

Drag Reduction in Pipeline by Polymer-Surfactant and Polymer-Polymer Mixtures

by

Weicong Huang

A thesis
presented to the University of Waterloo
in fulfillment of the
thesis requirement for the degree of
Master of Applied Science
in
Chemical Engineering

Waterloo, Ontario, Canada, 2015

© Weicong Huang 2015

Author's Declaration

I hereby declare that I am the sole author of this thesis. This is s true copy of the thesis, including any required final revisions, as accepted by my examiners.

I understand that my thesis may be made electronically available to the public.

Abstract

Extensive researches have been conducted to investigate into the drag reduction behavior of the polymer-surfactant mixture and the polymer-polymer mixture. The drag reduction effect of PAM (polyacrylamide), PEO (polyethylene oxide) and CMC (carboxymethyl cellulose) has already been studied respectively. However, the drag reduction effects of the combination of these polymers have not been studied before. It is interesting to investigate into these combinations because the synergy between different polymers can enhance the drag reduction effect under the right condition.

SDS (sodium dodecyl sulfate) is a surfactant widely used in many commercially available detergents. When dissolved in water and circulated in the flow loop, the drag reduction effect of SDS has also been observed. Therefore, the combination of PAM and SDS is also worth exploring. The synergy between the polymer and the surfactant may strengthen the drag reduction effect.

In this thesis, the drag reduction effects are investigated for the following combinations: the PAM-SDS system, the PAM-CMC system and the PEO-CMC system. The mixed solutions are circulated in the flow loop, where the pressure drop over a certain distance and the flow rate are recorded in order to plot the friction factor against the Reynolds number. In addition, the viscosity, conductivity and surface tension of the mixed solutions are studied at bench-scale to look for the synergy in the mixed system.

Acknowledgement

I am very grateful to Professor Rajinder Pal for giving me the opportunity to conduct researches in the labs and for his helpful advices on my researches. My gratitude is also given to Ali Asghar Mohsenipour for the training and the calibration data he gave me. Without their support, I could not have completed the researches.

In addition, a special thank is given to my parents and relatives for their love and support. Although I have not seen them for two years, their understanding is my driving force to accomplish the research goals.

Table of Contents

List of Tables.....	vii
List of Figures.....	viii
Chapter 1. Introduction to Drag Reduction Effect.....	1
1.1. Introduction and objective.....	1
1.2. Polymers used in the research	3
1.3. Surfactant used in the research.....	6
Chapter 2. Experimental Procedure	7
2.1. Flow loop experiment.....	7
2.2. Bench-scale experiment	11
2.3. Data processing	13
2.3.1. Viscometer	13
2.3.2. Flow loop.....	14
2.3.3. Sample calculation.....	17
Chapter 3. Literature Review	20
3.1. Concept of drag reduction effect.....	20
3.2. Mean velocity profiles.....	21
3.3. Drag reduction effect of polymer	23
3.4. Mechanism of polymer drag reduction effect	24
3.5. Drag reduction effect of surfactant.....	26
Chapter 4. Drag Reduction Effect of PAM-CMC System.....	27
4.1. Bench-scale experiment result	28
4.1.1. Viscosity.....	28
4.1.2. Surface tension	32
4.1.3. Conductivity.....	33
4.2. Flow loop experiment result.....	34
4.2.1. Experiments in 1.5-inch pipeline	34
4.2.2. Experiments in 1-inch pipeline	41
4.3. Conclusion.....	48

Chapter 5. Drag Reduction Effect of PEO-CMC System.....	49
5.1. Bench-scale experiment result	50
5.1.1. Viscosity.....	50
5.1.2. Surface tension	54
5.1.3. Conductivity.....	55
5.2. Flow loop experiment result.....	56
5.2.1. Experiments in 1.5-inch pipeline	56
5.2.2. Experiments in 1-inch pipeline	63
5.3. Conclusion.....	70
Chapter 6. Drag Reduction Effect of PAM-SDS System	71
6.1. Bench-scale experiment result	72
6.1.1. Viscosity.....	72
6.1.2. Surface tension	76
6.1.3. Conductivity.....	77
6.2. Flow loop experiment result.....	78
6.2.1. Experiments in 1.5-inch pipeline	78
6.2.2. Experiments in 1-inch pipeline	85
6.3. Conclusion.....	92
References.....	93
Appendices.....	97
Appendix A. PAM-CMC Experiment data.....	97
Appendix A-1. Bench-scale experiment data.....	97
Appendix A-2. Flow loop experiment data.....	105
Appendix B. PEO-CMC Experiment data	125
Appendix B-1. Bench-scale experiment data.....	125
Appendix B-2. Flow loop experiment data	133
Appendix C. PAM-SDS Experiment data.....	153
Appendix C-1. Bench-scale experiment data.....	153
Appendix C-2. Flow loop experiment data	161

List of Tables

Table 1.1 Polymers and surfactant used in this research.....	3
Table 2.1. Information of the equipment in the flow loop.....	9
Table 2.2. Tube dimension and test section length.....	10
Table 2.3. Calibration equations for the pressure transducers.....	10
Table 2.4. List of instruments in the bench-scale lab.....	11
Table 4.1. The total mass and weight fraction used in the experiments.....	27
Table 5.1. The total mass and weight fraction used in the experiments.....	49
Table 6.1. The concentrations of PAM and SDS used in the experiments.....	71

List of Figures

Figure 1.1. The structure of the repeating unit of PEO.....	3
Figure 1.2. The structure of the repeating unit of PAM.....	4
Figure 1.3. The structure of the repeating unit of CMC. R indicates the carboxymethyl group.....	5
Figure 1.4. The structure of the surfactant SDS.....	6
Figure 2.1. Picture of the flow loop.....	8
Figure 2.2. Picture of the flow loop.....	8
Figure 2.3. Schematic diagram of the flow loop.....	9
Figure 2.4. Picture of the viscometer.....	11
Figure 2.5. Picture of the tensiometer.....	12
Figure 2.6. Picture of the conductivity meter.....	12
Figure 3.1. Turbulent core velocity profile for Newtonian fluid and drag reducing fluids.....	22
Figure 3.2. Schematic of polymer stretching and relaxation, q is the vector of end-end distance and indicates the quantitative polymer stretching.....	24
Figure 4.1. Apparent viscosity (Pa·s) vs. PAM weight fraction for the PAM-CMC system (total concentration: 1000 ppm).....	29
Figure 4.2. Apparent viscosity (Pa·s) vs. PAM weight fraction for the PAM-CMC system (total concentration: 500 ppm).....	29
Figure 4.3. Power law parameter n vs. PAM weight fraction for the PAM-CMC system (total concentration: 500 ppm and 1000 ppm).....	31
Figure 4.4. Power law parameter k vs. PAM weight fraction for the PAM-CMC system (total concentration: 500 ppm and 1000 ppm).....	31
Figure 4.5. Surface tension (Dynes/cm) vs. PAM weight fraction for the PAM-CMC system....	32
Figure 4.6. Conductivity ($\mu\text{s}/\text{cm}$) vs. PAM weight fraction for the PAM-CMC system.....	33
Figure 4.7. Friction factor vs. Re number for the PAM-CMC system (1000ppm) in 1.5-inch pipe.....	35
Figure 4.8. Friction factor vs. Re number for the PAM-CMC system (500ppm) in 1.5-inch pipe.....	36

Figure 4.9. %DR vs. Re number for the PAM-CMC system (1000ppm in total) in 1.5-inch pipe (compared with Blasius equation).....	36
Figure 4.10. %DR vs. Re number for the PAM-CMC system (500ppm in total) in 1.5-inch pipe (compared with Blasius equation).....	37
Figure 4.11. %DR vs. Re number for the PAM-CMC system (1000ppm in total) in 1.5-inch pipe (compared with Dodge-Metzner equation).....	38
Figure 4.12. %DR vs. Re number for the PAM-CMC system (500ppm in total) in 1.5-inch pipe (compared with Dodge-Metzner equation).....	38
Figure 4.13. Friction factor vs. Re for the PAM-CMC system (1000ppm) in 1.5 inch pipe.....	39
Figure 4.14. Friction factor vs. Re for the PAM-CMC system (500ppm) in 1.5 inch pipe.....	40
Figure 4.15. Friction factor vs. Reynolds number for the PAM-CMC system (1000ppm in total) in 1-inch pipe.....	42
Figure 4.16. Friction factor vs. Reynolds number for the PAM-CMC system (500ppm in total) in 1-inch pipe.....	43
Figure 4.17. %DR vs. Reynolds number for the PAM-CMC system (1000ppm in total) in 1-inch pipe (compared with Blasius equation).....	43
Figure 4.18. %DR vs. Reynolds number for the PAM-CMC system (500ppm in total) in 1-inch pipe (compared with Blasius equation).....	44
Figure 4.19. %DR vs. Reynolds number for the PAM-CMC system (1000ppm in total) in 1-inch pipe compare (compared with Dodge-Metzner equation).....	45
Figure 4.20. %DR vs. Reynolds number for the PAM-CMC system (500ppm in total) in 1-inch pipe (compared with Dodge-Metzner equation).....	45
Figure 4.21. Friction factor vs. Re for the PAM-CMC system (1000ppm) in 1 inch pipe.....	46
Figure 4.22. Friction factor vs. Re for the PAM-CMC system (500ppm) in 1 inch pipe.....	47
Figure 5.1. Apparent viscosity (Pa·s) vs. PEO weight fraction for the PEO-CMC system (1000 ppm in total).....	51
Figure 5.2. Apparent viscosity (Pa·s) vs. PEO weight fraction for the PEO-CMC system (500 ppm in total).....	51
Figure 5.3. Power law parameter n vs. PEO weight fraction for the PEO-CMC system (total concentration: 500 ppm and 1000 ppm).....	53
Figure 5.4. Power law parameter k vs. PEO weight fraction for the PEO-CMC system	

(total concentration: 500 ppm and 1000 ppm).....	53
Figure 5.5. Surface tension (Dynes/cm) vs. PEO weight fraction for the PEO-CMC system.....	54
Figure 5.6. Conductivity ($\mu\text{s}/\text{cm}$) vs. PEO weight fraction for the PEO-CMC system.....	55
Figure 5.7. Friction factor vs. Re number for the PEO-CMC system (1000ppm) in 1.5-inch pipe.....	57
Figure 5.8. Friction factor vs. Re number for the PEO-CMC system (500ppm) in 1.5-inch pipe.....	58
Figure 5.9. %DR vs. Reynolds number for the PEO-CMC system (1000ppm in total) in 1.5-inch pipe (compared with Blasius equation).....	58
Figure 5.10. %DR vs. Reynolds number for the PEO-CMC system (500ppm in total) in 1.5-inch pipe (compared with Blasius equation).....	59
Figure 5.11. %DR vs. Reynolds number for the PEO-CMC system (1000ppm in total) in 1.5-inch pipe (compared with Dodge-Metzner equation).....	60
Figure 5.12. %DR vs. Reynolds number for the PEO-CMC system (500ppm in total) in 1.5-inch pipe (compared with Dodge-Metzner equation).....	60
Figure 5.13. Friction factor vs. Re for the PEO-CMC system (1000ppm) in 1.5 inch pipe.....	61
Figure 5.14. Friction factor vs. Re for the PEO-CMC system (500ppm) in 1.5 inch pipe.....	62
Figure 5.15. Friction factor vs. Re number for the PEO-CMC system (1000ppm) in 1-inch pipe.....	64
Figure 5.16. Friction factor vs. Re number for the PEO-CMC system (500ppm) in 1-inch pipe.....	65
Figure 5.17. %DR vs. Reynolds number for the PEO-CMC system (1000ppm in total) in 1-inch pipe (compared with Blasius equation).....	65
Figure 5.18. %DR vs. Reynolds number for the PEO-CMC system (500ppm in total) in 1-inch pipe (compared with Blasius equation).....	66
Figure 5.19. %DR vs. Reynolds number for the PAM-CMC system (1000ppm in total) in 1-inch pipe compare (compared with Dodge-Metzner equation).....	67
Figure 5.20. %DR vs. Reynolds number for the PAM-CMC system (500ppm in total) in 1-inch pipe (compared with Dodge-Metzner equation).....	67
Figure 5.21. Friction factor vs. Re for the PEO-CMC system (1000ppm) in 1 inch pipe.....	68
Figure 5.22. Friction factor vs. Re for the PEO-CMC system (500ppm) in 1 inch pipe.....	69

Figure 6.1. Apparent viscosity (Pa·s) vs. surfactant concentration (ppm) for the mixed system of PAM (500 ppm) and SDS.....	73
Figure 6.2. Apparent viscosity (Pa·s) vs. surfactant concentration (ppm) for the mixed system of PAM (1000 ppm) and SDS.....	73
Figure 6.3. Power law parameter n vs. SDS concentration for the PAM-SDS system.....	75
Figure 6.4. Power law parameter k vs. SDS concentration for the PAM-SDS system.....	75
Figure 6.5. Surface tension (Dynes/cm) vs. surfactant concentration (ppm) for the mixed system of PAM (500 and 1000 ppm) and SDS.....	76
Figure 6.6. Conductivity ($\mu\text{s}/\text{cm}$) vs. surfactant concentration (ppm) for the mixed system of PAM (500 and 1000 ppm) and SDS.....	77
Figure 6.7. Friction factor vs. Reynolds number for the mixed system of PAM (1000 ppm) and SDS (0, 5, 10, 50, 100 ppm) in 1.5-inch pipe.....	79
Figure 6.8. Friction factor vs. Reynolds number for the mixed system of PAM (500 ppm) and SDS (0, 5, 10, 50, 100 ppm) in 1.5-inch pipe.....	79
Figure 6.9. %DR vs. Reynolds number for the mixed system of PAM (1000 ppm) and SDS (0, 5, 10, 50, 100 ppm) in 1.5-inch pipe (compared with Blasius equation).....	80
Figure 6.10. %DR vs. Reynolds number for the mixed system of PAM (500 ppm) and SDS (0, 5, 10, 50, 100 ppm) in 1.5-inch pipe (compared with Blasius equation).....	80
Figure 6.11. %DR vs. Reynolds number for the mixed system of PAM (1000 ppm) and SDS (0, 5, 10, 50, 100 ppm) in 1.5-inch pipe (compared with Dodge-Metzner equation).....	82
Figure 6.12. %DR vs. Reynolds number for the mixed system of PAM (500 ppm) and SDS (0, 5, 10, 50, 100 ppm) in 1.5-inch pipe (compared with Dodge-Metzner equation).....	82
Figure 6.13. Friction factor vs. Re for the PAM-SDS system (1000ppm) in 1.5 inch pipe.....	83
Figure 6.14. Friction factor vs. Re for the PAM-SDS system (500ppm) in 1.5 inch pipe.....	84
Figure 6.15. Friction factor vs. Reynolds number for the mixed system of PAM (1000 ppm) and SDS (0, 5, 10, 50, 100 ppm) in 1-inch pipe.....	86
Figure 6.16. Friction factor vs. Reynolds number for the mixed system of PAM (500 ppm) and SDS (0, 5, 10, 50, 100 ppm) in 1-inch pipe.....	86
Figure 6.17. %DR vs. Reynolds number for the mixed system of PAM (1000 ppm) and SDS (0, 5, 10, 50, 100 ppm) in 1-inch pipe (compared with Blasius equation).....	87

Figure 6.18. %DR vs. Reynolds number for the mixed system of PAM (500 ppm) and SDS (0, 5, 10, 50, 100 ppm) in 1-inch pipe (compared with Blasius equation).....87

Figure 6.19. %DR vs. Reynolds number for the mixed system of PAM (1000 ppm) and SDS (0, 5, 10, 50, 100 ppm) in 1-inch pipe (compared with Dodge-Metzner equation).....89

Figure 6.20. %DR vs. Reynolds number for the mixed system of PAM (500 ppm) and SDS (0, 5, 10, 50, 100 ppm) in 1-inch pipe (compared with Dodge-Metzner equation).....89

Figure 6.21. Friction factor vs. Re for the PAM-SDS system (1000ppm) in 1 inch pipe.....90

Figure 6.22. Friction factor vs. Re for the PAM-SDS system (500ppm) in 1 inch pipe.....91

Chapter 1. Introduction to Drag Reduction Effect

1.1. Introduction and objective

The phenomenon that the addition of polymer or surfactant can result in the reduction of friction in turbulent pipe flow has been known for over fifty years, and this phenomenon is called drag reduction effect. In 1948, Tom published the first observation of the drag reduction effect ^[1]. During the following years, drag reduction effect has found many applications in many fields: transportation of oil, wastewater treatment, firefighting, heating and cooling systems, hydraulic machine, etc ^[2, 3, 4].

A large amount of researches have been conducted to study the drag reduction effect of polymer. Lumley (1973) concluded that the stretching of randomly coiled polymers due to a strong turbulent flow is relevant to the drag reduction effect ^[5]. The drag reduction effect of polymer is also explained by the viscoelastic effects of the polymer chains in the solution (Hinch 1977; Metzner 1970) ^[6, 7]. The high shear conditions of the turbulent flow induce the stretching of the polymer chain and the increase of elongational viscosity, which in turn increases effective viscosity in the buffer layer of the turbulent flow. Due to this increase, the buffer layer thickness causing a reduction in wall friction (Lumley 1973) ^[8]. In addition, the stream-wise and the span-wise fluctuations are suppressed.

Mysels (1949) was the first scientists to study the drag reduction effect of surfactant ^[9]. Dodge and Metzner (1959) also carefully studied the drag reduction effect of surfactant ^[10]. Surfactants demonstrate lower mechanical degradation and are considered as environmentally friendly chemicals (Harwigsson and Hellsten 1996; Zakin and Lui 1983) ^[2, 11]. Threadlike or wormlike micelles are believed to be the necessary factor for the surfactant drag reduction (Qi and Zakin 2002; Zakin 1998; Zakin 1996) ^[12, 13]. The morphology of micelles can be changed from spherical to threadlike by addition of oppositely charged substance. Although the mechanism of surfactant drag reduction is still unclear, it is proposed that the viscoelastic character of surfactant could be the reason for the drag reduction effect.

The drag reduction effect of polymer-surfactant mixtures find various applications in drug delivery, oil recovery, cosmetic recipe, etc (Bai 2010; Dan 2009; Harada and Kataoka 2006; Villetti 2011; Zhang 2011) ^[14~18]. The drag reduction effect of the polymer-surfactant combination can be adjusted by using different types of polymers and surfactants, as well as the physical properties of the solution, such as temperature and pH (Feitosa 1996; Jonsson 1998) ^[19, 20]. After the surfactant concentration increases beyond the critical aggregation concentration (CAC), the interaction between polymer and surfactant become obvious. Between positively or negatively charged polymer and oppositely charged surfactant, the electrostatic interaction play an important role in the polymer-surfactant interaction, and CAC has been reported to be several orders of magnitudes lower than the CMC of surfactant. Between non-ionic polymer and ionic surfactant, the hydrophobic interaction become the main driving force for the polymer-surfactant interaction, and CAC becomes close to the CMC of surfactant (Diamant and Andelman 1999; Hansson and Lindman 1996) ^[21, 22]. However, how the polymer-surfactant interaction affects the drag reduction effect is still unclear.

Although a lot of efforts have been directed to study the drag reduction effect of polymer solutions, the literature about the drag reduction effect of polymer-polymer mixtures is very limited. Preliminary study shows that mixing two interactive polymers may enhance the drag reduction effect of the solution. Therefore, the aim of this thesis is to investigate into the drag reduction effect of two polymer-polymer systems: the PAM-CMC system and the PEO-CMC system. Besides, the polymer-surfactant system PAM-SDS has also been studied.

1.2. Polymers used in the research

Three mixed systems are studied in this research and they are the PAM-CMC system, the PEO-CMC system and the PAM-SDS system. The three polymers and one surfactant used are:

Table 1.1 Polymers and surfactant used in this research

Polymer	PEO	Poly(ethylene oxide)
	PAM	Polyacrylamide
	CMC	Carboxymethyl cellulose
Surfactant	SDS	Sodium dodecyl sulfate

Poly(ethylene oxide), or polyoxyethylene, is prepared by the polymerization of ethylene oxide and is commercially available over a wide range of molecular weight. PEO has a low toxicity and is used in a variety of products. PEO is commonly used as a precipitant for plasmid DNA isolation and protein crystallization. PEO is the basis of many skin creams and personal lubricants. PEO is also used as an anti-foaming agent in food. PEO is non-ionic, but dissolvable in water. Given the same concentration, pure PEO solution is less viscous than pure PAM solution or pure CMC solution.

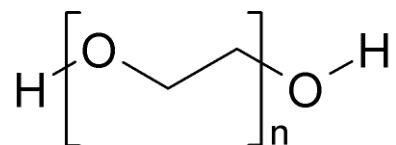


Figure 1.1. The structure of the repeating unit of PEO

Manufacturer information:

Name: Sentry™ Polyox™ WSR 303 – NF Grade

Manufacturer: The Dow Chemical Company

Molecular weight: 7,000,000

One of the largest uses of polyacrylamide is to flocculate solids in liquid, which applies to water treatment, paper making, screen printing, etc. The anionic form of cross-linked polyacrylamide is also frequently used as a soil conditioner on farm land and construction sites for erosion control. Another common use of polyacrylamide and its derivatives is in subsurface applications such as Enhanced Oil Recovery. High viscosity aqueous solutions can be generated with low concentrations of polyacrylamide polymers, and these can be injected to improve the economics of conventional water flooding.

The PAM used in this research is an anionic water-soluble copolymer of acrylamide and sodium acrylate with a molecular weight range of $11\sim 14\times 10^6$ g/mol and a charge density of approximately 30%. When dissolved in water sodium acrylate releases Na^+ ions into the water and leaves a negative charge on the polymer chains. The polymer chains have strong dipole and present a potential for strong interaction with other substances in the solution. The structures of the repeating units of PAM is shown in the following figure.

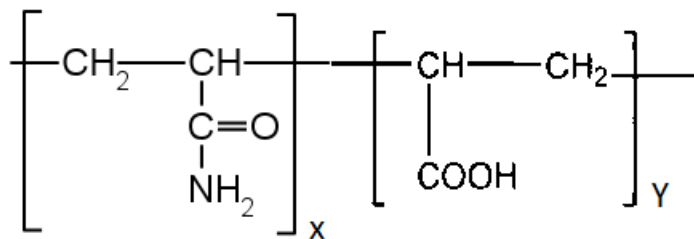


Figure 1.2. The structure of the repeating unit of PAM

Manufacturer information:

Name: HYPERFLOC AF 207

Manufacturer: hychem, inc.

Molecular weight: 10,000,000

Carboxymethyl cellulose, or Cellulose gum, is a cellulose derivative with carboxymethyl groups bound to some of the hydroxyl groups of the glucopyranose monomers that make up the cellulose backbone. It is often used as its sodium salt, sodium carboxymethyl cellulose. It is synthesized by the alkali-catalyzed reaction of cellulose with chloroacetic acid.

CMC is used in food as a viscosity modifier or thickener, and to stabilize emulsion in various products including ice cream. CMC is also used in pharmaceuticals as a thickening agent, and in the oil-drilling industry as an ingredient of drilling mud, where it acts as a viscosity modifier and water retention agent. CMC is also widely used as an anti-redeposition agent in many detergents. It is also used as an anti-abrasion and dispersive additive in granular detergents.

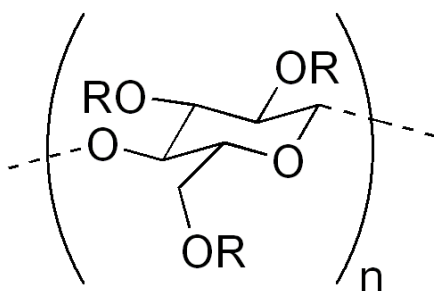


Figure 1.3. The structure of the repeating unit of CMC. R indicates the carboxymethyl group.

Manufacturer information:

Name: Hercules, Inc.

Manufacturer: Sodium Carboxymethyl Cellulose

Molecular weight: 700,000

1.3. Surfactant used in the research

Sodium dodecyl sulfate is an anionic surfactant used in many cleaning and hygiene products. The salt is of an organo-sulfate consisting of a 12-carbon tail attached to a sulfate group, giving the material the amphiphilic properties required of a detergent. SDS is mainly used in detergents for laundry with many cleaning applications. For example, it is used in many tasks requiring the removal of oily stains and residues.

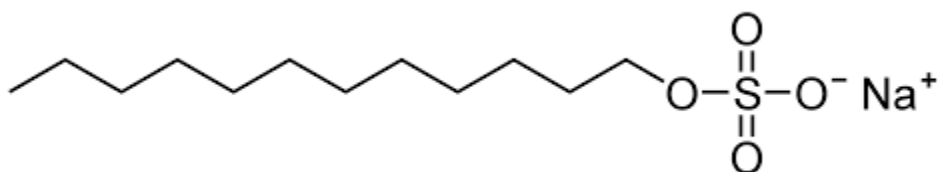


Figure 1.4. The structure of the surfactant SDS

Manufacturer information:

Name: Sodium Laurel Sulfate

Manufacturer: Duda Diesel LLC

Chapter 2. Experimental Procedure

The experiments in this thesis are divided into two parts: flow loop experiments and bench-scale experiments. In the flow loop experiment, the polymer-polymer solutions or the polymer-surfactant solutions are circulated in the flow loop. The flow rate and the pressure drop over a certain distance are recorded and converted into generalized Reynolds number and friction factor. In the bench-scale experiments, the polymer-polymer solutions or the polymer-surfactant solutions are tested in terms of viscosity, conductivity and surface tension. These results are used to characterize the interaction in the solutions and elucidate the mechanism of the drag reduction effect.

2.1. Flow loop experiments

The test fluid is prepared in a large mixing tank, which is equipped with a thermo insulation jacket and a mixer. A temperature controller is used to read and maintain the temperature of the test fluid at $20\pm 1^\circ\text{C}$. A pump is connected to circulate the test fluid in the flow loop. A flowmeter is connected after the pump to monitor and record the flow rate. After the flowmeter, there are six horizontally-installed tubes with different diameters. Each tube has a bypass which is connected to three pressure transducers, whose working ranges are different. The bypasses are located far enough from the tube entrances to ensure that the flow of the test fluid has been fully developed in the section of the tube where the measurement is taken. A data acquisition system is connected to the flowmeter and the three pressure transducers. The data is processed by the Labview software in the computer. Figure 2.3 illustrates the schematic diagram of the flow loop.



Figure 2.1. Picture of the flow loop

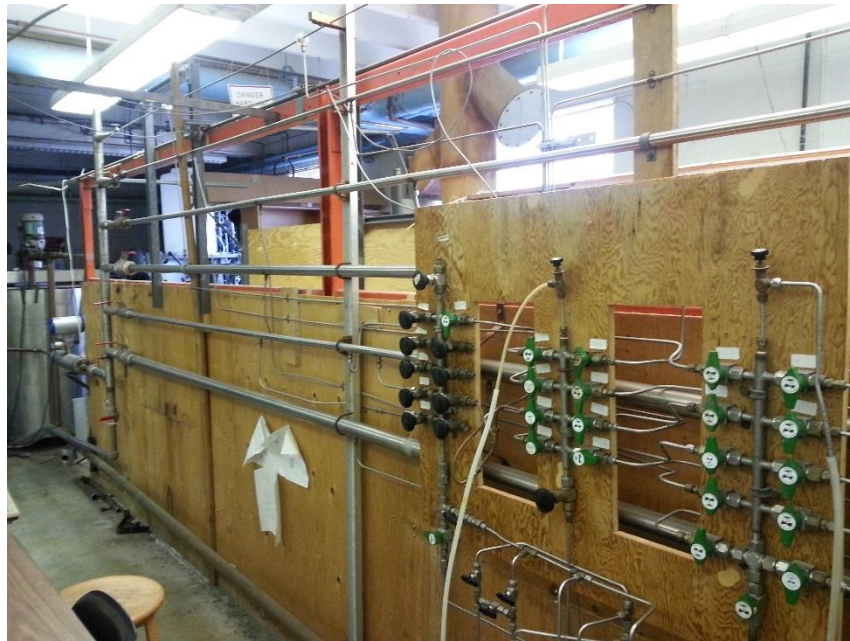


Figure 2.2. Picture of the flow loop

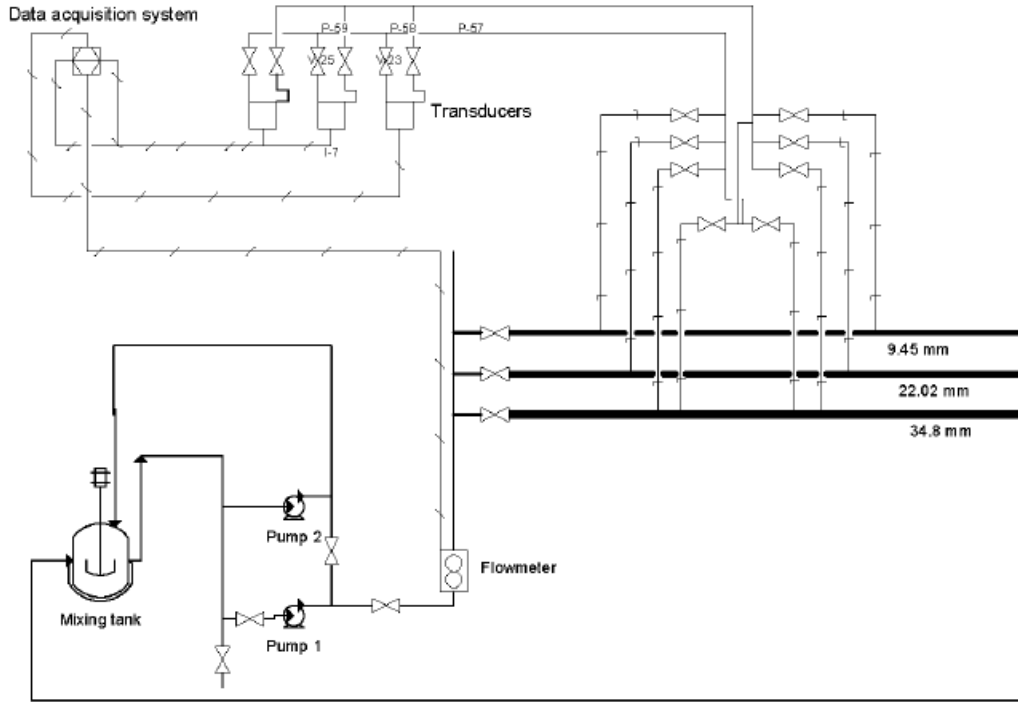


Figure 2.3. Schematic diagram of the flow loop

Table 2.1. Information of the equipment in the flow loop

	Equipment name	Description
1	Pump	Centrifugal pump, 7.5 HP
2	Flow meter	KrohneOptimass 7050 CT
3	Pressure transducer	Rosemont Model 3051 (0~0.5 psi)
4	Pressure transducer	Rosemont Model 3051 (0~5 psi)
5	Pressure transducer	Cole-Parmer Model 68071-52 (0~10 psi)
6	Transducer-PC interface	USB measurement computing interface model 1680 FS
7	Data processing system	Labview software

Table 2.2. Tube dimension and test section length

	Nominal Diameter	Inside diameter	Test section length
1	1 inch	22.02 mm	1.219 m
2	1.5 inch	34.8 mm	3.048 m

In this experiment, only the 1-inch tube and the 1.5-inch tube are used for the measurement. All the equipment has been calibrated by previous group members and the calibration data are presented in Ali Mohsenipour's thesis. The resulting calibration equations are summarized in the following figures and Table 2.3.

Table 2.3. Calibration equations for the pressure transducers

Range	Calibration equation
0~10 psi	Differential pressure = Reading voltage \times 2.5297 - 2.5573
0~5 psi	Differential pressure = Reading voltage \times 1.2581 - 1.2823
0~0.5 psi	Differential pressure = Reading voltage \times 0.1221 - 0.102

2.2. Bench-scale experiments

In order to reveal the mechanism of the drag reduction effect, the viscosity, conductivity and surface tension of the polymer-surfactant solutions and the polymer-polymer solutions are measured of bench-scale. The information of the instruments used in these experiments is given below:

Table 2.4. List of instruments in the bench-scale lab

	Instrument name	Description
1	Viscometer	Fann 35A/SR12 viscometer
2	Tensiometer	CSC-DuNouy
3	Conductivity meter	Thermo Orion 3 Star



Figure 2.4. Picture of the viscometer



Figure 2.5. Picture of the tensiometer



Figure 2.6. Picture of the conductivity meter

2.3. Data processing

2.3.1. Viscometer

In this coaxial cylinder viscometer, a rotor sleeve is rotated at a specific shear rate while a bob in the center measures the force exerted on the surface of the bob. The following equations are used in the calibration. Shear stress is given by:

$$\tau \text{ (pascal)} = \text{Dial reading} \times 0.0881 - 0.3694 \quad (2.1)$$

For non-Newtonian fluids:

$$\gamma = \frac{2N}{1-S^{-2N}} \Omega \quad (2.2)$$

N is the slope of $\ln(\Omega)$ vs. $\ln(\text{Shear stress})$ curve. N is equal to 1 for Newtonian fluid. S is the ratio between the rotor radius and the bob radius, which is 1.06551. Ω is defined as follows:

$$\Omega = \frac{2\pi \times RPM}{60} \quad (2.3)$$

2.3.2. Flow loop

For the flow loop, the purpose of the calculation is to convert the raw data from the flow meter and the pressure transducers into generalized Reynolds number, friction factor and percent drag reduction.

The calibration equation for the mass flowmeter:

$$\text{Mass flow rate (kg/s)} = \text{Voltage reading} \times 1.534 - 1.5272 \quad (2.4)$$

The flow velocity is obtained from mass flow rate using the following equation:

$$\text{Flow velocity} = \frac{\text{Mass flow rate}}{\text{Density} \times \text{Crosssectional area}} \quad (2.5)$$

The equation for calculating the generalized Reynolds number is ^[49]:

$$Re = \frac{\rho D^n V^{2-n}}{8^{n-1} k \left(\frac{3n+1}{4n} \right)^n} \quad (2.6)$$

ρ : Density

D: Tube diameter

V: Average flow rate

n: Power law parameter

k: Power law parameter

The calibration equations for the three pressure transducers are as follows:

Range	Calibration equation
0~10 psi	Differential pressure = Reading voltage \times 2.5297 - 2.5573
0~5 psi	Differential pressure = Reading voltage \times 1.2581 - 1.2823
0~0.5 psi	Differential pressure = Reading voltage \times 0.1221 - 0.102

The equation for calculating friction factor is:

$$f = \frac{\Delta P \cdot D}{2 \cdot \rho \cdot L \cdot V^2} \quad (2.7)$$

ΔP : Pressure drop

D: Tube diameter

ρ : Density

L: Length of the test section

V: Average flow rate

The percent drag reduction is calculated by:

$$\%DR = \frac{f_{\text{solvent}} - f_{\text{solution}}}{f_{\text{solvent}}} \times 100\% \quad (2.8)$$

f_{solvent} : friction factor of the solvent

f_{solution} : friction factor of the solution

The f_{solvent} of the turbulent flow of a Newtonian fluid such as water is calculated with the Blasius equation:

$$f = \frac{0.079}{Re^{0.25}} \quad (2.9)$$

The f_{solvent} of the turbulent flow of a non-Newtonian fluid is calculated using the following Dodge-Metzner equation:

$$\frac{1}{\sqrt{f}} = \frac{4}{n^{0.75}} \log \left(Re_g \cdot f^{1-\frac{n}{2}} \right) - \frac{0.4}{n^{1.2}} \quad (2.10)$$

The f_{solution} of the turbulent flow of a non-Newtonian fluid is obtained experimentally.

2.3.3. Sample calculation

The procedure here will go through the calculation step by step. For 1000ppm PAM solution in 1 inch pipe, the flowmeter signal is 2.727V, the pressure transducer signal is 1.497V, the tube diameter is 0.02202m, the length of the test section is 0.9144m, n is 0.3874, k is 0.525, and the density of the solution is 1013.11kg/m³.

Reynolds number calculation:

Mass flow rate is calculated with the following equation:

$$\begin{aligned}\text{Mass flow rate} &= \text{Voltage reading} \times 1.534 - 1.5272 \\ &= 2.727 \times 1.534 - 1.5272 \\ &= 2.656 \text{ kg/s}\end{aligned}$$

Velocity is calculated with the following equation:

$$\begin{aligned}\text{Velocity} &= \frac{\text{Mass flow rate}}{\text{Density} \times \text{Cross sectional area}} \\ &= \frac{2.656}{1013.11 \times 3.14 \times \left(\frac{0.02202}{2}\right)^2} \\ &= 6.888 \text{ m/s}\end{aligned}$$

Re is calculated with the following equation:

$$\begin{aligned}Re &= \frac{\rho D^n V^{2-n}}{8^{n-1} k \left(\frac{3n+1}{4n}\right)^n} \\ &= \frac{1013.11 \times 0.02202^{0.3874} \times 6.888^{2-0.3874}}{8^{0.3874-1} \times 0.525 \times \left(\frac{3 \times 0.3874 + 1}{4 \times 0.3874}\right)^{0.3874}} \\ &= 31057\end{aligned}$$

Friction factor calculation:

The calibration equations for the three pressure transducers are:

Range	Calibration equation
0~10 psi	Differential pressure (Pa) = Reading voltage \times 2.5297 - 2.5573
0~5 psi	Differential pressure (Pa) = Reading voltage \times 1.2581 - 1.2823
0~0.5 psi	Differential pressure (Pa) = Reading voltage \times 0.1221 - 0.102

The pressure drop signal here is 1.497V and the differential pressure is calculated with the second calibration equation:

$$\begin{aligned} \text{Differential pressure} &= 1.497 \times 1.2581 - 1.2823 \\ &= 0.601 \text{ Pa} \end{aligned}$$

The friction factor is calculated with the following equation. D is the tube diameter, L is the length of the test section, and V is velocity.

$$\begin{aligned} f_{\text{solution}} &= \frac{\Delta P \cdot D}{2 \cdot \rho \cdot L \cdot V^2} \\ &= \frac{0.601 \times 0.02202}{2 \times 1013.11 \times 0.9144 \times 6.888^2} \\ &= 0.00104 \end{aligned}$$

%DR calculation:

There are two ways to calculate %DR: using the Blasius equation (Method 1) and using the Dodge-Metzner equation (Method 2).

Method 1:

The Re number in this calculation is calculated with the following equation. The density of water is 998.2kg/m³ and the viscosity of water is 0.001002Pa.s.

$$Re = \frac{\rho DV}{\mu} = \frac{998.2 \times 0.02202 \times 6.888}{0.001002} = 151091$$

The Blasius equation is used to calculate $f_{solvent}$:

$$f_{solvent} = \frac{0.079}{Re^{0.25}} = \frac{0.079}{151091^{0.25}} = 0.00401$$

Therefore, %DR is calculated with the following equation:

$$\%DR = \frac{f_{solvent} - f_{solution}}{f_{solution}} = \frac{0.00401 - 0.00104}{0.00401} = 74.1\%$$

Method 2:

The Re number has already been calculated in previous section and is 31057 here. Use the Dodge-Metzner equation used to calculate $f_{solvent}$:

$$\frac{1}{\sqrt{f_{solvent}}} = \frac{4}{n^{0.75}} \log \left(Re_g \cdot f_{solvent}^{1-\frac{n}{2}} \right) - \frac{0.4}{n^{1.2}}$$

$$\frac{1}{\sqrt{f_{solvent}}} = \frac{4}{0.3874^{0.75}} \log \left(31057 \cdot f_{solvent}^{1-\frac{0.3874}{2}} \right) - \frac{0.4}{0.3874^{1.2}}$$

$$f_{solvent} = 0.00287$$

Thus, the %DR is:

$$\%DR = \frac{f_{solvent} - f_{solution}}{f_{solution}} = \frac{0.00287 - 0.00104}{0.00287} = 63.8\%$$

Chapter 3. Literature Review

3.1. Concept of drag reduction effect

Drag reduction effect was first observed by Toms in 1948^[1] and numerous studies conducted by following researchers found that the addition of polymer, surfactant or fiber in turbulent pipe flow can lead to drag reduction effect. The drag reduction effect was defined by Zakin in 1998^[23] as:

$$\%DR = \frac{f_{solvent} - f_{solution}}{f_{solvent}} \times 100\% \quad (3.1)$$

Where %DR is the percent drag reduction, $f_{solvent}$ and $f_{solution}$ are the friction factor of the solvent and the solution. Gyr and Bewersdorff described the drag reduction effect in detail^[24]. The early studies of Metzner and Park (1964)^[25], Lumley (1969; 1973)^[5, 8], Virk (1975)^[26], Zakin (1978, 1971)^[27, 28], Berman (1978)^[29], Tabor and Gennes (1986)^[30] have provided good qualitative understandings of drag reduction effect. The recent contributions of Escudier (1998)^[31], Zakin (2010; 1998)^[32, 23], Sreenivasan (2000)^[33], Ptaskinski (2001)^[34], Kim (2003)^[35], Vanapalli (2006)^[36], Shah and Zhou (2009)^[37], and Tamano (2010)^[38] have quantitatively discussed the effect in different situations. However, the mechanism of the drag reduction effect is still to be discovered and proved.

Many factors can influence drag reduction, such as polymer concentration, type of solvent, polymer flexibility, molecular weight, chemical composition and pipe diameter. Generally, drag reduction increases with increasing molecular weight, polymer concentration, polymer chain flexibility and flow rate, while it decreases with increasing pipe diameter. This is true for small pipe diameters, but as pipe diameter increases, the diameter effect becomes negligible. It is found that there is an asymptote for maximum polymer drag reduction (Virk and Merrill, 1969)^[39] and it is known as Virk's asymptote.

3.2. Mean velocity profiles

The turbulent flow velocity profile is divided into three regions by Zakin (1998)^[23]: the viscous sublayer, the buffer layer and the turbulent core.

At viscous sublayer:

$$U^+ = y^+ \quad (0 < y^+ < 5) \quad (3.2)$$

At buffer layer:

$$U^+ = 5.0 \times \ln(y^+) + 3.05 \quad (5 < y^+ < 30) \quad (3.3)$$

At turbulent core:

$$U^+ = 2.5 \times \ln(y^+) + 5.5 \quad (y^+ > 30) \quad (3.4)$$

Where:

$$U^* = \sqrt{\frac{\tau_w}{\rho}} \quad (3.5)$$

$$U^+ = \frac{U}{U^*} \quad (3.6)$$

$$y^+ = \frac{U^* y}{\nu} \quad (3.7)$$

Where U is the local mean velocity, y is the distance from wall, ν is the kinetic viscosity, U^* is the shear velocity, τ_w is the shear stress, ρ is density.

It is shown in some study that the velocity profile at the viscous sublayer of drag reducing fluid is similar to Newtonian fluids (Ohlendorf, 1986; Virk 1975; Wilson and Thomas 1985) [40, 26, 41]. The buffer layer is almost a part of the turbulent core velocity profile for the drag reducing fluid. For the core section, the profile can be expressed by the following equation:

$$U^+ = 2.5 \times \ln(y^+) + 5.5 + \Delta B \quad (3.8)$$

In this equation, ΔB is added to show the parallel profile for fluids with different drag reduction effect. This term causes a deviation from the Newtonian profile. The following figure demonstrates the turbulent core velocity for a Newtonian fluid and a drag reducing fluid in the pipe flow (Zakin 1998) [23].

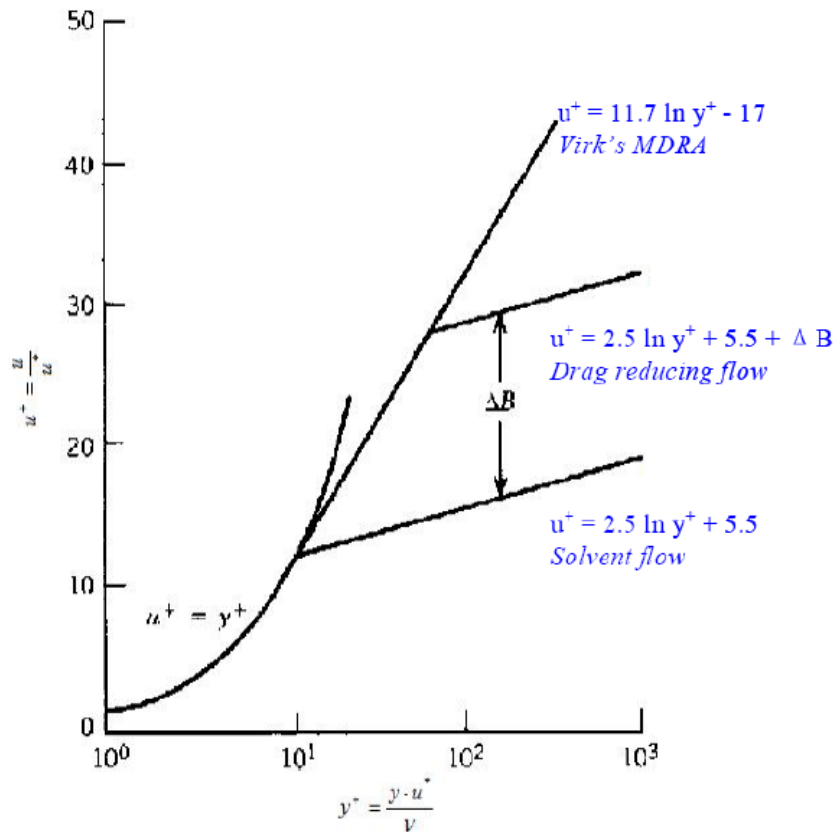


Figure 3.1. Turbulent core velocity profile for Newtonian fluid and drag reducing fluids

3.3. Drag reduction effect of polymer

Numerous researches have been conducted to investigate into the drag reduction effect of polymer in the past decades. The addition of a small amount of polymer (parts per million) can result in obvious drag reduction effect. For example, petroleum industry uses oil-soluble polymer in the pipeline system to reduce the pipeline friction. As a result the flow rate is increased and the drag reduction can be as high as 80% (Zakin 1998) ^[23].

Lumley (1973) ^[8] mentioned that the stretching of randomly coiled polymers due to strong turbulent flow is related to the drag reduction effect. Virk (1975) ^[26] suggested that the drag reduction effect is limited by an asymptotic. Tiederman (1989) ^[42] suggests that the changes of turbulent structures in the buffer layer also affect the drag reduction effect.

Warholic (1999) ^[43] suggested that the Reynolds shear stress become negligible near the maximum drag reduction . Kim (2003) ^[35] studied the pseudo plastic behavior of drag reducing polymer and used power law model for the non-Newtonian turbulent flow. Many researchers use Direct Numerical Simulation (DNS) to study the turbulent flow of polymer solutions. Graham (2004) ^[44] has provided a comprehensive review of the recent numerical investigations on drag reduction effect.

3.4. Mechanism of polymer drag reduction effect

In order to find out the mechanism of drag reduction effect, polymer is injected at certain locations in the flow and then the appearance of polymer is measured downstream as it spreads out. Injection experiment allows the testing of the dependence of drag reduction on the conformation of polymer in the flow. It is found that the polymer interacts with the turbulence at the turbulent core and the buffer layer (Tiederman and Luchik 1989) ^[42], while the viscous sublayer does not participate in the mechanism of drag reduction effect. Research has shown that drag reduction effect can occur at some onset shear stress. The most common explanation is the stretching and the aggregation of polymer due to shear stress increase (White and Mungal 2008) ^[45].

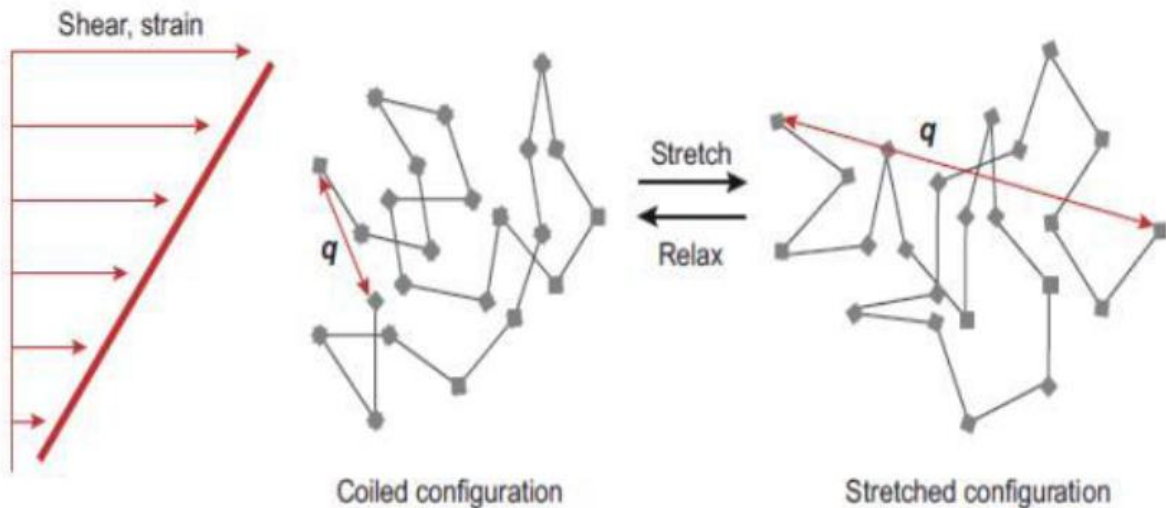


Figure 3.2. Schematic of polymer stretching and relaxation, q is the vector of end-end distance and indicates the quantitative polymer stretching

Two observations can justify that drag reduction effect is caused by an interaction between turbulence and polymer dynamics. Firstly, drag reduction effect is not seen until the transition from laminar region to turbulent region. Secondly, the onset of drag reduction effect at a fixed pipe diameter is determined by the length of polymer chain. For non-polymer drag reducing

solutions the turbulent structure is completely defined by the Reynolds number. However, in polymer drag reducing solutions, the polymer chain length and its conformation play a role. Drag reduction effect may be due to the molecular extension of the polymer chains. For the extension to occur, the elongation rate has to exceed the rotation rate.

Heterogeneous drag reduction is another form of drag reduction effect and has been observed by injecting concentrated polymer solution in the pipe flow. Sometimes it is observed that the injected polymer forms a stable thread in the flow, but significant drag reduction is still measured. This is in contradiction to the homogenous drag reduction effect where polymer had to be present in the buffer layer to take effect. Therefore, there must be a different mechanism (Hoyt, Sellin 1991, Vleggaar and Tels 1973) ^[46, 47]. Some studies show that this drag reduction is the result of a dissolving process. Consequently, the same mechanism as homogenous drag reduction happens (Bewersdorff, Gyr 1995) ^[24].

3.5. Drag reduction effect of surfactant

Surfactants have a hydrophilic head group which is capable of forming hydrogen bonds, and a hydrophobic tail group which is typically a non-polar long hydrocarbon chain. The surfactant molecules prefer to stay at the surface of water and reduce the surface tension. In water, the hydrophobic tail groups aggregate together in order to minimize the contact with water. At the same time, the hydrophilic head groups surround the aggregation of hydrocarbon tails and are in direct contact with the water molecules. The structure of the surfactant aggregation is called micelle.

Mysels (1949) is the first scientist to study the drag reduction effect of surfactant in turbulent flow ^[9]. However, it was not until Dodge and Metzner (1959) conducted researches on drag reduction that the study on drag reduction effect received enough attention ^[10]. Surfactants are more resistant to mechanical degradation than polymers and most of the surfactants can be considered as environmentally friendly chemicals (Harwigsson and Hellsten 1996; Zakin and Lui 1983; Zakin 1996) ^[2, 11, 13]. Threadlike or wormlike micelles are believed to be a necessity for the drag reducing performance of surfactant solutions (Qi and Zakin 2002; Zakin 1998; Zakin 1996) ^[12, 23, 13]. Micelles morphology can be changed from spherical to threadlike by adding to the ionic solutions an oppositely charged surfactant, organic counter-ions, or even uncharged small compounds like alcohols. Depending on system conditions, the micelle can be spherical, disk-like, cylindrical, thread-like, bilayer spherical (vesicle), hexagonal, lamellar and cubic crystal (Zakin 1998; Zhang 2005) ^[23, 48].

Chapter 4. Drag Reduction Effect of PAM-CMC System

The individual drag reduction effect of PAM and CMC has been studied in our group before. However, little effort has been put into the study of the mixed PAM-CMC system. Preliminary study of this combination shows that the drag reduction effect of the mixed system is bigger than the drag reduction effect of PAM or CMC alone. A more in-depth study demonstrates that synergistic drag reduction effect exists in the mixed PAM-CMC system.

In this study the total concentration of polymers added is fixed, and the weight fractions of PAM and CMC are varied. The following table (Table 4.1) shows the total concentration and the composition of the solutions prepared. The study is conducted at two levels of polymer concentration: 1000ppm in total and 500ppm in total. At each level, five compositions are studied. These solutions with different compositions are tested in the flow loop and the bench-scale equipment.

Table 4.1. The total mass and weight fractions used in the experiments

Total mass	Weight fractions of CMC and PAM				
500 ppm	100% CMC	75% CMC	50% CMC	25% CMC	0% CMC
	0% PAM	25% PAM	50% PAM	75% PAM	100% PAM
1000 ppm	100% CMC	75% CMC	50% CMC	25% CMC	0% CMC
	0% PAM	25% PAM	50% PAM	75% PAM	100% PAM

To study the drag reduction effect of the PAM-CMC system, PAM and CMC are dissolved in water and mixed in the flow loop tank. All solutions are freshly prepared before use. The tank is maintained at $20\pm 0.5^{\circ}\text{C}$ by the thermo jacket. All the solutions are tested in the 1-inch pipe and the 1.5-inch pipe. Flow rate and pressure drop are monitored, recorded and transferred to the data processing system. Then the flow rate and the pressure drop data are converted into Reynolds number and friction factor.

4.1. Bench-scale experiment result

4.1.1. Viscosity

Viscosity is an important parameter in the study of drag reduction effect. Since the polymer solutions of this study are non-Newtonian fluids, the viscosity measured here is the apparent viscosity, which is a function of the shear rate. To be more specific, the polymer solutions in this study are shear-thinning fluids, which means that the apparent viscosity of the fluids decrease as the shear rate is increased.

In Figures 4.1 and 4.2, the apparent viscosity is plotted against the PAM weight fraction. The viscosity of pure PAM solution is higher than that of pure CMC solution. Therefore, in theory, as the PAM weight fraction increases, the viscosity should also increase. However, this is not exactly the case for the PAM-CMC system.

For the 90rpm and 200rpm curves in both figures, the apparent viscosity first increases to the maximum between 25% and 50%, and then decreases as the PAM weight fraction approaches 100%. For the 30rpm curve in both figures, the maximum viscosity is located between 75% and 100%. This means that the mixed polymer solution may have a higher viscosity than the pure PAM solution or the pure CMC solution, which is different from the PEO-CMC system.

This phenomenon suggests that there is strong interaction between PAM and CMC in the solution. The anionic groups of PAM and CMC are neutralized by the cationic substances in the tap water. The polymer chain of PAM interacts with that of CMC and forms a network of polymer, which slightly increases the viscosity at high shear rate. This increased viscosity may affect the result of the flow loop experiment and enhance the drag reduction effect.

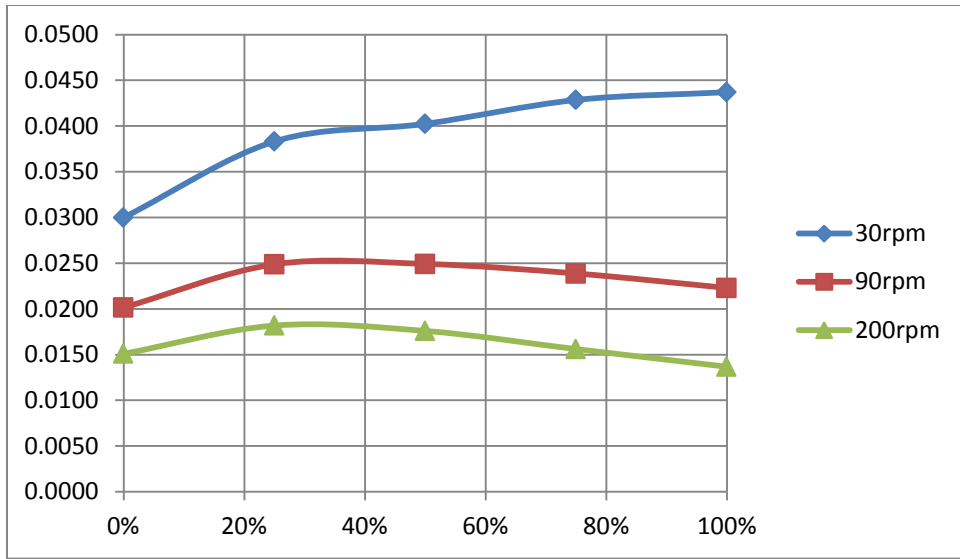


Figure 4.1. Apparent viscosity (Pa·s) vs. PAM weight fraction for the PAM-CMC system (total concentration: 1000 ppm)

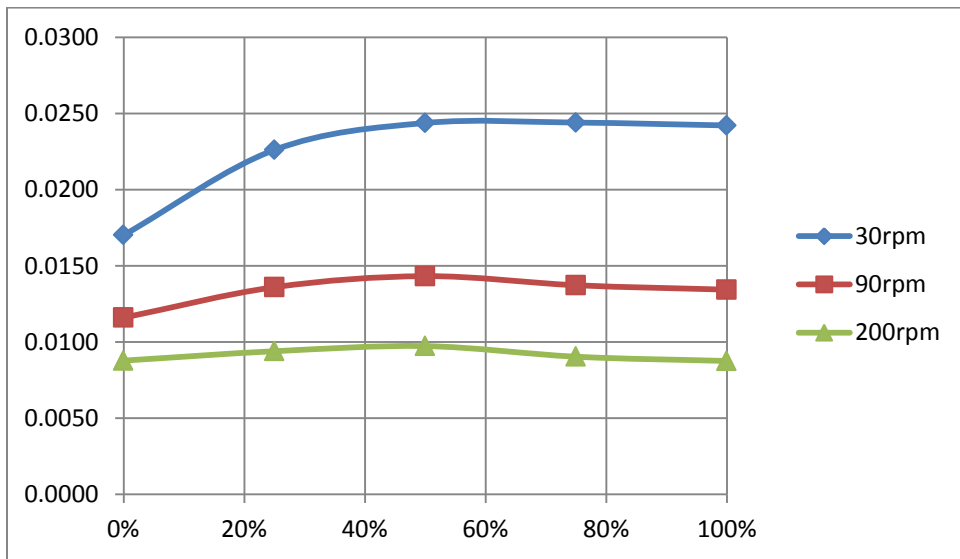


Figure 4.2. Apparent viscosity (Pa·s) vs. PAM weight fraction for the PAM-CMC system (total concentration: 500 ppm)

The power law parameters k and n are characteristic for each solution. They are used in the following equation, where η is the apparent viscosity and γ is the shear rate. The flow behavior index, n , indicates the degree of non-Newtonian behavior of the fluid. The flow consistency index, k , indicates the viscosity level at a certain shear rate of the fluid.

$$\eta = k \cdot \gamma^{n-1} \quad (4.1)$$

For a Newtonian fluid, n is equal to 1, which means that shear rate does not affect the viscosity. However, for a non-Newtonian fluid, such as the polymer solutions in this research, n has values between zero and one. Therefore, shear rate plays a role in the calculation of the apparent viscosity of the polymer solutions. In fact, as n increases, the shear rate makes a bigger contribution to the apparent viscosity.

In Figure 4.3, the power law parameter n decreases with increasing PAM weight fraction. This means that as the PAM weight fraction increases, the polymer solutions deviate more from the Newtonian fluid behavior. In Figure 4.4, the power law parameter k increases as the PAM weight fraction increases. This is because the viscosity of PAM is higher than that of CMC. Therefore, under the same shear rate, the apparent viscosity of the mixed polymer solutions increases as the PAM weight fraction increases.

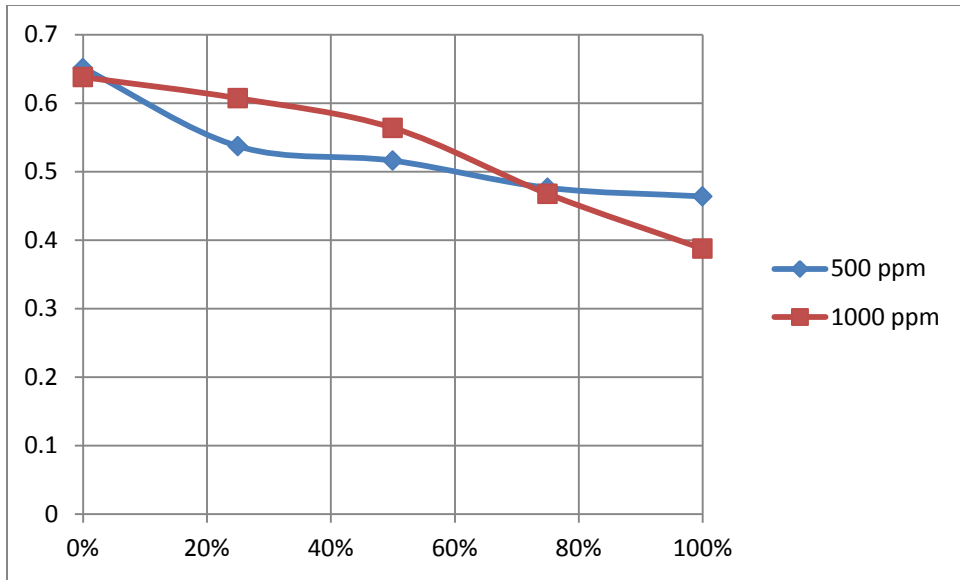


Figure 4.3. Power law parameter n vs. PAM weight fraction for the PAM-CMC system (total concentration: 500 ppm and 1000 ppm)

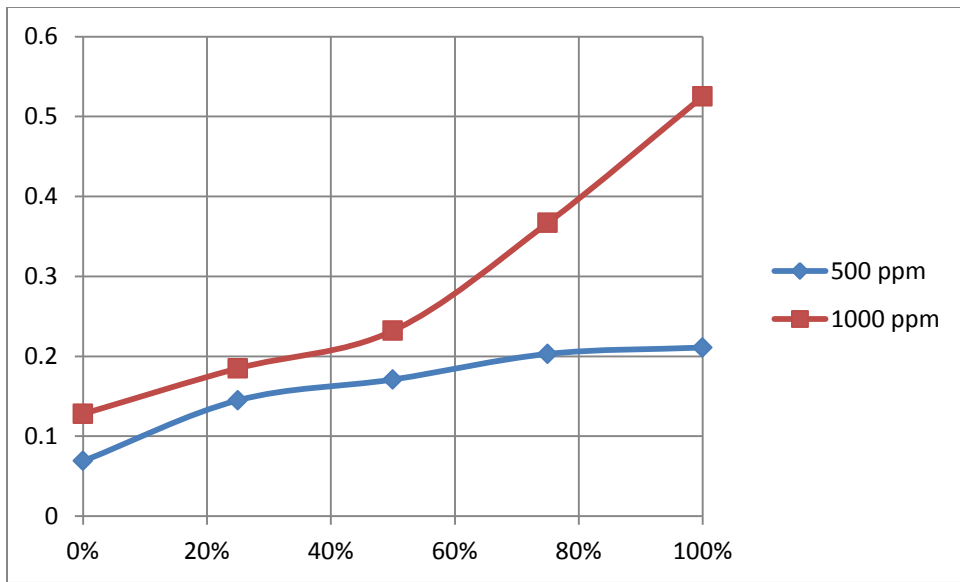


Figure 4.4. Power law parameter k vs. PAM weight fraction for the PAM-CMC system (total concentration: 500 ppm and 1000 ppm)

4.1.2. Surface tension

Typically surface tension is not used to study the polymer-polymer interaction. In this study, both PAM and CMC are not surface active. Measuring the surface tension of the PAM-CMC solutions with different concentrations and compositions may not provide useful information about the interaction between PAM and CMC.

In Figure 4.5, the surface tension of the PAM-CMC solutions at 500ppm level remains almost the same, while at 1000ppm level the surface tension drops slightly when the PAM weight fraction approaches 100%. This means that the surface tension is negatively affected only when the PAM concentration is very high (1000ppm) and the solution almost turns into pure PAM solution. Therefore, it is difficult to make any conclusions about the interaction between PAM and CMC from these data.

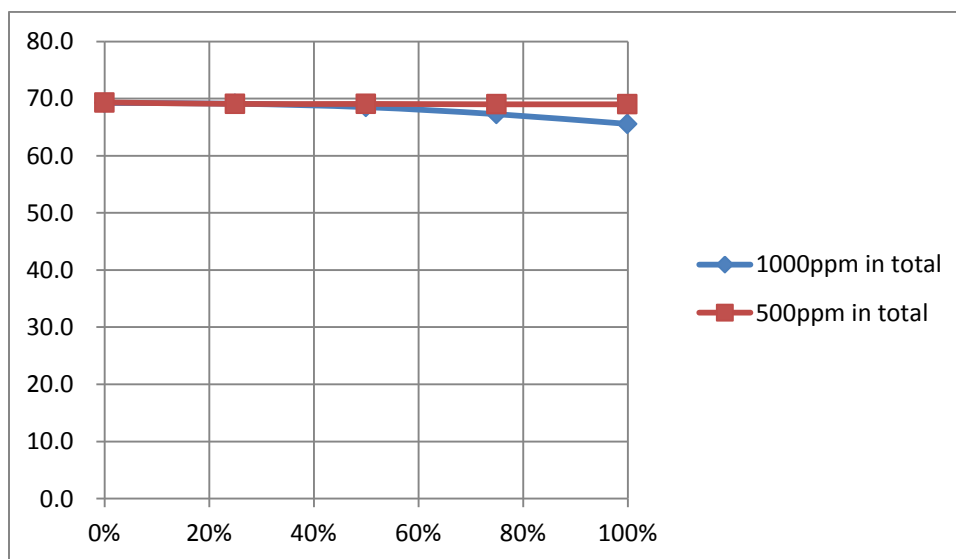


Figure 4.5. Surface tension (Dynes/cm) vs. PAM weight fraction for the PAM-CMC system

4.1.3. Conductivity

Conductivity is not commonly used to study the interaction between polymers. However, the conductivity is measured here as some polymers used in this research are ionic. Both PAM and CMC are anionic and water-soluble. In theory, these two polymers should repel each other, and the conductivity should be dictated by the total concentration and the degree of ionization of PAM and CMC.

In Figure 4.6, the conductivity almost remains constant and increases slightly only when the PAM weight fraction approaches 100%. This means that the PAM and CMC used in this research have almost the same degree of ionization. Therefore, as long as the total concentrations of the polymers in the solutions are the same, the conductivity of these solutions should be almost the same. In addition, the 1000ppm curve is higher than the 500ppm curve because higher total concentration leads to higher conductivity.

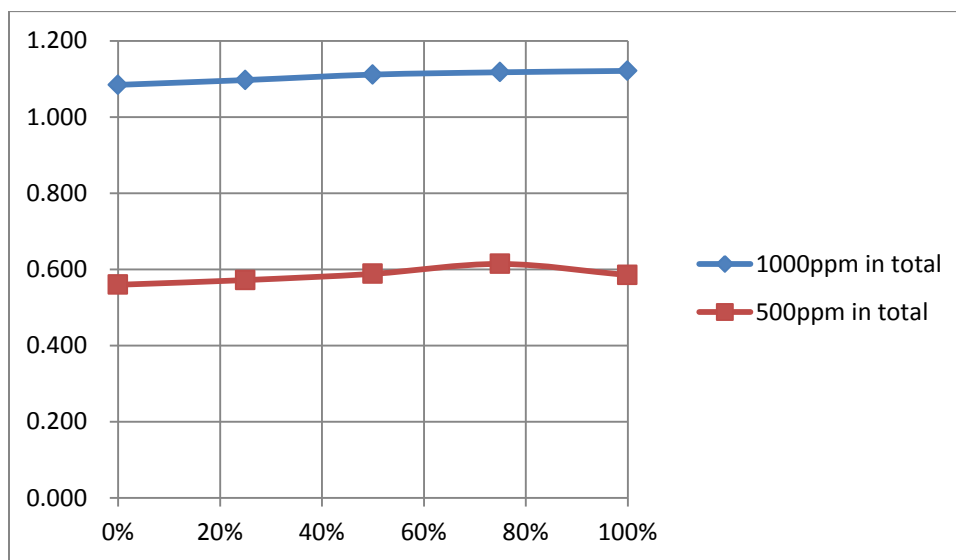


Figure 4.6. Conductivity ($\mu\text{s}/\text{cm}$) vs. PAM weight fraction for the PAM-CMC system

4.2. Flow loop experiment result

4.2.1. Experiments in 1.5-inch pipeline

In Figures 4.7 and 4.8, the friction factor is plotted against generalized Reynolds number and in all cases the friction factor decreases as the generalized Reynolds number increases. In a previous study of this group, both PAM and CMC demonstrated drag reduction effect when dissolved in water. It can be seen in Figures 4.7 and 4.8 that PAM has stronger drag reduction effect than CMC since the friction factor of the pure PAM curve is lower than that of the pure CMC curve.

For the five solutions with total concentration of 500ppm (Figure 4.8), the friction factor decreases in the order of CMC 500-PAM 0, CMC 375-PAM 125, CMC 250-PAM 250, CMC 125-PAM 375, CMC 0-PAM 500. This means that as the PAM weight fraction increases, the friction factor decreases, and therefore, the drag reduction effect strengthens. This predictable drag reduction behavior suggests that the synergy between PAM and CMC, if there is any, does not enhance the drag reduction effect of the mixed PAM-CMC solutions at the 500ppm level.

However, the five solutions with total concentration of 1000ppm (Figure 4.7) demonstrate a different drag reduction behavior. The pure PAM solution still has stronger drag reduction effect than the pure CMC solution. Now the drag reduction effect in the case of pure PAM solution is not the strongest. In fact, the CMC 500-PAM 500 solution has the strongest drag reduction effect, which can also be seen in Figures 4.9 and 4.11. This means that the synergy between PAM and CMC enhance the drag reduction effect at the 1000ppm level. This behavior coincides with the viscosity behavior shown in Figure 4.1, where the CMC 500-PAM 500 solution has higher viscosity than the pure PAM solution and the pure CMC solution.

In Figures 4.9 and 4.10, the percent drag reduction (%DR) is plotted against the generalized Reynolds number. In the calculation of the percent drag reduction here, the f_{solvent} is calculated from the Blasius equation which represents the turbulent flow of the pure solvent. It can be seen in Figure 4.10 that the percent drag reduction at 500ppm level increases in the order of CMC 500-PAM 0, CMC 375-PAM 125, CMC 250-PAM 250, CMC 125-PAM 375, CMC 0-PAM 500.

This indicates that as the PAM weight fraction increases, the drag reduction effect at 500ppm level also increases.

However, in Figure 4.9, the percent drag reduction at 1000ppm level increases in the order of CMC 1000-PAM 0, CMC 250-PAM 750, CMC 750-PAM 250, CMC 0-PAM 1000, CMC 500-PAM 500. The curves of CMC 250-PAM 750, CMC 750-PAM 250 and CMC 0-PAM 1000 are close to each other, while the CMC 500-PAM 500 curve is obviously higher than the other curves. This means that compared with pure PAM solution or pure CMC solution, mixing PAM and CMC (1:1) leads to enhanced drag reduction effect at 1000ppm level.

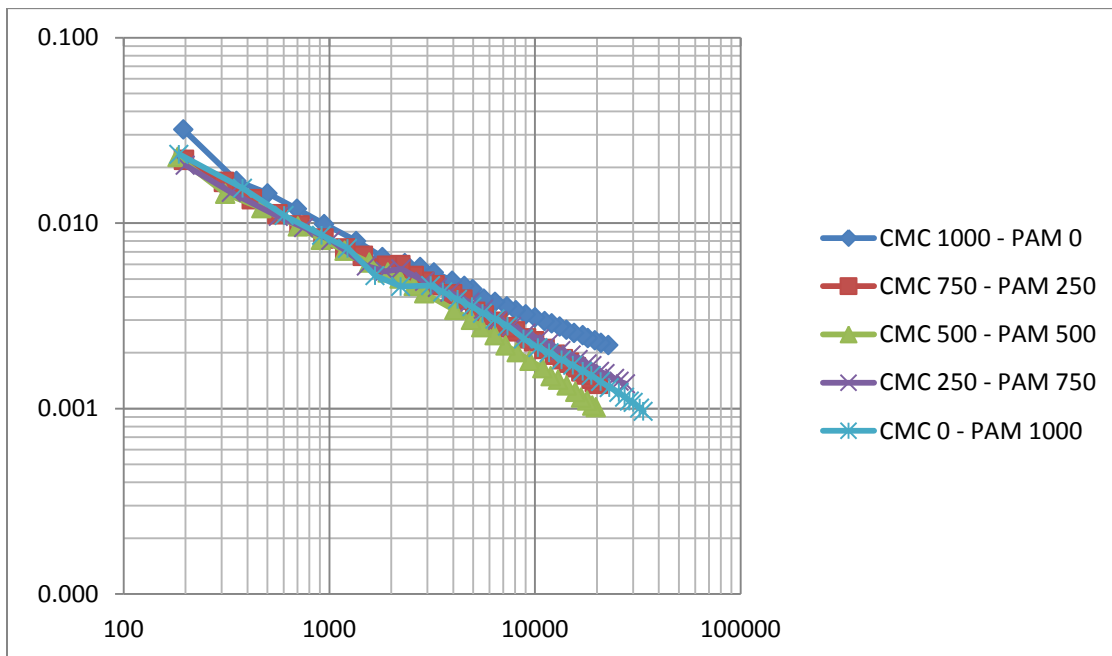


Figure 4.7. Friction factor vs. Re_g for the PAM-CMC system (1000ppm) in 1.5-inch pipe

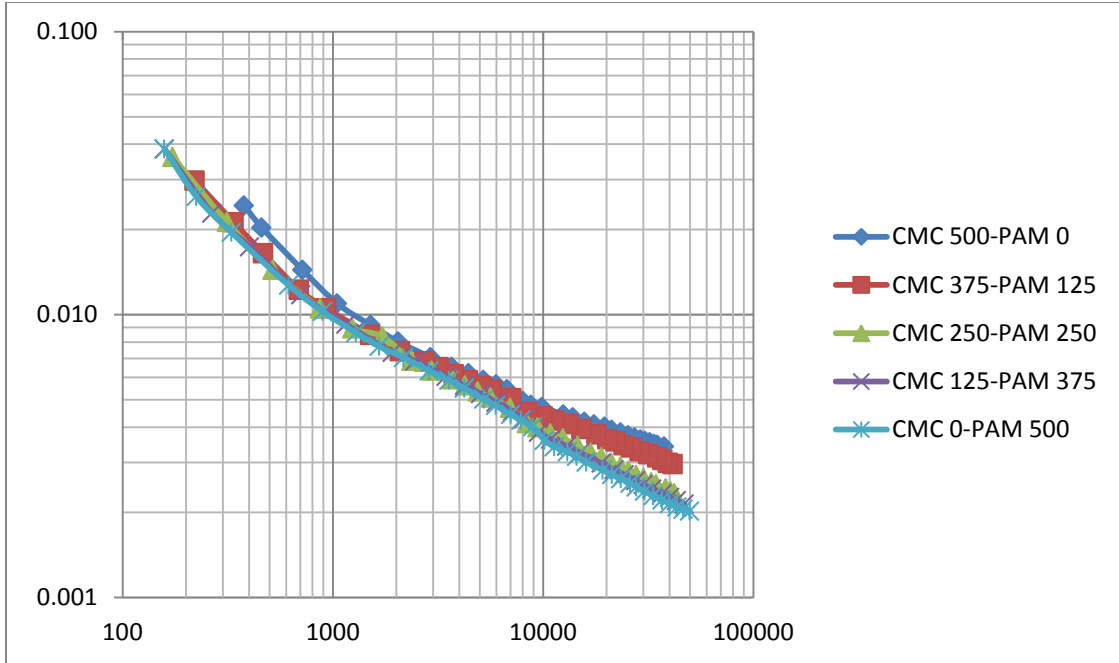


Figure 4.8. Friction factor vs. Re_g for the PAM-CMC system (500ppm) in 1.5-inch pipe

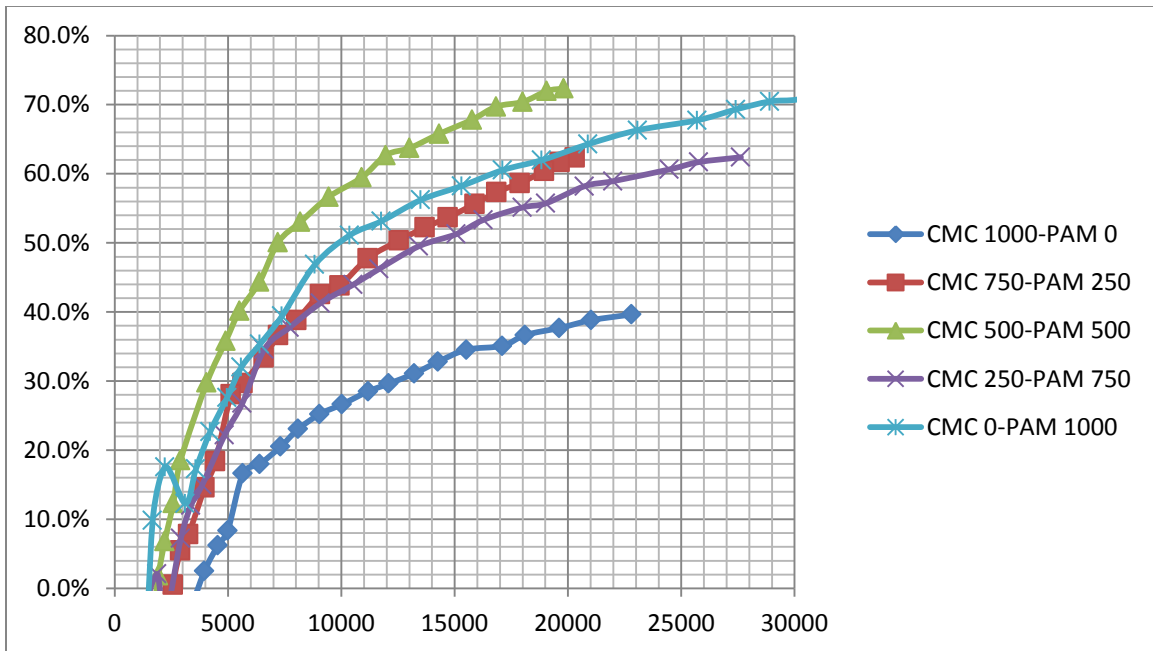


Figure 4.9. %DR vs. Re_s for the PAM-CMC system (1000ppm in total) in 1.5-inch pipe (compared with Blasius equation)

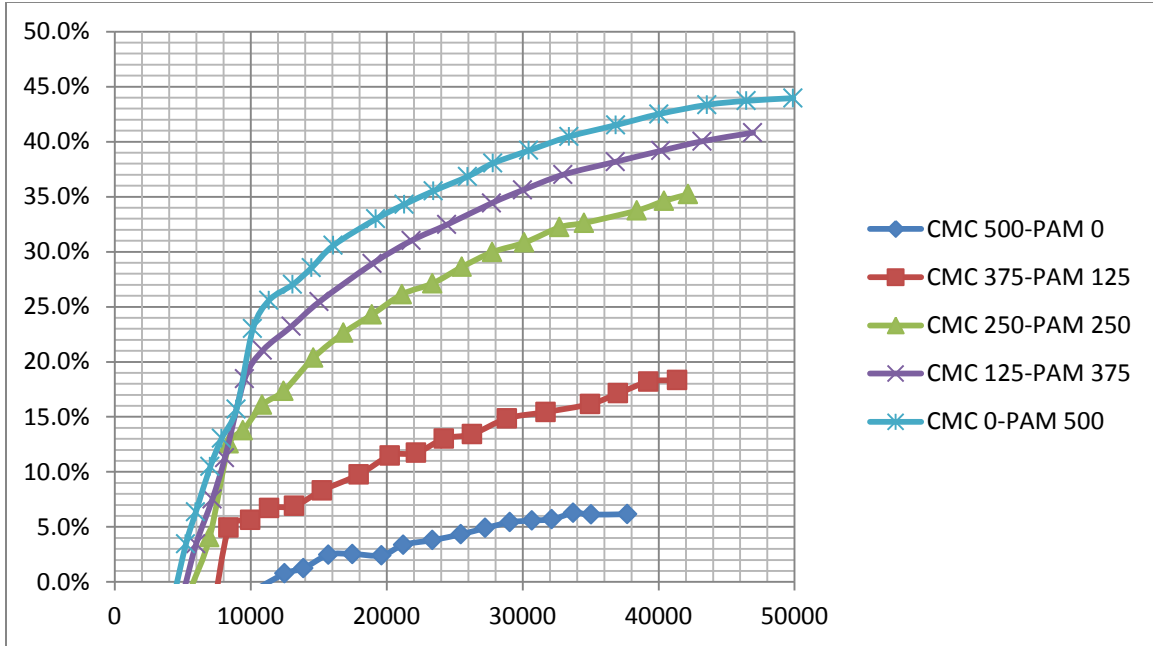


Figure 4.10. %DR vs. Re_s for the PAM-CMC system (500ppm in total) in 1.5-inch pipe (compared with Blasius equation)

In Figures 4.11 and 4.12, the percent drag reduction (%DR) is plotted against the generalized Reynolds number. In the calculation of the percent drag reduction here, the f_s is calculated from the Dodge-Metzner equation which represents the turbulent flow of non-Newtonian fluid. In Figure 4.12, the percent drag reduction at 500ppm level increases in the order of CMC 375-PAM 125, CMC 500-PAM 0, CMC 125-PAM 375, CMC 250-PAM 250, CMC 0-PAM 500. The pure PAM solution (CMC 0-PAM 500) still has the strongest drag reduction effect. But the positions of the CMC 375-PAM 125 and CMC 500-PAM 0 curves are switched. This may be due to the different methods used to calculate f_s .

In Figure 4.11, the percent drag reduction at 1000ppm level increases in the order of CMC 1000-PAM 0, CMC 0-PAM 1000, CMC 250-PAM 750, CMC 750-PAM 250, CMC 500-PAM 500. In this figure, all mixed polymer solutions have stronger drag reduction effect than the pure polymer solutions. This means that the mixed polymer solutions deviate more from the Dodge-Metzner equation, which can also be seen in Figure 4.13.

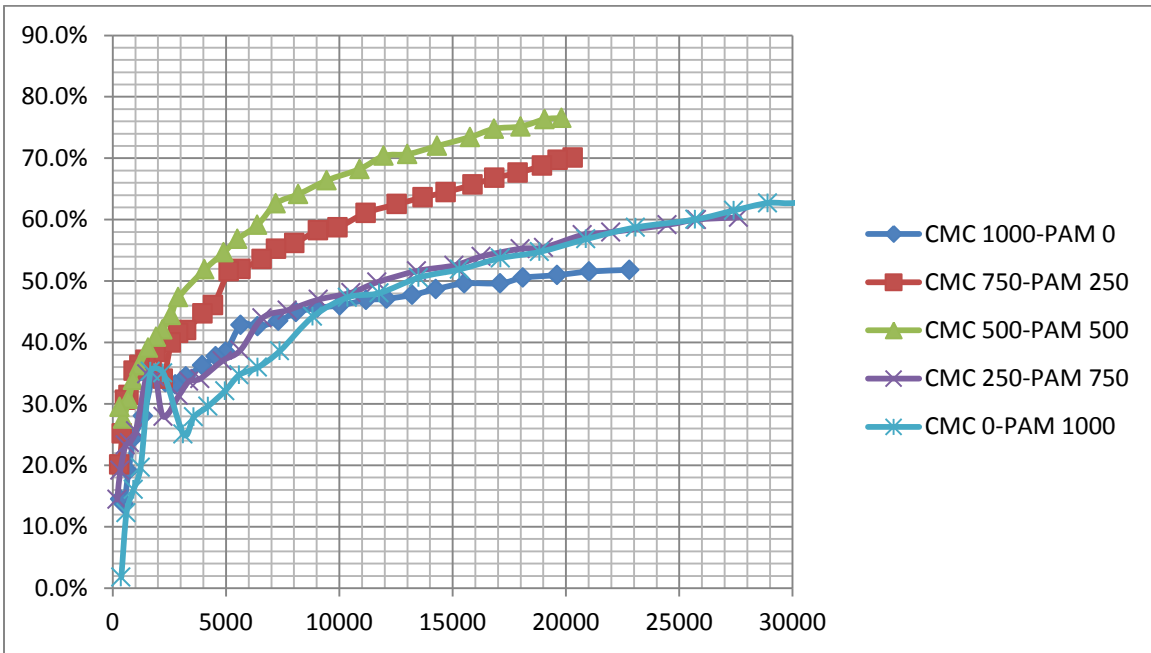


Figure 4.11. %DR vs. Re_g for the PAM-CMC system (1000ppm in total) in 1.5-inch pipe (compared with Dodge-Metzner equation)

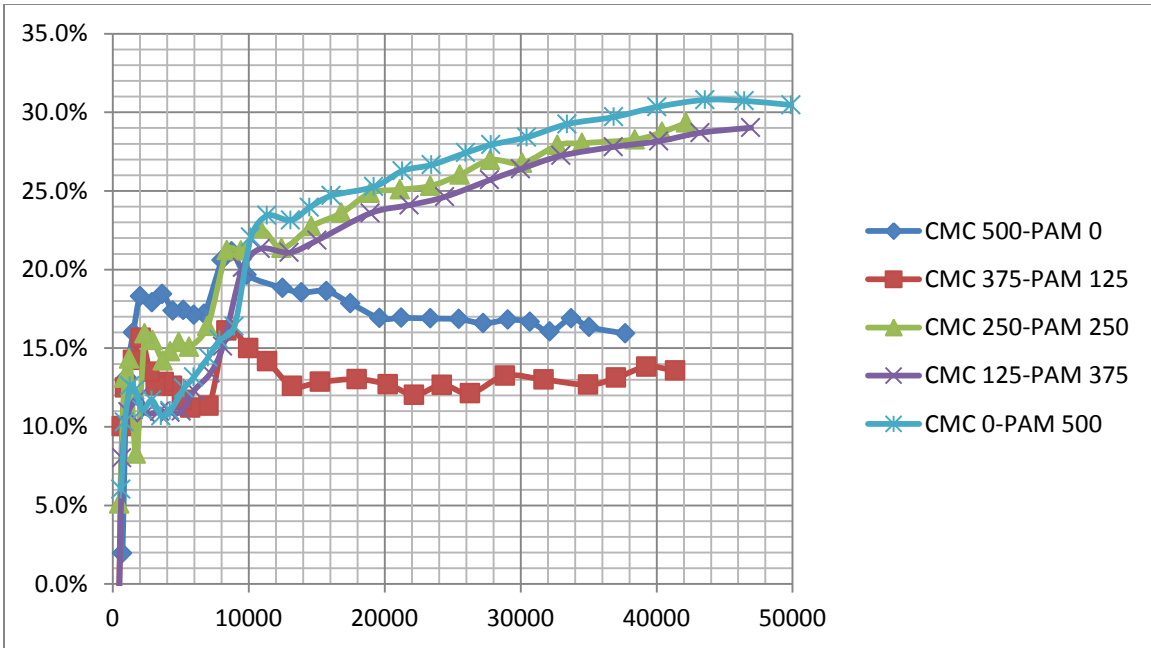


Figure 4.12. %DR vs. Re_g for the PAM-CMC system (500ppm in total) in 1.5-inch pipe (compared with Dodge-Metzner equation)

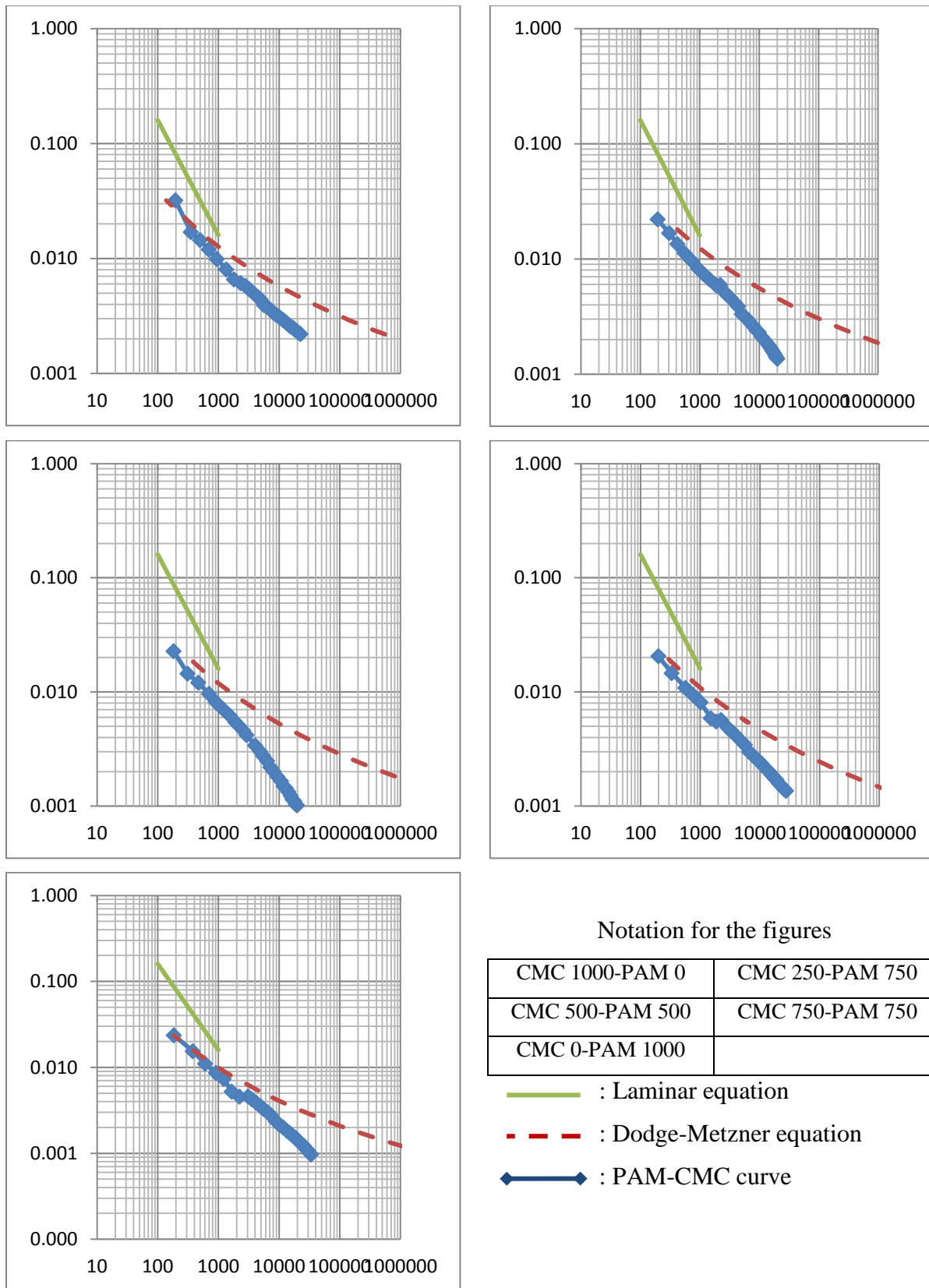


Figure 4.13. Friction factor vs. Re_g for the PAM-CMC system (1000ppm) in 1.5 inch pipe

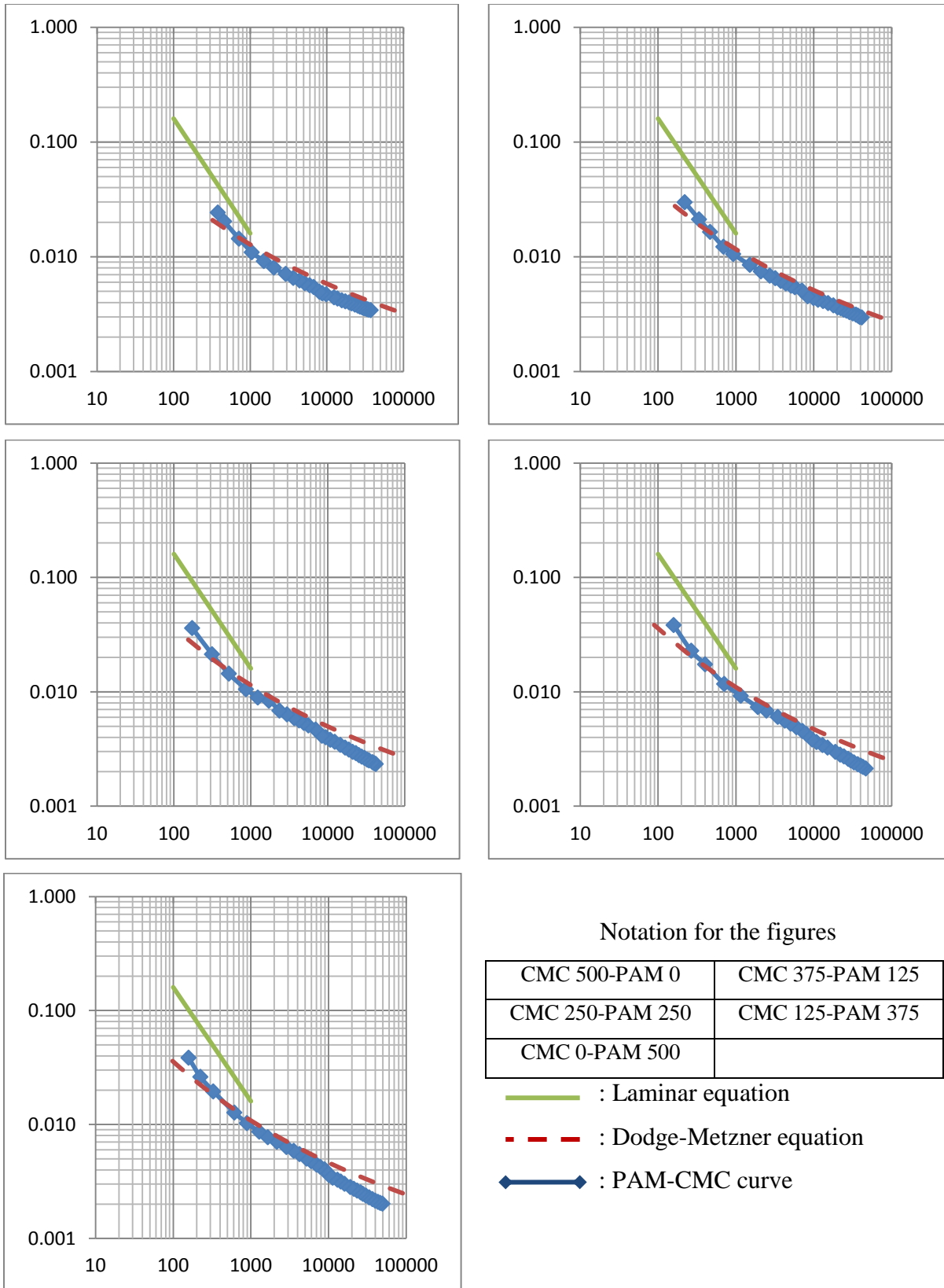


Figure 4.14. Friction factor vs. Re_g for the PAM-CMC system (500ppm) in 1.5 inch pipe

4.2.2. Experiments in 1-inch pipeline

The experiments in Figures 4.15 and 4.16 are carried out in the 1-inch pipe. Similarly, the friction factors of all curves decrease as the generalized Reynolds number increases. It can be seen in Figures 4.15 and 4.16 that PAM has stronger drag reduction effect than CMC since the friction factor of the pure PAM curve is lower than that of the pure CMC curve.

For the five solutions with total concentration of 500ppm (Figure 4.16), the friction factor decreases in the order of CMC 500-PAM 0, CMC 375-PAM 125, CMC 250-PAM 250, CMC 125-PAM 375, CMC 0-PAM 500. This means that as the PAM weight fraction increases, the friction factor decreases, and therefore, the drag reduction effect strengthens. Figure 4.18 also exhibits this trend clearly. This predictable drag reduction behavior suggests that the synergy between PAM and CMC, if there is any, does not enhance the drag reduction effect of the mixed PAM-CMC solutions at 500ppm level.

However, the five solutions with total concentration of 1000ppm (Figure 4.15) demonstrate a different drag reduction behavior. The pure PAM solution still has stronger drag reduction effect than the pure CMC solution. However, the drag reduction effect of the pure PAM solution is not the strongest. In fact, the CMC 500-PAM 500 solution and the CMC 750-PAM 250 solution have stronger drag reduction effect than the pure PAM solution. This means that the synergy between PAM and CMC enhance the drag reduction effect at 1000ppm level. This behavior coincides with the viscosity behavior shown in Figure 4.1, where the CMC 500-PAM 500 solution has higher viscosity than the pure PAM solution or the pure CMC solution.

In Figures 4.17 and 4.18, the percent drag reduction (%DR) is plotted against the generalized Reynolds number. In the calculation of the percent drag reduction here, the f_s is calculated from the Blasius equation which represents the turbulent flow of the pure solvent. It can be seen in Figure 4.18 that the percent drag reduction at 500ppm level increases in the order of CMC 500-PAM 0, CMC 375-PAM 125, CMC 250-PAM 250, CMC 125-PAM 375, CMC 0-PAM 500.

This indicates that as the PAM weight fraction increases, the drag reduction effect at 500ppm level also increases.

However, in Figure 4.17, the percent drag reduction at 1000ppm level increases in the order of CMC 1000-PAM 0, CMC 250-PAM 750, CMC 750-PAM 250, CMC 0-PAM 1000, CMC 500-PAM 500. The curves of CMC 500-PAM 500, CMC 750-PAM 250 and CMC 0-PAM 1000 are very close to each other, while the CMC 250-PAM 750 curve and the CMC 1000-PAM 0 curve are obviously lower than the other curves. This means that the mixed polymer solutions (CMC 500-PAM 500, CMC 750-PAM 250) can achieve almost the same drag reduction effect as the pure PAM solution.

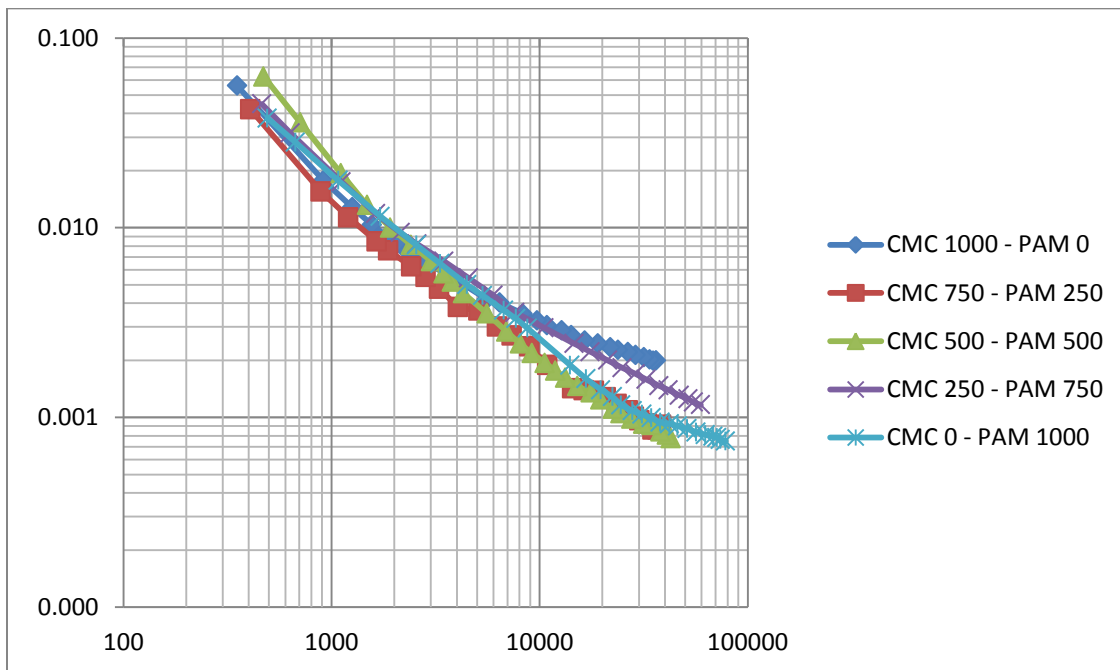


Figure 4.15. Friction factor vs. Re_g for the PAM-CMC system (1000ppm in total) in 1-inch pipe

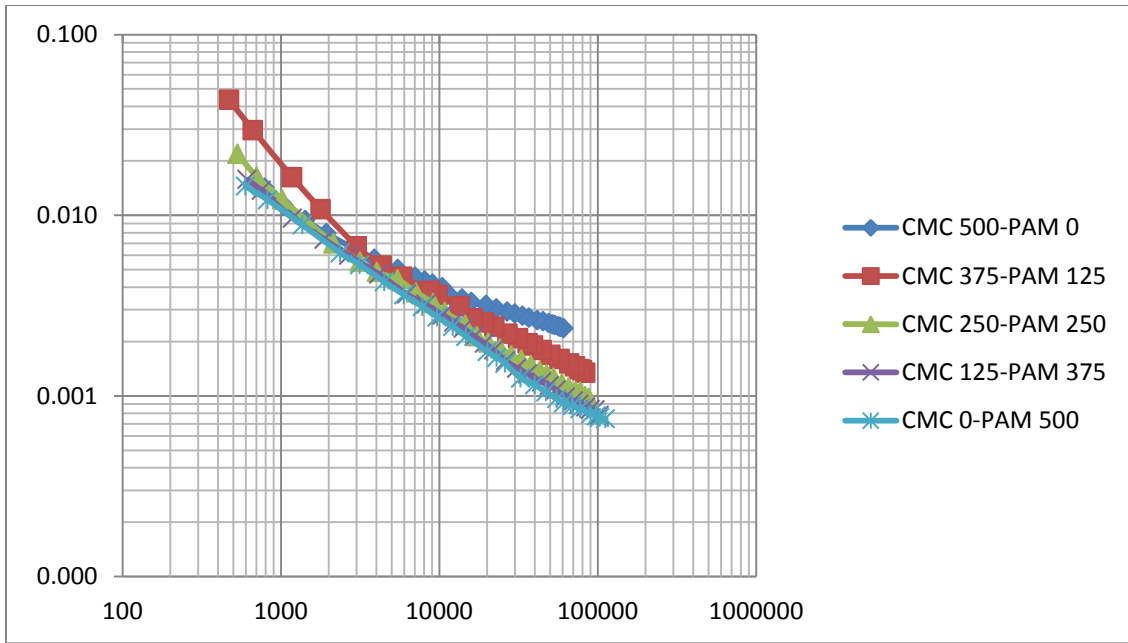


Figure 4.16. Friction factor vs. Re_g for the PAM-CMC system (500ppm in total) in 1-inch pipe

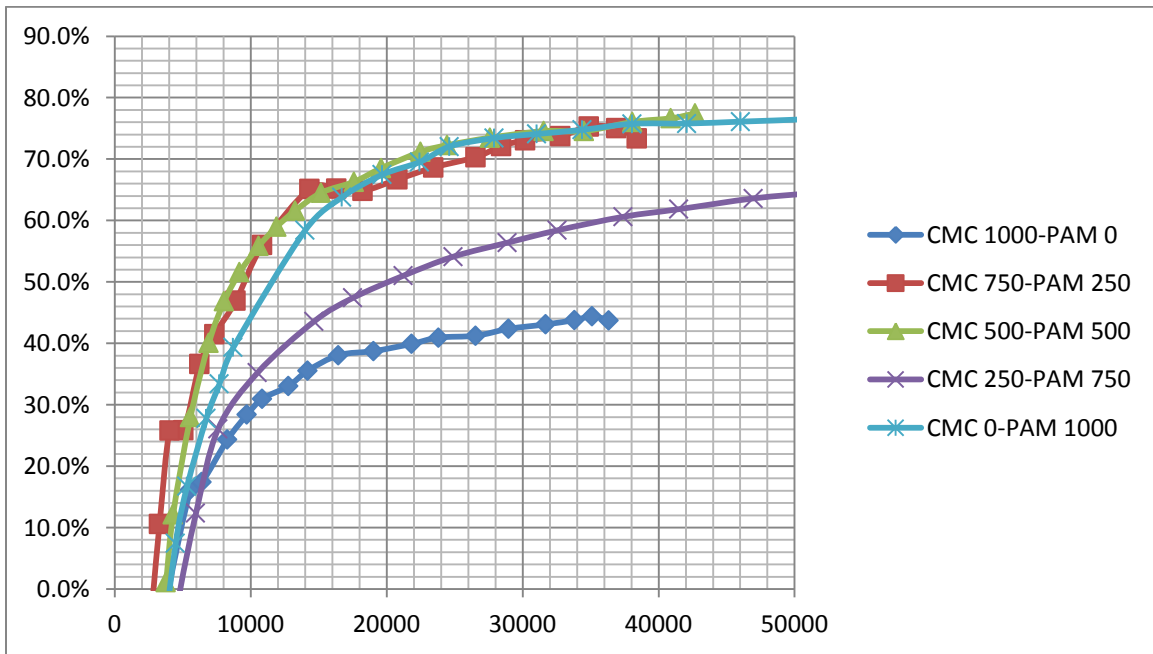


Figure 4.17. %DR vs. Re_s for the PAM-CMC system (1000ppm in total) in 1-inch pipe
(compared with Blasius equation)

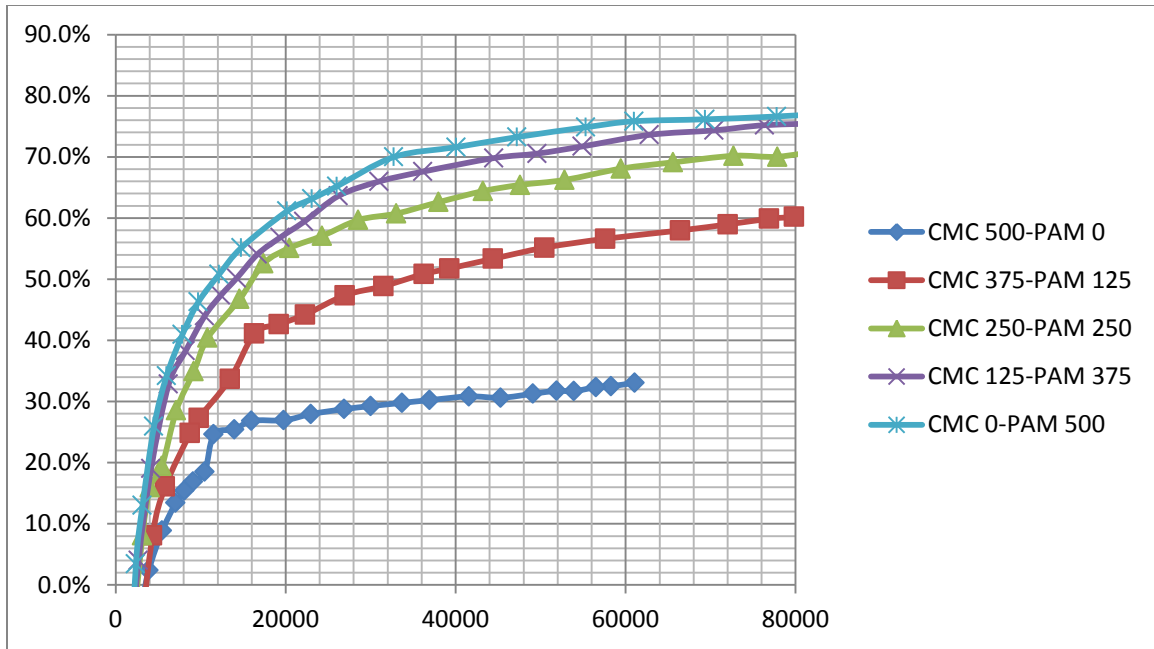


Figure 4.18. %DR vs. Re_s for the PAM-CMC system (500ppm in total) in 1-inch pipe (compared with Blasius equation)

In Figures 4.19 and 4.20, the percent drag reduction (%DR) is plotted against the generalized Reynolds number. In the calculation of the percent drag reduction here, the f_s is calculated from the Dodge-Metzner equation which represents the turbulent flow of non-Newtonian fluid. In Figure 4.20, the percent drag reduction at 500ppm level increases in the order of CMC 500-PAM 0, CMC 375-PAM 125, CMC 250-PAM 250, CMC 125-PAM 375, CMC 0-PAM 500, which it is also shown in Figure 4.22. This predictable drag reduction behavior indicates that at 500ppm level the drag reduction effect is a function of PAM weight fraction. The synergy between PAM and CMC, if there is any, does not enhance the drag reduction effect of the mixed PAM-CMC solutions at 500ppm level.

In Figure 4.19, the percent drag reduction at 1000ppm level increases in the order of CMC 250-PAM 750, CMC 1000-PAM 0, CMC 0-PAM 1000, CMC 750-PAM 250, CMC 500-PAM 500. In this figure, the mixed polymer solutions (CMC 750-PAM 250, CMC 500-PAM 500) have stronger drag reduction effect than the pure polymer solutions. This means that the mixed polymer solutions deviate more from the Dodge-Metzner equation, which can also be seen in Figure 4.21.

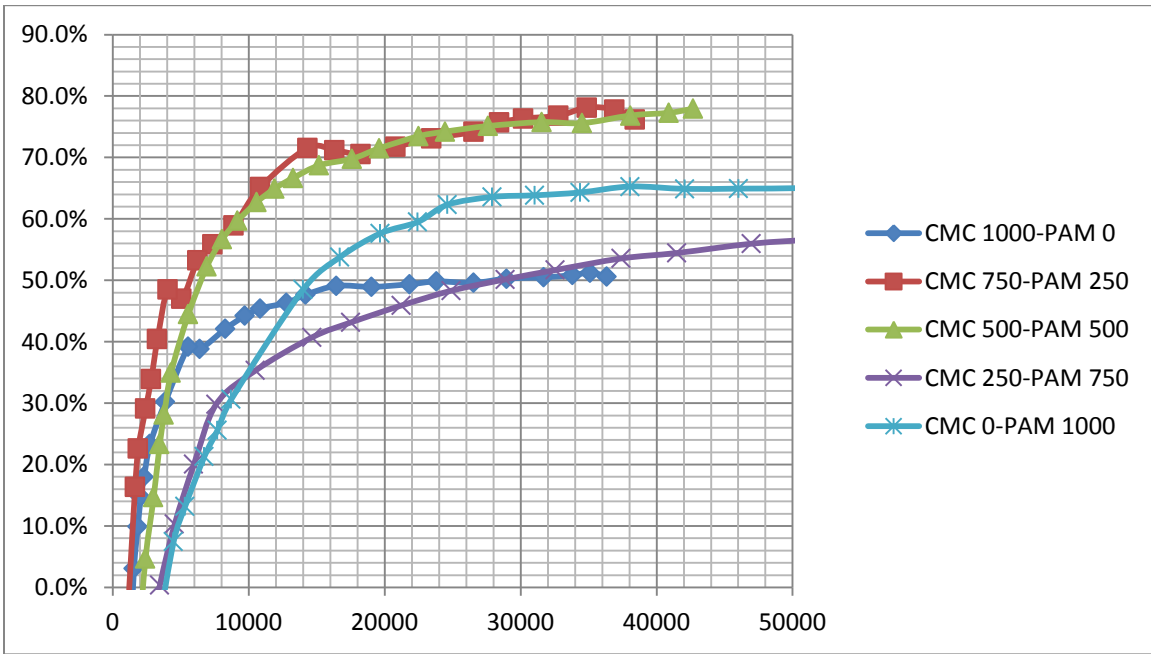


Figure 4.19. %DR vs. Re_g for the PAM-CMC system (1000ppm in total) in 1-inch pipe compare (compared with Dodge-Metzner equation)

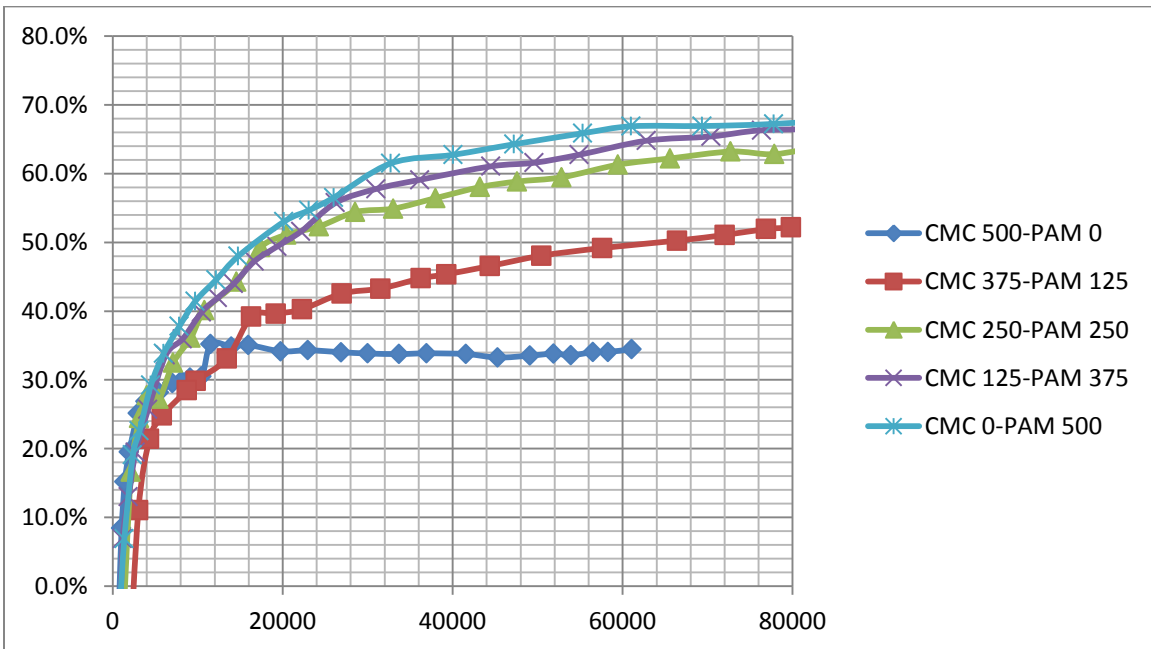


Figure 4.20. %DR vs. Re_g for the PAM-CMC system (500ppm in total) in 1-inch pipe (compared with Dodge-Metzner equation)

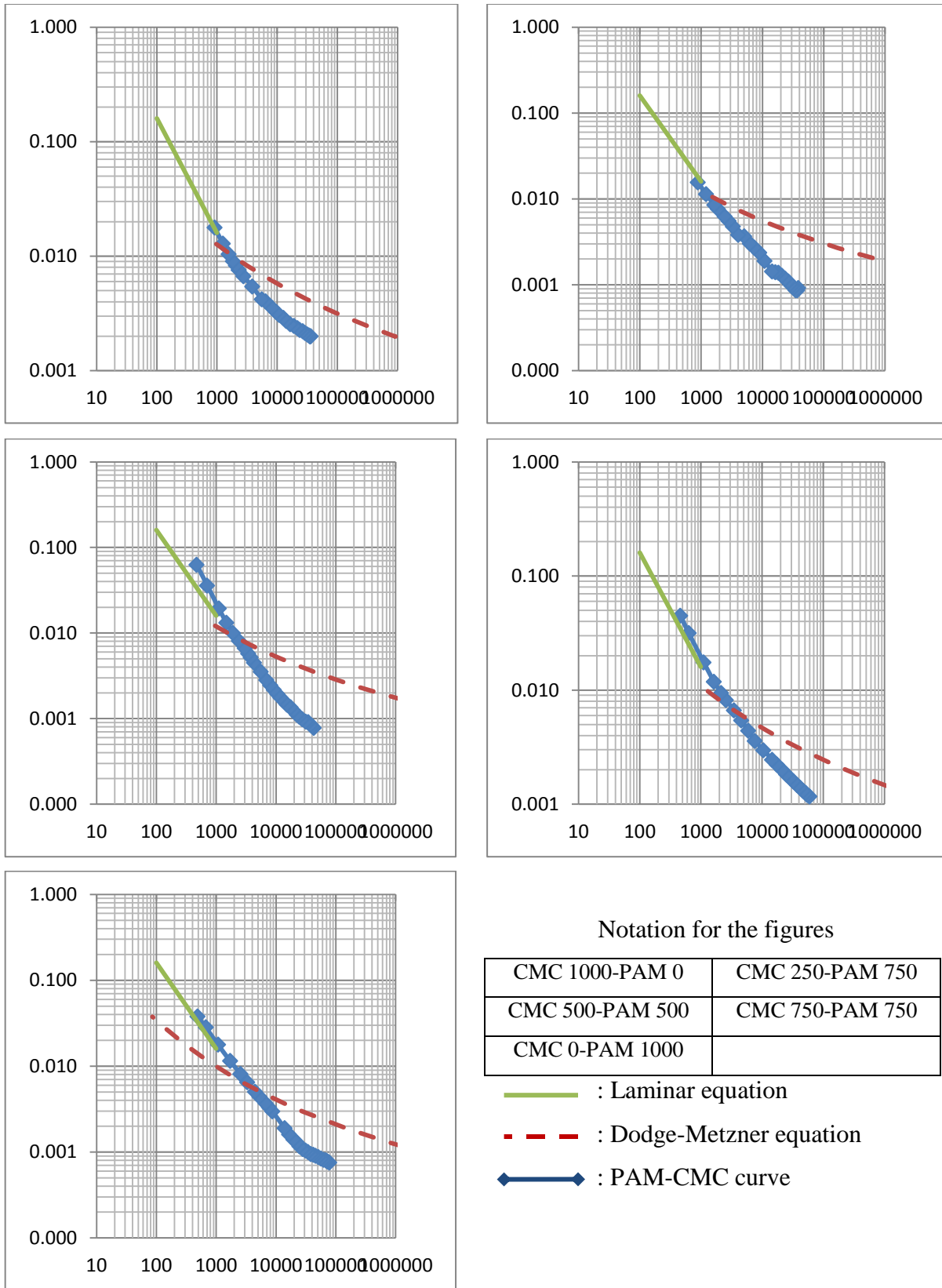


Figure 4.21. Friction factor vs. Re_g for the PAM-CMC system (1000ppm) in 1 inch pipe

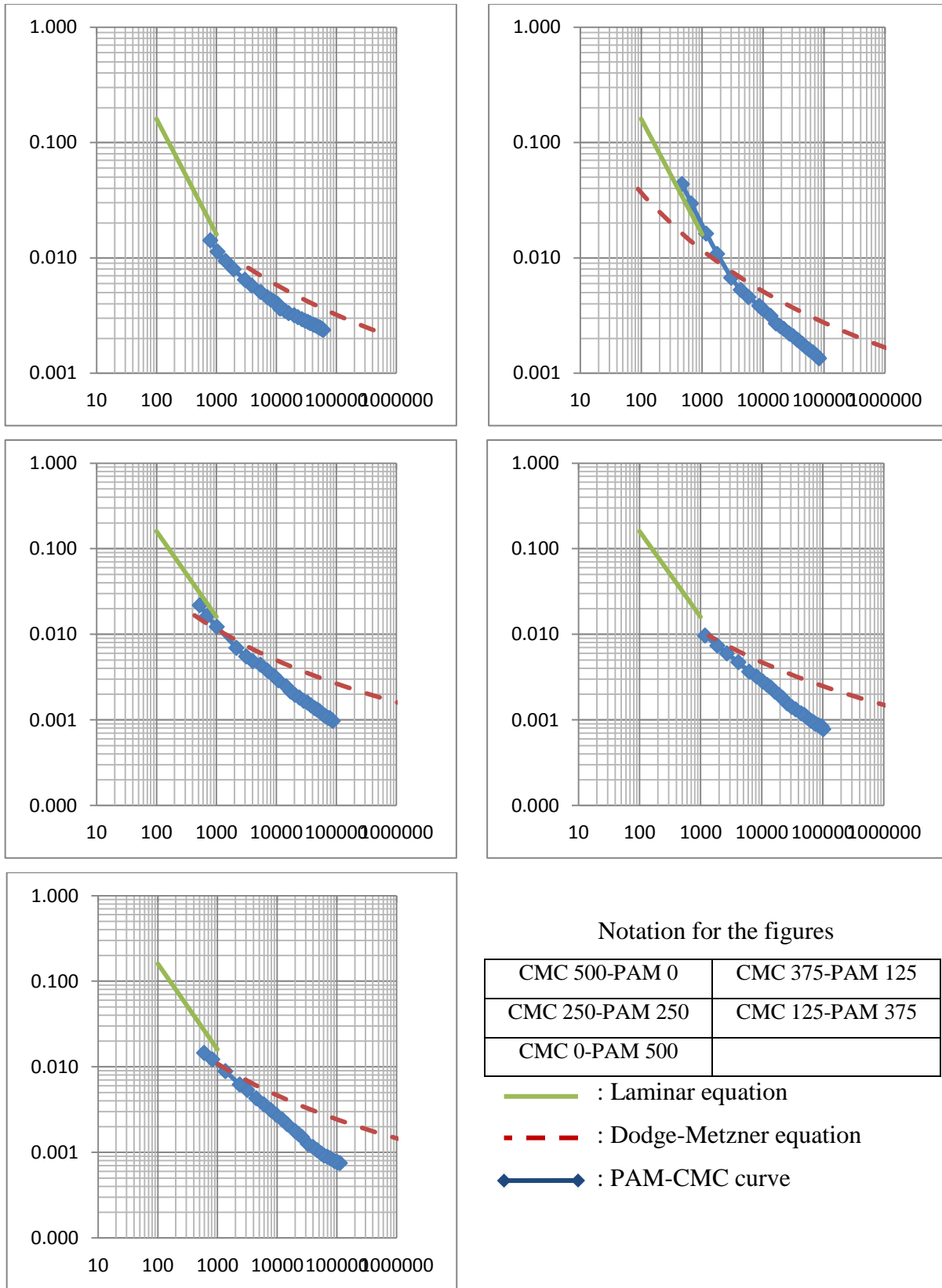


Figure 4.22. Friction factor vs. Re_g for the PAM-CMC system (500ppm) in 1 inch pipe

4.3. Conclusion

In summary, the solutions with total concentration of 500ppm do not show any enhanced drag reduction effect in both 1-inch pipe and 1.5-inch pipe. At the 500ppm level the drag reduction effect is determined by the PAM weight fraction. The drag reduction effect increases with increasing PAM weight fraction.

However, at the 1000ppm level, the mixed PAM-CMC solutions demonstrate enhanced drag reduction effect in both 1-inch pipe and 1.5-inch pipe. This enhancement is due to the synergy in the solutions between PAM and CMC chains. The PAM and CMC chains form an inter-entangled network of polymers, and thus, increase the viscosity of the solutions (Figure 4.1). The enhancement is also dependent on the total polymer concentration because at 1000ppm level the polymer concentration is high enough to form the polymer network, and therefore, suppressing the quasi-streamwise vortices. It is these streamwise vortices in the buffer layer that drive convective momentum transport, suppressing the vortices can lead to the drag reduction effect [50].

The curves in the 1-inch pipe (Figures 4.15 and 4.16) are more separate than those in the 1.5-inch pipe (Figures 4.7 and 4.8). This means that the change of polymer composition has a bigger impact on the friction in the 1-inch pipe than in the 1.5-inch pipe. This is possibly because the 1-inch pipe has bigger effective surface area, which means that a larger fraction of fluid is in contact with the pipeline inner surface. Therefore, the polymer in the 1-inch pipe has a more obvious impact on the interface between the pipeline and the fluid, and therefore, the friction.

Chapter 5. Drag Reduction Effect of PEO-CMC System

The drag reduction effect of the mixed PEO-CMC system is interesting to study. PEO is a linear polymer with large molecular weight, and it is a non-ionic polymer. PEO is weaker than CMC in terms of drag reduction effect. CMC is a water-soluble polymer and is widely used as anti-redeposition agent in many detergents. It is also used as anti-abrasion and dispersive additive in granular detergents. The drag reduction effect of the PEO-CMC system has not yet been studied before. The purpose of this study is to find out whether synergistic effect exists and whether it enhances the drag reduction effect.

In this study the total concentration of polymers added is fixed, and the weight fractions of PEO and CMC are varied. The following table (Table 5.1) shows the total concentration and the composition of the solutions prepared. The study is conducted at two levels of polymer concentrations: 1000ppm in total and 500ppm in total. At each level, five compositions are studied. These solutions with different compositions are tested in the flow loop and the bench-scale equipment.

Table 5.1. The total mass and weight fractions used in the experiments

Total mass	Weight fractions of CMC and PEO				
500 ppm	100% CMC	75% CMC	50% CMC	25% CMC	0% CMC
	0% PEO	25% PEO	50% PEO	75% PEO	100% PEO
1000 ppm	100% CMC	75% CMC	50% CMC	25% CMC	0% CMC
	0% PEO	25% PEO	50% PEO	75% PEO	100% PEO

To study the drag reduction effect of the PEO-CMC system, PEO and CMC are dissolved in water and mixed in the flow loop tank. All solutions are freshly prepared before use. The tank is maintained at $20\pm 0.5^\circ\text{C}$ by the thermo jacket. All the solutions are tested in the 1-inch pipe and the 1.5-inch pipe. Flow rate and pressure drop are monitored, recorded and transferred to the data processing system. Then the flow rate and the pressure drop data are converted into Reynolds number and friction factor.

5.1. Bench-scale experiment result

5.1.1. Viscosity

Viscosity is an important parameter in the study of drag reduction effect. Since the polymer solutions of this study are non-Newtonian fluids, the viscosity measured here is the apparent viscosity, which is a function of the shear rate. To be more specific, the polymer solutions in this study are shear-thinning fluids, which means that the apparent viscosity of the fluids decrease as the shear rate is increased.

In Figures 5.1 and 5.2, the apparent viscosity is plotted against the PEO weight fraction. Generally speaking, the apparent viscosity decreases with increasing PEO weight fraction. However, the viscosity does not decrease linearly as the PEO weight fraction increases. The viscosity remains almost the same as the PEO weight fraction increases from 0% to 25%, and then the viscosity decreases parabolically.

The viscosity of pure CMC solution is higher than that of pure PEO solution. Therefore, as the PEO weight fraction increases, the viscosity of the mixed solution should decrease. The plateau between 0% and 25% indicates that substitution of a small amount of CMC with PEO in the solution will not affect the viscosity at each shear rate. The parabolic decrease suggests that there is certain extent of synergy between CMC and PEO in the solution.

It is also noted that the maximum apparent viscosity of the mixed polymer solutions are no higher than the pure CMC solution (the viscosity of pure CMC solution is higher than that of pure PEO solution in this case), which is different from the PAM-CMC system. This suggests that the interaction between PEO and CMC in the solutions is weak. This phenomenon may affect the result of the flow loop experiments.

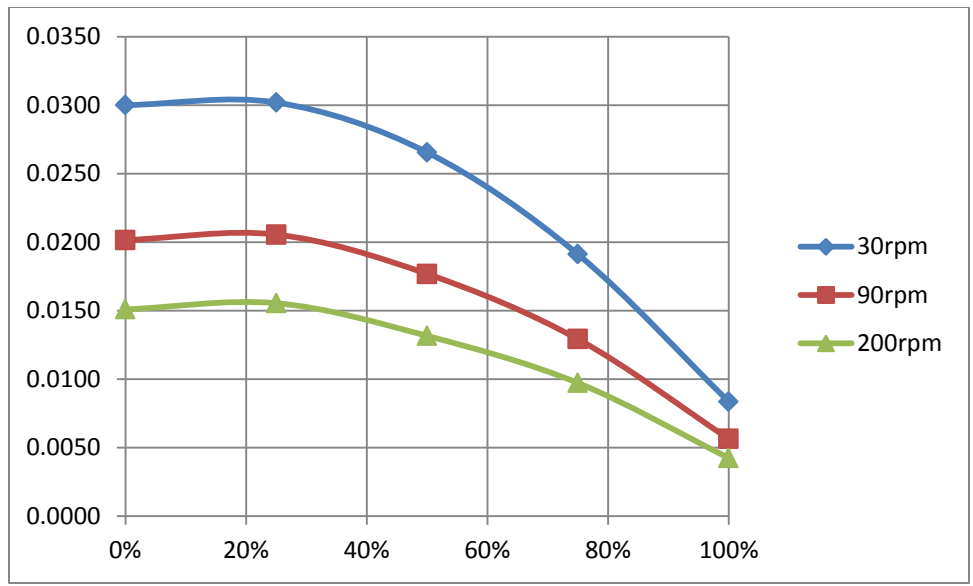


Figure 5.1. Apparent viscosity (Pa·s) vs. PEO weight fraction for the PEO-CMC system (1000 ppm in total)

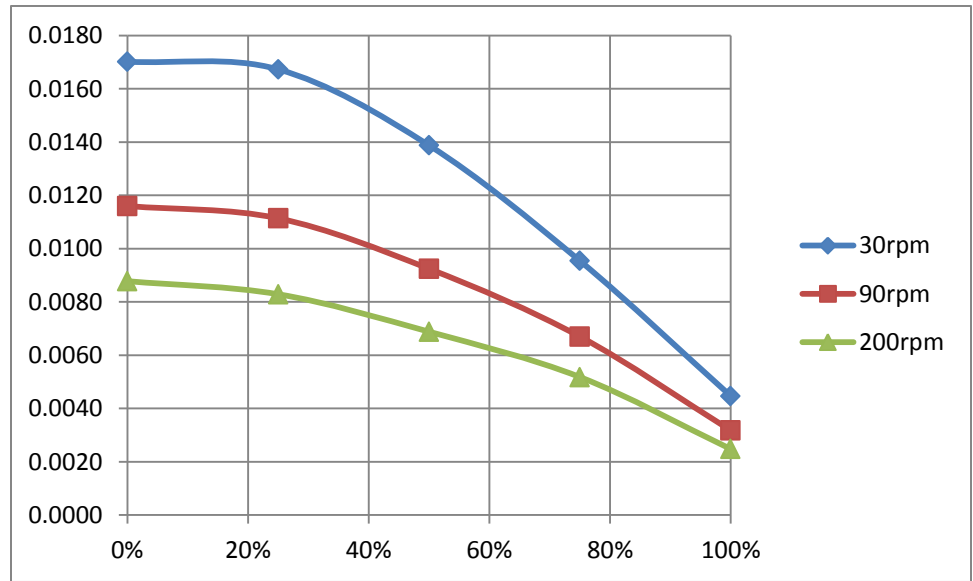


Figure 5.2. Apparent viscosity (Pa·s) vs. PEO weight fraction for the PEO-CMC system (500 ppm in total)

The power law parameters k and n are characteristic for each solution. They are used in the following equation, where η is the apparent viscosity and $\dot{\gamma}$ is the shear rate. The flow behavior index, n , indicates the degree of non-Newtonian behavior of the fluid. The flow consistency index, k , indicates the viscosity level at a certain shear rate of the fluid.

$$\eta = k \cdot \dot{\gamma}^{n-1} \quad (5.1)$$

For a Newtonian fluid, n is equal to 1, which means that shear rate does not affect the viscosity. However, for a non-Newtonian fluid, such as the polymer solutions in this research, n has values between zero and one. Therefore, shear rate plays a role in the calculation of the apparent viscosity of the polymer solutions. In fact, as n increases, the shear rate makes a bigger contribution to the apparent viscosity.

In Figure 5.3, the power law parameter n is almost independent of the PEO weight fraction. This means that as the PEO weight fraction increases, the polymer solutions maintain the same degree of non-Newtonian fluid behavior. In Figure 5.4, the power law parameter k decreases as the PEO weight fraction increases. This is because the viscosity of CMC is higher than that of PEO. However, the plateau between 0% and 25% indicates that substitution of a small amount of CMC with PEO in the solution does not affect the viscosity.

This phenomenon coincides with the surface tension decrease in Figure 5.5. The surface tension decreases dramatically from 0% to 25%, which means that in this range PEO gathers at the surface and does not enter the CMC network. That is why the power law meter k remains almost constant below 25% and then decreases as PEO weight fraction increases beyond 25%.

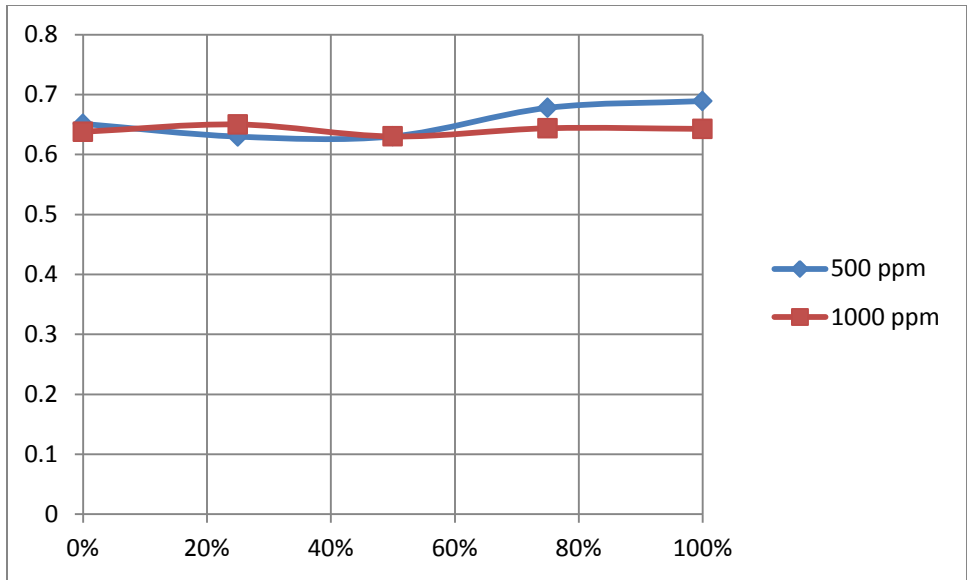


Figure 5.3. Power law parameter n vs. PEO weight fraction for the PEO-CMC system (total concentration: 500 ppm and 1000 ppm)

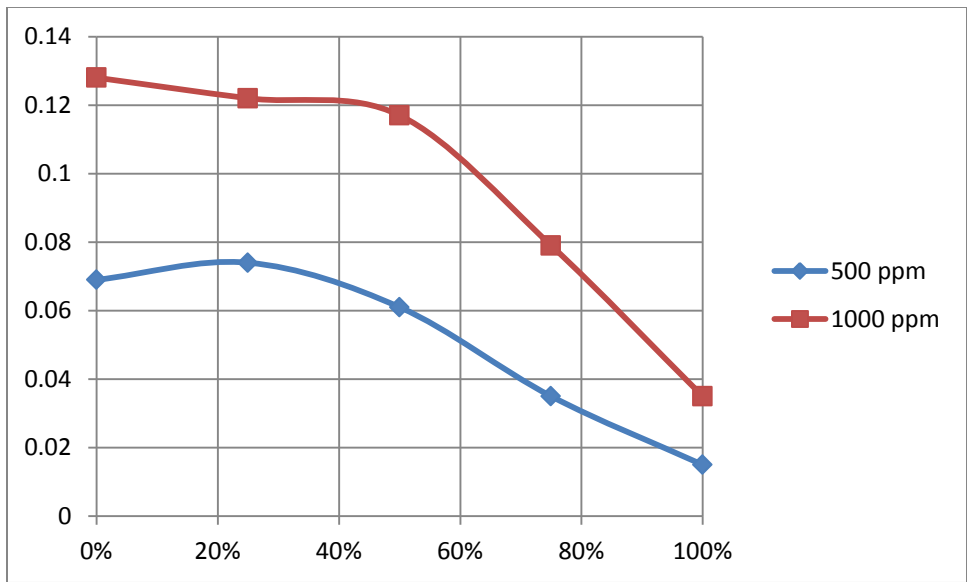


Figure 5.4. Power law parameter k vs. PEO weight fraction for the PEO-CMC system (total concentration: 500 ppm and 1000 ppm)

5.1.2. Surface tension

Typically surface tension is not used to study the polymer-polymer interaction. However, PEO is a surface active polymer with a minimum surface tension of 62 dynes/cm, while CMC is not surface active and does not cause a decrease in surface tension with increasing polymer concentration. Measuring the surface tension may allow for the determination of critical micelle concentration while other polymer is present.

In Figure 5.5, the surface tension decreases as the PEO weight fraction increases. However, the surface tension does not decrease linearly with the PEO weight fraction. The surface tension decreases dramatically as the PEO weight fraction increases from 0% to 25%. In this range PEO gathers at the surface and does not enter the CMC network. The surface tension decreases to about 59.5 dynes/cm initially, and then it slightly increases to about 60.5 dynes/cm. The surface tension of the CMC 500-PEO 500 solution is slightly lower than that of the pure PEO solution. This indicates that the interaction between PEO and CMC is not very strong.

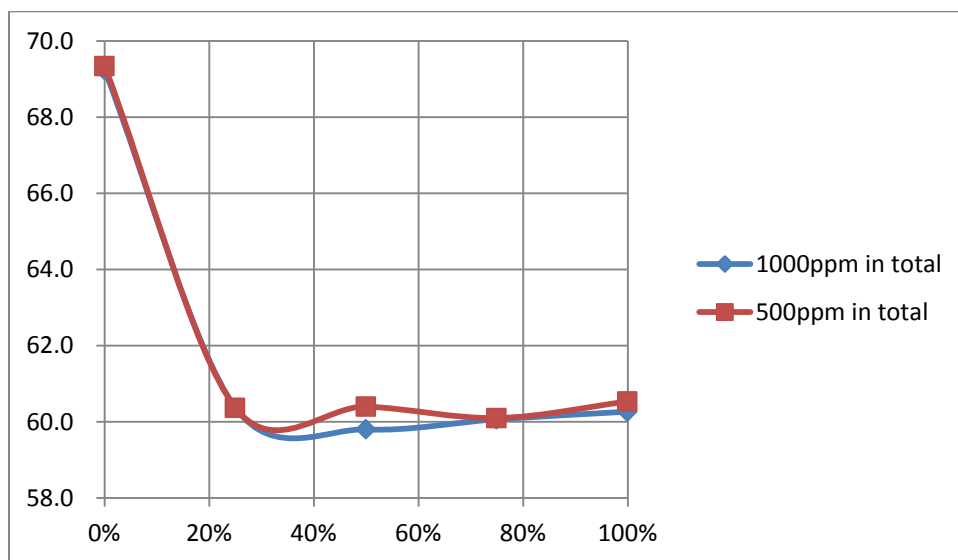


Figure 5.5. Surface tension (Dynes/cm) vs. PEO weight fraction for the PEO-CMC system

5.1.3. Conductivity

Conductivity is not commonly used to study the interaction between polymers. The conductivity is measured here as some polymers used in this research are ionic. In this study, CMC is an anionic and water-soluble polymer, while PEO is non-ionic. Therefore, it can be expected that the conductivity of the mixed solutions is dictated by the concentration of CMC in the solutions.

In Figure 5.6, the conductivity decreases linearly as the PEO weight fraction increases. The conductivity almost decreases to zero as the PEO weight fraction approaches 100%. This means that the PEO makes no contribution to the conductivity of the mixed solutions, and the conductivity is completely controlled by the CMC concentration. In addition, the 1000 ppm curve is higher than the 500 ppm curve since higher concentration of CMC leads to higher conductivity.

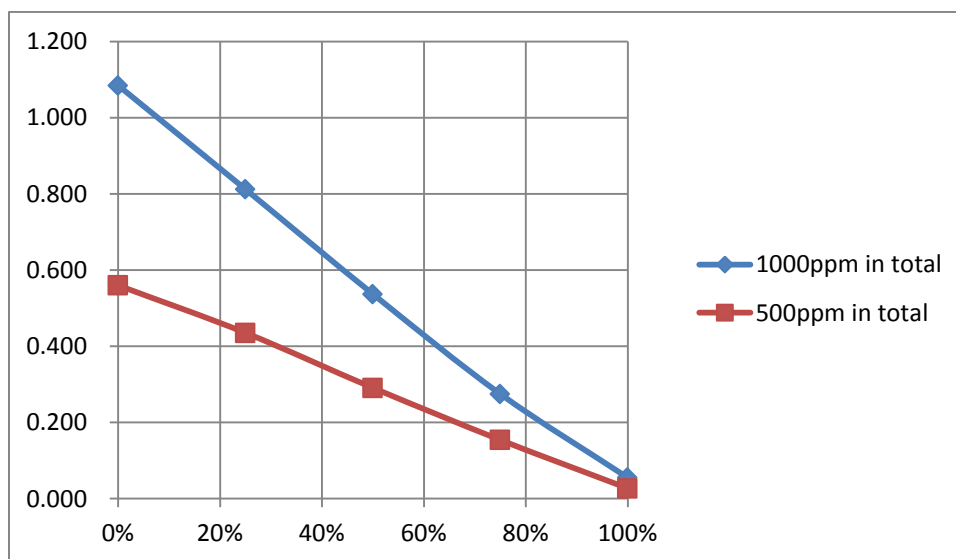


Figure 5.6. Conductivity ($\mu\text{s}/\text{cm}$) vs. PEO weight fraction for the PEO-CMC system

5.2. Flow loop experiment result

5.2.1. Experiments in 1.5-inch pipeline

In Figures 5.7 and 5.8, the friction factor is plotted against generalized Reynolds number and in all cases the friction factor decreases as the generalized Reynolds number increases. In a previous study of this group, both PEO and CMC respectively demonstrated drag reduction effect when dissolved in water. It can be seen in Figures 5.7 and 5.8 that CMC has stronger drag reduction effect than PEO since the friction factor of the pure CMC curve is lower than that of the pure PEO curve.

For the five solutions with total concentration of 500ppm (Figure 5.8), the friction factor increases in the order of CMC 500-PEO 0, CMC 375-PEO 125, CMC 250-PEO 250, CMC 125-PEO 375, CMC 0-PEO 500. This means that as the PEO weight fraction increases, the friction factor increases, and therefore, the drag reduction effect weakens. This predictable drag reduction behavior suggests that the synergy between PEO and CMC, if there is any, does not enhance the drag reduction effect of the mixed PEO-CMC solutions at the 500ppm level.

However, the five solutions with total concentration of 1000ppm (Figure 5.7) demonstrate a slightly different drag reduction behavior. The pure CMC solution has stronger drag reduction effect than the pure PEO solution. Now the drag reduction effect in the case of pure CMC solution is not the strongest. In fact, the CMC 750-PEO 250 solution has the strongest drag reduction effect, which can also be seen in Figure 5.9. This means that the synergy between PEO and CMC enhances the drag reduction effect at the 1000ppm level. This behavior coincides with the viscosity behavior shown in Figure 5.1, where the CMC 750-PEO 250 solution has higher viscosity than the pure PEO solution and the pure CMC solution.

In Figures 5.9 and 5.10, the percent drag reduction (%DR) is plotted against the generalized Reynolds number. In the calculation of the percent drag reduction here, the f_{solvent} is calculated from the Blasius equation which represents the turbulent flow of the pure solvent. It can be seen in Figure 5.10 that the percent drag reduction at 500ppm level increases in the order of CMC 0-

PEO 500, CMC 125-PEO 375, CMC 375-PEO 125, CMC 250-PEO 250, CMC 500-PEO 0. This suggests that as the PEO weight fraction increases, the drag reduction effect at 500ppm level decreases.

However, in Figure 5.9, the percent drag reduction at 1000ppm level increases in the order of CMC 0-PEO 1000, CMC 250-PEO 750, CMC 500-PEO 500, CMC 1000-PEO 0, CMC 750-PEO 250. The CMC 750-PEO 250 curve is slightly higher than the other curves. This means that compared with pure PEO solution or pure CMC solution, mixing PEO and CMC (3:1) leads to enhanced drag reduction effect at 1000ppm level. This coincides with the viscosity data shown in Figure 5.1, where the CMC 750-PEO 250 solution has higher viscosity than the other solutions.

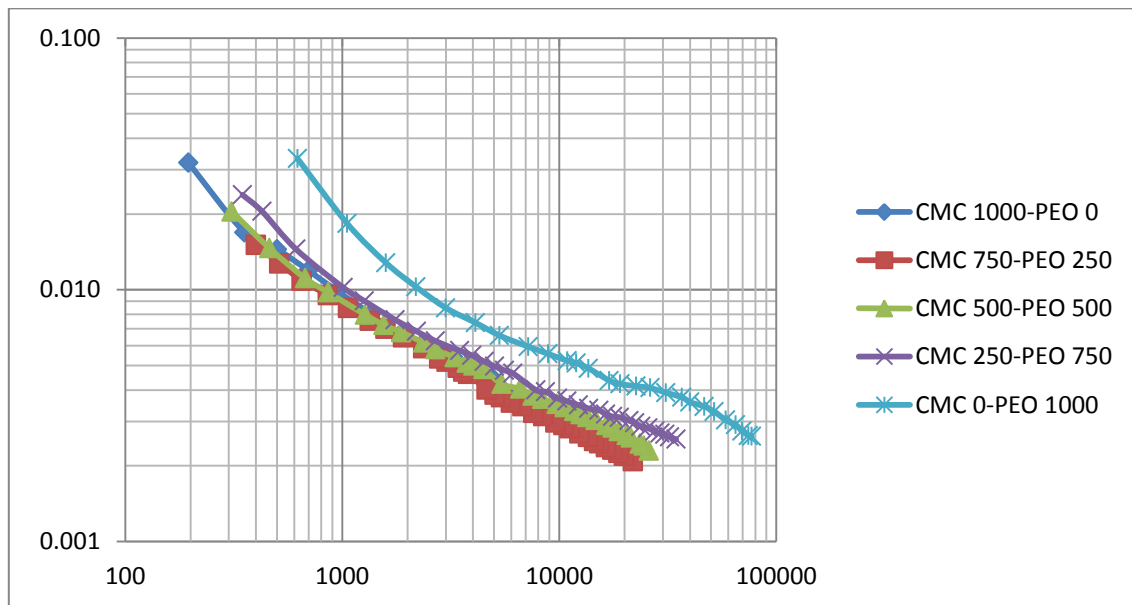


Figure 5.7. Friction factor vs. Re_g for the PEO-CMC system (1000ppm) in 1.5-inch pipe

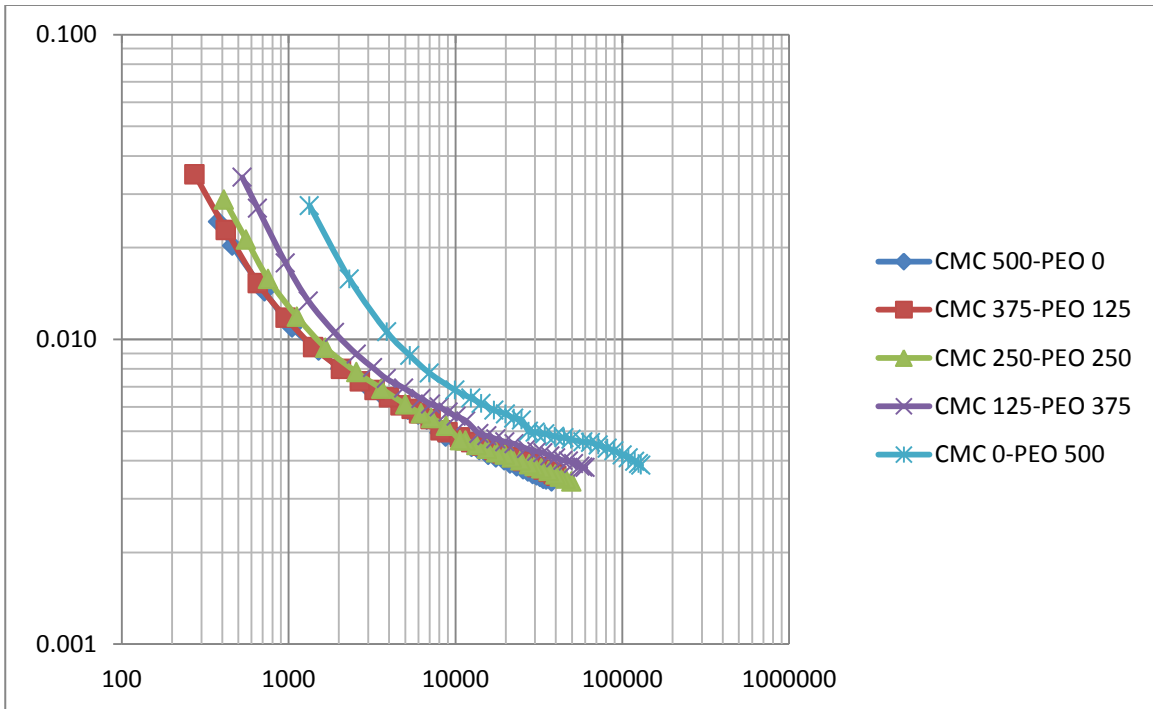


Figure 5.8. Friction factor vs. Re_g for the PEO-CMC system (500ppm) in 1.5-inch pipe

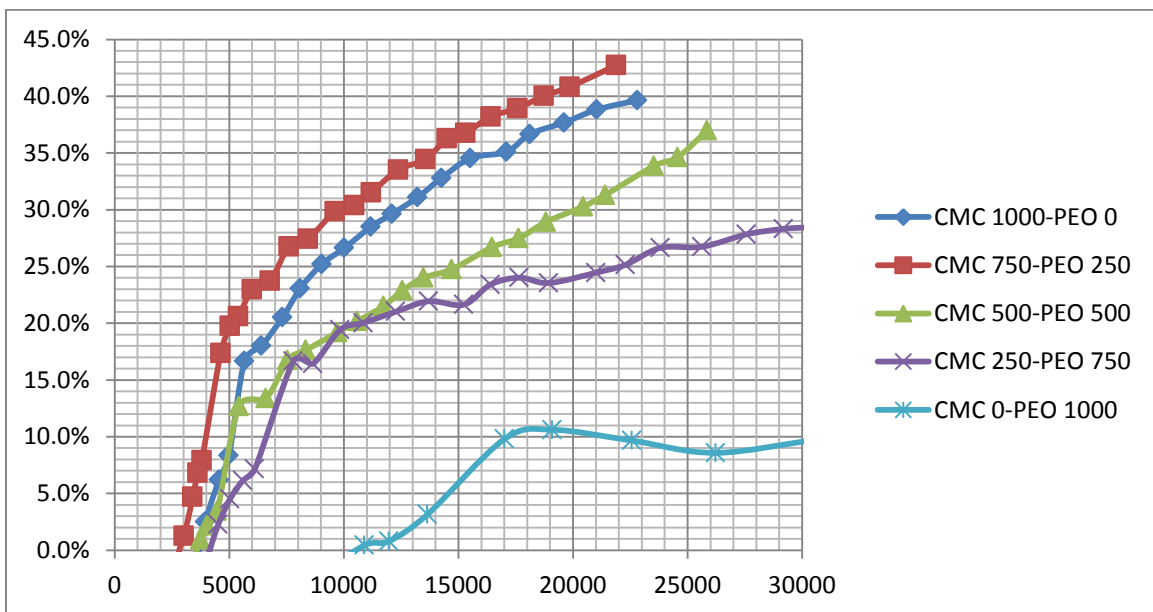


Figure 5.9. %DR vs. Re_s for the PEO-CMC system (1000ppm in total) in 1.5-inch pipe (compared with Blasius equation)

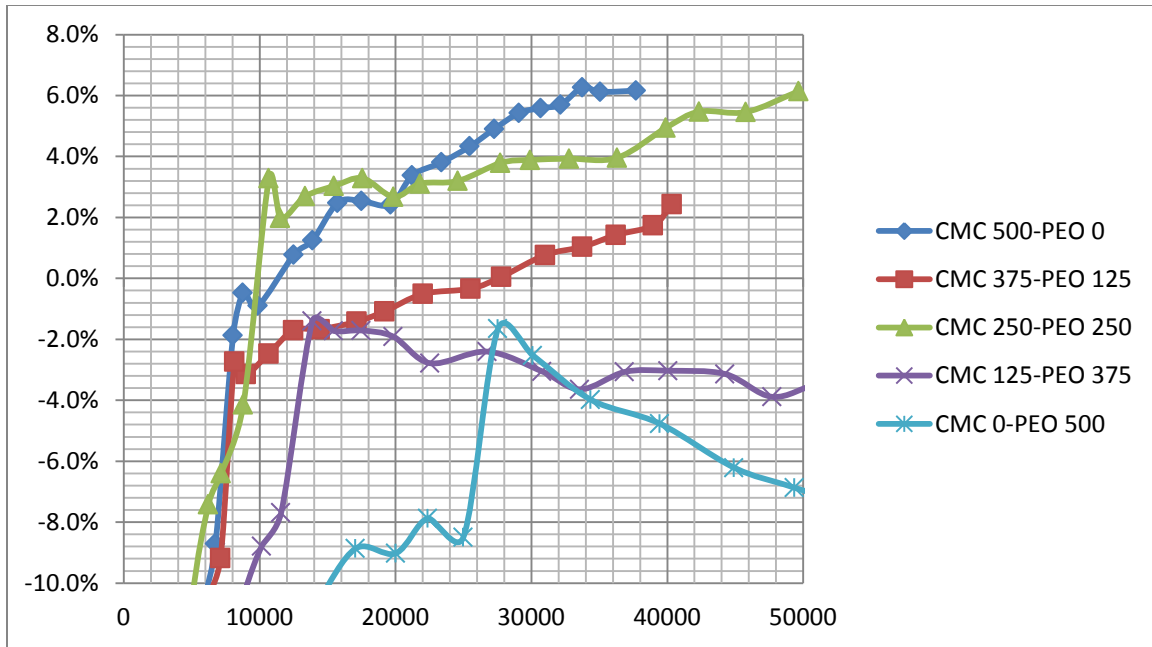


Figure 5.10. %DR vs. Re_s for the PEO-CMC system (500ppm in total) in 1.5-inch pipe (compared with Blasius equation)

In Figures 5.11 and 5.12, the percent drag reduction (%DR) is plotted against the generalized Reynolds number. In the calculation of the percent drag reduction here, the f_s is calculated from the Dodge-Metzner equation which represents the turbulent flow of non-Newtonian fluid. In Figure 5.12, the percent drag reduction at 500ppm level increases in the order of CMC 0-PEO 500, CMC 125-PEO 375, CMC 250-PEO 250, CMC 375-PEO 125, CMC 500-PEO 0. The predictable drag reduction behavior indicates that the drag reduction effect of the PEO-CMC solutions increases as the PEO weight fraction decreases.

In Figure 5.11, the percent drag reduction at 1000ppm level increases in the order of CMC 0-PEO 1000, CMC 250-PEO 750, CMC 500-PEO 500, CMC 1000-PEO 0, CMC 750-PEO 250. In this figure, the CMC 750-PEO 250 solution has stronger drag reduction effect than the other solutions. This coincides with the viscosity data shown in Figure 5.1, where the CMC 750-PEO 250 solution has higher viscosity than the other solutions.

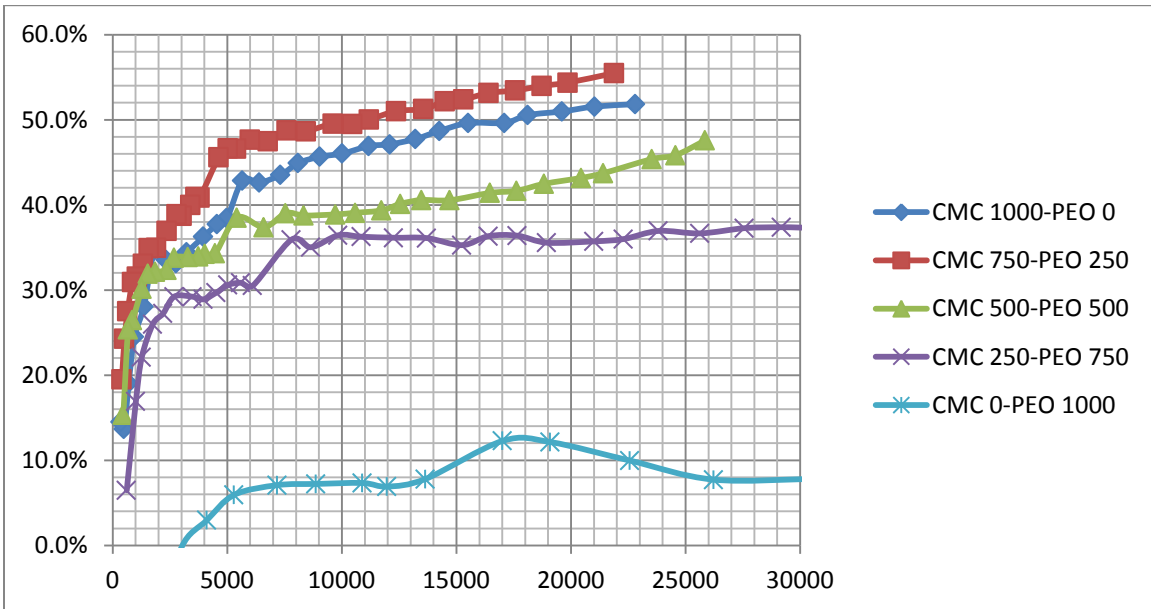


Figure 5.11. %DR vs. Re_g for the PEO-CMC system (1000ppm in total) in 1.5-inch pipe (compared with Dodge-Metzner equation)

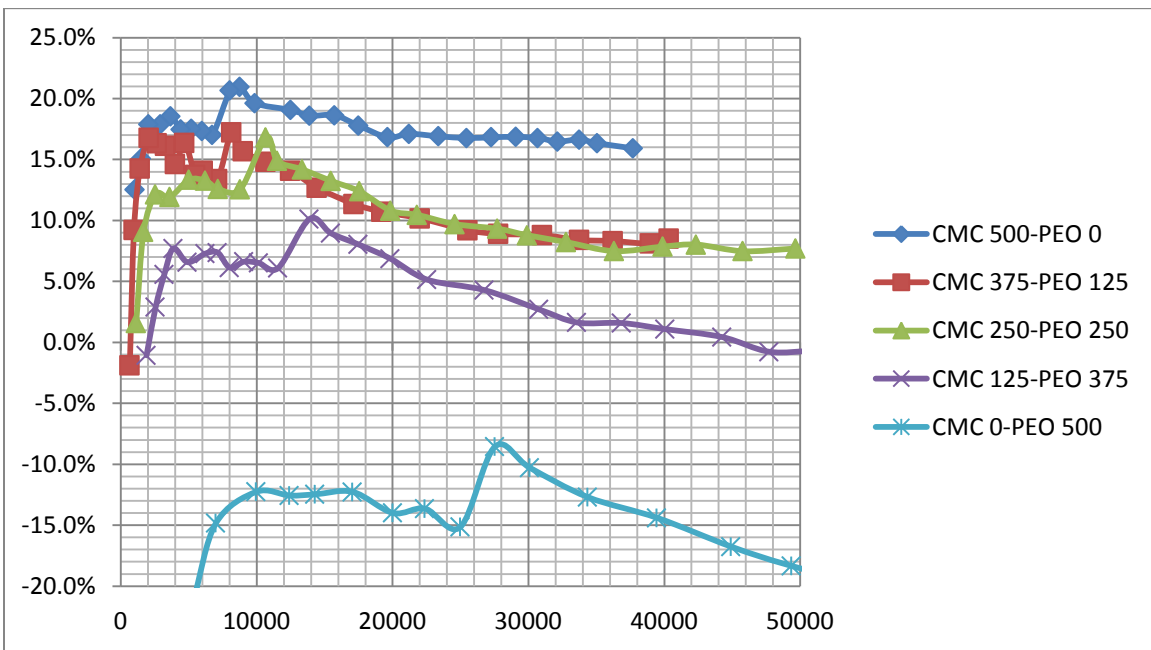


Figure 5.12. %DR vs. Re_g for the PEO-CMC system (500ppm in total) in 1.5-inch pipe (compared with Dodge-Metzner equation)

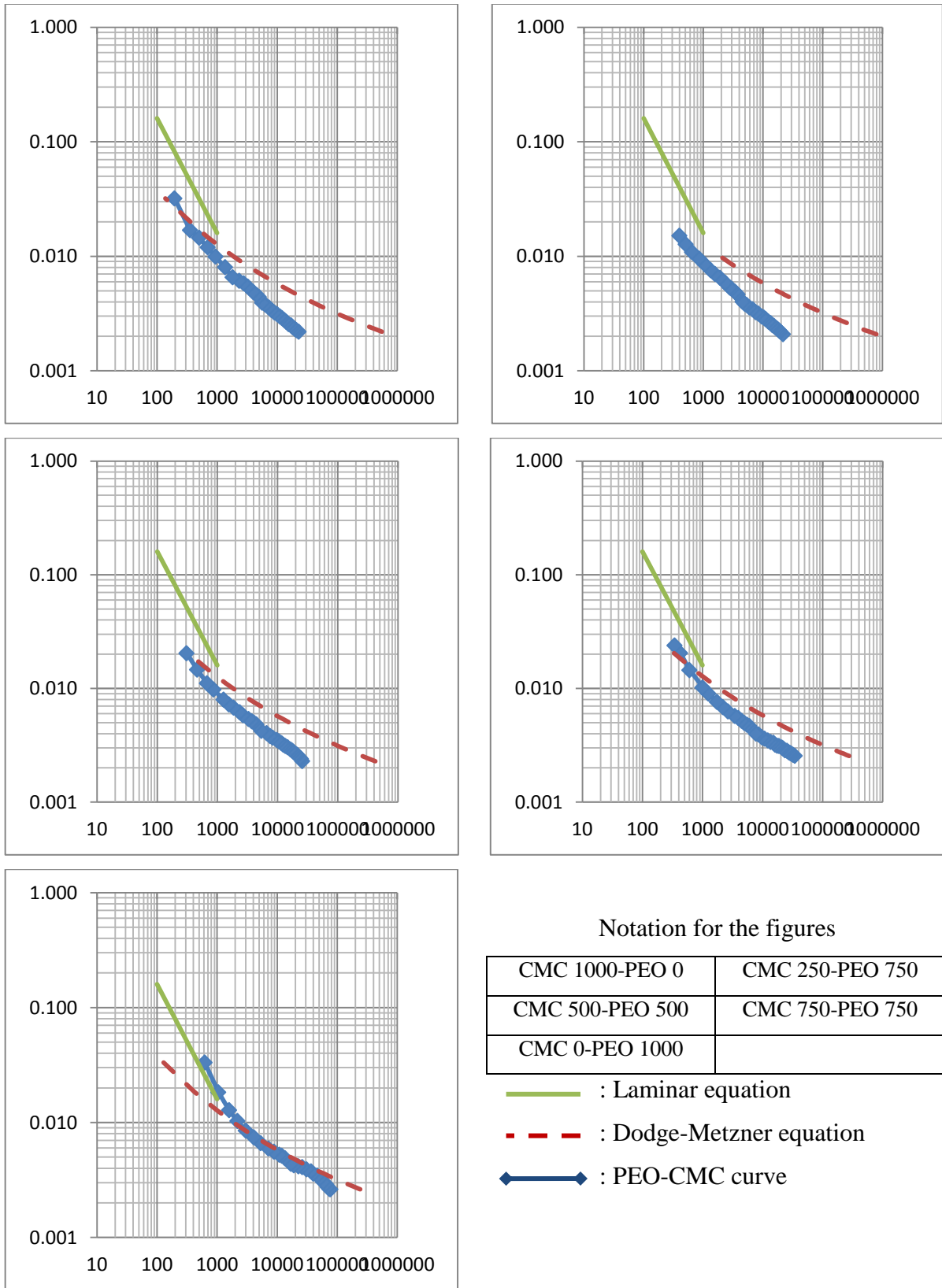


Figure 5.13. Friction factor vs. Re_g for the PEO-CMC system (1000ppm) in 1.5 inch pipe

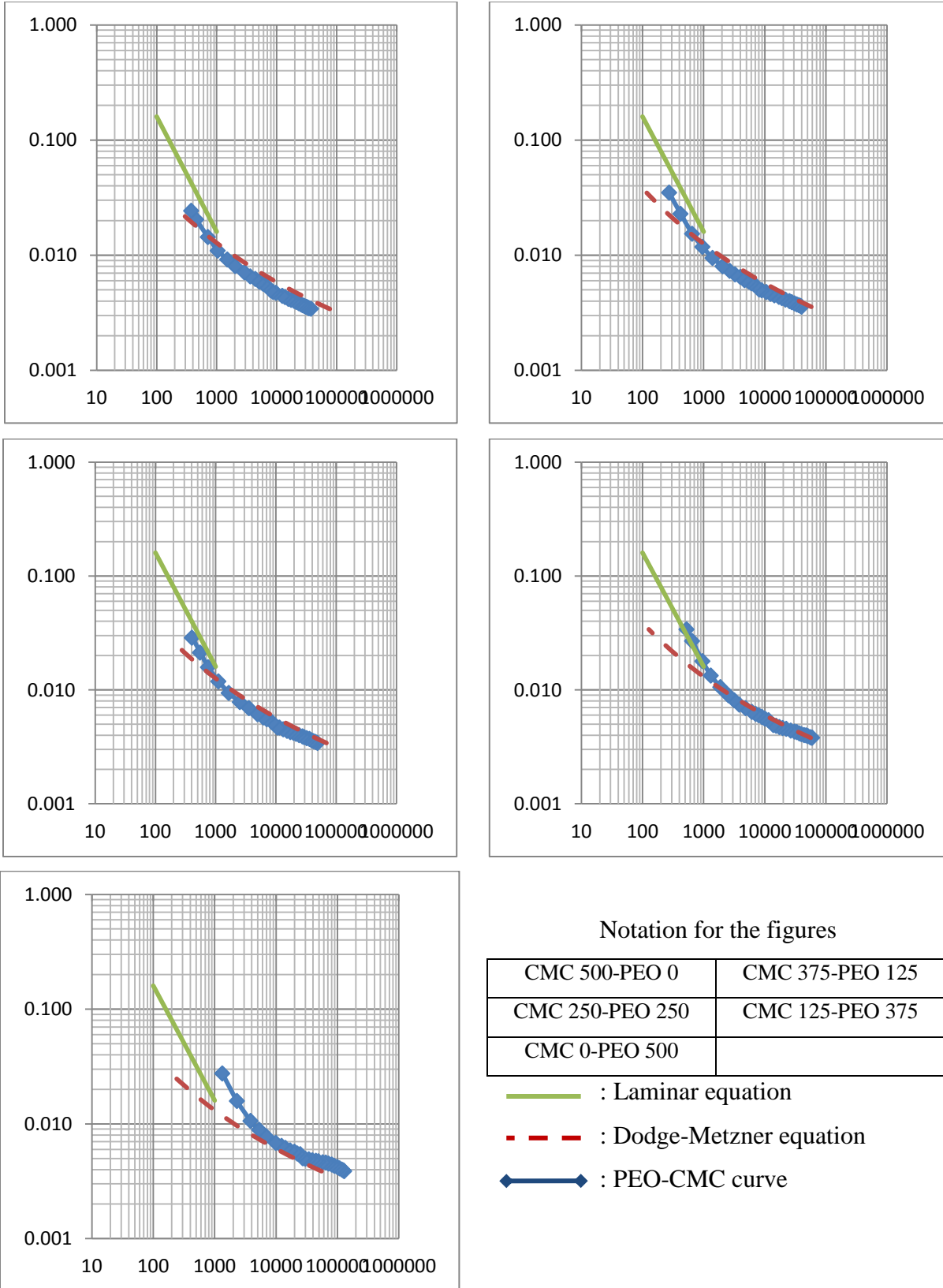


Figure 5.14. Friction factor vs. Re_g for the PEO-CMC system (500ppm) in 1.5 inch pipe

5.2.2. Experiments in 1-inch pipeline

The experiments of Figures 5.15 and 5.16 are carried out in 1-inch pipe. Similarly, the friction factors of all curves decrease as the generalized Reynolds number increases. It can be seen in Figures 5.15 and 5.16 that CMC has stronger drag reduction effect than PEO since the friction factor of the pure CMC curve is lower than that of the pure PEO curve.

For the five solutions with total concentration of 500ppm (Figure 5.16), the friction factor increases in the order of CMC 500-PEO 0, CMC 375-PEO 125, CMC 250-PEO 250, CMC 125-PEO 375, CMC 0-PEO 500. This means that as the PEO weight fraction increases, the friction factor increases, and therefore, the drag reduction effect weakens. Figure 5.18 also exhibits this trend clearly. This predictable drag reduction behavior suggests that the synergy between PEO and CMC, if there is any, does not enhance the drag reduction effect of the mixed PEO-CMC solutions at the 500ppm level.

However, the five solutions with total concentration of 1000ppm (Figure 5.15) demonstrate a slightly different drag reduction behavior. The pure CMC solution still has stronger drag reduction effect than the pure PEO solution. However, the drag reduction effect of the pure CMC solution is not the strongest. The CMC 750-PEO 250 solution has slightly stronger drag reduction effect than the pure CMC solution, which is also shown in Figure 5.17. This means that synergy between PEO and CMC enhance the drag reduction effect at the 1000ppm level. This behavior coincides with the viscosity behavior shown in Figure 5.1, where the viscosity of the CMC 750-PEO 250 solution is slightly higher than the pure PEO solution and the pure CMC solution.

In Figures 5.17 and 5.18, the percent drag reduction (%DR) is plotted against the generalized Reynolds number. In the calculation of the percent drag reduction here, the f_s is calculated from the Blasius equation which represents the turbulent flow of the pure solvent. It can be seen in Figure 5.18 that the percent drag reduction at 500ppm level decreases in the order of CMC 500-PEO 0, CMC 375-PEO 125, CMC 250-PEO 250, CMC 125-PEO 375, CMC 0-PEO 500. This

indicates that as the PEO weight fraction decreases, the drag reduction effect at 500ppm level increases.

However, in Figure 5.17, the percent drag reduction at 1000ppm level decreases in the order of CMC 750-PEO 250, CMC 1000-PEO 0, CMC 500-PEO 500, CMC 250-PEO 750, CMC 0-PEO 1000. The CMC 750-PEO 250 curve is slightly higher than the CMC 1000-PEO 0 curve, which means that mixing PEO and CMC (1:3) can enhance the drag reduction effect. This behavior coincides with the viscosity data shown in Figure 5.1, where the viscosity of the CMC 750-PEO 250 solution is slightly higher than the pure PEO solution and the pure CMC solution.

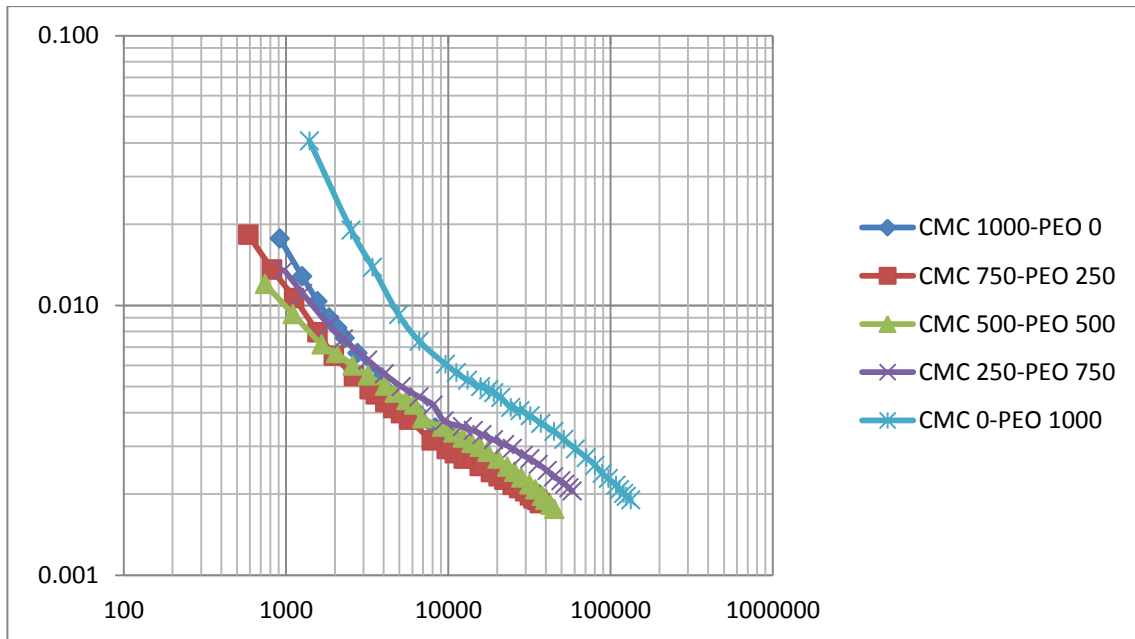


Figure 5.15. Friction factor vs. Re_g for the PEO-CMC system (1000ppm) in 1-inch pipe

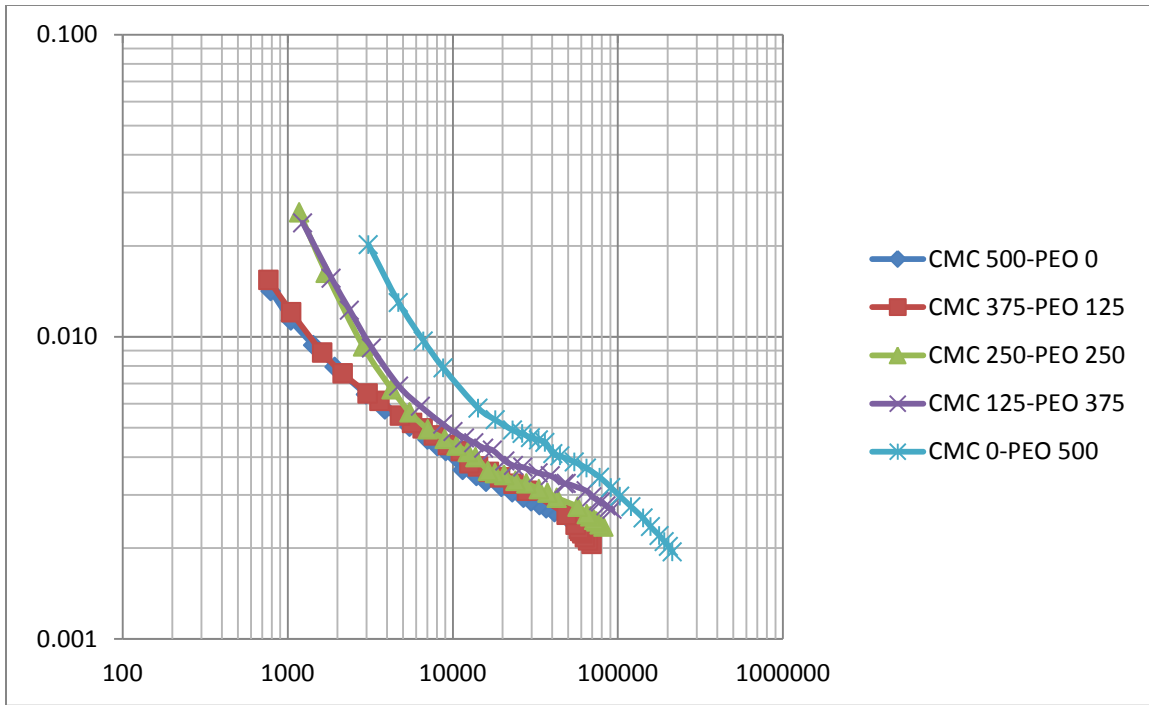


Figure 5.16. Friction factor vs. Re_g for the PEO-CMC system (500ppm) in 1-inch pipe

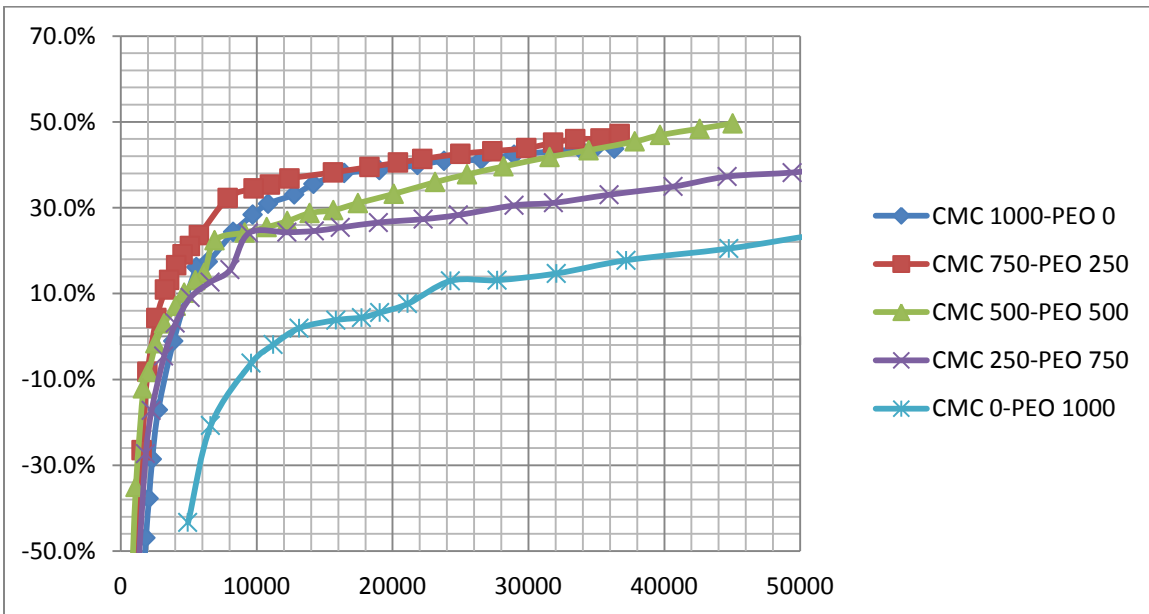


Figure 5.17. %DR vs. Re_s for the PEO-CMC system (1000ppm in total) in 1-inch pipe (compared with Blasius equation)

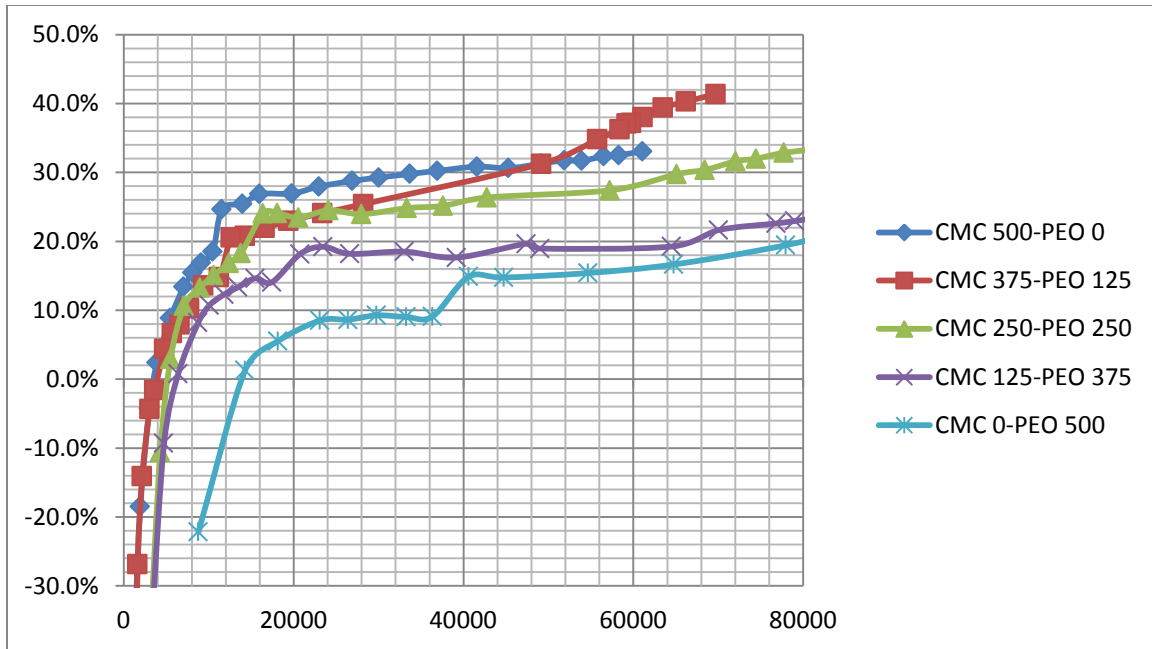


Figure 5.18. %DR vs. Re_s for the PEO-CMC system (500ppm in total) in 1-inch pipe (compared with Blasius equation)

In Figures 5.19 and 5.20, the percent drag reduction (%DR) is plotted against the generalized Reynolds number. In the calculation of the percent drag reduction here, the f_s is calculated from the Dodge-Metzner equation which represents the turbulent flow of non-Newtonian fluid. In Figure 5.20, the percent drag reduction at 500ppm level decreases in the order of CMC 500-PEO 0, CMC 375-PEO 125, CMC 250-PEO 250, CMC 125-PEO 375, CMC 0-PEO 500, which it is also shown in Figure 5.22. This predictable drag reduction behavior indicates that at 500ppm level the drag reduction effect is a function of PEO weight fraction. The synergy between PEO and CMC, if there is any, does not enhance the drag reduction effect of the mixed PEO-CMC solutions at 500ppm level.

In Figure 5.19, the percent drag reduction at 1000ppm level increases in the order of CMC 0-PEO 1000, CMC 250-PEO 750, CMC 500-PEO 500, CMC 1000-PEO 0, CMC 750-PEO 250. The CMC 750-PEO 250 curve is slightly higher than the CMC 1000-PEO 0 curve, which means that mixing PEO and CMC (1:3) can enhance the drag reduction effect. This behavior coincides with the viscosity data shown in Figure 5.1, where the viscosity of the CMC 750-PEO 250 solution is slightly higher than the pure PEO solution and the pure CMC solution.

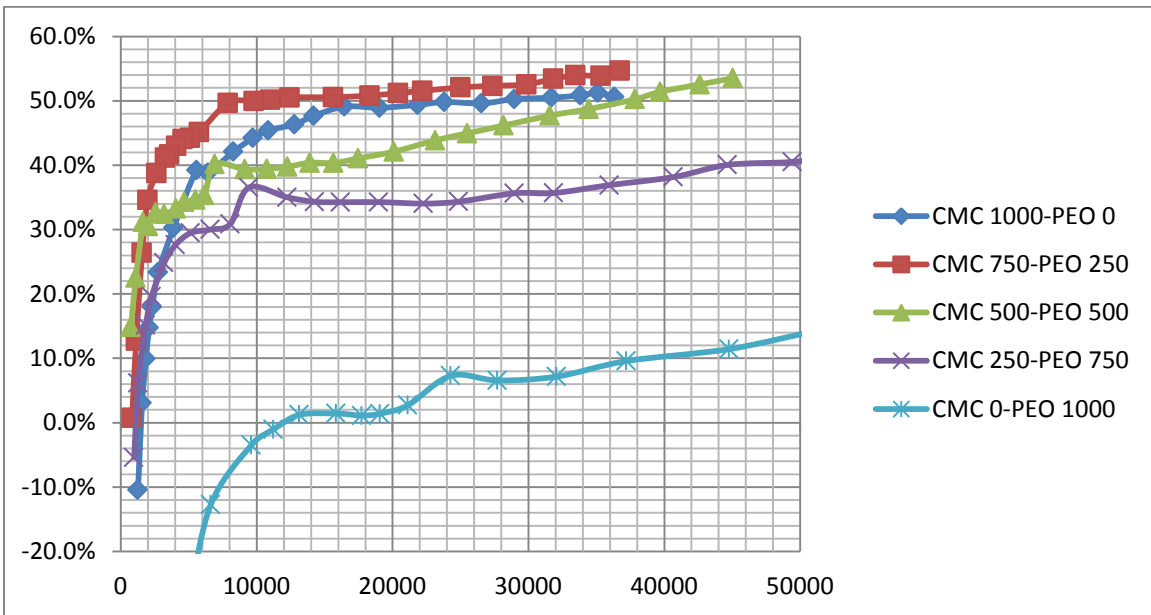


Figure 5.19. %DR vs. Re_g for the PEO-CMC system (1000ppm in total) in 1-inch pipe compare (compared with Dodge-Metzner equation)

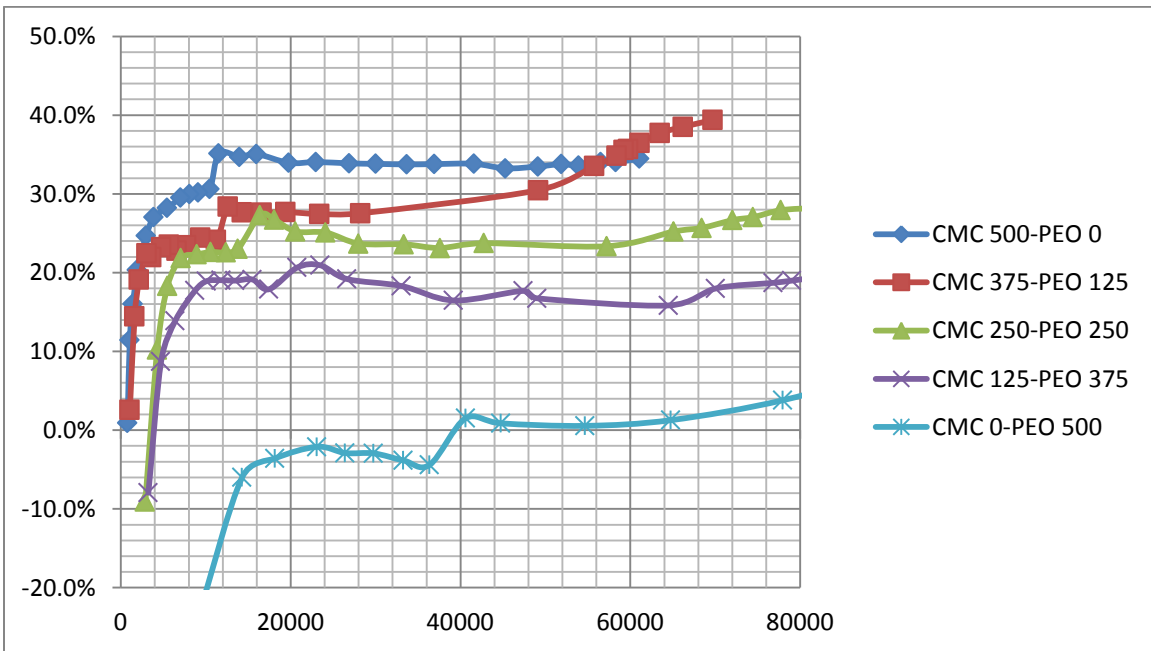


Figure 5.20. %DR vs. Re_g for the PEO-CMC system (500ppm in total) in 1-inch pipe (compared with Dodge-Metzner equation)

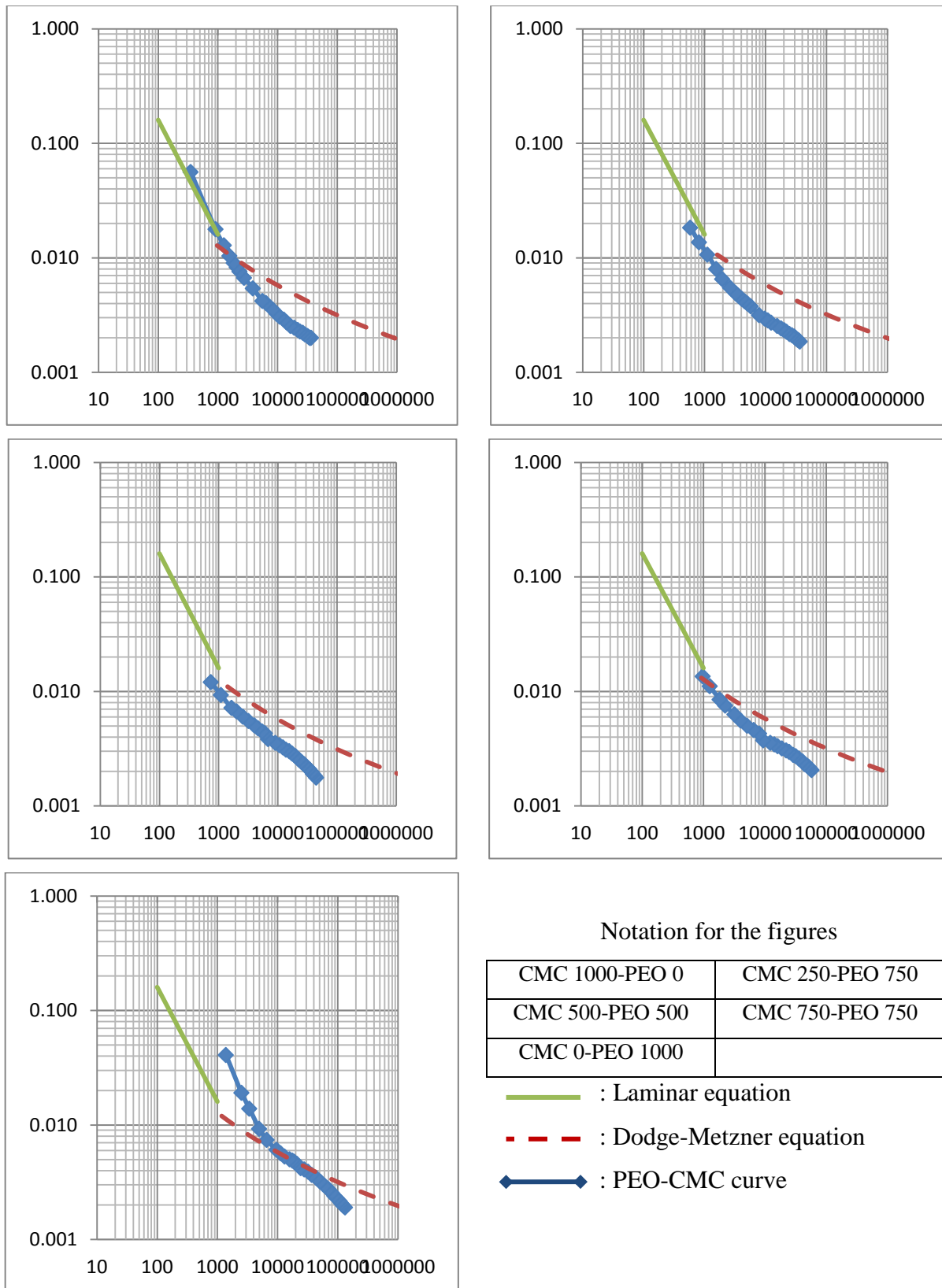


Figure 5.21. Friction factor vs. Re_g for the PEO-CMC system (1000ppm) in 1 inch pipe

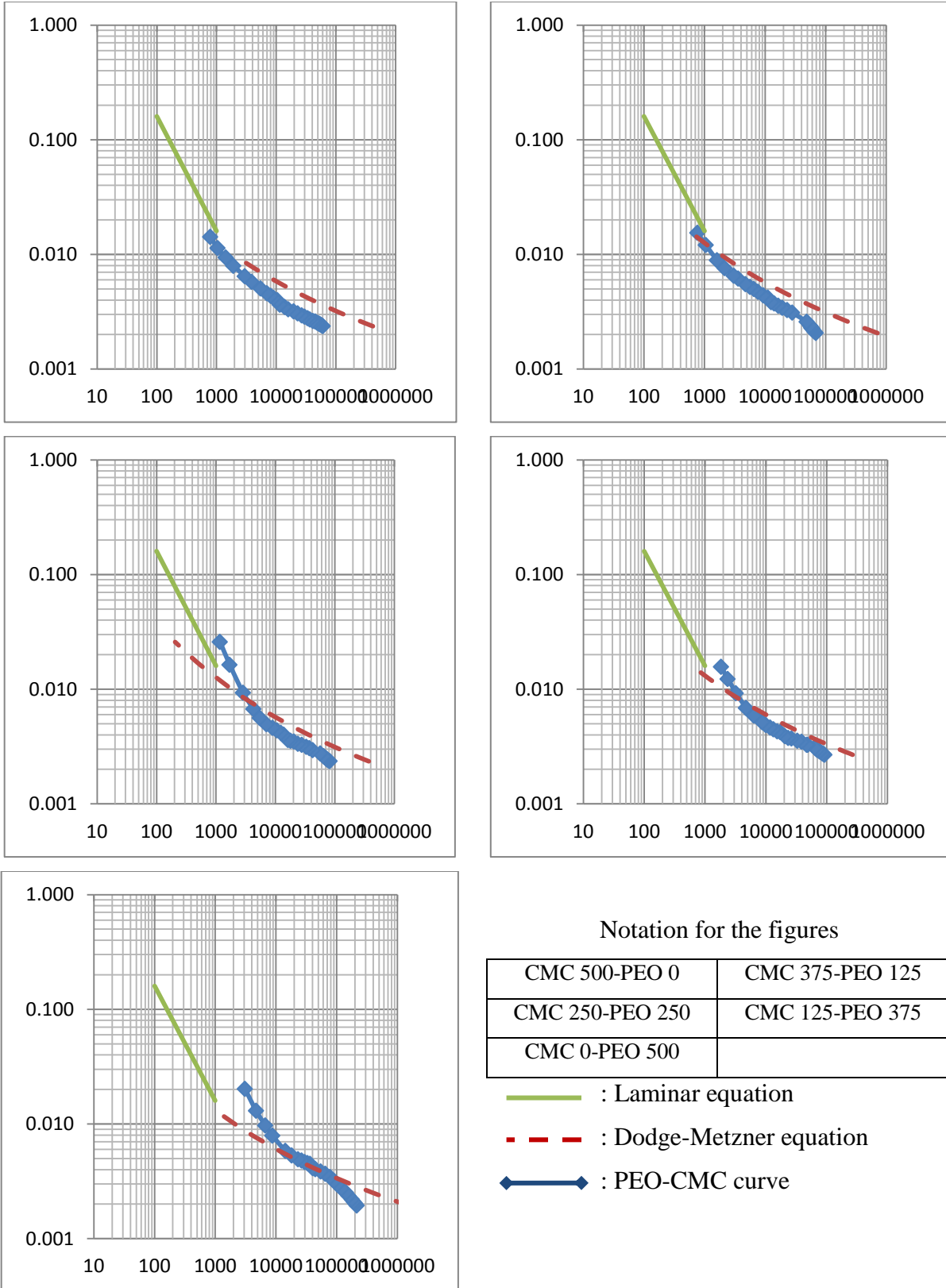


Figure 5.22. Friction factor vs. Re_g for the PEO-CMC system (500ppm) in 1 inch pipe

5.3. Conclusion

In summary, the solutions with total concentration of 500ppm do not show any enhanced drag reduction effect in both 1-inch pipe and 1.5-inch pipe. At the 500ppm level the drag reduction effect is determined by the PEO weight fraction. The drag reduction effect increases as the PEO weight fraction decreases.

However, at the 1000ppm level, mixed PEO-CMC solutions demonstrate enhanced drag reduction effect in both 1-inch pipe and 1.5-inch pipe. This enhancement is due to the synergy in the solution between PEO and CMC chains. The PEO and CMC chains form an inter-entangled network of polymers, which slightly increases the viscosity of the solutions (Figure 5.1), and therefore, leads to enhanced drag reduction effect. The enhancement is also dependent on the total polymer concentration because at 1000ppm level the polymer concentration is high enough to form the polymer network, and therefore, suppressing the quasi-streamwise vortices. It is these streamwise vortices in the buffer layer that drive convective momentum transport, suppressing the vortices can lead to the drag reduction effect ^[50].

The curves in the 1-inch pipe (Figures 5.15 and 5.16) are more separate than those in the 1.5-inch pipe (Figures 5.7 and 5.8). This means that the change of polymer composition has a bigger impact on the friction in the 1-inch pipe than in the 1.5-inch pipe. This is possibly because the 1-inch pipe has bigger effective surface area, which means that a larger fraction of fluid is in contact with the pipeline inner surface. Therefore, the polymer in the fluid has a more obvious impact on the interface between the pipeline and the fluid, and therefore, the friction.

Chapter 6. Drag Reduction Effect of PAM-SDS System

The drag reduction effect of pure PAM solution has been well studied in previous research. Previous study also shows that OTAC (octadecyltrimethylammonium chloride) can enhance drag reduction effect when mixed with PAM. Another researcher shows that anionic surfactant SDS is able to enhance the drag reduction effect when working together with PEO. Hence, both PAM and SDS show great promises for enhanced drag reduction effect. The purpose of this research is to find out whether SDS can enhance the drag reduction effect of PAM in turbulent pipe flow.

In this study the concentration of PAM is fixed at 500ppm and 1000ppm, and different amounts of SDS are added in the solutions. The following table (Table 6.1) illustrates the composition of the solutions prepared. These solutions with different compositions are tested with the flow loop and the bench-scale equipment.

Table 6.1. The concentrations of PAM and SDS used in the experiments

PAM concentration	SDS concentration				
500 ppm	0 ppm	5 ppm	10 ppm	50 ppm	100 ppm
1000 ppm	0 ppm	5 ppm	10 ppm	50 ppm	100 ppm

To study the drag reduction effect of the PAM-SDS system, PAM and SDS are dissolved in water and mixed in the flow loop tank. All solutions are freshly prepared before use. The tank is maintained at $20\pm 0.5^{\circ}\text{C}$ by the thermo jacket. All the solutions are tested in the 1-inch pipe and the 1.5-inch pipe. Flow rate and pressure drop are monitored, recorded and transferred to the data processing system. Then the flow rate and the pressure drop data are converted into Reynolds number and friction factor.

6.1. Bench-scale experiment result

6.1.1. Viscosity

Viscosity is an important parameter in the study of drag reduction effect. Since the polymer solutions in this study are non-Newtonian fluids, therefore, the viscosity measured here is apparent viscosity, which is a function of the shear rate. To be more specific, the polymer solutions in this study are shear-thinning fluids, which means that the apparent viscosity of the fluids will decrease as the shear rate increases.

In Figures 6.1 and 6.2, the apparent viscosity is plotted against the SDS concentration. In both figures the apparent viscosity remains almost the same as the SDS concentration increases. This indicates that SDS does not increase the apparent viscosity of the mixed solutions and the viscosity is almost controlled by the PAM concentration, which is different from the PAM-CMC system and the PEO-CMC system. Therefore, it is difficult to confirm the synergy between PAM and SDS from the viscosity data.

In both figures the apparent viscosity decrease in the order of 30rpm, 90rpm, 200rpm. This means that the PAM-SDS solutions in this study are shear-thinning fluids, therefore, the apparent viscosity decreases with increasing shear rate. In addition, the comparison between Figures 6.1 and 6.2 indicates that the viscosity of the 1000ppm PAM solutions is higher than that of the 500ppm PAM solutions because higher PAM concentration leads to higher viscosity.

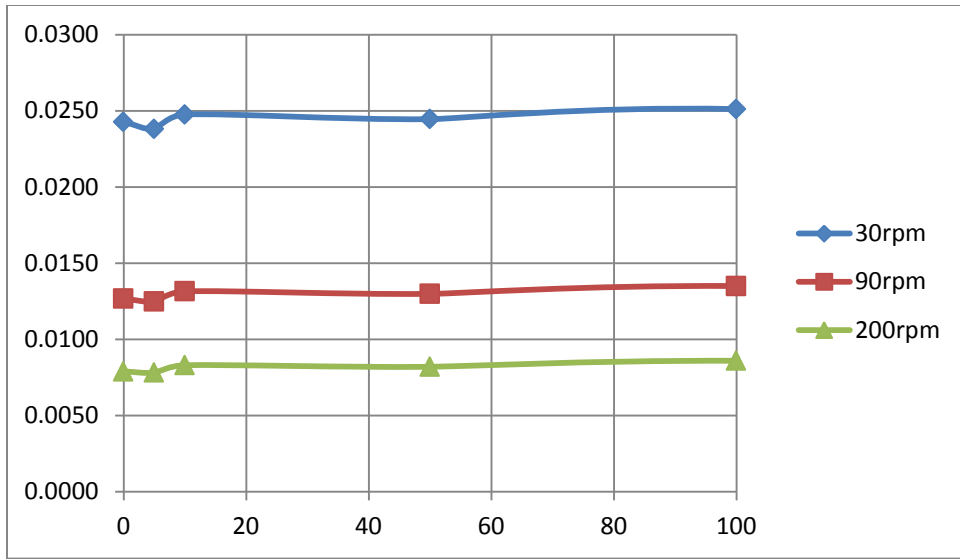


Figure 6.1. Apparent viscosity (Pa·s) vs. surfactant concentration (ppm) for the mixed system of PAM (500 ppm) and SDS

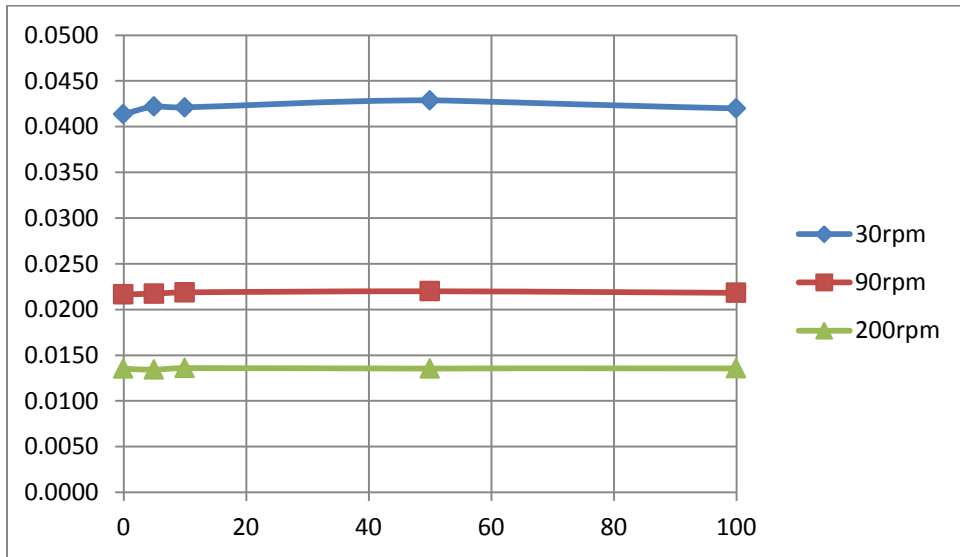


Figure 6.2. Apparent viscosity (Pa·s) vs. surfactant concentration (ppm) for the mixed system of PAM (1000 ppm) and SDS

The power law parameters k and n are characteristic for each solution. They are used in the following equation, where η is the apparent viscosity and γ is the shear rate. The flow behavior index, n , indicates the degree of non-Newtonian behavior of the fluid. The flow consistency index, k , indicates the viscosity level at certain shear rate of the fluid.

$$\eta = k \cdot \gamma^{n-1} \quad (6.1)$$

For Newtonian fluid, n is equal to 1, which means that shear rate does not affect the viscosity. However, for non-Newtonian fluid, such as the polymer solutions in this research, n has values between zero and one. Therefore, shear rate plays a role in the calculation of the apparent viscosity of the polymer solutions. In fact, as n increases, shear rate makes a bigger contribution to the apparent viscosity.

In Figure 6.3, the power law parameter n is almost independent of the SDS concentration. This means that as the SDS concentration increases, the polymer solutions maintain the same degree of non-Newtonian fluid behavior. In Figure 6.4, the power law parameter k remains almost constant. This is because the viscosity of the solutions is almost dictated by the PAM concentration.

This phenomenon coincides with the surface tension decrease in Figure 6.5. The surface tension decreases gradually in the whole range, which means that SDS prefers to gather at the surface. That is why the power law parameter k and n remain almost the same in the whole range.

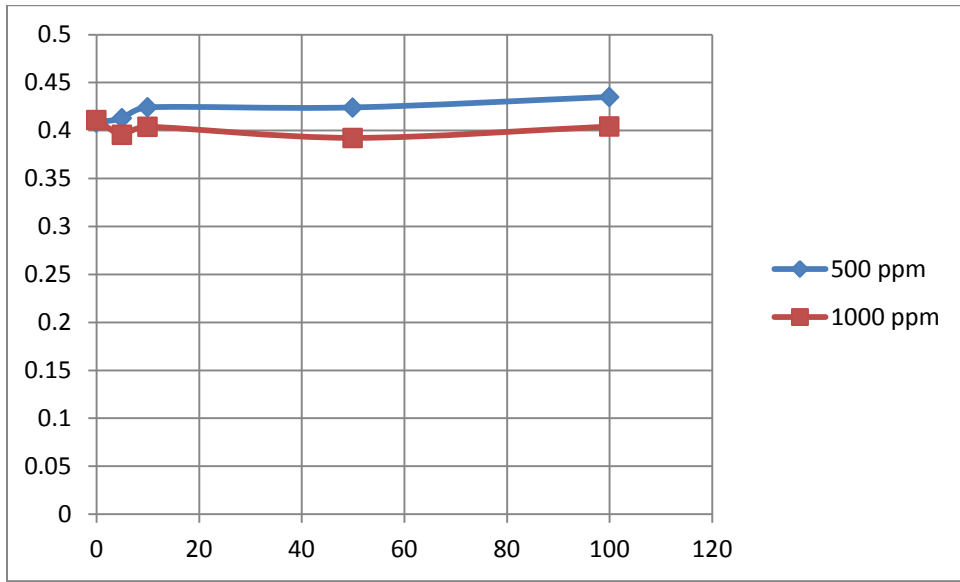


Figure 6.3. Power law parameter n vs. SDS concentration for the PAM-SDS system

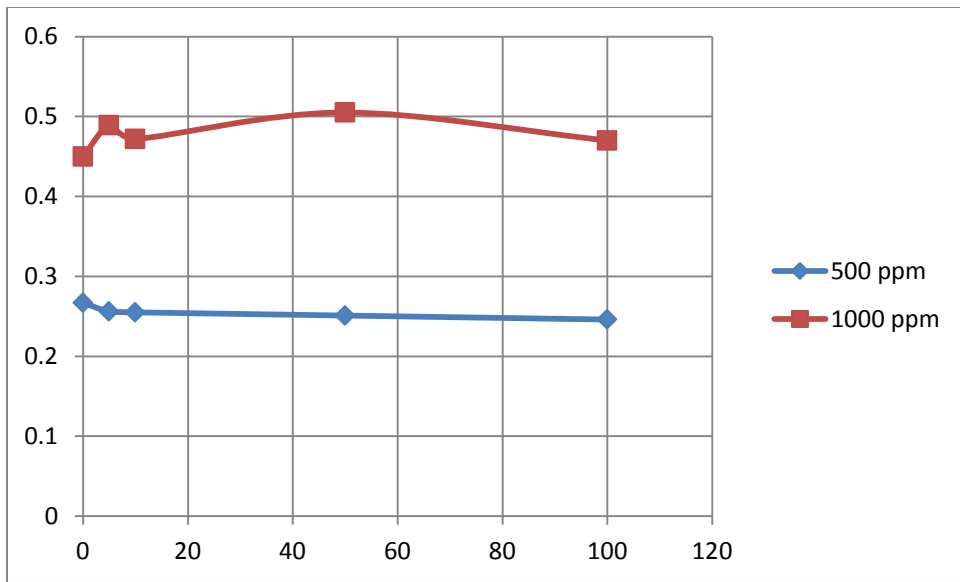


Figure 6.4. Power law parameter k vs. SDS concentration for the PAM-SDS system

6.1.2. Surface tension

Surface tension is measured to study the polymer-surfactant interaction. In this study, SDS is an anionic surfactant, while PAM is not surface active and does not cause a decrease in surface tension. In Figure 6.5, the surface tension of the PAM-SDS solutions decreases gradually as the SDS concentration increases, and there is no turning point shown in the figure. This phenomenon indicates that the surfactant molecules prefer to stay at the surface rather than entering the polymer network in this range (0ppm - 100ppm).

In addition, although PAM is not a surface active polymer, it decreases the surface tension when a high PAM concentration (1000ppm) is achieved. This indicates that the PAM molecules exist not only in the bulk solution but also at the surface, where the SDS molecules gather. Therefore, there may be synergy between PAM and SDS in the solution.

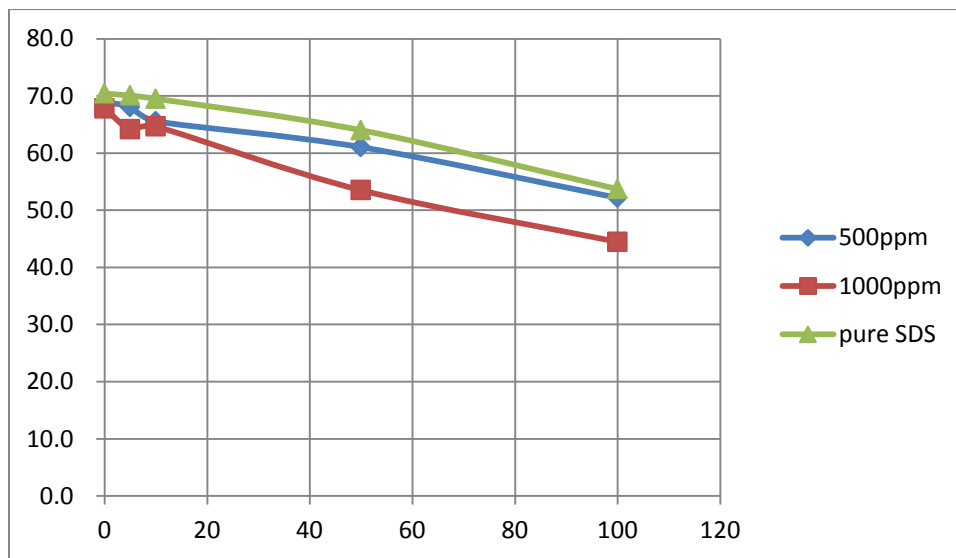


Figure 6.5. Surface tension (Dynes/cm) vs. surfactant concentration (ppm) for the mixed system of PAM (500 and 1000 ppm) and SDS

6.1.3. Conductivity

Conductivity is not a common tool to study the polymer-surfactant interaction. However, the conductivity is also measured here because both PAM and SDS used in this research are anionic. However, the anionic groups of PAM and SDS are neutralized by the cationic substances in tap water. Therefore, the interaction between PAM and SDS is not likely to be electrostatic.

It can be expected that the conductivity of the mixed solutions is dictated by the amounts of PAM and SDS added in the solutions. In Figure 6.6, the conductivity slightly increases as the SDS concentration increases, which indicates that the addition of SDS increases the conductivity of the solutions. Besides, the 1000ppm curve is higher than the 500ppm curve and the pure SDS curve, which means that the PAM concentration also affects the conductivity of the solutions.

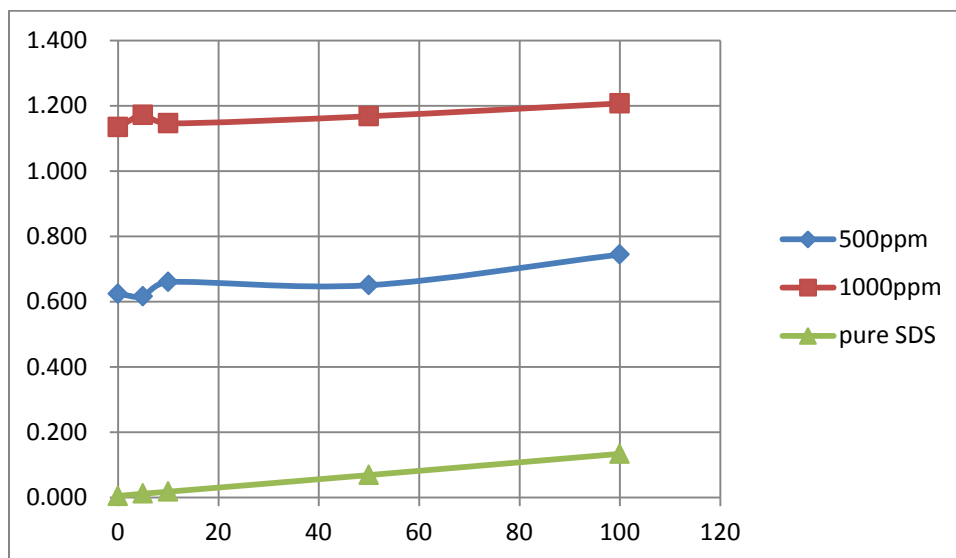


Figure 6.6. Conductivity ($\mu\text{s/cm}$) vs. surfactant concentration (ppm) for the mixed system of PAM (500 and 1000 ppm) and SDS

6.2. Flow loop experiment result

6.2.1. Experiments in 1.5-inch pipeline

In Figures 6.7 and 6.8, the friction factor is plotted against generalized Reynolds number and in all cases the friction factor decreases as the generalized Reynolds number increases. In Figures 6.9 and 6.10, the percent drag reduction (%DR) is plotted against the generalized Reynolds number. In the calculation of the percent drag reduction here, the f_s is calculated from the Blasius equation which represents the turbulent flow of the pure solvent.

For the 1000ppm PAM series (Figure 6.7), the five curves almost overlap with each other. After converting the friction factor data into percent drag reduction data (Figure 6.9), the difference of the five curves is more explicit. In Figure 6.9, the pure PAM solution exhibits the lowest drag reduction effect, while the PAM 1000-SDS 100 solution has the highest drag reduction effect. The other three solutions have almost the same moderate drag reduction effect. This trend implies that the drag reduction effect of the PAM solutions increases as the SDS concentration increases.

For the 500ppm PAM series (Figure 6.8), the five curves are close to each other in the low Re number region and become separate in the high Re number region, which means that the enhancement of the drag reduction effect become more obvious in the high Re number region. After converting the friction factor data into percent drag reduction data (Figure 6.10), the difference of the five curves is more clear. It can be seen in Figure 6.10 that the PAM 500-SDS 5 solution demonstrates the greatest drag reduction effect. However, as the SDS concentration continues to increase, the drag reduction effect decreases.

The comparison between Figures 6.9 and 6.10 shows that the PAM 500-SDS 5 solution has higher drag reduction effect than the PAM 1000-SDS 0 solution. This means that the addition of 5ppm SDS into 500ppm PAM solution can achieve a higher drag reduction effect than the 1000ppm PAM solution.

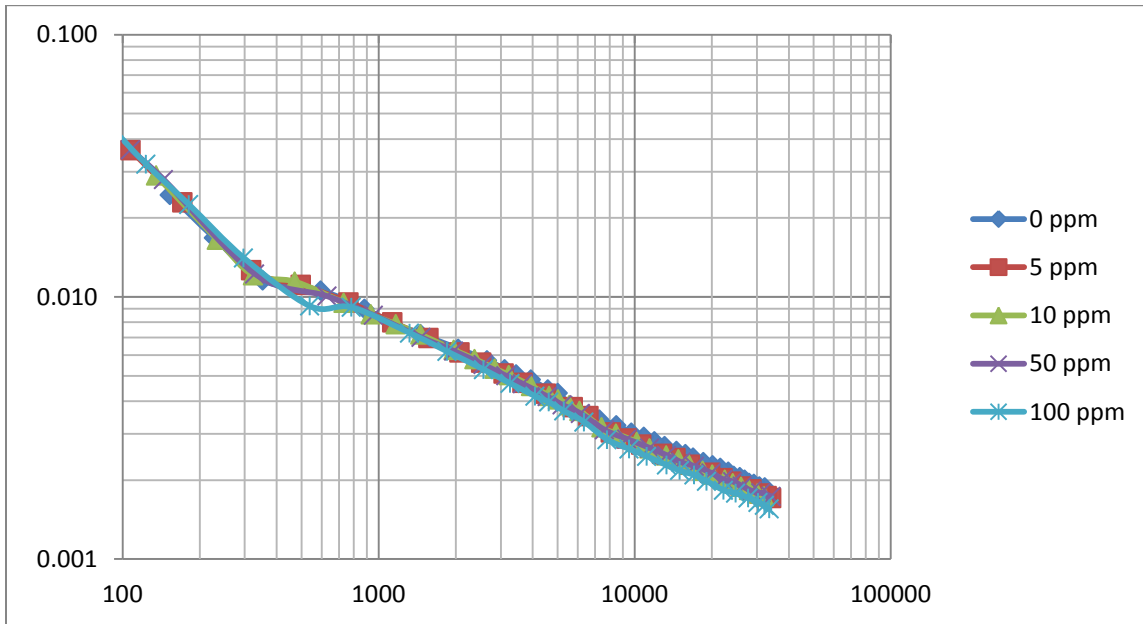


Figure 6.7. Friction factor vs. Re_g for the mixed system of PAM (1000 ppm) and SDS (0, 5, 10, 50, 100 ppm) in 1.5-inch pipe

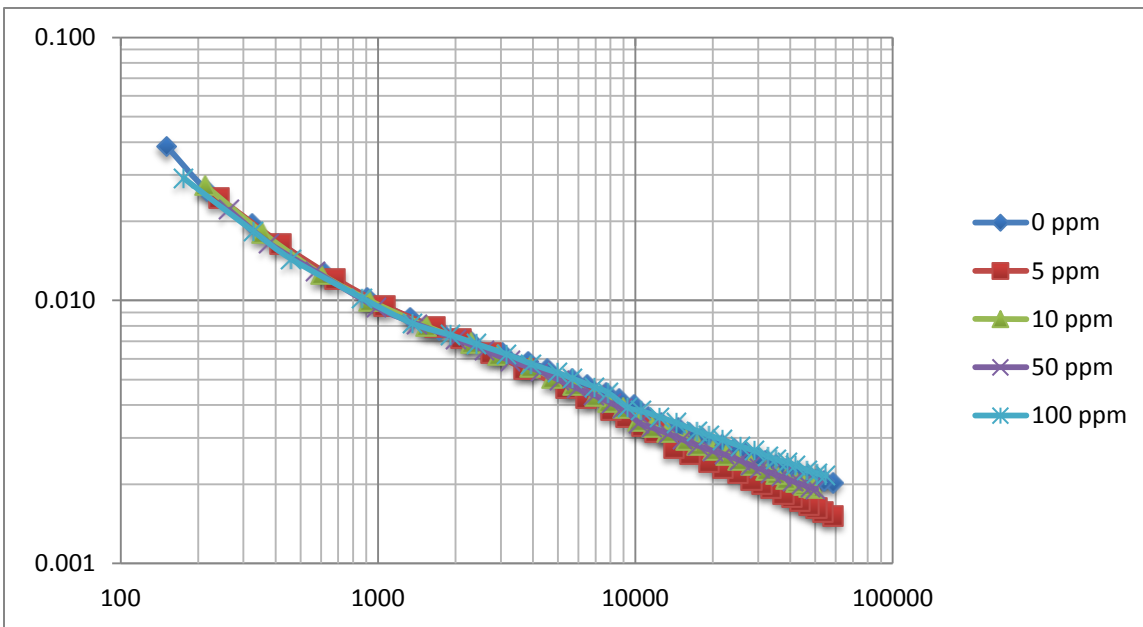


Figure 6.8. Friction factor vs. Re_g for the mixed system of PAM (500 ppm) and SDS (0, 5, 10, 50, 100 ppm) in 1.5-inch pipe

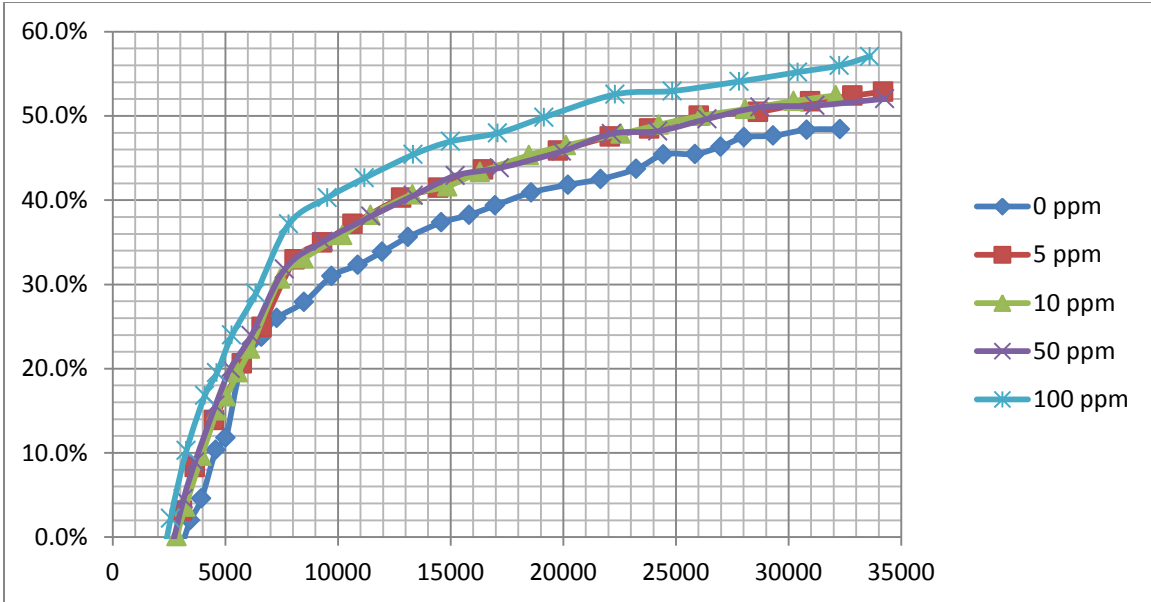


Figure 6.9. %DR vs. Re_s for the mixed system of PAM (1000 ppm) and SDS (0, 5, 10, 50, 100 ppm) in 1.5-inch pipe (compared with Blasius equation)

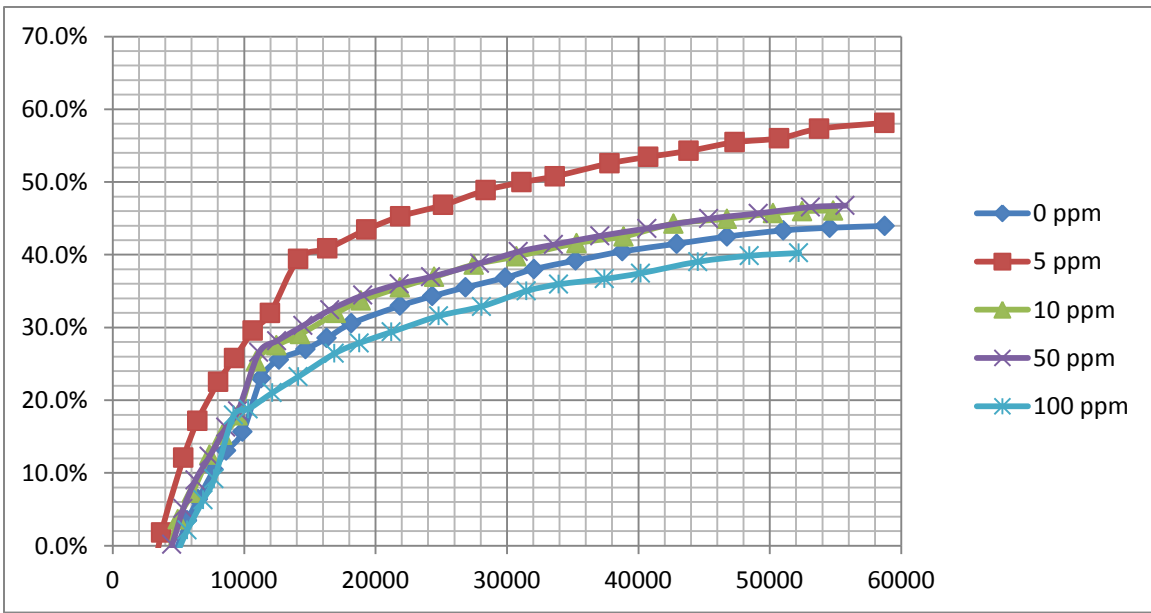


Figure 6.10. %DR vs. Re_s for the mixed system of PAM (500 ppm) and SDS (0, 5, 10, 50, 100 ppm) in 1.5-inch pipe (compared with Blasius equation)

In Figures 6.11 and 6.12, the percent drag reduction (%DR) is plotted against the generalized Reynolds number. In the calculation of the percent drag reduction here, the f_s is calculated from the Dodge-Metzner equation which represents the turbulent flow of non-Newtonian fluid. For the 1000ppm PAM series (Figure 6.11), the PAM 1000-SDS 0 solution has the lowest drag reduction effect, while the PAM 1000-SDS 100 solution has the highest drag reduction effect. The other three solutions almost have the same drag reduction effect.

For the 500ppm PAM series (Figure 6.12), the PAM 500-SDS 5 solution demonstrates the greatest drag reduction effect. As the SDS concentration continues to increase, the drag reduction effect decreases. Since the viscosity of the solutions remains almost the same in the whole range (Figures 6.1 and 6.2), viscosity change is not likely to cause the change of the drag reduction effect in the PAM-SDS system. Therefore, the stretching and shrinkage of the polymer chains plays an important role on the drag reduction effect. For the 500ppm PAM series, adding a small amount of SDS can lead to the stretching of PAM chains and increase the drag reduction effect. However, adding more SDS into the PAM solutions causes the shrinkage of the polymer chains and decreases the drag reduction effect.

It is found that the addition of SDS has bigger impact on the drag reduction effect of the 500ppm PAM solutions than the 1000ppm PAM solutions. For example, adding 5ppm SDS into 500ppm PAM solution incurs a large increase in drag reduction. However, adding 5ppm SDS into 1000ppm PAM solution only leads to a small increase in drag reduction. This suggests that the 1000ppm PAM solution is less accessible to SDS molecules because of the formation of an interconnected network of polymers. Consequently, SDS is less effective in interacting with the polymer at high PAM concentration.

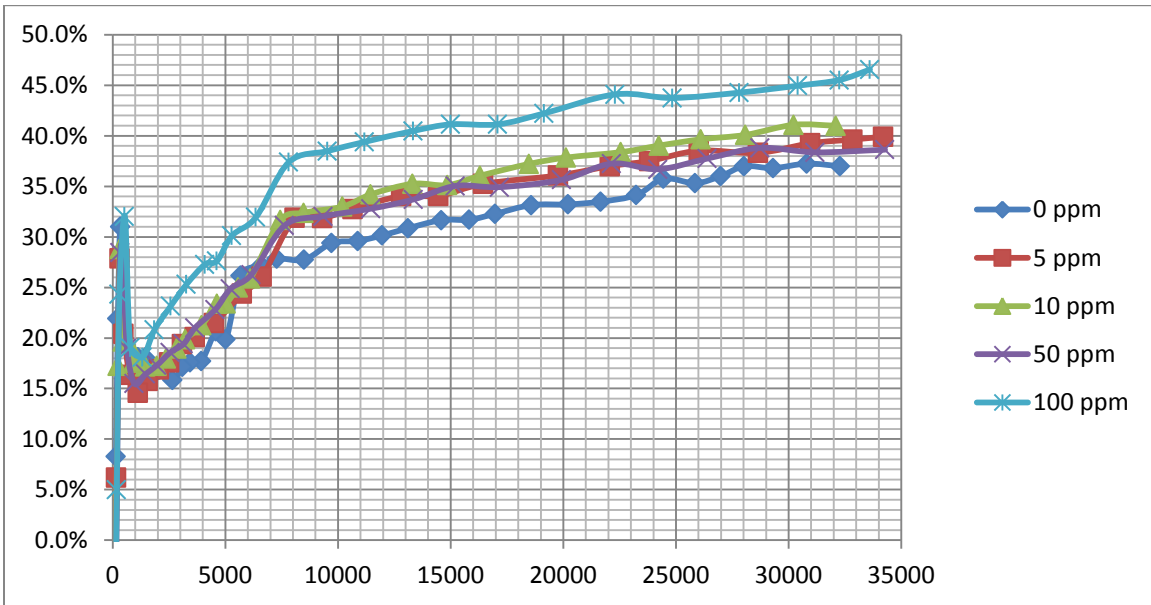


Figure 6.11. %DR vs. Re_g for the mixed system of PAM (1000 ppm) and SDS (0, 5, 10, 50, 100 ppm) in 1.5-inch pipe (compared with Dodge-Metzner equation)

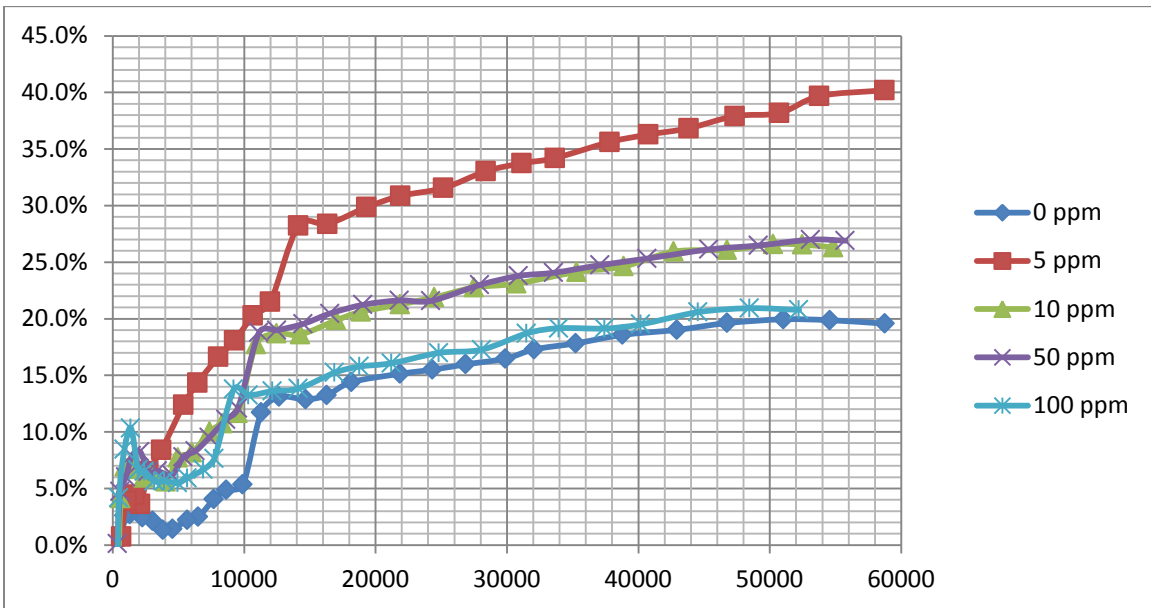


Figure 6.12. %DR vs. Re_g for the mixed system of PAM (500 ppm) and SDS (0, 5, 10, 50, 100 ppm) in 1.5-inch pipe (compared with Dodge-Metzner equation)

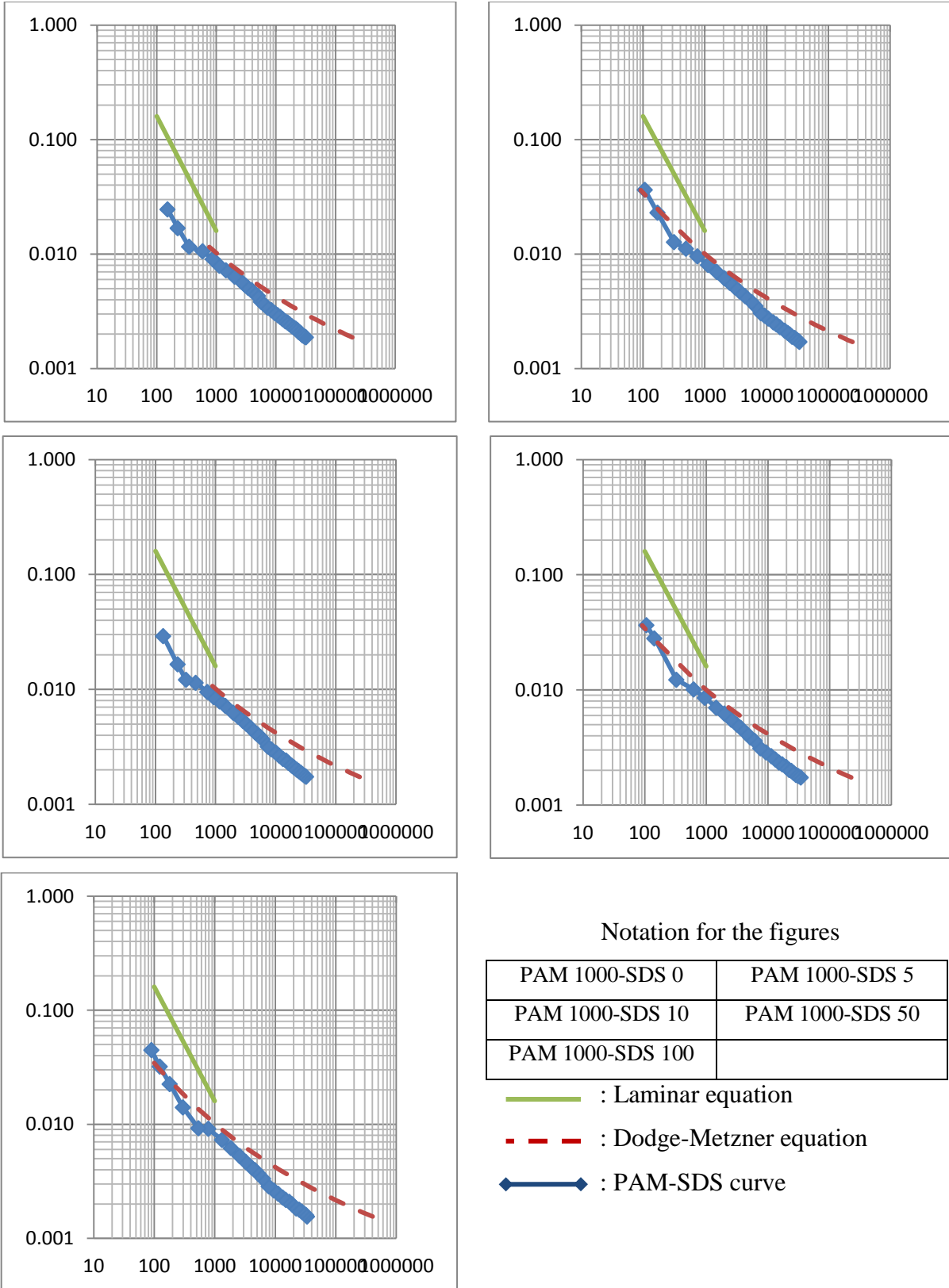


Figure 6.13. Friction factor vs. Re_g for the PAM-SDS system (1000ppm) in 1.5 inch pipe

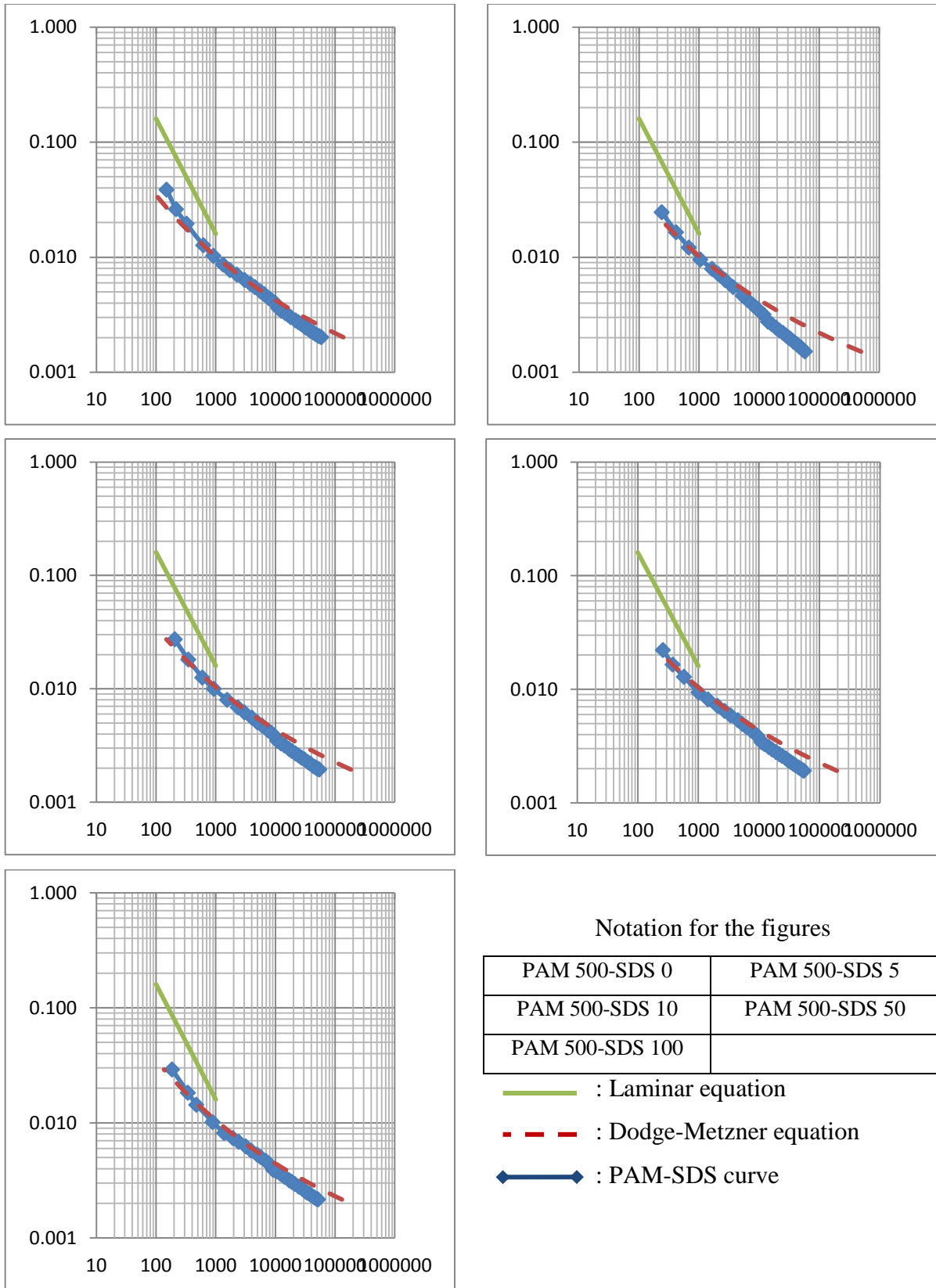


Figure 6.14. Friction factor vs. Re_g for the PAM-SDS system (500ppm) in 1.5 inch pipe

6.2.2. Experiments in 1-inch pipeline

In Figures 6.15 and 6.16, the friction factor is plotted against generalized Reynolds number and in all cases the friction factor decreases as the generalized Reynolds number increases. In Figures 6.17 and 6.18, the percent drag reduction (%DR) is plotted against the generalized Reynolds number. In the calculation of the percent drag reduction here, the f_s is calculated from the Blasius equation which represents the turbulent flow of the pure solvent.

For the 1000ppm PAM series (Figure 6.15), the five curves almost overlap with each other. After converting the friction factor data into percent drag reduction data (Figure 6.17), the difference of the five curves is still very small. Both figures tell us that the addition of SDS to the 1000ppm PAM solutions in 1-inch pipe does not enhance the drag reduction effect.

For the 500ppm PAM series (Figure 6.16), the five curves are close to each other in the low Re number region and become separate in the high Re number region, which means that the enhancement of drag reduction effect become more obvious in the high Re number region. After converting the friction factor data into percent drag reduction data (Figure 6.18), the difference of the five curves becomes more obvious. It can be seen in Figure 6.18 that initially the drag reduction effect increases as the SDS concentration increases. The PAM 500-SDS 50 solution demonstrates the highest drag reduction effect. When the SDS concentration increases to 100ppm, the drag reduction effect decreases.

The comparison between Figures 6.17 and 6.18 shows that the PAM 500-SDS 50 solution has almost the same drag reduction effect as the PAM 1000-SDS 0 solution. This means that the addition of 50ppm SDS into 500ppm PAM solution can achieve the same drag reduction effect as the 1000ppm PAM solution.

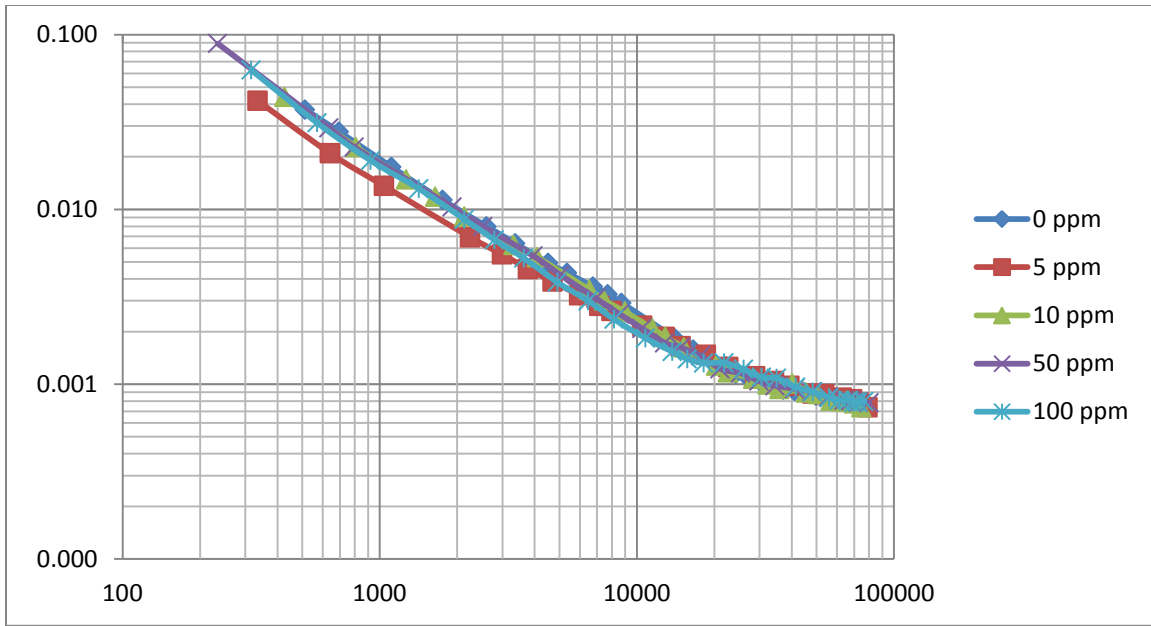


Figure 6.15. Friction factor vs. Re_g for the mixed system of PAM (1000 ppm) and SDS (0, 5, 10, 50, 100 ppm) in 1-inch pipe

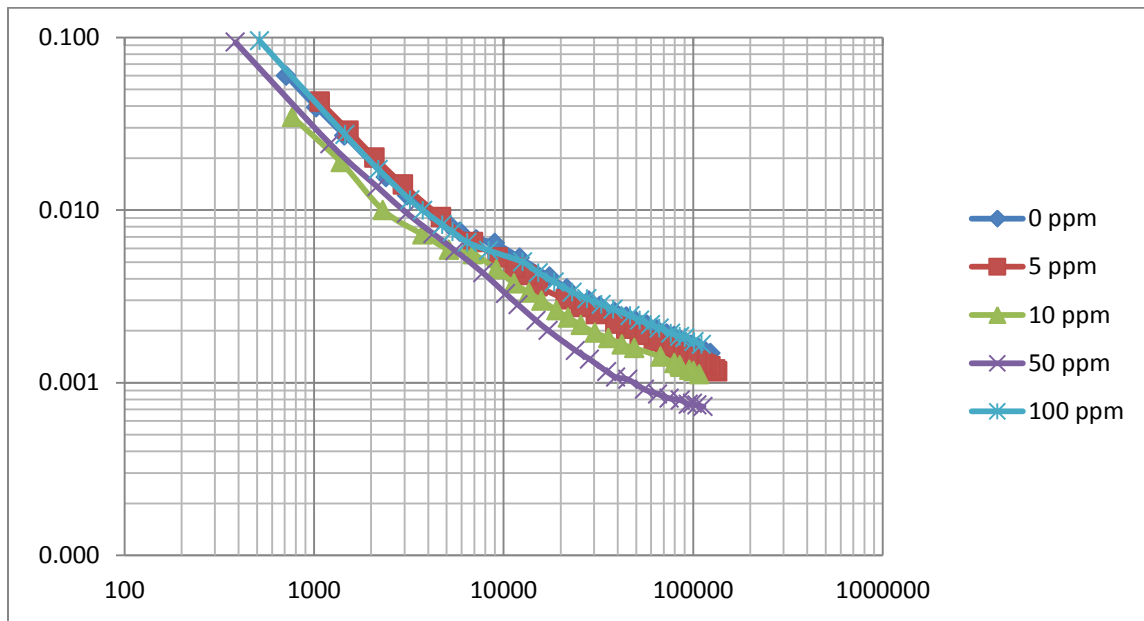


Figure 6.16. Friction factor vs. Re_g for the mixed system of PAM (500 ppm) and SDS (0, 5, 10, 50, 100 ppm) in 1-inch pipe

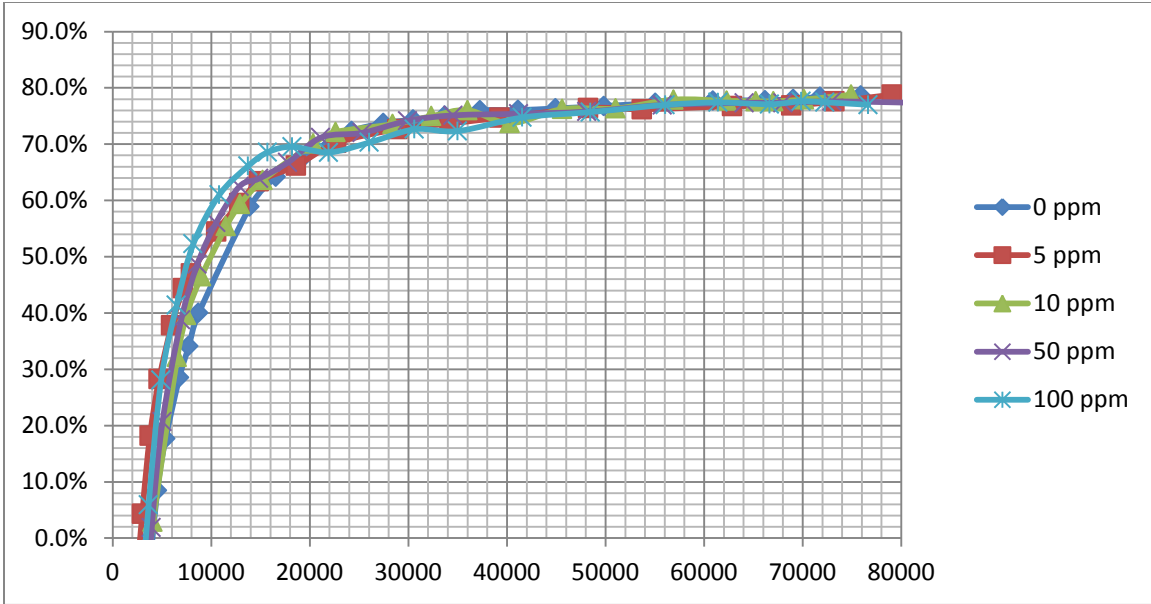


Figure 6.17. %DR vs. Re_s for the mixed system of PAM (1000 ppm) and SDS (0, 5, 10, 50, 100 ppm) in 1-inch pipe (compared with Blasius equation)

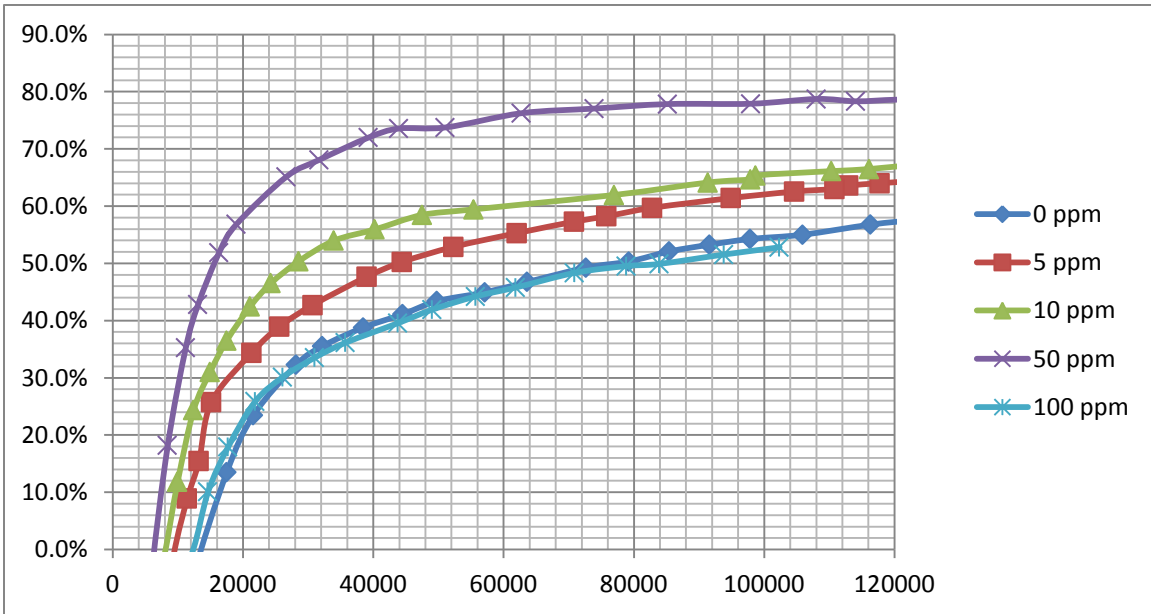


Figure 6.18. %DR vs. Re_s for the mixed system of PAM (500 ppm) and SDS (0, 5, 10, 50, 100 ppm) in 1-inch pipe (compared with Blasius equation)

In Figures 6.19 and 6.20, the percent drag reduction (%DR) is plotted against the generalized Reynolds number. In the calculation of the percent drag reduction here, the f_s is calculated from the Dodge-Metzner equation which represents the turbulent flow of non-Newtonian fluid. For the 1000ppm PAM series (Figure 6.19), the five curves almost overlap with each other and it is difficult to tell which one has the highest drag reduction effect.

For the 500ppm PAM series (Figure 6.20), the drag reduction effect increases as the SDS concentration increases initially. The PAM 500 -SDS 50 solution demonstrates the greatest drag reduction effect. However, when the SDS concentration increases to 100ppm, the drag reduction effect decreases. Since the viscosity of the solutions remains almost the same in the whole range (Figures 6.1 and 6.2), viscosity change is not likely to cause the change of the drag reduction effect in the PAM-SDS system. Therefore, the stretching and shrinkage of the polymer chains plays an important role on the drag reduction effect. For the 500ppm PAM series, adding a small amount of SDS can lead to the stretching of PAM chains and increase the drag reduction effect. However, adding more SDS into the PAM solutions causes the shrinkage of the polymer chains and decreases the drag reduction effect.

It is found that the addition of SDS has bigger impact on the drag reduction effect of the 500ppm PAM solutions than the 1000ppm PAM solutions. For example, adding 50ppm SDS into 500ppm PAM solution incurs a large increase in drag reduction. However, the drag reduction effect almost remains the same when 50ppm SDS is added into the 1000ppm PAM solution. This suggests that the 1000ppm PAM solution is less accessible to SDS molecules because of the formation of an interconnected polymer network. Consequently, SDS is less effective in interacting with the polymer at high PAM concentration.

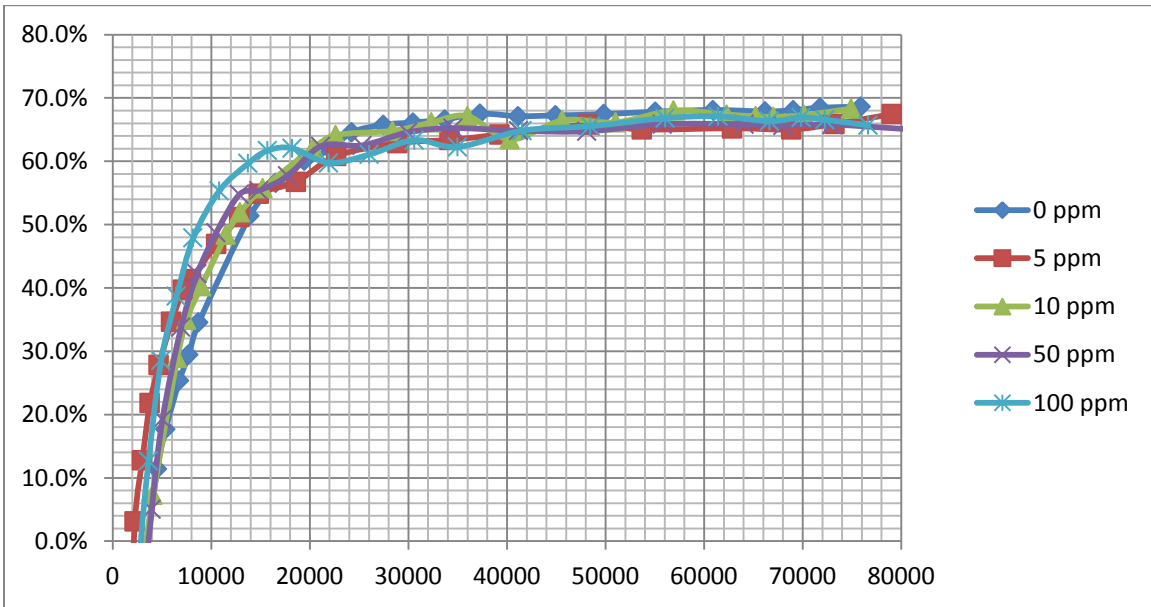


Figure 6.19. %DR vs. Re_g for the mixed system of PAM (1000 ppm) and SDS (0, 5, 10, 50, 100 ppm) in 1-inch pipe (compared with Dodge-Metzner equation)

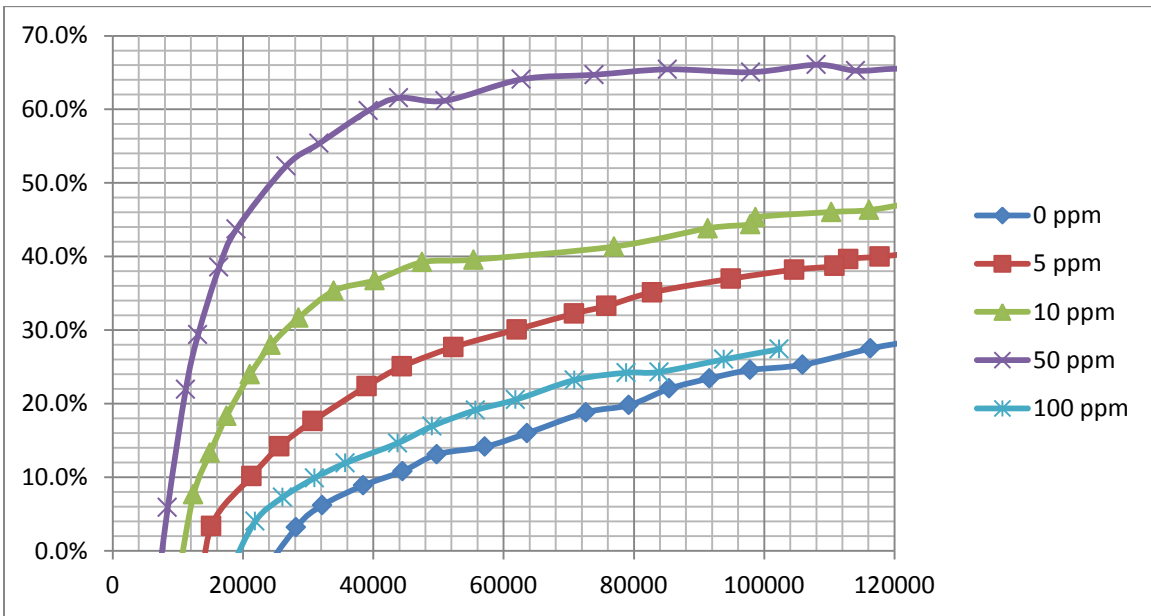


Figure 6.20. %DR vs. Re_g for the mixed system of PAM (500 ppm) and SDS (0, 5, 10, 50, 100 ppm) in 1-inch pipe (compared with Dodge-Metzner equation)

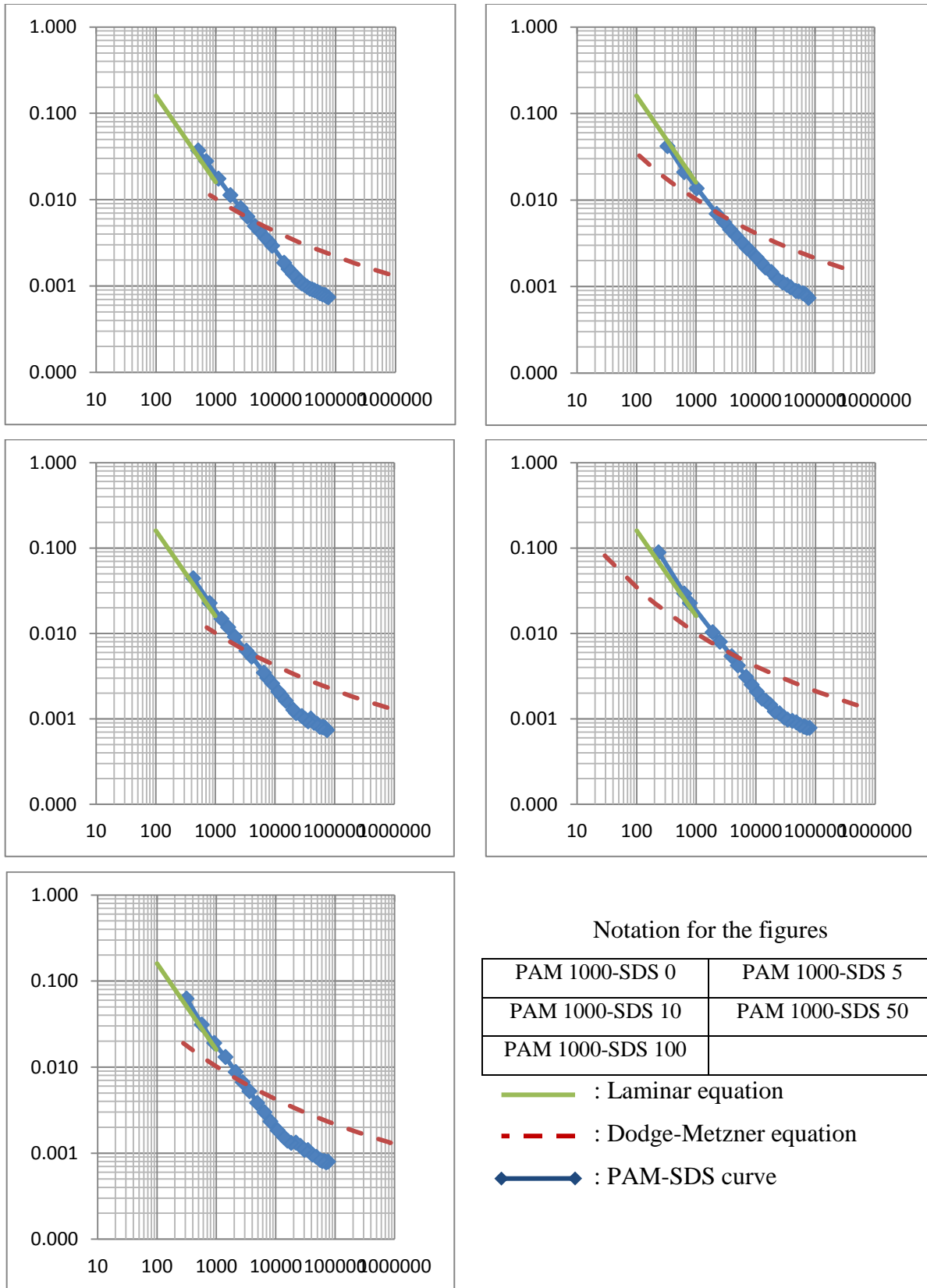


Figure 6.21. Friction factor vs. Re_g for the PAM-SDS system (1000ppm) in 1 inch pipe

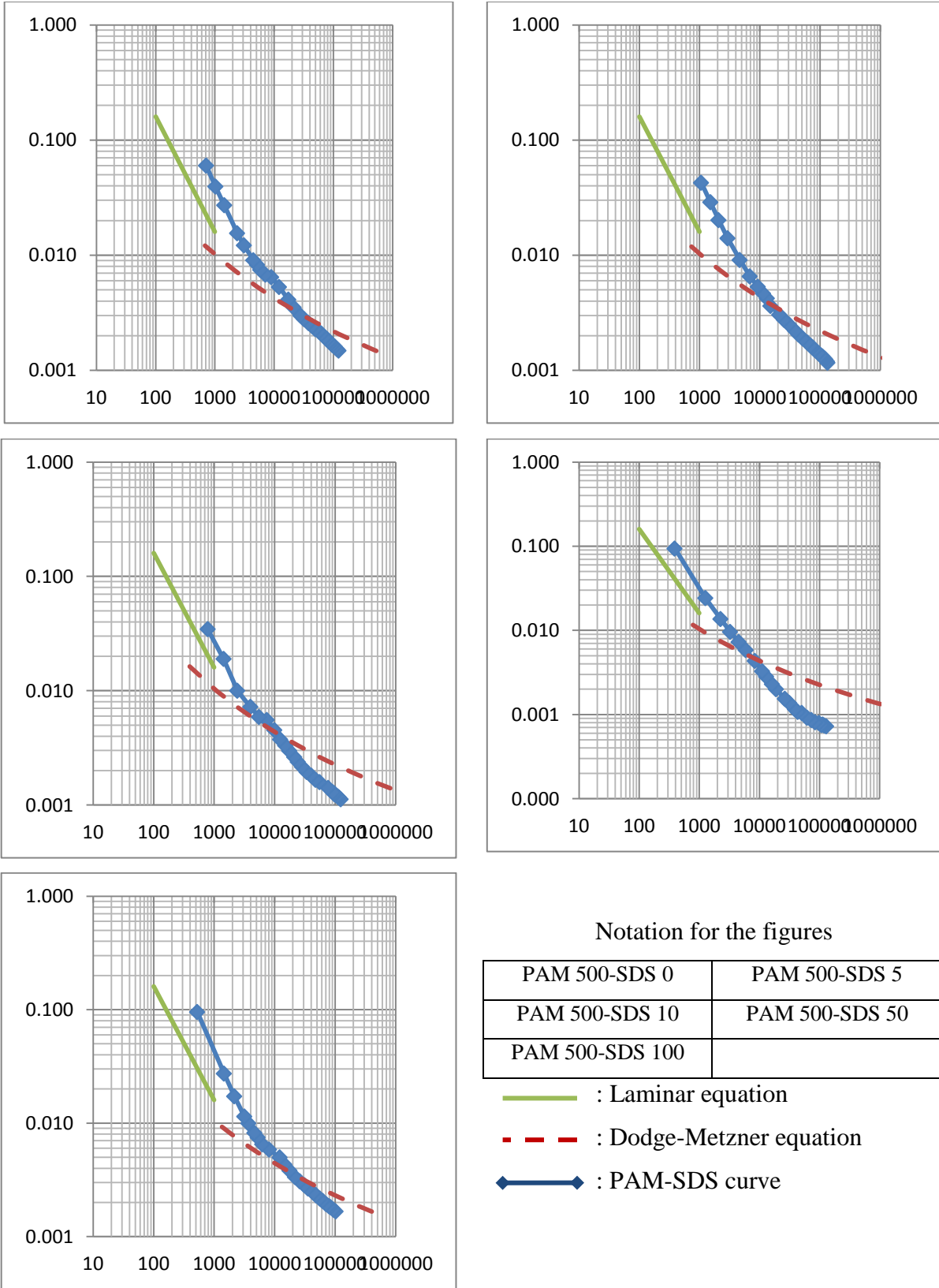


Figure 6.22. Friction factor vs. Re_g for the PAM-SDS system (500ppm) in 1 inch pipe

6.3. Conclusion

In summary, for the 1000ppm PAM solutions, the addition of SDS does not have a big impact on the drag reduction effect of in 1-inch pipe and 1.5-inch pipe. On contrary, the drag reduction effect of the 500ppm PAM solutions are greatly affected by the addition of SDS. The interaction between PAM and SDS is not likely to be electrostatic because both substances have anionic groups. Therefore, the hydrophobic interaction plays an important role between SDS and PAM.

Since the viscosity of the solutions remains almost the same in the whole range (Figures 6.1 and 6.2), viscosity change is not likely to cause the change of the drag reduction effect in the PAM-SDS system. Hence, the stretching and shrinkage of the polymer chains plays an important role on the drag reduction effect. Adding SDS in the solution can alter the polymer conformation and the structure of the polymer network. Therefore, the drag reduction effect of the PAM-SDS system can be changed by the addition of SDS.

The comparison between the 500ppm and the 1000ppm PAM series finds that the addition of SDS has bigger impact on the drag reduction effect of the 500ppm PAM solutions than the 1000ppm PAM solutions. This suggests that the 1000ppm PAM solution is less accessible to SDS molecules because of the formation of an interconnected polymer network. Consequently, SDS is less effective in interacting with the polymer at high PAM concentration.

References

- [1] Toms, B. Some observations on the flow of linear polymer solutions through straight tubes at large Reynolds numbers, North Holland, Amsterdam.(1948).
- [2] Harwigsson, I. and M. Hellsten "Environmentally acceptable drag-reducing surfactants for district heating and cooling." Journal of the American Oil Chemists' Society **73**(7): 921-928 (1996).
- [3] Stoll, M., H. Al-Shureqi, J. Finol, S. Al-Harthy, S. Oyemade, A. de Kruijf, J. Van Wunnik, F. Arkesteijn, R. Bouwmeester and M. Faber Alkaline-Surfactant-Polymer Flood: From the Laboratory to the Field. SPE EOR Conference at Oil & Gas West Asia, Muscat, Oman.(2010), DOI: 10.2118/129164-MS.
- [4] Yoo, S. S. (1974). Heat transfer and friction factors for non-Newtonian fluids in turbulent pipe flow, University of Illinois at Chicago Circle.
- [5] Lumley, J. "Drag reduction by additives." Annual Review of Fluid Mechanics **1**(1): 367-384 (1969).
- [6] Hinch, E. "Mechanical models of dilute polymer solutions in strong flows." Physics of Fluids **20**: S22 (1977).
- [7] Metzner, A. and A. Metzner "Stress levels in rapid extensional flows of polymeric fluids." Rheologica Acta **9**(2): 174-181 (1970).
- [8] Lumley, J. "Drag reduction in turbulent flow by polymer additives." Journal of Polymer Science: Macromolecular Reviews **7**(1): 263-290 (1973).
- [9] Mysels, K. J. "Napalm. Mixture of Aluminum Disoaps." Industrial & Engineering Chemistry **41**(7): 1435-1438 (1949).
- [10] Dodge, D. and A. Metzner "Turbulent flow of non Newtonian systems." AIChE Journal **5**(2): 189-204 (1959).
- [11] Zakin, J. L. and H. L. Lui "VARIABLES AFFECTING DRAG REDUCTION BY NONIONIC SURFACTANT ADDITIVES†." Chemical Engineering Communications **23**(1): 77-88 (1983).
- [12] Qi, Y. and J. L. Zakin "Chemical and rheological characterization of drag-reducing cationic surfactant systems." Industrial & engineering chemistry research **41**(25): 6326-6336 (2002).
- [13] Zakin, J. L., J. Myska and Z. Chara "New limiting drag reduction and velocity profile asymptotes for nonpolymeric additives systems." AIChE Journal **42**(12): 3544-3546 (1996).

- [14] Bai, G., M. Nichifor and M. Bastos "Cationic Polyelectrolytes as Drug Delivery Vectors: Calorimetric and Fluorescence Study of Rutin Partitioning[†]." *The Journal of Physical Chemistry B* **114**(49) (2010).
- [15] Dan, A., S. Ghosh and S. P. Moulik "Physicochemistry of the Interaction between Inulin and Alkyltrimethylammonium Bromides in Aqueous Medium and the Formed Coacervates." *The Journal of Physical Chemistry B* **113**(25): 8505-8513 (2009).
- [16] Harada, A. and K. Kataoka "Supramolecular assemblies of block copolymers in aqueous media as nanocontainers relevant to biological applications." *Progress in polymer science* **31**(11): 949-982 (2006).
- [17] Villetti, M. A., C. I. D. Bica, I. T. S. Garcia, F. V. Pereira, F. I. Ziembowicz, C. L. Kloster and C. Giacomelli "Physicochemical Properties of Methylcellulose and Dodecyltrimethylammonium Bromide in Aqueous Medium." *The Journal of Physical Chemistry B* **115**(19) (2011).
- [18] Zhang, X., D. Taylor, R. Thomas and J. Penfold "The role of electrolyte and polyelectrolyte on the adsorption of the anionic surfactant, sodium dodecylbenzenesulfonate, at the air-water interface." *Journal of colloid and interface science* **365**(2): P:656-664 (2011).
- [19] Feitosa, E., W. Brown and P. Hansson "Interactions between the Non-ionic Surfactant C12E5 and Poly (ethylene oxide) Studied Using Dynamic Light Scattering and Fluorescence Quenching." *Macromolecules* **29**(6): 2169-2178 (1996).
- [20] Jönsson, B., B. Lindman, K. Holmberg and B. Kronberg, *Surfactants and polymers in aqueous solution*, John Wiley & Sons Chichester, UK (1998).
- [21] Diamant, H. and D. Andelman "Onset of self-assembly in polymer-surfactant systems." *EPL (Europhysics Letters)* **48**: 170 (1999).
- [22] Hansson, P. and B. Lindman "Surfactant-polymer interactions." *Current opinion in colloid & interface science* **1**(5): 604-613 (1996).
- [23] Zakin, J. L., B. Lu and H. W. Bewersdorff "Surfactant drag reduction." *Reviews in Chemical Engineering* **14**(4-5): 253-320 (1998).
- [24] Gyr, A. and H. W. Bewersdorff, *Drag reduction of turbulent flows by additives*, Kluwer Academic (Dordrecht and Boston) (1995).
- [25] Metzner, A. and M. G. Park "Turbulent flow characteristics of viscoelastic fluids." *Journal of Fluid Mechanics* **20**(02): 291-303 (1964).
- [26] Virk, P. "Drag reduction fundamentals." *AIChE Journal* **21**(4): 625-656 (1975).

- [27] Zakin, J. and D. Hunston "Effects of solvent nature on the mechanical degradation of high polymer solutions." *Journal of Applied Polymer Science* **22**(6): 1763-1766 (1978).
- [28] Zakin, J. L., M. Poreh, A. Brosh and M. Warshavsky Exploratory study of friction reduction in slurry flows.(1971).
- [29] Berman, N. S. "Drag reduction by polymers." *Annual Review of Fluid Mechanics* **10**(1): 47-64 (1978).
- [30] Tabor, M. and P. G. Gennes "A cascade theory of drag reduction." *EPL (Europhysics Letters)* **2**: 519 (1986).
- [31] Escudier, M., F. Presti and S. Smith "Drag reduction in the turbulent pipe flow of polymers." *Journal of non-newtonian fluid mechanics* **81**(3): 197-213 (1998).
- [32] Zakin, J. L. (2010) "Polymer and Surfactant Drag Reduction in Turbulent Flows." *Polymer Physics: From Suspensions to Nanocomposites and Beyond* DOI: 10.1002 / 9780470600160.ch2.
- [33] Sreenivasan, K. R. and C. M. White "The onset of drag reduction by dilute polymer additives, and the maximum drag reduction asymptote." *Journal of Fluid Mechanics* **409** (2000).
- [34] Ptasinski, P., F. Nieuwstadt, B. Van Den Brule and M. Hulsen "Experiments in turbulent pipe flow with polymer additives at maximum drag reduction." *Flow, Turbulence and Combustion* **66**(2): 159-182 (2001).
- [35] Kim, S. (2003). Turbulent drag reduction behavior of pseudoplastic fluids in straight pipes. Canada, University of Waterloo (Canada). **Ph.D.:** 335.
- [36] Vanapalli, S. A., S. L. Ceccio and M. J. Solomon "Universal scaling for polymer chain scission in turbulence." *Proceedings of the National Academy of Sciences* **103**(45): 16660 (2006).
- [37] Shah, S. N. and Y. Zhou "Maximum Drag Reduction Asymptote of Polymeric Fluid Flow in Coiled Tubing." *Journal of fluids engineering* **131**: 011201 (2009).
- [38] Tamano, S., M. Itoh, K. Kato and K. Yokota "Turbulent drag reduction in nonionic surfactant solutions." *Physics of Fluids* **22**: 055102 (2010).
- [39] Virk, P. and E. W. Merrill (1969). "The Onset of Dilute Polymer Solution Phenomena". in *Viscous Drag Reduction*, CS Wells(Ed.), , Plenum Press, New York: p107-130.
- [40] Ohlendorf, D., W. Interthal and H. Hoffmann "Surfactant systems for drag reduction: physico-chemical properties and rheological behaviour." *Rheologica Acta* **25**(5): 468-486 (1986).
- [41] Wilson, K. and A. Thomas "Analytic Model of Laminar Turbulent Transition for Bingham Plastics." *The Canadian Journal of Chemical Engineering* **84**(5): 520-526 (2006).

- [42] Tiederman, W. The effect of dilute polymer solutions on viscous drag and turbulent structure.(1989).
- [43] Warholic, M., H. Massah and T. Hanratty "Influence of drag-reducing polymers on turbulence: effects of Reynolds number, concentration and mixing." *Experiments in fluids* **27**(5): 461-472 (1999).
- [44] Graham, M. "Drag reduction in turbulent flow of polymer solutions." *Rheology Reviews*: 143 (2004).
- [45] White, C. M. Mungal, M. G. "Mechanics and prediction of turbulent drag reduction with polymer additives". *Fluid mechanics*: 40, 235-256 (2008).
- [46] Hoyt, J. W. Sellin, R. H. J. "Polymer threads and drag reduction". *Rheol. Acta.* (1991) 30, 307-315.
- [47] Vleggaar, J. Tels, M. "Drag reduction by polymer threads". *Chemical engineering science.* (1973) Vol 28, Issue 3, 965-968.
- [48] Zhang, Y. (2005). Correlations among surfactant drag reduction, additive chemical structures, rheological properties and microstructures in water and water/co-solvent systems, The Ohio State University,Phd Thesis.
- [49] K. Madlener, B. Frey, and H.K. Ciezki. Generalized Reynolds number for non-Newtonian fluids. *Progress in Propulsion Physics* 1 (2009) 237-250.
- [50] M. D. Graham. Drag reduction in turbulent flow of polymer solutions. *Rheology reviews* 2004, 143-170.

Appendices

Appendix A. PAM-CMC Experiment data

Appendix A-1. Bench-scale experiment data

Surface tension vs. PAM weight fraction for the PAM-CMC system (total concentration 1000ppm)

PAM weight fraction	Surface tension (Dynes/cm)				
	1	2	3	Average	RSD
0%	69.4	69.2	69.1	69.2	0.2
25%	69.1	69.2	69.0	69.1	0.1
50%	68.7	68.3	68.5	68.5	0.3
75%	67.3	67.2	67.3	67.3	0.1
100%	65.6	65.6	65.5	65.6	0.1

Conductivity vs. PAM weight fraction for the PAM-CMC system (total concentration 1000ppm)

PAM weight fraction	Conductivity ($\mu\text{S}/\text{cm}$)				
	1	2	3	Average	RSD
0%	1.086	1.084	1.083	1.084	0.1
25%	1.095	1.097	1.099	1.097	0.2
50%	1.11	1.111	1.113	1.111	0.1
75%	1.116	1.117	1.119	1.117	0.1
100%	1.122	1.122	1.119	1.121	0.2

Viscosity data for the PAM-CMC solution (1000ppm CMC - 0ppm PAM)

RPM	0.9	1.8	30	60	90	100	200
Ω	0.094	0.188	3.140	6.280	9.420	10.467	20.933
$\ln(\Omega)$	-2.362	-1.669	1.144	1.837	2.243	2.348	3.041
Dail Reading	6.5	7	22.5	33	42.5	45	65
Shear stress	0.2033	0.2473	1.6129	2.5379	3.3749	3.5951	5.3571
$\ln(\text{Shear stress})$	-1.593	-1.397	0.478	0.931	1.216	1.280	1.678
N	1.5644	1.5644	1.5644	1.5644	1.5644	1.5644	1.5644
Shear rate	1.6368	3.2736	54.5597	109.1193	163.6790	181.8655	363.7311
$\log(\text{Shear rate})$	0.2140	0.5150	1.7369	2.0379	2.2140	2.2598	2.5608
$\log(\text{Shear stress})$	-0.692	-0.607	0.208	0.404	0.528	0.556	0.729
n	0.6379	0.6379	0.6379	0.6379	0.6379	0.6379	0.6379
k	0.128	0.128	0.128	0.128	0.128	0.128	0.128
η	0.1068	0.0831	0.0300	0.0233	0.0202	0.0194	0.0151

Viscosity data for the PAM-CMC solution (750ppm CMC - 250ppm PAM)

RPM	0.9	1.8	30	60	90	100	200
Ω	0.094	0.188	3.140	6.280	9.420	10.467	20.933
$\ln(\Omega)$	-2.362	-1.669	1.144	1.837	2.243	2.348	3.041
Dail Reading	7.5	9	28	40.5	51	53.5	79.5
Shear stress	0.2914	0.4235	2.0974	3.1987	4.1237	4.3440	6.6346
$\ln(\text{shear stress})$	-1.233	-0.859	0.741	1.163	1.417	1.469	1.892
N	1.647	1.647	1.647	1.647	1.647	1.647	1.647
Shear rate	1.6451	3.2902	54.8366	109.6732	164.5099	182.7887	365.5774
$\log(\text{shear rate})$	0.2162	0.5172	1.7391	2.0401	2.2162	2.2619	2.5630
$\log(\text{Shear stress})$	-0.536	-0.373	0.322	0.505	0.615	0.638	0.822
n	0.6071	0.6071	0.6071	0.6071	0.6071	0.6071	0.6071
k	0.185	0.185	0.185	0.185	0.185	0.185	0.185
η	0.1519	0.1157	0.0383	0.0292	0.0249	0.0239	0.0182

Viscosity data for the PAM-CMC solution (500ppm CMC - 500ppm PAM)

RPM	0.9	1.8	30	60	90	100	200
Ω	0.094	0.188	3.140	6.280	9.420	10.467	20.933
$\ln(\Omega)$	-2.362	-1.669	1.144	1.837	2.243	2.348	3.041
Dail Reading	10	11	29	42	52	54	76.5
Shear stress	0.5116	0.5997	2.1855	3.3308	4.2118	4.3880	6.3703
$\ln(\text{shear stress})$	-0.670	-0.511	0.782	1.203	1.438	1.479	1.852
N	1.771	1.771	1.771	1.771	1.771	1.771	1.771
Shear rate	1.6576	3.3151	55.2524	110.5048	165.7572	184.1746	368.3493
$\log(\text{shear rate})$	0.2195	0.5205	1.7424	2.0434	2.2195	2.2652	2.5663
$\log(\text{Shear stress})$	-0.291	-0.222	0.340	0.523	0.624	0.642	0.804
n	0.5638	0.5638	0.5638	0.5638	0.5638	0.5638	0.5638
k	0.232	0.232	0.232	0.232	0.232	0.232	0.232
η	0.1858	0.1373	0.0402	0.0297	0.0249	0.0238	0.0176

Viscosity data for the PAM-CMC solution (250ppm CMC - 750ppm PAM)

RPM	0.9	1.8	30	60	90	100	200
Ω	0.094	0.188	3.140	6.280	9.420	10.467	20.933
$\ln(\Omega)$	-2.362	-1.669	1.144	1.837	2.243	2.348	3.041
Dail Reading	13	16	32	42	50	51.5	72
Shear stress	0.7759	1.0402	2.4498	3.3308	4.0356	4.1678	5.9738
$\ln(\text{shear stress})$	-0.254	0.039	0.896	1.203	1.395	1.427	1.787
N	2.1347	2.1347	2.1347	2.1347	2.1347	2.1347	2.1347
Shear rate	1.6947	3.3894	56.4902	112.9805	169.4707	188.3008	376.6017
$\log(\text{shear rate})$	0.2291	0.5301	1.7520	2.0530	2.2291	2.2749	2.5759
$\log(\text{Shear stress})$	-0.110	0.017	0.389	0.523	0.606	0.620	0.776
n	0.4675	0.4675	0.4675	0.4675	0.4675	0.4675	0.4675
k	0.367	0.367	0.367	0.367	0.367	0.367	0.367
η	0.2773	0.1917	0.0429	0.0296	0.0239	0.0226	0.0156

Viscosity data for the PAM-CMC solution (0ppm CMC - 1000ppm PAM)

RPM	0.9	1.8	30	60	90	100	200
Ω	0.094	0.188	3.140	6.280	9.420	10.467	20.933
$\ln(\Omega)$	-2.362	-1.669	1.144	1.837	2.243	2.348	3.041
Dail Reading	17	20	34	41	47	48	67
Shear stress	1.1283	1.3926	2.6260	3.2427	3.7713	3.8594	5.5333
$\ln(\text{shear stress})$	0.121	0.331	0.965	1.176	1.327	1.351	1.711
N	2.5235	2.5235	2.5235	2.5235	2.5235	2.5235	2.5235
Shear rate	1.7349	3.4699	57.8310	115.6620	173.4930	192.7700	385.5401
$\log(\text{shear rate})$	0.2393	0.5403	1.7622	2.0632	2.2393	2.2850	2.5861
$\log(\text{Shear stress})$	0.052	0.144	0.419	0.511	0.576	0.587	0.743
n	0.3874	0.3874	0.3874	0.3874	0.3874	0.3874	0.3874
k	0.525	0.525	0.525	0.525	0.525	0.525	0.525
η	0.3745	0.2449	0.0437	0.0286	0.0223	0.0209	0.0137

Apparent viscosity vs. PAM weight fraction for the PAM-CMC system (total concentration 1000ppm)

PAM weight fraction	30rpm	90rpm	200rpm
0%	0.0300	0.0202	0.0151
25%	0.0383	0.0249	0.0182
50%	0.0402	0.0249	0.0176
75%	0.0429	0.0239	0.0156
100%	0.0437	0.0223	0.0137

Surface tension vs. PAM weight fraction for the PAM-CMC system (total concentration 500ppm)

PAM weight fraction	Surface tension (Dynes/cm)				
	1	2	3	Average	RSD
0%	69.3	69.3	69.4	69.3	0.1
25%	69.1	69.1	69.0	69.1	0.1
50%	69.0	69.1	69.1	69.1	0.1
75%	69.0	69.0	69.0	69.0	0.0
100%	69.0	69.0	69.0	69.0	0.0

Conductivity vs. PAM weight fraction for the PAM-CMC system (total concentration 500ppm)

PAM weight fraction	Conductivity ($\mu\text{S}/\text{cm}$)				
	1	2	3	Average	RSD
0%	0.56	0.56	0.559	0.560	0.1
25%	0.570	0.573	0.573	0.572	0.3
50%	0.588	0.587	0.59	0.588	0.3
75%	0.617	0.614	0.612	0.614	0.4
100%	0.586	0.583	0.586	0.585	0.3

Viscosity data for the PAM-CMC solution (500ppm CMC - 0ppm PAM)

RPM	0.9	1.8	30	60	90	100	200
Ω	0.094	0.188	3.140	6.280	9.420	10.467	20.933
$\ln(\Omega)$	-2.362	-1.669	1.144	1.837	2.243	2.348	3.041
Dail Reading	6	6.5	14.5	20.5	26.5	28	39
Shear stress	0.1592	0.2033	0.9081	1.4367	1.9653	2.0974	3.0665
$\ln(\text{Shear stress})$	-1.8376	-1.5933	-0.0965	0.3623	0.6756	0.7407	1.1205
N	1.5276	1.5276	1.5276	1.5276	1.5276	1.5276	1.5276
Shear rate	1.63	3.27	54.44	108.87	163.31	181.46	362.91
$\log(\text{Shear rate})$	0.2130	0.5140	1.7359	2.0369	2.2130	2.2588	2.5598
$\log(\text{Shear stress})$	-0.798	-0.692	-0.042	0.157	0.293	0.322	0.487
n	0.6511	0.6511	0.6511	0.6511	0.6511	0.6511	0.6511
k	0.069	0.069	0.069	0.069	0.069	0.069	0.069
η	0.0578	0.0454	0.0170	0.0134	0.0116	0.0112	0.0088

Viscosity data for the PAM-CMC solution (375ppm CMC - 125ppm PAM)

RPM	0.9	1.8	30	60	90	100	200
Ω	0.094	0.188	3.140	6.280	9.420	10.467	20.933
$\ln(\Omega)$	-2.362	-1.669	1.144	1.837	2.243	2.348	3.041
Dail Reading	8	8.5	19	24	29.5	31	45
Shear stress	0.3354	0.3795	1.3045	1.7450	2.2296	2.3617	3.5951
$\ln(\text{Shear stress})$	-1.0924	-0.9690	0.2658	0.5568	0.8018	0.8594	1.2796
N	1.8458	1.8458	1.8458	1.8458	1.8458	1.8458	1.8458
Shear rate	1.67	3.33	55.51	111.01	166.52	185.02	370.05
$\log(\text{Shear rate})$	0.2215	0.5225	1.7443	2.0454	2.2215	2.2672	2.5683
$\log(\text{Shear stress})$	-0.474	-0.421	0.115	0.242	0.348	0.373	0.556
n	0.5371	0.5371	0.5371	0.5371	0.5371	0.5371	0.5371
k	0.145	0.145	0.145	0.145	0.145	0.145	0.145
η	0.1146	0.0831	0.0226	0.0164	0.0136	0.0129	0.0094

Viscosity data for the PAM-CMC solution (250ppm CMC - 250ppm PAM)

RPM	0.9	1.8	30	60	90	100	200
Ω	0.094	0.188	3.140	6.280	9.420	10.467	20.933
$\ln(\Omega)$	-2.362	-1.669	1.144	1.837	2.243	2.348	3.041
Dail Reading	8.5	9	19.5	26.5	31.5	33	45
Shear stress	0.3795	0.4235	1.3486	1.9653	2.4058	2.5379	3.5951
$\ln(\text{Shear stress})$	-0.9690	-0.8592	0.2990	0.6756	0.8779	0.9313	1.2796
N	1.937	1.937	1.937	1.937	1.937	1.937	1.937
Shear rate	1.67	3.35	55.82	111.63	167.45	186.05	372.11
$\log(\text{Shear rate})$	0.2239	0.5249	1.7468	2.0478	2.2239	2.2696	2.5707
$\log(\text{Shear stress})$	-0.421	-0.373	0.130	0.293	0.381	0.404	0.556
n	0.516	0.516	0.516	0.516	0.516	0.516	0.516
k	0.171	0.171	0.171	0.171	0.171	0.171	0.171
η	0.1330	0.0951	0.0244	0.0174	0.0143	0.0136	0.0097

Viscosity data for the PAM-CMC solution (125ppm CMC - 375ppm PAM)

RPM	0.9	1.8	30	60	90	100	200
Ω	0.094	0.188	3.140	6.280	9.420	10.467	20.933
$\ln(\Omega)$	-2.362	-1.669	1.144	1.837	2.243	2.348	3.041
Dail Reading	12	14	20	27	30.5	31.5	44
Shear stress	0.6878	0.8640	1.3926	2.0093	2.3177	2.4058	3.5070
$\ln(\text{Shear stress})$	-0.3743	-0.1462	0.3312	0.6978	0.8406	0.8779	1.2548
N	2.357	2.357	2.357	2.357	2.357	2.357	2.357
Shear rate	1.72	3.44	57.25	114.51	171.76	190.85	381.70
$\log(\text{Shear rate})$	0.2349	0.5360	1.7578	2.0588	2.2349	2.2807	2.5817
$\log(\text{Shear stress})$	-0.163	-0.063	0.144	0.303	0.365	0.381	0.545
n	0.4764	0.4764	0.4764	0.4764	0.4764	0.4764	0.4764
k	0.203	0.203	0.203	0.203	0.203	0.203	0.203
η	0.1530	0.1064	0.0244	0.0170	0.0137	0.0130	0.0090

Viscosity data for the PAM-CMC solution (0ppm CMC - 500ppm PAM)

RPM	0.9	1.8	30	60	90	100	200
Ω	0.094	0.188	3.140	6.280	9.420	10.467	20.933
$\ln(\Omega)$	-2.362	-1.669	1.144	1.837	2.243	2.348	3.041
Dail Reading	10	11.5	20	25.5	29.5	31	42.5
Shear stress	0.5116	0.6438	1.3926	1.8772	2.2296	2.3617	3.3749
$\ln(\text{Shear stress})$	-0.6702	-0.4404	0.3312	0.6298	0.8018	0.8594	1.2164
N	2.1487	2.1487	2.1487	2.1487	2.1487	2.1487	2.1487
Shear rate	1.70	3.39	56.54	113.08	169.61	188.46	376.92
$\log(\text{Shear rate})$	0.2295	0.5305	1.7523	2.0534	2.2295	2.2752	2.5763
$\log(\text{Shear stress})$	-0.291	-0.191	0.144	0.273	0.348	0.373	0.528
n	0.4638	0.4638	0.4638	0.4638	0.4638	0.4638	0.4638
k	0.211	0.211	0.211	0.211	0.211	0.211	0.211
η	0.1587	0.1094	0.0242	0.0167	0.0134	0.0127	0.0088

Apparent viscosity vs. PAM weight fraction for the PAM-CMC system (total concentration 500ppm)

PEO weight fraction	30rpm	90rpm	200rpm
0%	0.0170	0.0116	0.0088
25%	0.0226	0.0136	0.0094
50%	0.0244	0.0143	0.0097
75%	0.0265	0.0140	0.0088
100%	0.0242	0.0134	0.0088

Appendix A-2. Flow loop experiment data

Flow loop data for the PAM-CMC solution (1000ppm CMC - 0ppm PAM) in 1.5-inch pipe

FR signal	PD signal	Velocity	Re	f	%DR*	fs	%DR**
5.025	2.871	6.427	22820	0.002	39.7%	0.005	51.8%
4.791	2.710	6.054	21035	0.002	38.8%	0.005	51.5%
4.602	2.594	5.752	19621	0.002	37.7%	0.005	51.0%
4.397	2.464	5.425	18118	0.002	36.7%	0.005	50.5%
4.256	2.394	5.200	17102	0.002	35.1%	0.005	49.6%
4.033	2.244	4.845	15529	0.003	34.5%	0.005	49.6%
3.850	2.147	4.553	14269	0.003	32.8%	0.005	48.7%
3.695	2.068	4.305	13224	0.003	31.1%	0.005	47.7%
3.525	1.975	4.034	12103	0.003	29.6%	0.005	47.1%
3.383	1.897	3.808	11187	0.003	28.5%	0.006	46.9%
3.199	1.802	3.514	10029	0.003	26.6%	0.006	46.0%
3.038	1.718	3.258	9044	0.003	25.2%	0.006	45.7%
2.879	1.643	3.004	8099	0.003	23.1%	0.006	44.9%
2.746	1.586	2.792	7330	0.004	20.5%	0.006	43.5%
2.581	1.511	2.529	6405	0.004	18.0%	0.007	42.6%
2.444	1.446	2.310	5663	0.004	16.7%	0.007	42.9%
2.315	4.942	2.104	4988	0.004	8.4%	0.007	38.5%
2.230	4.576	1.969	4555	0.005	6.2%	0.007	37.7%
2.111	4.091	1.779	3968	0.005	2.5%	0.008	36.3%
1.957	3.513	1.533	3241	0.005	-4.0%	0.008	34.4%
1.853	3.114	1.368	2773	0.006	-8.1%	0.009	33.2%
1.752	2.699	1.206	2338	0.006	-10.1%	0.009	33.5%
1.625	2.224	1.004	1820	0.007	-13.2%	0.010	34.6%
1.503	1.939	0.809	1357	0.008	-31.1%	0.011	28.0%
1.385	1.638	0.621	946	0.010	-51.5%	0.013	24.5%
1.307	1.455	0.497	698	0.012	-73.0%	0.015	19.1%
1.240	1.298	0.390	502	0.014	-97.3%	0.017	13.7%
1.185	1.160	0.302	355	0.017	-116.3%	0.020	14.5%
1.118	1.092	0.195	196	0.032	-267.1%	0.026	-21.7%

* Percent drag reduction based on Blasius equation

** Percent drag reduction based on Dodge-Metzner equation

Flow loop data for the PAM-CMC solution (750ppm CMC - 250ppm PAM) in 1.5-inch pipe

FR signal	PD signal	Velocity	Re	f	%DR*	fs	%DR**
5.106	2.230	6.660	20321	0.001	62.3%	0.005	70.1%
5.008	2.200	6.501	19649	0.001	61.7%	0.005	69.7%
4.906	2.186	6.336	18957	0.001	60.4%	0.005	68.8%
4.746	2.151	6.077	17885	0.002	58.7%	0.005	67.6%
4.589	2.103	5.822	16851	0.002	57.3%	0.005	66.8%
4.441	2.066	5.583	15892	0.002	55.7%	0.005	65.7%
4.254	2.011	5.280	14704	0.002	53.7%	0.005	64.5%
4.091	1.954	5.016	13689	0.002	52.2%	0.005	63.6%
3.903	1.890	4.711	12545	0.002	50.4%	0.005	62.5%
3.671	1.811	4.335	11173	0.002	47.8%	0.005	61.1%
3.454	1.754	3.983	9931	0.002	43.8%	0.006	58.7%
3.301	1.690	3.735	9081	0.002	42.6%	0.006	58.3%
3.105	1.631	3.418	8024	0.003	38.8%	0.006	56.2%
2.953	1.575	3.172	7230	0.003	36.7%	0.006	55.3%
2.826	1.539	2.966	6585	0.003	33.4%	0.006	53.6%
2.638	1.473	2.661	5662	0.003	29.7%	0.007	52.0%
2.527	1.430	2.481	5137	0.003	28.1%	0.007	51.6%
2.377	4.845	2.238	4450	0.004	18.4%	0.007	46.1%
2.269	4.475	2.063	3973	0.004	14.6%	0.007	44.7%
2.101	3.901	1.791	3262	0.005	7.9%	0.008	42.0%
2.014	3.559	1.650	2910	0.005	5.5%	0.008	41.6%
1.930	3.302	1.514	2581	0.005	0.5%	0.009	40.0%
1.835	3.112	1.360	2223	0.006	-10.8%	0.009	34.1%
1.749	2.652	1.221	1912	0.006	-6.8%	0.010	38.4%
1.617	2.234	1.007	1462	0.007	-15.2%	0.011	37.2%
1.535	1.988	0.874	1201	0.007	-21.6%	0.011	36.4%
1.448	1.753	0.733	940	0.008	-31.7%	0.013	35.4%
1.369	1.572	0.605	719	0.010	-47.9%	0.014	31.4%
1.308	1.427	0.506	561	0.011	-62.3%	0.016	30.7%
1.25	1.309	0.412	422	0.013	-86.1%	0.018	25.2%
1.199	1.211	0.330	309	0.017	-118.3%	0.021	20.1%
1.143	1.095	0.239	197	0.022	-165.1%	0.026	14.9%

* Percent drag reduction based on Blasius equation

** Percent drag reduction based on Dodge-Metzner equation

Flow loop data for the PAM-CMC solution (500ppm CMC - 500ppm PAM) in 1.5-inch pipe

FR signal	PD signal	Velocity	Re	f	%DR*	fs	%DR**
4.810	1.799	6.177	19817	0.001	72.3%	0.004	76.5%
4.709	1.773	6.013	19068	0.001	72.0%	0.004	76.3%
4.565	1.762	5.780	18015	0.001	70.4%	0.004	75.2%
4.401	1.719	5.515	16839	0.001	69.7%	0.005	74.8%
4.250	1.706	5.270	15777	0.001	67.8%	0.005	73.5%
4.039	1.669	4.928	14329	0.001	65.8%	0.005	72.0%
3.842	1.632	4.609	13016	0.001	63.7%	0.005	70.7%
3.680	1.588	4.347	11965	0.001	62.7%	0.005	70.4%
3.512	1.571	4.075	10905	0.002	59.5%	0.005	68.2%
3.274	1.515	3.690	9454	0.002	56.7%	0.005	66.4%
3.059	1.471	3.341	8200	0.002	53.0%	0.006	64.1%
2.883	1.430	3.056	7214	0.002	50.1%	0.006	62.7%
2.731	4.908	2.810	6395	0.002	44.4%	0.006	59.2%
2.560	4.489	2.533	5510	0.003	40.2%	0.006	56.8%
2.438	4.236	2.336	4903	0.003	35.8%	0.007	54.7%
2.262	3.797	2.051	4067	0.003	29.8%	0.007	51.9%
1.998	3.118	1.623	2907	0.004	18.5%	0.008	47.4%
1.919	2.963	1.495	2584	0.005	12.3%	0.008	44.5%
1.823	2.702	1.340	2207	0.005	6.8%	0.009	42.1%
1.749	2.504	1.220	1929	0.005	1.9%	0.009	40.9%
1.649	2.257	1.058	1572	0.006	-7.3%	0.010	39.1%
1.534	1.955	0.872	1191	0.007	-18.6%	0.011	36.3%
1.443	1.721	0.725	913	0.008	-29.7%	0.012	33.9%
1.370	1.566	0.606	707	0.010	-46.1%	0.014	30.8%
1.277	1.353	0.456	469	0.012	-70.6%	0.017	27.6%
1.208	1.189	0.344	313	0.014	-90.6%	0.020	29.5%
1.142	1.100	0.237	184	0.023	-173.6%	0.026	13.3%

* Percent drag reduction based on Blasius equation

** Percent drag reduction based on Dodge-Metzner equation

Flow loop data for the PAM-CMC solution (250ppm CMC - 750ppm PAM) in 1.5-inch pipe

FR signal	PD signal	Velocity	Re	f	%DR*	fs	%DR**
5.115	2.218	6.566	27630	0.001	62.4%	0.003	60.4%
4.932	2.147	6.274	25772	0.001	61.7%	0.004	60.0%
4.802	2.112	6.067	24479	0.001	60.6%	0.004	59.2%
4.545	2.028	5.657	21992	0.002	58.9%	0.004	58.0%
4.411	1.979	5.444	20733	0.002	58.2%	0.004	57.5%
4.225	1.941	5.147	19028	0.002	55.7%	0.004	55.5%
4.110	1.896	4.964	17999	0.002	55.1%	0.004	55.3%
3.912	1.832	4.648	16275	0.002	53.3%	0.004	54.0%
3.770	1.797	4.422	15077	0.002	51.3%	0.004	52.6%
3.568	1.725	4.100	13428	0.002	49.5%	0.004	51.6%
3.344	1.660	3.743	11678	0.002	46.3%	0.004	49.8%
3.191	1.613	3.499	10532	0.002	44.0%	0.005	48.1%
2.990	1.545	3.179	9091	0.003	41.3%	0.005	47.0%
2.789	1.482	2.859	7725	0.003	37.8%	0.005	45.3%
2.615	1.426	2.581	6607	0.003	34.6%	0.005	44.0%
2.455	4.747	2.326	5633	0.003	26.8%	0.006	38.7%
2.319	4.339	2.109	4849	0.004	22.2%	0.006	37.0%
2.137	3.790	1.819	3865	0.004	15.0%	0.006	34.1%
2.038	3.445	1.662	3364	0.004	12.0%	0.007	33.7%
1.946	3.175	1.515	2920	0.005	7.3%	0.007	31.4%
1.794	2.768	1.273	2235	0.006	-3.9%	0.008	27.9%
1.708	2.327	1.136	1877	0.005	2.1%	0.008	34.4%
1.616	2.044	0.989	1519	0.006	-1.1%	0.009	34.9%
1.474	1.824	0.763	1020	0.008	-30.3%	0.011	25.6%
1.388	1.615	0.625	753	0.009	-45.3%	0.012	23.7%
1.322	1.454	0.520	568	0.011	-59.1%	0.014	23.3%
1.227	1.254	0.369	335	0.015	-96.6%	0.018	19.2%
1.161	1.135	0.264	200	0.020	-153.2%	0.024	14.4%

* Percent drag reduction based on Blasius equation

** Percent drag reduction based on Dodge-Metzner equation

Flow loop data for the PAM-CMC solution (0ppm CMC - 1000ppm PAM) in 1.5-inch pipe

FR signal	PD signal	Velocity	Re	f	%DR*	fs	%DR**
5.071	1.851	6.491	33700	0.001	73.4%	0.003	65.6%
4.968	1.843	6.327	32337	0.001	72.4%	0.003	64.6%
4.803	1.830	6.064	30199	0.001	70.8%	0.003	62.8%
4.702	1.801	5.903	28918	0.001	70.5%	0.003	62.7%
4.581	1.786	5.711	27410	0.001	69.3%	0.003	61.5%
4.441	1.771	5.488	25705	0.001	67.7%	0.003	60.0%
4.219	1.718	5.134	23088	0.001	66.3%	0.003	58.7%
4.026	1.684	4.827	20900	0.001	64.3%	0.003	56.8%
3.838	1.652	4.527	18849	0.002	62.0%	0.003	54.8%
3.674	1.611	4.266	17126	0.002	60.5%	0.003	53.8%
3.495	1.574	3.981	15319	0.002	58.3%	0.004	51.9%
3.308	1.527	3.683	13513	0.002	56.2%	0.004	50.6%
3.118	1.487	3.380	11768	0.002	53.1%	0.004	48.1%
2.959	1.445	3.127	10380	0.002	51.1%	0.004	47.3%
2.773	1.408	2.831	8841	0.002	46.9%	0.004	44.2%
2.585	4.592	2.532	7382	0.003	39.4%	0.005	38.6%
2.452	4.276	2.320	6412	0.003	35.3%	0.005	36.0%
2.333	3.952	2.130	5588	0.003	32.0%	0.005	34.7%
2.238	3.752	1.979	4962	0.004	27.6%	0.005	32.1%
2.118	3.444	1.788	4213	0.004	22.7%	0.006	29.6%
2.011	3.177	1.617	3584	0.004	17.3%	0.006	27.9%
1.927	2.970	1.484	3118	0.005	12.3%	0.006	25.1%
1.752	2.229	1.205	2229	0.005	17.6%	0.007	35.0%
1.629	1.953	1.009	1674	0.005	9.8%	0.008	35.3%
1.519	1.906	0.834	1231	0.007	-20.6%	0.009	19.6%
1.433	1.715	0.697	922	0.009	-35.7%	0.010	16.1%
1.333	1.504	0.537	606	0.011	-62.4%	0.013	12.3%
1.248	1.361	0.402	380	0.015	-112.1%	0.016	1.8%
1.158	1.167	0.259	187	0.024	-189.5%	0.024	1.0%

* Percent drag reduction based on Blasius equation

** Percent drag reduction based on Dodge-Metzner equation

Flow loop data for the PAM-CMC solution (1000ppm CMC - 0ppm PAM) in 1-inch pipe

FR signal	PD signal	Velocity	Re	f	%DR*	fs	%DR**
3.809	3.447	11.208	36350	0.002	43.8%	0.004	50.6%
3.739	3.315	10.929	35124	0.002	44.4%	0.004	51.3%
3.664	3.231	10.630	33822	0.002	43.8%	0.004	50.9%
3.541	3.081	10.140	31717	0.002	43.1%	0.004	50.5%
3.378	2.879	9.491	28983	0.002	42.4%	0.004	50.3%
3.230	2.714	8.901	26558	0.002	41.2%	0.004	49.6%
3.059	2.501	8.220	23829	0.002	40.9%	0.005	49.8%
2.932	2.368	7.714	21854	0.002	39.9%	0.005	49.4%
2.747	2.173	6.977	19060	0.002	38.7%	0.005	48.9%
2.569	1.986	6.268	16471	0.003	38.1%	0.005	49.1%
2.407	1.851	5.623	14205	0.003	35.6%	0.005	47.7%
2.302	1.774	5.204	12786	0.003	33.1%	0.005	46.3%
2.154	1.650	4.615	10854	0.003	31.0%	0.006	45.4%
2.065	1.588	4.260	9734	0.003	28.4%	0.006	44.2%
1.947	1.509	3.790	8301	0.004	24.3%	0.006	42.1%
1.784	1.404	3.141	6427	0.004	17.4%	0.007	38.8%
1.706	4.189	2.830	5576	0.004	16.2%	0.007	39.2%
1.540	3.373	2.169	3881	0.005	-1.1%	0.008	30.3%
1.419	2.729	1.687	2756	0.007	-17.1%	0.009	23.4%
1.367	2.489	1.480	2305	0.008	-28.6%	0.009	18.0%
1.339	2.380	1.368	2072	0.008	-37.8%	0.010	14.8%
1.311	2.255	1.257	1845	0.009	-46.9%	0.010	9.9%
1.275	2.118	1.113	1564	0.010	-64.1%	0.011	3.1%
1.234	1.989	0.950	1260	0.013	-94.8%	0.012	-10.4%
1.184	1.831	0.751	915	0.018	-153.9%	0.013	-35.1%
1.089	1.610	0.372	352	0.056	-574.1%	0.020	-184.4%

* Percent drag reduction based on Blasius equation

** Percent drag reduction based on Dodge-Metzner equation

Flow loop data for the PAM-CMC solution (750ppm CMC - 250ppm PAM) in 1-inch pipe

FR signal	PD signal	Velocity	Re	f	%DR*	fs	%DR**
4.170	2.456	12.846	38430	0.001	73.4%	0.004	76.2%
4.080	2.299	12.482	36920	0.001	75.1%	0.004	77.8%
3.957	2.198	11.985	34886	0.001	75.3%	0.004	78.1%
3.828	2.180	11.462	32787	0.001	73.7%	0.004	76.8%
3.666	2.093	10.807	30205	0.001	73.1%	0.004	76.3%
3.553	2.049	10.350	28440	0.001	72.1%	0.004	75.7%
3.431	2.026	9.856	26568	0.001	70.3%	0.004	74.2%
3.222	1.929	9.010	23447	0.001	68.6%	0.004	73.1%
3.040	1.851	8.274	20821	0.001	66.7%	0.005	71.8%
2.856	1.764	7.529	18257	0.001	64.8%	0.005	70.6%
2.713	1.660	6.950	16333	0.001	65.2%	0.005	71.2%
2.560	1.564	6.331	14342	0.001	65.2%	0.005	71.6%
2.278	1.505	5.190	10874	0.002	56.0%	0.005	65.2%
2.108	1.476	4.502	8920	0.002	47.0%	0.006	59.0%
1.965	4.914	3.923	7364	0.003	41.5%	0.006	55.9%
1.858	4.437	3.490	6257	0.003	36.6%	0.006	53.3%
1.738	4.078	3.005	5078	0.004	25.8%	0.007	47.0%
1.627	3.279	2.555	4053	0.004	25.8%	0.007	48.5%
1.540	3.107	2.203	3297	0.005	10.6%	0.008	40.5%
1.484	2.948	1.977	2834	0.006	-0.5%	0.008	33.9%
1.432	2.747	1.766	2423	0.006	-10.8%	0.009	29.1%
1.359	2.447	1.471	1878	0.008	-28.7%	0.010	22.6%
1.327	2.328	1.341	1651	0.008	-40.0%	0.010	16.4%
1.260	2.111	1.070	1206	0.011	-77.6%	0.011	-0.3%
1.208	1.963	0.860	889	0.016	-130.4%	0.013	-18.5%
1.117	1.832	0.491	408	0.042	-441.8%	0.018	-129.5%

* Percent drag reduction based on Blasius equation

** Percent drag reduction based on Dodge-Metzner equation

Flow loop data for the PAM-CMC solution (500ppm CMC - 500ppm PAM) in 1-inch pipe

FR signal	PD signal	Velocity	Re	f	%DR*	fs	%DR**
4.115	2.199	12.617	42702	0.001	77.4%	0.004	78.0%
4.024	2.179	12.249	40925	0.001	76.6%	0.004	77.3%
3.876	2.109	11.650	38083	0.001	76.0%	0.004	76.8%
3.687	2.047	10.886	34546	0.001	74.6%	0.004	75.6%
3.523	1.940	10.222	31564	0.001	74.6%	0.004	75.8%
3.299	1.835	9.316	27625	0.001	73.5%	0.004	75.1%
3.112	1.755	8.560	24462	0.001	72.3%	0.004	74.2%
2.993	1.710	8.079	22511	0.001	71.2%	0.004	73.5%
2.810	1.657	7.338	19609	0.001	68.5%	0.004	71.5%
2.679	1.618	6.809	17609	0.001	66.3%	0.004	69.8%
2.515	1.546	6.145	15198	0.001	64.5%	0.005	68.7%
2.379	1.503	5.595	13283	0.002	61.6%	0.005	66.7%
2.278	1.472	5.187	11913	0.002	59.0%	0.005	64.9%
2.178	1.442	4.782	10602	0.002	55.9%	0.005	62.8%
2.067	4.856	4.333	9202	0.002	51.6%	0.005	59.8%
1.972	4.588	3.949	8053	0.002	46.8%	0.006	56.7%
1.875	4.356	3.557	6930	0.003	40.1%	0.006	52.3%
1.751	4.079	3.055	5571	0.004	28.0%	0.006	44.5%
1.626	3.719	2.550	4296	0.005	12.2%	0.007	35.0%
1.573	3.620	2.335	3787	0.005	1.1%	0.007	28.2%
1.538	3.555	2.194	3462	0.006	-7.8%	0.008	23.4%
1.488	3.429	1.992	3013	0.007	-21.7%	0.008	14.7%
1.417	3.152	1.704	2409	0.008	-42.8%	0.009	4.7%
1.355	2.914	1.454	1917	0.010	-69.2%	0.009	-8.7%
1.296	2.746	1.215	1482	0.013	-112.9%	0.010	-29.0%
1.241	2.710	0.993	1108	0.019	-197.6%	0.011	-71.2%
1.175	2.693	0.726	707	0.036	-410.2%	0.014	-161.9%
1.131	2.680	0.548	472	0.063	-728.8%	0.017	-274.5%

* Percent drag reduction based on Blasius equation

** Percent drag reduction based on Dodge-Metzner equation

Flow loop data for the PAM-CMC solution (250ppm CMC - 750ppm PAM) in 1-inch pipe

FR signal	PD signal	Velocity	Re	f	%DR*	fs	%DR**
4.123	2.772	12.450	59471	0.001	66.2%	0.003	58.2%
3.962	2.644	11.809	54844	0.001	65.7%	0.003	57.8%
3.852	2.588	11.371	51758	0.001	64.6%	0.003	56.7%
3.677	2.463	10.674	46979	0.001	63.6%	0.003	56.0%
3.469	2.333	9.846	41511	0.001	61.9%	0.003	54.5%
3.307	2.224	9.202	37418	0.001	60.6%	0.003	53.6%
3.107	2.105	8.405	32572	0.002	58.4%	0.003	51.7%
2.948	2.012	7.772	28889	0.002	56.4%	0.003	50.2%
2.768	1.901	7.056	24909	0.002	54.1%	0.004	48.3%
2.593	1.804	6.359	21241	0.002	51.0%	0.004	45.9%
2.405	1.696	5.611	17532	0.002	47.4%	0.004	43.2%
2.251	1.612	4.998	14684	0.002	43.6%	0.004	40.7%
2.005	1.484	4.018	10512	0.003	35.2%	0.005	35.3%
1.813	1.386	3.254	7608	0.004	26.1%	0.005	29.8%
1.694	4.237	2.780	5978	0.004	12.4%	0.006	20.1%
1.581	3.779	2.331	4561	0.005	-3.3%	0.006	10.3%
1.485	3.359	1.948	3466	0.007	-21.1%	0.007	0.4%
1.399	2.946	1.606	2578	0.008	-42.1%	0.007	-9.7%
1.353	2.741	1.423	2141	0.009	-58.6%	0.008	-18.7%
1.295	2.516	1.192	1633	0.012	-90.6%	0.009	-34.1%
1.229	2.339	0.929	1115	0.017	-163.7%	0.010	-69.2%
1.157	2.138	0.643	633	0.032	-335.6%	0.013	-137.4%
1.127	2.062	0.523	462	0.045	-487.8%	0.016	-189.2%

* Percent drag reduction based on Blasius equation

** Percent drag reduction based on Dodge-Metzner equation

Flow loop data for the PAM-CMC solution (0ppm CMC - 1000ppm PAM) in 1-inch pipe

FR signal	PD signal	Velocity	Re	f	%DR*	fs	%DR**
4.069	2.107	12.226	78352	0.001	78.4%	0.002	66.3%
3.963	2.053	11.804	74041	0.001	78.2%	0.002	66.1%
3.892	2.027	11.522	71205	0.001	77.8%	0.002	65.7%
3.816	1.991	11.220	68216	0.001	77.6%	0.002	65.5%
3.672	1.909	10.647	62688	0.001	77.5%	0.002	65.7%
3.507	1.830	9.990	56575	0.001	77.1%	0.002	65.5%
3.354	1.763	9.382	51121	0.001	76.5%	0.002	65.0%
3.206	1.695	8.793	46048	0.001	76.1%	0.003	64.9%
3.086	1.640	8.316	42084	0.001	75.8%	0.003	64.9%
2.960	1.577	7.815	38070	0.001	75.7%	0.003	65.3%
2.840	1.539	7.337	34391	0.001	74.8%	0.003	64.3%
2.727	1.497	6.888	31057	0.001	74.1%	0.003	63.8%
2.617	1.456	6.450	27938	0.001	73.4%	0.003	63.6%
2.495	1.420	5.965	24627	0.001	72.0%	0.003	62.3%
2.411	4.905	5.631	22441	0.001	69.5%	0.003	59.5%
2.301	4.604	5.193	19696	0.001	67.5%	0.003	57.7%
2.175	4.349	4.692	16722	0.002	63.8%	0.003	53.8%
2.053	4.167	4.206	14022	0.002	58.4%	0.004	48.6%
1.784	3.743	3.136	8734	0.003	39.4%	0.004	30.7%
1.725	3.623	2.902	7705	0.003	33.4%	0.004	25.6%
1.667	3.450	2.671	6741	0.004	27.8%	0.005	21.3%
1.576	3.171	2.309	5330	0.004	16.8%	0.005	13.2%
1.517	2.988	2.074	4484	0.005	7.5%	0.005	7.5%
1.429	2.757	1.724	3328	0.006	-14.2%	0.006	-7.4%
1.364	2.575	1.466	2561	0.008	-37.3%	0.007	-21.1%
1.283	2.333	1.143	1716	0.011	-82.6%	0.008	-46.2%
1.211	2.138	0.857	1078	0.018	-163.0%	0.010	-80.1%
1.156	1.984	0.638	670	0.028	-288.5%	0.012	-137.9%
1.128	1.882	0.527	492	0.038	-395.2%	0.014	-170.1%

* Percent drag reduction based on Blasius equation

** Percent drag reduction based on Dodge-Metzner equation

Flow loop data for the PAM-CMC solution (500ppm CMC - 0ppm PAM) in 1.5-inch pipe

FR signal	PD signal	Velocity	Re	f	%DR*	fs	%DR**
4.945	3.831	6.395	37723	0.003	6.2%	0.004	15.9%
4.737	3.578	6.058	35068	0.003	6.1%	0.004	16.3%
4.632	3.450	5.888	33747	0.003	6.3%	0.004	16.9%
4.504	3.316	5.681	32154	0.004	5.7%	0.004	16.1%
4.385	3.184	5.488	30692	0.004	5.6%	0.004	16.7%
4.253	3.042	5.275	29091	0.004	5.4%	0.004	16.8%
4.101	2.890	5.028	27275	0.004	4.9%	0.004	16.6%
3.948	2.742	4.781	25478	0.004	4.3%	0.005	16.8%
3.766	2.569	4.486	23382	0.004	3.8%	0.005	16.9%
3.575	2.393	4.177	21235	0.004	3.4%	0.005	16.9%
3.430	2.273	3.942	19640	0.004	2.4%	0.005	16.9%
3.230	2.097	3.618	17496	0.004	2.5%	0.005	17.8%
3.061	1.959	3.344	15735	0.004	2.5%	0.005	18.6%
2.879	1.829	3.050	13894	0.004	1.2%	0.005	18.5%
2.739	1.730	2.823	12519	0.004	0.8%	0.005	18.8%
2.457	1.550	2.366	9868	0.005	-0.9%	0.006	19.7%
2.335	1.473	2.169	8773	0.005	-0.5%	0.006	21.1%
2.251	1.430	2.033	8039	0.005	-1.9%	0.006	20.6%
2.098	4.433	1.785	6746	0.005	-8.7%	0.007	17.2%
2.005	3.967	1.635	5990	0.006	-10.4%	0.007	17.1%
1.906	3.483	1.474	5212	0.006	-11.8%	0.007	17.4%
1.803	3.032	1.307	4432	0.006	-14.5%	0.008	17.4%
1.698	2.586	1.137	3673	0.007	-16.4%	0.008	18.4%
1.588	2.183	0.959	2919	0.007	-20.7%	0.009	17.9%
1.451	1.739	0.737	2047	0.008	-28.3%	0.010	18.3%
1.360	1.498	0.590	1516	0.009	-38.9%	0.011	16.0%
1.273	1.293	0.449	1049	0.011	-54.6%	0.013	13.1%
1.205	1.178	0.339	718	0.014	-89.4%	0.015	2.0%
1.146	1.085	0.244	459	0.020	-146.2%	0.018	-14.5%
1.126	1.060	0.211	379	0.024	-184.4%	0.019	-25.3%

* Percent drag reduction based on Blasius equation

** Percent drag reduction based on Dodge-Metzner equation

Flow loop data for the PAM-CMC solution (375ppm CMC - 125ppm PAM) in 1.5-inch pipe

FR signal	PD signal	Velocity	Re	f	%DR*	fs	%DR**
5.018	3.547	6.517	41395	0.003	18.3%	0.003	13.6%
4.876	3.397	6.287	39275	0.003	18.2%	0.003	13.8%
4.724	3.265	6.041	37045	0.003	17.1%	0.004	13.1%
4.581	3.141	5.809	34985	0.003	16.2%	0.004	12.7%
4.349	2.923	5.433	31724	0.003	15.4%	0.004	13.0%
4.139	2.731	5.093	28860	0.003	14.9%	0.004	13.3%
3.945	2.576	4.779	26292	0.003	13.4%	0.004	12.1%
3.785	2.438	4.519	24232	0.003	13.0%	0.004	12.7%
3.622	2.315	4.255	22189	0.004	11.7%	0.004	12.0%
3.464	2.185	3.999	20264	0.004	11.5%	0.004	12.7%
3.270	2.049	3.685	17977	0.004	9.8%	0.004	13.0%
3.030	1.880	3.296	15271	0.004	8.3%	0.005	12.9%
2.838	1.754	2.985	13209	0.004	6.9%	0.005	12.6%
2.659	1.635	2.695	11375	0.004	6.7%	0.005	14.2%
2.517	1.552	2.465	9983	0.004	5.6%	0.005	15.0%
2.348	1.456	2.191	8403	0.005	5.0%	0.005	16.1%
2.198	4.816	1.948	7076	0.005	-3.3%	0.006	11.3%
2.036	4.025	1.686	5726	0.005	-6.6%	0.006	11.2%
1.959	3.655	1.561	5117	0.006	-7.8%	0.006	11.7%
1.864	3.238	1.407	4396	0.006	-10.2%	0.007	12.6%
1.778	2.883	1.268	3774	0.006	-12.7%	0.007	12.8%
1.695	2.568	1.133	3203	0.007	-16.0%	0.007	12.6%
1.623	2.299	1.017	2732	0.007	-18.5%	0.008	13.5%
1.519	1.942	0.848	2096	0.007	-23.1%	0.009	15.6%
1.414	1.643	0.678	1510	0.008	-32.9%	0.010	14.2%
1.296	1.352	0.487	930	0.011	-51.8%	0.012	12.5%
1.241	1.236	0.398	692	0.012	-67.7%	0.014	10.0%
1.183	1.15	0.304	467	0.016	-111.1%	0.016	-0.7%
1.146	1.096	0.244	338	0.021	-156.9%	0.019	-11.3%
1.108	1.040	0.182	221	0.030	-235.8%	0.024	-26.2%

* Percent drag reduction based on Blasius equation

** Percent drag reduction based on Dodge-Metzner equation

Flow loop data for the PAM-CMC solution (250ppm CMC - 250ppm PAM) in 1.5-inch pipe

FR signal	PD signal	Velocity	Re	f	%DR*	fs	%DR**
5.112	3.105	6.661	42195	0.002	35.2%	0.003	29.3%
4.994	3.020	6.470	40413	0.002	34.6%	0.003	28.7%
4.861	2.930	6.255	38434	0.002	33.8%	0.003	28.3%
4.593	2.733	5.821	34547	0.003	32.6%	0.003	28.0%
4.465	2.637	5.614	32738	0.003	32.2%	0.004	27.9%
4.277	2.517	5.310	30141	0.003	30.8%	0.004	26.8%
4.102	2.397	5.027	27786	0.003	30.0%	0.004	27.0%
3.931	2.291	4.750	25547	0.003	28.6%	0.004	26.0%
3.761	2.189	4.475	23382	0.003	27.1%	0.004	25.3%
3.581	2.073	4.184	21160	0.003	26.1%	0.004	25.1%
3.395	1.967	3.883	18941	0.003	24.3%	0.004	24.9%
3.213	1.863	3.588	16848	0.003	22.6%	0.004	23.6%
3.011	1.754	3.261	14622	0.003	20.4%	0.004	22.8%
2.804	1.650	2.926	12449	0.004	17.4%	0.005	21.4%
2.646	1.565	2.671	10870	0.004	16.1%	0.005	22.6%
2.498	1.495	2.431	9455	0.004	13.8%	0.005	21.2%
2.385	1.440	2.248	8419	0.004	12.6%	0.005	21.2%
2.220	4.649	1.981	6979	0.005	4.1%	0.006	16.4%
2.056	3.940	1.716	5638	0.005	-0.5%	0.006	15.1%
1.960	3.534	1.561	4897	0.005	-3.1%	0.006	15.4%
1.873	3.182	1.420	4256	0.006	-5.8%	0.007	14.8%
1.794	2.877	1.292	3700	0.006	-8.5%	0.007	14.2%
1.682	2.458	1.111	2957	0.006	-12.4%	0.008	15.5%
1.587	2.138	0.957	2370	0.007	-17.1%	0.008	15.9%
1.473	1.870	0.773	1725	0.008	-35.3%	0.009	8.3%
1.378	1.545	0.619	1241	0.009	-36.8%	0.010	14.3%
1.297	1.354	0.488	872	0.011	-51.6%	0.012	13.1%
1.208	1.188	0.344	519	0.014	-90.2%	0.015	5.1%
1.147	1.1	0.245	314	0.021	-158.1%	0.019	-11.7%
1.097	1.037	0.164	173	0.036	-296.5%	0.026	-38.3%

* Percent drag reduction based on Blasius equation

** Percent drag reduction based on Dodge-Metzner equation

Flow loop data for the PAM-CMC solution (125ppm CMC - 375ppm PAM) in 1.5-inch pipe

FR signal	PD signal	Velocity	Re	f	%DR*	fs	%DR**
5.115	2.910	6.585	46945	0.002	40.8%	0.003	29.0%
4.897	2.761	6.237	43213	0.002	40.0%	0.003	28.7%
4.716	2.645	5.948	40196	0.002	39.2%	0.003	28.2%
4.510	2.515	5.618	36854	0.002	38.2%	0.003	27.8%
4.263	2.361	5.223	32981	0.002	37.0%	0.003	27.2%
4.067	2.250	4.910	30015	0.003	35.6%	0.003	26.4%
3.912	2.164	4.662	27738	0.003	34.4%	0.003	25.7%
3.680	2.039	4.291	24447	0.003	32.5%	0.004	24.6%
3.488	1.934	3.984	21833	0.003	31.0%	0.004	24.1%
3.268	1.821	3.633	18966	0.003	28.9%	0.004	23.6%
2.948	1.664	3.121	15050	0.003	25.5%	0.004	21.9%
2.770	1.581	2.837	13010	0.003	23.2%	0.004	21.1%
2.574	1.490	2.523	10885	0.004	21.0%	0.005	21.3%
2.445	1.438	2.317	9559	0.004	18.5%	0.005	20.1%
2.296	4.718	2.079	8103	0.004	11.3%	0.005	15.1%
2.197	4.359	1.921	7182	0.005	7.5%	0.005	13.4%
2.062	3.821	1.705	5989	0.005	3.5%	0.006	12.3%
1.951	3.409	1.527	5066	0.005	-0.9%	0.006	11.0%
1.848	3.019	1.363	4258	0.006	-4.5%	0.006	10.9%
1.740	2.631	1.190	3464	0.006	-8.9%	0.007	11.0%
1.592	2.143	0.953	2471	0.007	-16.9%	0.008	10.9%
1.502	1.846	0.810	1926	0.007	-20.3%	0.008	11.9%
1.358	1.486	0.579	1157	0.009	-39.1%	0.010	10.9%
1.258	1.269	0.420	707	0.012	-63.1%	0.013	8.0%
1.177	1.142	0.290	403	0.017	-120.0%	0.017	-3.9%
1.134	1.070	0.221	267	0.023	-170.2%	0.020	-11.7%
1.094	1.035	0.157	159	0.038	-317.6%	0.027	-40.7%

* Percent drag reduction based on Blasius equation

** Percent drag reduction based on Dodge-Metzner equation

Flow loop data for the PAM-CMC solution (0ppm CMC - 500ppm PAM) in 1.5-inch pipe

FR signal	PD signal	Velocity	Re	f	%DR*	fs	%DR**
5.121	2.833	6.687	49906	0.002	44.0%	0.003	30.5%
4.934	2.699	6.384	46474	0.002	43.7%	0.003	30.7%
4.772	2.590	6.121	43570	0.002	43.3%	0.003	30.8%
4.570	2.467	5.794	40041	0.002	42.5%	0.003	30.3%
4.383	2.360	5.491	36869	0.002	41.5%	0.003	29.7%
4.174	2.240	5.152	33433	0.002	40.5%	0.003	29.2%
3.988	2.141	4.850	30475	0.002	39.2%	0.003	28.4%
3.816	2.050	4.572	27826	0.002	38.0%	0.003	27.9%
3.693	1.991	4.372	25983	0.003	36.8%	0.003	27.4%
3.519	1.902	4.090	23454	0.003	35.5%	0.004	26.7%
3.367	1.826	3.844	21319	0.003	34.3%	0.004	26.3%
3.213	1.751	3.594	19229	0.003	33.0%	0.004	25.3%
2.970	1.638	3.200	16089	0.003	30.6%	0.004	24.7%
2.839	1.584	2.988	14479	0.003	28.5%	0.004	23.9%
2.723	1.534	2.800	13103	0.003	27.0%	0.004	23.1%
2.569	1.465	2.550	11352	0.003	25.6%	0.004	23.4%
2.460	1.426	2.374	10167	0.004	23.0%	0.005	22.1%
2.344	4.808	2.186	8956	0.004	15.7%	0.005	16.4%
2.235	4.370	2.009	7868	0.004	13.1%	0.005	15.5%
2.148	4.039	1.868	7036	0.004	10.5%	0.005	14.4%
2.031	3.614	1.678	5969	0.005	6.4%	0.005	13.2%
1.947	3.306	1.542	5241	0.005	3.5%	0.006	12.4%
1.824	2.883	1.343	4237	0.005	-1.9%	0.006	11.0%
1.738	2.591	1.203	3581	0.006	-5.9%	0.007	10.7%
1.640	2.264	1.045	2881	0.006	-10.4%	0.007	11.7%
1.532	1.939	0.870	2173	0.007	-17.5%	0.008	11.1%
1.447	1.69	0.732	1667	0.008	-23.1%	0.009	12.3%
1.378	1.521	0.620	1292	0.009	-32.0%	0.010	12.6%
1.297	1.342	0.489	897	0.010	-47.9%	0.011	10.3%
1.232	1.221	0.383	617	0.013	-72.3%	0.013	6.0%
1.153	1.098	0.255	331	0.019	-139.0%	0.018	-7.9%
1.118	1.048	0.198	225	0.026	-200.5%	0.022	-17.3%
1.093	1.034	0.158	158	0.038	-318.6%	0.027	-41.9%

* Percent drag reduction based on Blasius equation

** Percent drag reduction based on Dodge-Metzner equation

Flow loop data for the PAM-CMC solution (500ppm CMC - 0ppm PAM) in 1-inch pipe

FR signal	PD signal	Velocity	Re	f	%DR*	fs	%DR**
3.815	3.952	11.402	61089	0.002	33.1%	0.004	34.5%
3.719	3.803	11.014	58300	0.002	32.5%	0.004	34.1%
3.658	3.701	10.767	56546	0.002	32.3%	0.004	34.0%
3.566	3.565	10.395	53926	0.002	31.7%	0.004	33.6%
3.494	3.440	10.104	51899	0.002	31.7%	0.004	33.8%
3.395	3.290	9.704	49144	0.003	31.3%	0.004	33.5%
3.255	3.083	9.138	45316	0.003	30.6%	0.004	33.3%
3.116	2.860	8.576	41597	0.003	30.8%	0.004	33.8%
2.938	2.612	7.856	36957	0.003	30.2%	0.004	33.9%
2.810	2.442	7.338	33710	0.003	29.8%	0.004	33.8%
2.661	2.253	6.735	30030	0.003	29.3%	0.004	33.8%
2.531	2.097	6.210	26912	0.003	28.8%	0.004	34.0%
2.362	1.908	5.526	22995	0.003	28.0%	0.005	34.3%
2.218	1.761	4.944	19788	0.003	26.9%	0.005	34.2%
2.040	1.583	4.224	16003	0.003	26.9%	0.005	35.1%
1.941	1.502	3.824	13992	0.003	25.4%	0.005	34.8%
1.816	1.400	3.318	11556	0.004	24.6%	0.006	35.2%
1.759	4.575	3.087	10486	0.004	18.5%	0.006	30.5%
1.684	4.018	2.784	9121	0.004	16.9%	0.006	30.3%
1.627	3.619	2.554	8117	0.004	15.4%	0.006	29.9%
1.565	3.214	2.303	7061	0.005	13.4%	0.006	29.5%
1.468	2.641	1.911	5489	0.005	8.9%	0.007	28.2%
1.362	2.075	1.482	3896	0.006	2.4%	0.008	26.9%
1.297	1.776	1.219	2994	0.006	-4.2%	0.009	25.1%
1.214	1.444	0.883	1939	0.008	-18.5%	0.010	19.5%
1.170	1.294	0.705	1431	0.009	-32.3%	0.011	15.2%
1.134	1.184	0.560	1048	0.011	-50.8%	0.012	8.5%
1.108	1.123	0.455	792	0.014	-79.0%	0.014	-0.7%

* Percent drag reduction based on Blasius equation

** Percent drag reduction based on Dodge-Metzner equation

Flow loop data for the PAM-CMC solution (375ppm CMC - 125ppm PAM) in 1-inch pipe

FR signal	PD signal	Velocity	Re	f	%DR*	fs	%DR**
4.077	3.012	12.469	83642	0.001	61.1%	0.003	53.1%
3.981	2.947	12.081	79857	0.001	60.2%	0.003	52.2%
3.905	2.877	11.773	76901	0.001	59.9%	0.003	51.9%
3.778	2.777	11.259	72040	0.001	59.0%	0.003	51.1%
3.628	2.653	10.652	66431	0.002	58.0%	0.003	50.2%
3.384	2.442	9.665	57619	0.002	56.6%	0.003	49.2%
3.177	2.274	8.827	50463	0.002	55.2%	0.003	48.1%
2.995	2.140	8.091	44425	0.002	53.4%	0.003	46.6%
2.834	2.020	7.439	39290	0.002	51.8%	0.003	45.4%
2.737	1.946	7.047	36295	0.002	50.9%	0.004	44.8%
2.577	1.834	6.399	31522	0.002	48.9%	0.004	43.3%
2.418	1.716	5.756	26996	0.002	47.4%	0.004	42.6%
2.244	1.607	5.052	22305	0.002	44.2%	0.004	40.3%
2.123	1.525	4.562	19215	0.003	42.6%	0.004	39.6%
2.005	1.447	4.085	16345	0.003	41.1%	0.004	39.2%
1.879	1.367	3.575	13449	0.003	33.7%	0.005	33.1%
1.707	1.285	2.879	9797	0.004	27.3%	0.005	29.9%
1.655	1.206	2.668	8768	0.004	24.8%	0.005	28.5%
1.495	1.168	2.021	5839	0.005	16.1%	0.006	24.8%
1.403	1.141	1.649	4335	0.005	8.1%	0.007	21.5%
1.314	1.131	1.289	3023	0.007	-10.2%	0.008	11.1%
1.218	1.194	0.900	1788	0.011	-61.9%	0.009	-15.9%
1.163	1.567	0.678	1180	0.016	-126.7%	0.011	-46.8%
1.109	1.447	0.459	668	0.030	-274.6%	0.014	-111.0%
1.085	1.395	0.362	472	0.043	-419.6%	0.016	-167.5%

* Percent drag reduction based on Blasius equation

** Percent drag reduction based on Dodge-Metzner equation

Flow loop data for the PAM-CMC solution (250ppm CMC - 250ppm PAM) in 1-inch pipe

FR signal	PD signal	Velocity	Re	f	%DR*	fs	%DR**
4.169	2.544	12.826	88094	0.001	71.7%	0.003	64.5%
4.062	2.481	12.393	83722	0.001	71.2%	0.003	64.0%
3.916	2.415	11.803	77875	0.001	70.0%	0.003	62.8%
3.785	2.301	11.274	72748	0.001	70.2%	0.003	63.2%
3.598	2.195	10.518	65630	0.001	69.1%	0.003	62.2%
3.431	2.101	9.843	59478	0.001	68.1%	0.003	61.3%
3.245	2.015	9.091	52863	0.001	66.2%	0.003	59.5%
3.092	1.921	8.473	47616	0.001	65.4%	0.003	58.8%
2.961	1.848	7.943	43268	0.001	64.4%	0.003	58.0%
2.797	1.767	7.281	38020	0.001	62.6%	0.003	56.4%
2.635	1.685	6.626	33058	0.002	60.7%	0.004	54.9%
2.482	1.595	6.008	28585	0.002	59.7%	0.004	54.4%
2.329	1.526	5.389	24330	0.002	57.1%	0.004	52.3%
2.183	1.452	4.799	20483	0.002	55.1%	0.004	51.1%
2.060	1.397	4.302	17415	0.002	52.6%	0.004	49.3%
1.941	4.384	3.821	14605	0.002	46.8%	0.004	44.3%
1.769	3.630	3.126	10842	0.003	40.4%	0.005	40.1%
1.688	3.350	2.799	9200	0.003	35.0%	0.005	36.1%
1.579	2.882	2.358	7135	0.004	28.6%	0.006	32.5%
1.482	2.514	1.966	5448	0.004	19.5%	0.006	27.3%
1.394	2.071	1.610	4051	0.005	15.9%	0.007	27.7%
1.333	1.845	1.364	3166	0.006	8.1%	0.007	24.5%
1.256	1.594	1.053	2156	0.007	-8.6%	0.008	16.7%
1.153	1.323	0.636	1021	0.012	-68.5%	0.011	-10.8%
1.118	1.229	0.495	703	0.016	-111.1%	0.013	-23.3%
1.097	1.197	0.410	532	0.022	-169.6%	0.015	-45.9%

* Percent drag reduction based on Blasius equation

** Percent drag reduction based on Dodge-Metzner equation

Flow loop data for the PAM-CMC solution (125ppm CMC - 375ppm PAM) in 1-inch pipe

FR signal	PD signal	Velocity	Re	f	%DR*	fs	%DR**
4.178	2.236	12.707	102755	0.001	77.3%	0.002	68.4%
4.056	2.227	12.220	96814	0.001	75.9%	0.003	66.6%
3.914	2.122	11.653	90054	0.001	76.1%	0.003	67.0%
3.797	2.068	11.185	84611	0.001	75.6%	0.003	66.5%
3.615	1.966	10.459	76380	0.001	75.2%	0.003	66.3%
3.479	1.911	9.916	70421	0.001	74.3%	0.003	65.4%
3.300	1.824	9.201	62835	0.001	73.6%	0.003	64.8%
3.105	1.758	8.422	54916	0.001	71.7%	0.003	62.7%
2.969	1.704	7.879	49613	0.001	70.5%	0.003	61.6%
2.834	1.639	7.340	44536	0.001	69.8%	0.003	61.0%
2.599	1.543	6.402	36159	0.001	67.6%	0.003	59.1%
2.445	1.480	5.787	31003	0.001	66.0%	0.003	57.8%
2.295	1.426	5.188	26249	0.002	63.6%	0.004	55.8%
2.159	4.691	4.645	22180	0.002	59.4%	0.004	51.6%
2.060	4.345	4.250	19369	0.002	56.8%	0.004	49.4%
1.961	3.982	3.855	16693	0.002	54.1%	0.004	47.3%
1.866	3.683	3.475	14255	0.002	50.2%	0.004	44.0%
1.789	3.394	3.168	12379	0.003	47.4%	0.004	42.0%
1.707	3.084	2.841	10484	0.003	44.0%	0.005	39.9%
1.603	2.715	2.425	8240	0.003	38.3%	0.005	36.0%
1.502	2.323	2.022	6246	0.004	32.9%	0.006	33.6%
1.384	1.963	1.551	4169	0.005	19.1%	0.006	25.7%
1.287	1.644	1.164	2691	0.006	4.0%	0.007	19.5%
1.226	1.455	0.920	1882	0.007	-10.9%	0.008	13.0%
1.166	1.280	0.680	1188	0.010	-34.9%	0.010	6.9%
1.122	1.183	0.505	754	0.014	-77.9%	0.012	-10.6%
1.106	1.140	0.441	614	0.016	-97.5%	0.014	-15.2%

* Percent drag reduction based on Blasius equation

** Percent drag reduction based on Dodge-Metzner equation

Flow loop data for the PAM-CMC solution (0ppm CMC - 500ppm PAM) in 1-inch pipe

FR signal	PD signal	Velocity	Re	f	%DR*	fs	%DR**
4.210	2.223	13.013	112247	0.001	78.2%	0.002	68.4%
4.041	2.120	12.329	103310	0.001	78.1%	0.002	68.5%
3.950	2.075	11.961	98606	0.001	77.8%	0.002	68.2%
3.791	1.987	11.317	90572	0.001	77.6%	0.002	68.2%
3.528	1.869	10.252	77817	0.001	76.6%	0.003	67.2%
3.346	1.780	9.516	69393	0.001	76.1%	0.003	66.9%
3.157	1.685	8.750	61009	0.001	75.8%	0.003	66.9%
3.024	1.639	8.212	55338	0.001	74.9%	0.003	65.9%
2.826	1.570	7.410	47260	0.001	73.3%	0.003	64.3%
2.640	1.504	6.657	40087	0.001	71.6%	0.003	62.7%
2.437	1.426	5.836	32742	0.001	70.0%	0.003	61.5%
2.237	4.579	5.026	26028	0.002	65.2%	0.003	56.5%
2.145	4.297	4.653	23125	0.002	63.2%	0.004	54.7%
2.047	3.960	4.257	20166	0.002	61.1%	0.004	53.0%
1.855	3.369	3.479	14794	0.002	55.2%	0.004	48.0%
1.753	3.063	3.066	12185	0.002	50.8%	0.004	44.6%
1.650	2.719	2.649	9734	0.003	46.3%	0.005	41.5%
1.565	2.458	2.305	7861	0.003	41.0%	0.005	37.8%
1.473	2.164	1.933	5997	0.004	34.2%	0.005	33.8%
1.392	1.916	1.605	4507	0.004	25.9%	0.006	29.3%
1.310	1.681	1.273	3157	0.005	13.1%	0.007	22.6%
1.257	1.515	1.058	2377	0.006	3.5%	0.008	19.1%
1.178	1.309	0.739	1368	0.009	-26.3%	0.010	6.9%
1.127	1.173	0.532	827	0.012	-59.8%	0.012	-3.0%
1.102	1.099	0.431	598	0.014	-80.5%	0.014	-5.9%

* Percent drag reduction based on Blasius equation

** Percent drag reduction based on Dodge-Metzner equation

Appendix B. PEO-CMC Experiment data

Appendix B-1. Bench-scale experiment data

Surface tension vs. PEO weight fraction for the PEO-CMC system (total concentration 1000ppm)

PEO weight fraction	Surface tension (Dynes/cm)				
	1	2	3	Average	RSD
0%	69.4	69.2	69.1	69.2	0.2
25%	60.3	60.5	60.3	60.4	0.2
50%	59.8	59.8	59.8	59.8	0.0
75%	60.1	60.1	60.0	60.1	0.1
100%	60.2	60.3	60.3	60.3	0.1

Conductivity vs. PEO weight fraction for the PEO-CMC system (total concentration 1000ppm)

PEO weight fraction	Conductivity ($\mu\text{S}/\text{cm}$)				
	1	2	3	Average	RSD
0%	1.086	1.084	1.083	1.084	0.1
25%	0.811	0.811	0.813	0.812	0.1
50%	0.537	0.536	0.537	0.537	0.1
75%	0.275	0.275	0.274	0.275	0.2
100%	0.055	0.055	0.055	0.055	0.0

Viscosity data for the PEO-CMC solution (1000ppm CMC - 0ppm PEO)

RPM	0.9	1.8	30	60	90	100	200
Ω	0.094	0.188	3.140	6.280	9.420	10.467	20.933
$\ln(\Omega)$	-2.362	-1.669	1.144	1.837	2.243	2.348	3.041
Dail Reading	6.5	7.0	22.5	33.0	42.5	45.0	65.0
Shear stress	0.2033	0.2473	1.6129	2.5379	3.3749	3.5951	5.3571
$\ln(\text{Shear stress})$	-1.593	-1.397	0.478	0.931	1.216	1.280	1.678
N	1.5644	1.5644	1.5644	1.5644	1.5644	1.5644	1.5644
Shear rate	1.64	3.27	54.56	109.12	163.68	181.87	363.73
$\log(\text{Shear rate})$	0.2140	0.5150	1.7369	2.0379	2.2140	2.2598	2.5608
$\log(\text{Shear stress})$	-0.692	-0.607	0.208	0.404	0.528	0.556	0.729
n	0.6379	0.6379	0.6379	0.6379	0.6379	0.6379	0.6379
k	0.128	0.128	0.128	0.128	0.128	0.128	0.128
η	0.1068	0.0831	0.0300	0.0233	0.0202	0.0194	0.0151

Viscosity data for the PEO-CMC solution (750ppm CMC - 250ppm PEO)

RPM	0.9	1.8	30	60	90	100	200
Ω	0.094	0.188	3.140	6.280	9.420	10.467	20.933
$\ln(\Omega)$	-2.362	-1.669	1.144	1.837	2.243	2.348	3.041
Dail Reading	6.5	7	23	33	43	44.5	68.5
Shear stress	0.2033	0.2473	1.6569	2.5379	3.4189	3.5511	5.6655
$\ln(\text{Shear stress})$	-1.593	-1.397	0.505	0.931	1.229	1.267	1.734
N	1.5367	1.5367	1.5367	1.5367	1.5367	1.5367	1.5367
Shear rate	1.63	3.27	54.47	108.93	163.40	181.56	363.11
$\log(\text{Shear rate})$	0.2133	0.5143	1.7361	2.0372	2.2133	2.2590	2.5600
$\log(\text{Shear stress})$	-0.692	-0.607	0.219	0.404	0.534	0.550	0.753
n	0.6501	0.6501	0.6501	0.6501	0.6501	0.6501	0.6501
k	0.122	0.122	0.122	0.122	0.122	0.122	0.122
η	0.1030	0.0808	0.0302	0.0237	0.0206	0.0198	0.0155

Viscosity data for the PEO-CMC solution (500ppm CMC - 500ppm PEO)

RPM	0.9	1.8	30	60	90	100	200
Ω	0.094	0.188	3.140	6.280	9.420	10.467	20.933
$\ln(\Omega)$	-2.362	-1.669	1.144	1.837	2.243	2.348	3.041
Dail Reading	8.5	10	21	29	37	39	59.5
Shear stress	0.3795	0.5116	1.4807	2.1855	2.8903	3.0665	4.8726
$\ln(\text{Shear stress})$	-0.969	-0.670	0.393	0.782	1.061	1.121	1.584
N	1.5841	1.5841	1.5841	1.5841	1.5841	1.5841	1.5841
Shear rate	1.64	3.28	54.63	109.25	163.88	182.09	364.17
$\log(\text{Shear rate})$	0.2145	0.5155	1.7374	2.0384	2.2145	2.2603	2.5613
$\log(\text{Shear stress})$	-0.421	-0.291	0.170	0.340	0.461	0.487	0.688
n	0.6301	0.6301	0.6301	0.6301	0.6301	0.6301	0.6301
k	0.117	0.117	0.117	0.117	0.117	0.117	0.117
η	0.0971	0.0752	0.0265	0.0205	0.0177	0.0170	0.0132

Viscosity data for the PEO-CMC solution (250ppm CMC - 750ppm PEO)

RPM	0.9	1.8	30	60	90	100	200
Ω	0.094	0.188	3.140	6.280	9.420	10.467	20.933
$\ln(\Omega)$	-2.362	-1.669	1.144	1.837	2.243	2.348	3.041
Dail Reading	6	6.5	16	22.5	28.5	30	44
Shear stress	0.1592	0.2033	1.0402	1.6129	2.1415	2.2736	3.5070
$\ln(\text{Shear stress})$	-1.838	-1.593	0.039	0.478	0.761	0.821	1.255
N	1.5526	1.5526	1.5526	1.5526	1.5526	1.5526	1.5526
Shear rate	1.64	3.27	54.52	109.04	163.56	181.73	363.47
$\log(\text{Shear rate})$	0.2137	0.5147	1.7366	2.0376	2.2137	2.2594	2.5605
$\log(\text{Shear stress})$	-0.798	-0.692	0.017	0.208	0.331	0.357	0.545
n	0.6438	0.6438	0.6438	0.6438	0.6438	0.6438	0.6438
k	0.079	0.079	0.079	0.079	0.079	0.079	0.079
η	0.0666	0.0521	0.0191	0.0149	0.0129	0.0124	0.0097

Viscosity data for the PEO-CMC solution (0ppm CMC - 1000ppm PEO)

RPM	0.9	1.8	30	60	90	100	200
Ω	0.094	0.188	3.140	6.280	9.420	10.467	20.933
$\ln(\Omega)$	-2.362	-1.669	1.144	1.837	2.243	2.348	3.041
Dail Reading	5	5.5	9.5	12	14.5	15.5	22
Shear stress	0.0711	0.1152	0.4676	0.6878	0.9081	0.9962	1.5688
$\ln(\text{Shear stress})$	-2.644	-2.162	-0.760	-0.374	-0.096	-0.004	0.450
N	1.5513	1.5513	1.5513	1.5513	1.5513	1.5513	1.5513
Shear rate	1.64	3.27	54.52	109.03	163.55	181.72	363.44
$\log(\text{Shear rate})$	0.2136	0.5147	1.7365	2.0376	2.2136	2.2594	2.5604
$\log(\text{Shear stress})$	-1.148	-0.939	-0.330	-0.163	-0.042	-0.002	0.196
n	0.6427	0.6427	0.6427	0.6427	0.6427	0.6427	0.6427
k	0.035	0.035	0.035	0.035	0.035	0.035	0.035
η	0.0293	0.0228	0.0084	0.0065	0.0056	0.0054	0.0042

Apparent viscosity vs. PEO weight fraction for the PEO-CMC system (total concentration 1000ppm)

PEO weight fraction	30rpm	90rpm	200rpm
0%	0.0300	0.0202	0.0151
25%	0.0302	0.0206	0.0155
50%	0.0265	0.0177	0.0132
75%	0.0191	0.0129	0.0097
100%	0.0084	0.0056	0.0042

Surface tension vs. PEO weight fraction for the PEO-CMC system (total concentration 500ppm)

PEO weight fraction	Surface tension (Dynes/cm)				
	1	2	3	Average	RSD
0%	69.3	69.3	69.4	69.3	0.1
25%	60.4	60.4	60.3	60.4	0.1
50%	60.3	60.5	60.4	60.4	0.2
75%	60.0	60.2	60.1	60.1	0.2
100%	60.5	60.5	60.6	60.5	0.1

Conductivity vs. PEO weight fraction for the PEO-CMC system (total concentration 500ppm)

PEO weight fraction	Conductivity ($\mu\text{S}/\text{cm}$)				
	1	2	3	Average	RSD
0%	0.56	0.56	0.559	0.560	0.1
25%	0.436	0.435	0.434	0.435	0.2
50%	0.29	0.29	0.292	0.291	0.4
75%	0.154	0.154	0.154	0.154	0.0
100%	0.027	0.027	0.027	0.027	0.0

Viscosity data for the PEO-CMC solution (500ppm CMC - 0ppm PEO)

RPM	0.9	1.8	30	60	90	100	200
Ω	0.094	0.188	3.140	6.280	9.420	10.467	20.933
$\ln(\Omega)$	-2.362	-1.669	1.144	1.837	2.243	2.348	3.041
Dail Reading	6	6.5	14.5	20.5	26.5	28	39
Shear stress	0.1592	0.2033	0.9081	1.4367	1.9653	2.0974	3.0665
$\ln(\text{Shear stress})$	-1.838	-1.593	-0.096	0.362	0.676	0.741	1.121
N	1.5276	1.5276	1.5276	1.5276	1.5276	1.5276	1.5276
Shear rate	1.63	3.27	54.44	108.87	163.31	181.46	362.91
$\log(\text{Shear rate})$	0.2130	0.5140	1.7359	2.0369	2.2130	2.2588	2.5598
$\log(\text{Shear stress})$	-0.798	-0.692	-0.042	0.157	0.293	0.322	0.487
n	0.6511	0.6511	0.6511	0.6511	0.6511	0.6511	0.6511
k	0.069	0.069	0.069	0.069	0.069	0.069	0.069
η	0.0578	0.0454	0.0170	0.0134	0.0116	0.0112	0.0088

Viscosity data for the PEO-CMC solution (375ppm CMC - 125ppm PEO)

RPM	0.9	1.8	30	60	90	100	200
Ω	0.094	0.188	3.140	6.280	9.420	10.467	20.933
$\ln(\Omega)$	-2.362	-1.669	1.144	1.837	2.243	2.348	3.041
Dail Reading	6	6.5	14.5	20.5	25	26	38.5
Shear stress	0.1592	0.2033	0.9081	1.4367	1.8331	1.9212	3.0225
$\ln(\text{Shear stress})$	-1.838	-1.593	-0.096	0.362	0.606	0.653	1.106
N	1.5867	1.5867	1.5867	1.5867	1.5867	1.5867	1.5867
Shear rate	1.64	3.28	54.63	109.27	163.90	182.11	364.23
$\log(\text{Shear rate})$	0.2146	0.5156	1.7375	2.0385	2.2146	2.2603	2.5614
$\log(\text{Shear stress})$	-0.798	-0.692	-0.042	0.157	0.263	0.284	0.480
n	0.6298	0.6298	0.6298	0.6298	0.6298	0.6298	0.6298
k	0.074	0.074	0.074	0.074	0.074	0.074	0.074
η	0.0613	0.0474	0.0167	0.0129	0.0111	0.0107	0.0083

Viscosity data for the PEO-CMC solution (250ppm CMC - 250ppm PEO)

RPM	0.9	1.8	30	60	90	100	200
Ω	0.094	0.188	3.140	6.280	9.420	10.467	20.933
$\ln(\Omega)$	-2.362	-1.669	1.144	1.837	2.243	2.348	3.041
Dail Reading	6	6.5	13	17	21.5	22.5	33
Shear stress	0.1592	0.2033	0.7759	1.1283	1.5248	1.6129	2.5379
$\ln(\text{Shear stress})$	-1.838	-1.593	-0.254	0.121	0.422	0.478	0.931
N	1.582	1.582	1.582	1.582	1.582	1.582	1.582
Shear rate	1.64	3.28	54.62	109.24	163.86	182.06	364.12
$\log(\text{Shear rate})$	0.2145	0.5155	1.7373	2.0384	2.2145	2.2602	2.5612
$\log(\text{Shear stress})$	-0.798	-0.692	-0.110	0.052	0.183	0.208	0.404
n	0.6302	0.6302	0.6302	0.6302	0.6302	0.6302	0.6302
k	0.061	0.061	0.061	0.061	0.061	0.061	0.061
η	0.0507	0.0393	0.0139	0.0107	0.0092	0.0089	0.0069

Viscosity data for the PEO-CMC solution (125ppm CMC - 375ppm PEO)

RPM	0.9	1.8	30	60	90	100	200
Ω	0.094	0.188	3.140	6.280	9.420	10.467	20.933
$\ln(\Omega)$	-2.362	-1.669	1.144	1.837	2.243	2.348	3.041
Dail Reading	6	6	10.5	13	16	17	27
Shear stress	0.1592	0.1592	0.5557	0.7759	1.0402	1.1283	2.0093
$\ln(\text{Shear stress})$	-1.838	-1.838	-0.588	-0.254	0.039	0.121	0.698
N	1.4467	1.4467	1.4467	1.4467	1.4467	1.4467	1.4467
Shear rate	1.62	3.25	54.17	108.33	162.50	180.56	361.11
$\log(\text{Shear rate})$	0.2109	0.5119	1.7337	2.0348	2.2109	2.2566	2.5576
$\log(\text{Shear stress})$	-0.798	-0.798	-0.255	-0.110	0.017	0.052	0.303
n	0.6778	0.6778	0.6778	0.6778	0.6778	0.6778	0.6778
k	0.035	0.035	0.035	0.035	0.035	0.035	0.035
η	0.0295	0.0236	0.0095	0.0076	0.0067	0.0065	0.0052

Viscosity data for the PEO-CMC solution (0ppm CMC - 500ppm PEO)

RPM	0.9	1.8	30	60	90	100	200
Ω	0.094	0.188	3.140	6.280	9.420	10.467	20.933
$\ln(\Omega)$	-2.362	-1.669	1.144	1.837	2.243	2.348	3.041
Dail Reading	5	5.5	7	8.5	10	10.5	14.5
Shear stress	0.0711	0.1152	0.2473	0.3795	0.5116	0.5557	0.9081
$\ln(\text{Shear stress})$	-2.644	-2.162	-1.397	-0.969	-0.670	-0.588	-0.096
N	1.4488	1.4488	1.4488	1.4488	1.4488	1.4488	1.4488
Shear rate	1.63	3.25	54.17	108.35	162.52	180.58	361.16
$\log(\text{Shear rate})$	0.2109	0.5119	1.7338	2.0348	2.2109	2.2567	2.5577
$\log(\text{Shear stress})$	-1.148	-0.939	-0.607	-0.421	-0.291	-0.255	-0.042
n	0.6891	0.6891	0.6891	0.6891	0.6891	0.6891	0.6891
k	0.015	0.015	0.015	0.015	0.015	0.015	0.015
η	0.0133	0.0107	0.0045	0.0036	0.0032	0.0031	0.0025

Apparent viscosity vs. PEO weight fraction for the PEO-CMC system (total concentration 500ppm)

PEO weight fraction	30rpm	90rpm	200rpm
0%	0.0170	0.0116	0.0088
25%	0.0167	0.0111	0.0083
50%	0.0139	0.0092	0.0069
75%	0.0095	0.0067	0.0052
100%	0.0045	0.0032	0.0025

Appendix B-2. Flow loop experiment data

Flow loop data for the PEO-CMC solution (1000ppm CMC - 0ppm PEO) in 1.5-inch pipe

FR signal	PD signal	Velocity	Re	f	%DR*	fs	%DR**
5.025	2.871	6.427	22820	0.002	39.7%	0.005	51.8%
4.791	2.710	6.054	21035	0.002	38.8%	0.005	51.5%
4.602	2.594	5.752	19621	0.002	37.7%	0.005	51.0%
4.397	2.464	5.425	18118	0.002	36.7%	0.005	50.5%
4.256	2.394	5.200	17102	0.002	35.1%	0.005	49.6%
4.033	2.244	4.845	15529	0.003	34.5%	0.005	49.6%
3.850	2.147	4.553	14269	0.003	32.8%	0.005	48.7%
3.695	2.068	4.305	13224	0.003	31.1%	0.005	47.7%
3.525	1.975	4.034	12103	0.003	29.6%	0.005	47.1%
3.383	1.897	3.808	11187	0.003	28.5%	0.006	46.9%
3.199	1.802	3.514	10029	0.003	26.6%	0.006	46.0%
3.038	1.718	3.258	9044	0.003	25.2%	0.006	45.7%
2.879	1.643	3.004	8099	0.003	23.1%	0.006	44.9%
2.746	1.586	2.792	7330	0.004	20.5%	0.006	43.5%
2.581	1.511	2.529	6405	0.004	18.0%	0.007	42.6%
2.444	1.446	2.310	5663	0.004	16.7%	0.007	42.9%
2.315	4.942	2.104	4988	0.004	8.4%	0.007	38.5%
2.230	4.576	1.969	4555	0.005	6.2%	0.007	37.7%
2.111	4.091	1.779	3968	0.005	2.5%	0.008	36.3%
1.957	3.513	1.533	3241	0.005	-4.0%	0.008	34.4%
1.853	3.114	1.368	2773	0.006	-8.1%	0.009	33.2%
1.752	2.699	1.206	2338	0.006	-10.1%	0.009	33.5%
1.625	2.224	1.004	1820	0.007	-13.2%	0.010	34.6%
1.503	1.939	0.809	1357	0.008	-31.1%	0.011	28.0%
1.385	1.638	0.621	946	0.010	-51.5%	0.013	24.5%
1.307	1.455	0.497	698	0.012	-73.0%	0.015	19.1%
1.240	1.298	0.390	502	0.014	-97.3%	0.017	13.7%
1.185	1.160	0.302	355	0.017	-116.3%	0.020	14.5%
1.118	1.092	0.195	196	0.032	-267.1%	0.026	-21.7%

* Percent drag reduction based on Blasius equation

** Percent drag reduction based on Dodge-Metzner equation

Flow loop data for the PEO-CMC solution (750ppm CMC - 250ppm PEO) in 1.5-inch pipe

FR signal	PD signal	Velocity	Re	f	%DR*	fs	%DR**
5.014	2.770	6.420	21892	0.002	42.7%	0.005	55.5%
4.736	2.615	5.976	19872	0.002	40.8%	0.005	54.4%
4.577	2.518	5.722	18741	0.002	40.0%	0.005	54.0%
4.411	2.424	5.457	17578	0.002	38.9%	0.005	53.4%
4.242	2.320	5.187	16414	0.002	38.2%	0.005	53.2%
4.080	2.236	4.928	15318	0.002	36.8%	0.005	52.4%
3.958	2.162	4.733	14506	0.003	36.3%	0.005	52.2%
3.816	2.098	4.506	13575	0.003	34.4%	0.005	51.3%
3.630	1.990	4.209	12381	0.003	33.5%	0.005	51.0%
3.441	1.897	3.907	11197	0.003	31.5%	0.006	50.0%
3.322	1.837	3.717	10468	0.003	30.4%	0.006	49.5%
3.181	1.758	3.492	9621	0.003	29.8%	0.006	49.6%
2.979	1.664	3.169	8440	0.003	27.4%	0.006	48.7%
2.832	1.588	2.934	7607	0.003	26.8%	0.006	48.8%
2.683	1.530	2.696	6786	0.003	23.7%	0.007	47.5%
2.536	1.459	2.461	6000	0.004	23.0%	0.007	47.7%
2.421	1.415	2.277	5404	0.004	20.6%	0.007	46.6%
2.350	1.385	2.164	5043	0.004	19.8%	0.007	46.7%
2.266	1.356	2.030	4626	0.004	17.4%	0.007	45.6%
2.094	3.833	1.755	3801	0.005	7.9%	0.008	40.9%
2.055	3.683	1.693	3620	0.005	6.8%	0.008	41.0%
2.009	3.530	1.619	3409	0.005	4.7%	0.008	40.0%
1.924	3.230	1.483	3029	0.005	1.3%	0.008	38.7%
1.873	3.035	1.402	2807	0.005	-0.1%	0.009	38.9%
1.768	2.710	1.234	2363	0.006	-6.6%	0.009	37.0%
1.656	2.348	1.055	1913	0.006	-13.2%	0.010	35.0%
1.570	2.074	0.918	1584	0.007	-18.3%	0.011	34.9%
1.503	1.876	0.811	1340	0.008	-23.5%	0.011	33.1%
1.424	1.669	0.684	1066	0.008	-33.0%	0.012	31.6%
1.361	1.517	0.584	860	0.010	-43.7%	0.014	31.0%
1.293	1.351	0.475	652	0.011	-55.8%	0.015	27.5%
1.245	1.260	0.399	514	0.013	-74.6%	0.017	24.3%
1.203	1.183	0.331	401	0.015	-97.4%	0.019	19.5%
1.075	1.078	0.127	110	0.072	-639.0%	0.036	-100.1%

* Percent drag reduction based on Blasius equation

** Percent drag reduction based on Dodge-Metzner equation

Flow loop data for the PEO-CMC solution (500ppm CMC - 500ppm PEO) in 1.5-inch pipe

FR signal	PD signal	Velocity	Re	f	%DR*	fs	%DR**
4.951	2.911	6.401	25862	0.002	37.0%	0.004	47.6%
4.806	2.858	6.166	24572	0.002	34.6%	0.004	45.8%
4.688	2.780	5.975	23535	0.002	33.9%	0.004	45.4%
4.442	2.640	5.577	21414	0.003	31.3%	0.005	43.7%
4.329	2.571	5.394	20458	0.003	30.3%	0.005	43.2%
4.133	2.442	5.077	18829	0.003	28.9%	0.005	42.5%
3.986	2.354	4.839	17631	0.003	27.5%	0.005	41.7%
3.841	2.256	4.605	16470	0.003	26.7%	0.005	41.4%
3.617	2.119	4.242	14720	0.003	24.8%	0.005	40.6%
3.454	2.012	3.978	13481	0.003	24.0%	0.005	40.6%
3.331	1.940	3.779	12566	0.003	22.9%	0.005	40.1%
3.217	1.878	3.595	11733	0.003	21.5%	0.005	39.4%
3.058	1.786	3.337	10598	0.003	20.2%	0.006	39.1%
2.933	1.715	3.135	9728	0.004	19.2%	0.006	38.9%
2.729	1.603	2.805	8353	0.004	17.6%	0.006	38.8%
2.606	1.538	2.606	7552	0.004	16.8%	0.006	39.0%
2.456	1.474	2.363	6605	0.004	13.4%	0.006	37.4%
2.261	1.376	2.048	5428	0.004	12.7%	0.007	38.5%
2.095	4.013	1.779	4477	0.005	3.5%	0.007	34.3%
2.015	3.657	1.650	4037	0.005	2.2%	0.008	34.3%
1.963	3.442	1.566	3757	0.005	1.0%	0.008	33.9%
1.875	3.100	1.423	3297	0.005	-1.7%	0.008	33.9%
1.753	2.645	1.226	2687	0.006	-5.5%	0.009	33.8%
1.686	2.433	1.117	2367	0.006	-9.5%	0.009	32.4%
1.577	2.081	0.941	1870	0.007	-15.4%	0.010	32.1%
1.503	1.849	0.821	1552	0.007	-19.1%	0.011	31.9%
1.435	1.671	0.711	1275	0.008	-26.3%	0.011	30.1%
1.326	1.414	0.535	862	0.010	-44.1%	0.013	26.5%
1.272	1.296	0.447	675	0.011	-56.7%	0.015	25.4%
1.205	1.184	0.339	462	0.015	-92.8%	0.017	15.4%
1.152	1.107	0.253	310	0.020	-150.3%	0.021	3.1%

* Percent drag reduction based on Blasius equation

** Percent drag reduction based on Dodge-Metzner equation

Flow loop data for the PEO-CMC solution (250ppm CMC - 750ppm PEO) in 1.5-inch pipe

FR signal	PD signal	Velocity	Re	f	%DR*	fs	%DR**
4.933	3.098	6.357	34516	0.003	30.1%	0.004	38.1%
4.744	2.945	6.051	32288	0.003	29.4%	0.004	37.9%
4.602	2.841	5.822	30641	0.003	28.6%	0.004	37.4%
4.476	2.737	5.619	29198	0.003	28.3%	0.004	37.4%
4.333	2.626	5.388	27583	0.003	27.8%	0.004	37.3%
4.157	2.503	5.104	25629	0.003	26.7%	0.004	36.7%
3.991	2.371	4.836	23821	0.003	26.6%	0.005	36.9%
3.849	2.286	4.607	22303	0.003	25.2%	0.005	36.0%
3.726	2.203	4.408	21009	0.003	24.5%	0.005	35.7%
3.526	2.068	4.085	18950	0.003	23.5%	0.005	35.6%
3.398	1.971	3.878	17661	0.003	24.0%	0.005	36.4%
3.270	1.891	3.672	16398	0.003	23.4%	0.005	36.3%
3.151	1.831	3.480	15245	0.003	21.6%	0.005	35.3%
2.988	1.724	3.217	13703	0.003	21.9%	0.005	36.1%
2.833	1.638	2.966	12278	0.003	21.0%	0.005	36.1%
2.674	1.554	2.710	10859	0.004	20.0%	0.006	36.3%
2.557	1.494	2.521	9846	0.004	19.4%	0.006	36.4%
2.415	1.436	2.292	8651	0.004	16.4%	0.006	35.0%
2.311	1.383	2.124	7803	0.004	16.7%	0.006	35.9%
2.095	3.886	1.775	6118	0.005	7.2%	0.007	30.5%
2.025	3.584	1.662	5596	0.005	6.2%	0.007	30.9%
1.948	3.276	1.538	5036	0.005	4.5%	0.007	30.6%
1.875	3.008	1.420	4520	0.005	2.3%	0.007	29.7%
1.794	2.732	1.289	3965	0.005	-1.0%	0.008	28.9%
1.722	2.474	1.173	3488	0.006	-3.0%	0.008	29.2%
1.595	2.054	0.968	2688	0.006	-7.2%	0.009	29.2%
1.513	1.828	0.835	2201	0.007	-12.9%	0.009	27.2%
1.433	1.623	0.706	1753	0.008	-20.2%	0.010	26.0%
1.340	1.415	0.556	1268	0.009	-34.4%	0.012	22.1%
1.287	1.305	0.470	1011	0.010	-45.9%	0.012	16.9%
1.197	1.154	0.325	612	0.014	-89.0%	0.015	6.5%
1.150	1.100	0.249	427	0.020	-149.8%	0.018	-11.8%
1.128	1.062	0.214	347	0.024	-180.0%	0.020	-19.1%

* Percent drag reduction based on Blasius equation

** Percent drag reduction based on Dodge-Metzner equation

Flow loop data for the PEO-CMC solution (0ppm CMC - 1000ppm PEO) in 1.5-inch pipe

FR signal	PD signal	Velocity	Re	f	%DR*	fs	%DR**
4.881	3.101	6.279	77140	0.003	28.4%	0.003	22.4%
4.782	3.008	6.119	74484	0.003	28.4%	0.003	22.6%
4.597	2.892	5.820	69588	0.003	26.4%	0.003	20.8%
4.416	2.813	5.528	64885	0.003	22.9%	0.004	17.3%
4.166	2.627	5.124	58533	0.003	21.1%	0.004	15.8%
3.895	2.471	4.686	51848	0.003	16.7%	0.004	11.8%
3.678	2.321	4.335	46653	0.003	14.4%	0.004	10.0%
3.393	2.103	3.874	40056	0.004	13.2%	0.004	9.6%
3.245	2.016	3.635	36737	0.004	10.8%	0.004	7.6%
2.981	1.829	3.209	31011	0.004	9.8%	0.004	7.8%
2.751	1.681	2.837	26238	0.004	8.6%	0.004	7.7%
2.567	1.558	2.540	22577	0.004	9.7%	0.005	10.0%
2.385	1.449	2.245	19103	0.004	10.6%	0.005	12.1%
2.272	1.393	2.063	17026	0.004	9.8%	0.005	12.3%
2.080	3.945	1.752	13646	0.005	3.2%	0.005	7.8%
1.981	3.529	1.593	11983	0.005	0.8%	0.005	6.9%
1.915	3.230	1.486	10907	0.005	0.4%	0.006	7.3%
1.786	2.723	1.277	8884	0.006	-2.2%	0.006	7.2%
1.672	2.311	1.093	7191	0.006	-5.0%	0.006	7.1%
1.536	1.879	0.873	5303	0.007	-10.0%	0.007	5.9%
1.444	1.642	0.725	4116	0.007	-17.8%	0.008	3.0%
1.351	1.416	0.574	3002	0.008	-27.4%	0.008	-0.2%
1.277	1.277	0.455	2187	0.010	-45.8%	0.009	-8.5%
1.218	1.179	0.359	1589	0.013	-71.2%	0.011	-19.4%
1.160	1.104	0.266	1055	0.018	-127.1%	0.013	-45.4%
1.107	1.059	0.180	622	0.033	-273.4%	0.015	-114.9%

* Percent drag reduction based on Blasius equation

** Percent drag reduction based on Dodge-Metzner equation

Flow loop data for the PEO-CMC solution (1000ppm CMC - 0ppm PEO) in 1-inch pipe

FR signal	PD signal	Velocity	Re	f	%DR*	fs	%DR**
3.809	3.447	11.208	36350	0.002	43.8%	0.004	50.6%
3.739	3.315	10.929	35124	0.002	44.4%	0.004	51.3%
3.664	3.231	10.630	33822	0.002	43.8%	0.004	50.9%
3.541	3.081	10.140	31717	0.002	43.1%	0.004	50.5%
3.378	2.879	9.491	28983	0.002	42.4%	0.004	50.3%
3.230	2.714	8.901	26558	0.002	41.2%	0.004	49.6%
3.059	2.501	8.220	23829	0.002	40.9%	0.005	49.8%
2.932	2.368	7.714	21854	0.002	39.9%	0.005	49.4%
2.747	2.173	6.977	19060	0.002	38.7%	0.005	48.9%
2.569	1.986	6.268	16471	0.003	38.1%	0.005	49.1%
2.407	1.851	5.623	14205	0.003	35.6%	0.005	47.7%
2.302	1.774	5.204	12786	0.003	33.1%	0.005	46.3%
2.154	1.650	4.615	10854	0.003	31.0%	0.006	45.4%
2.065	1.588	4.260	9734	0.003	28.4%	0.006	44.2%
1.947	1.509	3.790	8301	0.004	24.3%	0.006	42.1%
1.784	1.404	3.141	6427	0.004	17.4%	0.007	38.8%
1.706	4.189	2.830	5576	0.004	16.2%	0.007	39.2%
1.540	3.373	2.169	3881	0.005	-1.1%	0.008	30.3%
1.419	2.729	1.687	2756	0.007	-17.1%	0.009	23.4%
1.367	2.489	1.480	2305	0.008	-28.6%	0.009	18.0%
1.339	2.380	1.368	2072	0.008	-37.8%	0.010	14.8%
1.311	2.255	1.257	1845	0.009	-46.9%	0.010	9.9%
1.275	2.118	1.113	1564	0.010	-64.1%	0.011	3.1%
1.234	1.989	0.950	1260	0.013	-94.8%	0.012	-10.4%
1.184	1.831	0.751	915	0.018	-153.9%	0.013	-35.1%
1.089	1.610	0.372	352	0.056	-574.1%	0.020	-184.4%

* Percent drag reduction based on Blasius equation

** Percent drag reduction based on Dodge-Metzner equation

Flow loop data for the PEO-CMC solution (750ppm CMC - 250ppm PEO) in 1-inch pipe

FR signal	PD signal	Velocity	Re	f	%DR*	fs	%DR**
3.940	3.490	11.749	36760	0.002	47.2%	0.004	54.7%
3.855	3.415	11.410	35335	0.002	46.1%	0.004	53.9%
3.743	3.258	10.963	33479	0.002	46.0%	0.004	54.0%
3.643	3.150	10.564	31845	0.002	45.2%	0.004	53.4%
3.520	3.026	10.073	29864	0.002	43.9%	0.004	52.5%
3.362	2.833	9.443	27369	0.002	43.2%	0.004	52.3%
3.209	2.650	8.832	25008	0.002	42.6%	0.005	52.1%
3.023	2.448	8.090	22213	0.002	41.3%	0.005	51.6%
2.901	2.319	7.603	20428	0.002	40.5%	0.005	51.2%
2.754	2.168	7.017	18330	0.002	39.5%	0.005	50.8%
2.560	1.975	6.243	15654	0.003	38.2%	0.005	50.6%
2.316	1.746	5.269	12452	0.003	36.8%	0.005	50.5%
2.200	1.652	4.806	10998	0.003	35.4%	0.006	50.1%
2.102	1.572	4.415	9808	0.003	34.5%	0.006	50.0%
1.938	1.451	3.761	7898	0.003	32.3%	0.006	49.7%
1.742	4.172	2.978	5765	0.004	23.6%	0.007	45.1%
1.679	3.790	2.727	5118	0.004	21.1%	0.007	44.2%
1.625	3.455	2.512	4580	0.004	19.2%	0.007	44.1%
1.575	3.173	2.312	4096	0.004	16.6%	0.008	43.0%
1.520	2.879	2.093	3580	0.005	13.2%	0.008	41.7%
1.487	2.707	1.961	3279	0.005	11.0%	0.008	41.2%
1.413	2.347	1.666	2631	0.005	4.3%	0.009	38.8%
1.333	2.013	1.346	1974	0.007	-8.2%	0.010	34.6%
1.280	1.856	1.135	1567	0.008	-26.4%	0.011	26.4%
1.218	1.671	0.888	1125	0.011	-59.2%	0.012	12.8%
1.172	1.507	0.704	823	0.014	-91.9%	0.014	0.7%
1.133	1.383	0.548	587	0.018	-142.3%	0.016	-12.1%

* Percent drag reduction based on Blasius equation

** Percent drag reduction based on Dodge-Metzner equation

Flow loop data for the PEO-CMC solution (500ppm CMC - 500ppm PEO) in 1-inch pipe

FR signal	PD signal	Velocity	Re	f	%DR*	fs	%DR**
3.927	3.380	11.848	45055	0.002	49.7%	0.004	53.5%
3.811	3.273	11.379	42631	0.002	48.4%	0.004	52.6%
3.669	3.137	10.805	39713	0.002	46.9%	0.004	51.4%
3.577	3.067	10.433	37853	0.002	45.4%	0.004	50.2%
3.406	2.903	9.742	34461	0.002	43.4%	0.004	48.7%
3.258	2.752	9.144	31595	0.002	41.9%	0.004	47.7%
3.078	2.575	8.417	28203	0.002	39.6%	0.004	46.2%
2.931	2.430	7.822	25512	0.002	37.8%	0.004	44.9%
2.799	2.302	7.289	23159	0.003	36.0%	0.005	43.9%
2.623	2.137	6.578	20120	0.003	33.2%	0.005	42.1%
2.464	1.983	5.935	17477	0.003	31.1%	0.005	41.1%
2.351	1.877	5.478	15661	0.003	29.4%	0.005	40.3%
2.239	1.764	5.026	13916	0.003	28.8%	0.005	40.4%
2.131	1.671	4.589	12287	0.003	26.9%	0.005	39.8%
2.026	1.580	4.165	10758	0.003	25.5%	0.006	39.4%
1.910	1.482	3.696	9134	0.004	24.2%	0.006	39.4%
1.743	1.352	3.021	6929	0.004	22.4%	0.006	40.1%
1.681	4.071	2.770	6154	0.004	14.8%	0.007	35.4%
1.629	3.710	2.560	5524	0.004	13.1%	0.007	34.6%
1.557	3.241	2.269	4682	0.005	10.2%	0.007	34.3%
1.503	2.920	2.051	4077	0.005	7.1%	0.008	33.3%
1.421	2.434	1.719	3202	0.005	3.0%	0.008	32.4%
1.359	2.107	1.469	2581	0.006	-1.6%	0.009	32.7%
1.301	1.835	1.234	2034	0.007	-8.3%	0.010	30.6%
1.259	1.634	1.065	1661	0.007	-12.1%	0.010	31.1%
1.191	1.406	0.790	1103	0.009	-35.0%	0.012	22.5%
1.142	1.249	0.592	743	0.012	-62.2%	0.014	14.9%

* Percent drag reduction based on Blasius equation

** Percent drag reduction based on Dodge-Metzner equation

Flow loop data for the PEO-CMC solution (250ppm CMC - 750ppm PEO) in 1-inch pipe

FR signal	PD signal	Velocity	Re	f	%DR*	fs	%DR**
3.869	3.652	11.586	58027	0.002	41.8%	0.004	43.4%
3.772	3.546	11.195	55387	0.002	40.6%	0.004	42.5%
3.661	3.422	10.747	52405	0.002	39.4%	0.004	41.4%
3.549	3.291	10.296	49441	0.002	38.2%	0.004	40.5%
3.365	3.042	9.554	44672	0.002	37.3%	0.004	40.0%
3.207	2.879	8.917	40681	0.002	34.9%	0.004	38.2%
3.015	2.652	8.143	35967	0.003	33.0%	0.004	36.9%
2.843	2.456	7.449	31876	0.003	31.1%	0.004	35.7%
2.718	2.301	6.945	28987	0.003	30.6%	0.004	35.6%
2.534	2.105	6.203	24869	0.003	28.3%	0.004	34.3%
2.415	1.975	5.723	22297	0.003	27.4%	0.005	34.0%
2.257	1.805	5.086	18999	0.003	26.6%	0.005	34.3%
2.116	1.668	4.518	16178	0.003	25.4%	0.005	34.2%
2.017	1.577	4.119	14270	0.003	24.6%	0.005	34.3%
1.908	1.479	3.679	12245	0.004	24.3%	0.005	35.0%
1.748	1.348	3.034	9428	0.004	24.1%	0.006	36.5%
1.666	3.914	2.703	8062	0.004	15.6%	0.006	30.9%
1.574	3.295	2.332	6600	0.005	12.7%	0.007	30.0%
1.476	2.686	1.937	5131	0.005	9.1%	0.007	29.5%
1.398	2.282	1.623	4035	0.006	3.1%	0.008	27.7%
1.334	1.988	1.365	3190	0.006	-4.5%	0.008	24.8%
1.258	1.664	1.058	2260	0.008	-17.3%	0.009	19.6%
1.221	1.525	0.909	1839	0.008	-27.3%	0.010	15.2%
1.167	1.357	0.691	1268	0.011	-55.5%	0.012	6.2%
1.137	1.268	0.570	977	0.013	-80.6%	0.013	-5.4%

* Percent drag reduction based on Blasius equation

** Percent drag reduction based on Dodge-Metzner equation

Flow loop data for the PEO-CMC solution (0ppm CMC - 1000ppm PEO) in 1-inch pipe

FR signal	PD signal	Velocity	Re	f	%DR*	fs	%DR**
3.884	3.487	11.658	133139	0.002	45.9%	0.003	36.2%
3.757	3.348	11.146	125256	0.002	44.8%	0.003	35.0%
3.684	3.277	10.851	120783	0.002	43.9%	0.003	34.1%
3.568	3.158	10.383	113765	0.002	42.6%	0.003	32.9%
3.476	3.085	10.012	108278	0.002	40.9%	0.003	30.8%
3.285	2.881	9.241	97119	0.002	38.7%	0.003	28.7%
3.139	2.726	8.651	88810	0.002	37.0%	0.003	27.0%
2.986	2.595	8.034	80317	0.003	33.8%	0.003	23.6%
2.810	2.419	7.323	70833	0.003	30.8%	0.003	20.8%
2.618	2.223	6.549	60856	0.003	27.6%	0.004	17.9%
2.431	2.042	5.794	51537	0.003	23.8%	0.004	14.4%
2.290	1.910	5.225	44789	0.003	20.5%	0.004	11.4%
2.125	1.745	4.559	37222	0.004	17.8%	0.004	9.6%
2.008	1.641	4.086	32087	0.004	14.7%	0.004	7.2%
1.905	1.544	3.671	27739	0.004	13.1%	0.004	6.6%
1.820	1.462	3.328	24280	0.004	13.0%	0.005	7.3%
1.740	4.885	3.005	21139	0.005	7.6%	0.005	2.7%
1.686	4.464	2.787	19085	0.005	5.6%	0.005	1.4%
1.650	4.180	2.641	17747	0.005	4.4%	0.005	1.1%
1.598	3.747	2.432	15861	0.005	3.8%	0.005	1.4%
1.520	3.164	2.117	13140	0.005	2.0%	0.005	1.2%
1.463	2.814	1.887	11240	0.006	-1.9%	0.006	-1.0%
1.412	2.520	1.681	9609	0.006	-6.2%	0.006	-3.5%
1.312	2.020	1.277	6619	0.007	-20.7%	0.007	-12.7%
1.251	1.802	1.031	4949	0.009	-43.3%	0.007	-28.2%
1.190	1.676	0.785	3417	0.014	-100.9%	0.008	-72.1%
1.151	1.573	0.627	2522	0.019	-160.8%	0.009	-111.6%
1.096	1.495	0.405	1394	0.041	-400.9%	0.011	-263.8%

* Percent drag reduction based on Blasius equation

** Percent drag reduction based on Dodge-Metzner equation

Flow loop data for the PEO-CMC solution (500ppm CMC - 0ppm PEO) in 1.5-inch pipe

FR signal	PD signal	Velocity	Re	f	%DR*	fs	%DR**
4.945	3.831	6.395	37723	0.003	6.2%	0.004	15.9%
4.737	3.578	6.058	35068	0.003	6.1%	0.004	16.3%
4.632	3.450	5.888	33747	0.003	6.3%	0.004	16.6%
4.504	3.316	5.681	32154	0.004	5.7%	0.004	16.5%
4.385	3.184	5.488	30692	0.004	5.6%	0.004	16.8%
4.253	3.042	5.275	29091	0.004	5.4%	0.004	16.9%
4.101	2.890	5.028	27275	0.004	4.9%	0.004	16.8%
3.948	2.742	4.781	25478	0.004	4.3%	0.005	16.8%
3.766	2.569	4.486	23382	0.004	3.8%	0.005	16.9%
3.575	2.393	4.177	21235	0.004	3.4%	0.005	17.1%
3.430	2.273	3.942	19640	0.004	2.4%	0.005	16.8%
3.230	2.097	3.618	17496	0.004	2.5%	0.005	17.8%
3.061	1.959	3.344	15735	0.004	2.5%	0.005	18.6%
2.879	1.829	3.050	13894	0.004	1.2%	0.005	18.6%
2.739	1.730	2.823	12519	0.004	0.8%	0.005	19.1%
2.457	1.550	2.366	9868	0.005	-0.9%	0.006	19.6%
2.335	1.473	2.169	8773	0.005	-0.5%	0.006	21.0%
2.251	1.430	2.033	8039	0.005	-1.9%	0.006	20.7%
2.098	4.433	1.785	6746	0.005	-8.7%	0.007	17.0%
2.005	3.967	1.635	5990	0.006	-10.4%	0.007	17.3%
1.906	3.483	1.474	5212	0.006	-11.8%	0.007	17.5%
1.803	3.032	1.307	4432	0.006	-14.5%	0.008	17.5%
1.698	2.586	1.137	3673	0.007	-16.4%	0.008	18.5%
1.588	2.183	0.959	2919	0.007	-20.7%	0.009	17.9%
1.451	1.739	0.737	2047	0.008	-28.3%	0.010	17.9%
1.360	1.498	0.590	1516	0.009	-38.9%	0.011	15.1%
1.273	1.293	0.449	1049	0.011	-54.6%	0.013	12.5%
1.205	1.178	0.339	718	0.014	-89.4%	0.014	-0.2%
1.146	1.085	0.244	459	0.020	-146.2%	0.018	-14.8%
1.126	1.060	0.211	379	0.024	-184.4%	0.019	-25.7%

* Percent drag reduction based on Blasius equation

** Percent drag reduction based on Dodge-Metzner equation

Flow loop data for the PEO-CMC solution (375ppm CMC - 125ppm PEO) in 1.5-inch pipe

FR signal	PD signal	Velocity	Re	f	%DR*	fs	%DR**
4.911	3.889	6.311	40351	0.004	2.4%	0.004	8.5%
4.813	3.784	6.153	38974	0.004	1.7%	0.004	8.1%
4.615	3.546	5.834	36231	0.004	1.4%	0.004	8.3%
4.433	3.337	5.541	33758	0.004	1.0%	0.004	8.4%
4.227	3.105	5.209	31017	0.004	0.8%	0.004	8.8%
3.978	2.845	4.807	27790	0.004	0.1%	0.004	8.9%
3.800	2.665	4.520	25543	0.004	-0.3%	0.004	9.2%
3.513	2.384	4.058	22030	0.004	-0.5%	0.005	10.2%
3.273	2.171	3.671	19204	0.004	-1.1%	0.005	10.7%
3.092	2.019	3.379	17144	0.004	-1.4%	0.005	11.4%
2.845	1.824	2.981	14439	0.004	-1.7%	0.005	12.7%
2.659	1.688	2.681	12487	0.005	-1.7%	0.005	14.1%
2.478	1.570	2.390	10664	0.005	-2.5%	0.006	14.8%
2.306	1.466	2.112	9006	0.005	-3.1%	0.006	15.7%
2.214	1.411	1.964	8151	0.005	-2.7%	0.006	17.2%
2.099	4.442	1.779	7115	0.005	-9.2%	0.006	13.4%
1.978	3.818	1.584	6069	0.006	-10.6%	0.007	14.1%
1.908	3.500	1.471	5484	0.006	-12.5%	0.007	13.7%
1.810	3.013	1.313	4693	0.006	-12.2%	0.007	16.4%
1.721	2.673	1.169	4005	0.006	-15.9%	0.008	14.6%
1.623	2.287	1.011	3283	0.007	-18.0%	0.008	16.1%
1.536	1.987	0.871	2676	0.007	-21.6%	0.009	16.3%
1.443	1.702	0.721	2066	0.008	-27.3%	0.010	16.8%
1.334	1.420	0.546	1409	0.009	-40.0%	0.011	14.3%
1.252	1.254	0.413	963	0.012	-62.9%	0.013	9.2%
1.189	1.145	0.312	655	0.015	-97.3%	0.015	-1.9%
1.136	1.079	0.226	422	0.023	-171.9%	0.018	-24.0%
1.098	1.033	0.165	274	0.035	-283.2%	0.022	-55.8%

* Percent drag reduction based on Blasius equation

** Percent drag reduction based on Dodge-Metzner equation

Flow loop data for the PEO-CMC solution (250ppm CMC - 250ppm PEO) in 1.5-inch pipe

FR signal	PD signal	Velocity	Re	f	%DR*	fs	%DR**
4.959	3.846	6.409	49692	0.003	6.1%	0.004	7.7%
4.730	3.585	6.039	45802	0.003	5.5%	0.004	7.5%
4.523	3.341	5.704	42361	0.004	5.5%	0.004	8.0%
4.373	3.183	5.461	39913	0.004	4.9%	0.004	7.9%
4.148	2.957	5.098	36316	0.004	4.0%	0.004	7.5%
3.921	2.720	4.731	32782	0.004	3.9%	0.004	8.2%
3.732	2.533	4.425	29916	0.004	3.9%	0.004	8.8%
3.585	2.395	4.187	27737	0.004	3.8%	0.004	9.3%
3.367	2.206	3.835	24589	0.004	3.2%	0.004	9.7%
3.169	2.039	3.515	21821	0.004	3.1%	0.005	10.5%
3.024	1.927	3.280	19852	0.004	2.7%	0.005	10.8%
2.851	1.791	3.000	17570	0.004	3.3%	0.005	12.4%
2.688	1.678	2.737	15491	0.004	3.0%	0.005	13.2%
2.514	1.566	2.455	13351	0.005	2.7%	0.005	14.2%
2.360	1.476	2.206	11532	0.005	2.0%	0.005	14.9%
2.286	1.428	2.087	10684	0.005	3.3%	0.006	16.8%
2.115	4.372	1.810	8794	0.005	-4.1%	0.006	12.6%
1.960	3.619	1.560	7170	0.006	-6.4%	0.006	12.6%
1.866	3.184	1.408	6230	0.006	-7.4%	0.007	13.3%
1.738	2.666	1.201	5010	0.006	-10.6%	0.007	13.3%
1.579	2.109	0.943	3602	0.007	-17.3%	0.008	11.9%
1.449	1.707	0.733	2550	0.008	-24.8%	0.009	12.1%
1.328	1.398	0.538	1667	0.009	-38.7%	0.010	9.1%
1.245	1.236	0.403	1125	0.012	-63.2%	0.012	1.6%
1.182	1.133	0.301	755	0.016	-101.9%	0.014	-12.2%
1.145	1.093	0.242	557	0.021	-157.3%	0.016	-32.8%
1.115	1.058	0.193	410	0.029	-229.1%	0.018	-56.0%

* Percent drag reduction based on Blasius equation

** Percent drag reduction based on Dodge-Metzner equation

Flow loop data for the PEO-CMC solution (125ppm CMC - 375ppm PEO) in 1.5-inch pipe

FR signal	PD signal	Velocity	Re	f	%DR*	fs	%DR**
4.886	4.001	6.195	60023	0.004	-3.5%	0.004	-1.6%
4.795	3.870	6.050	58174	0.004	-3.1%	0.004	-1.0%
4.681	3.724	5.868	55877	0.004	-3.2%	0.004	-0.9%
4.448	3.438	5.497	51255	0.004	-3.4%	0.004	-0.7%
4.267	3.230	5.209	47732	0.004	-3.9%	0.004	-0.8%
4.086	3.006	4.921	44272	0.004	-3.1%	0.004	0.4%
3.861	2.758	4.563	40061	0.004	-3.0%	0.004	1.1%
3.687	2.578	4.286	36876	0.004	-3.1%	0.004	1.6%
3.503	2.404	3.993	33580	0.004	-3.6%	0.004	1.6%
3.344	2.247	3.739	30794	0.004	-3.1%	0.004	2.7%
3.107	2.032	3.362	26753	0.004	-2.4%	0.005	4.3%
2.851	1.830	2.954	22551	0.005	-2.8%	0.005	5.1%
2.680	1.698	2.682	19845	0.005	-1.9%	0.005	6.9%
2.526	1.592	2.437	17482	0.005	-1.7%	0.005	8.0%
2.390	1.506	2.220	15458	0.005	-1.7%	0.005	9.0%
2.281	1.440	2.047	13881	0.005	-1.4%	0.005	10.1%
2.116	1.456	1.784	11575	0.005	-7.7%	0.006	6.1%
2.010	3.909	1.615	10150	0.006	-8.8%	0.006	6.5%
1.927	3.513	1.483	9066	0.006	-10.0%	0.006	6.6%
1.844	3.143	1.351	8014	0.006	-11.7%	0.006	6.1%
1.772	2.813	1.236	7127	0.006	-11.8%	0.007	7.4%
1.697	2.515	1.117	6231	0.006	-13.4%	0.007	7.3%
1.581	2.104	0.932	4907	0.007	-17.5%	0.007	6.6%
1.484	1.783	0.778	3862	0.007	-20.5%	0.008	7.7%
1.419	1.610	0.674	3197	0.008	-26.5%	0.009	5.6%
1.353	1.446	0.569	2555	0.009	-34.1%	0.009	2.9%
1.28	1.291	0.453	1889	0.011	-49.3%	0.010	-1.1%
1.212	1.17	0.345	1316	0.013	-76.8%	0.012	-13.4%
1.166	1.112	0.271	960	0.018	-122.1%	0.013	-34.3%
1.123	1.069	0.203	653	0.027	-211.9%	0.016	-72.5%
1.104	1.049	0.173	528	0.034	-278.4%	0.017	-99.5%

* Percent drag reduction based on Blasius equation

** Percent drag reduction based on Dodge-Metzner equation

Flow loop data for the PEO-CMC solution (0ppm CMC - 500ppm PEO) in 1.5-inch pipe

FR signal	PD signal	Velocity	Re	f	%DR*	fs	%DR**
4.879	4.099	6.295	129752	0.004	-5.8%	0.003	-21.9%
4.785	3.988	6.142	125650	0.004	-6.4%	0.003	-22.4%
4.628	3.791	5.888	118870	0.004	-7.0%	0.003	-22.9%
4.393	3.511	5.507	108892	0.004	-8.1%	0.003	-23.8%
4.188	3.268	5.175	100360	0.004	-8.8%	0.003	-24.3%
3.920	2.964	4.740	89463	0.004	-9.7%	0.003	-24.7%
3.719	2.741	4.414	81490	0.004	-10.0%	0.004	-24.7%
3.475	2.478	4.019	72055	0.004	-9.9%	0.004	-23.9%
3.284	2.287	3.709	64868	0.005	-9.9%	0.004	-23.0%
3.101	2.098	3.413	58154	0.005	-8.2%	0.004	-20.9%
2.854	1.876	3.012	49378	0.005	-6.9%	0.004	-18.3%
2.725	1.770	2.803	44934	0.005	-6.2%	0.004	-16.8%
2.562	1.642	2.539	39466	0.005	-4.8%	0.004	-14.4%
2.405	1.533	2.285	34363	0.005	-4.0%	0.004	-12.7%
2.270	1.444	2.066	30114	0.005	-2.5%	0.004	-10.3%
2.186	1.393	1.930	27539	0.005	-1.7%	0.005	-8.5%
2.101	4.446	1.792	24991	0.005	-8.5%	0.005	-15.1%
2.012	3.935	1.648	22387	0.006	-7.9%	0.005	-13.6%
1.929	3.534	1.513	20021	0.006	-9.0%	0.005	-14.0%
1.822	3.013	1.340	17068	0.006	-8.9%	0.005	-12.3%
1.718	2.584	1.171	14309	0.006	-10.6%	0.005	-12.5%
1.644	2.303	1.051	12419	0.006	-12.2%	0.006	-12.6%
1.544	1.951	0.889	9971	0.007	-14.3%	0.006	-12.3%
1.414	1.574	0.678	6994	0.008	-21.5%	0.007	-14.8%
1.336	1.394	0.552	5336	0.009	-31.8%	0.007	-21.2%
1.263	1.247	0.433	3889	0.011	-48.2%	0.008	-30.5%
1.176	1.115	0.292	2322	0.016	-100.5%	0.010	-63.3%
1.114	1.045	0.192	1337	0.027	-214.0%	0.012	-133.1%

* Percent drag reduction based on Blasius equation

** Percent drag reduction based on Dodge-Metzner equation

Flow loop data for the PEO-CMC solution (500ppm CMC - 0ppm PEO) in 1-inch pipe

FR signal	PD signal	Velocity	Re	f	%DR*	fs	%DR**
3.815	3.952	11.402	61089	0.002	33.1%	0.004	34.5%
3.719	3.803	11.014	58300	0.002	32.5%	0.004	34.1%
3.658	3.701	10.767	56546	0.002	32.3%	0.004	34.0%
3.566	3.565	10.395	53926	0.002	31.7%	0.004	33.6%
3.494	3.440	10.104	51899	0.002	31.7%	0.004	33.8%
3.395	3.290	9.704	49144	0.003	31.3%	0.004	33.5%
3.255	3.083	9.138	45316	0.003	30.6%	0.004	33.2%
3.116	2.860	8.576	41597	0.003	30.8%	0.004	33.8%
2.938	2.612	7.856	36957	0.003	30.2%	0.004	33.8%
2.810	2.442	7.338	33710	0.003	29.8%	0.004	33.7%
2.661	2.253	6.735	30030	0.003	29.3%	0.004	33.8%
2.531	2.097	6.210	26912	0.003	28.8%	0.004	33.9%
2.362	1.908	5.526	22995	0.003	28.0%	0.005	34.0%
2.218	1.761	4.944	19788	0.003	26.9%	0.005	33.9%
2.040	1.583	4.224	16003	0.003	26.9%	0.005	35.1%
1.941	1.502	3.824	13992	0.003	25.4%	0.005	34.7%
1.816	1.400	3.318	11556	0.004	24.6%	0.006	35.1%
1.759	4.575	3.087	10486	0.004	18.5%	0.006	30.6%
1.684	4.018	2.784	9121	0.004	16.9%	0.006	30.2%
1.627	3.619	2.554	8117	0.004	15.4%	0.006	30.0%
1.565	3.214	2.303	7061	0.005	13.4%	0.006	29.5%
1.468	2.641	1.911	5489	0.005	8.9%	0.007	28.2%
1.362	2.075	1.482	3896	0.006	2.4%	0.008	27.1%
1.297	1.776	1.219	2994	0.006	-4.2%	0.009	24.7%
1.214	1.444	0.883	1939	0.008	-18.5%	0.010	20.3%
1.170	1.294	0.705	1431	0.009	-32.3%	0.011	16.0%
1.134	1.184	0.560	1048	0.011	-50.8%	0.013	11.4%
1.108	1.123	0.455	792	0.014	-79.0%	0.014	0.9%

* Percent drag reduction based on Blasius equation

** Percent drag reduction based on Dodge-Metzner equation

Flow loop data for the PEO-CMC solution (375ppm CMC - 125ppm PEO) in 1-inch pipe

FR signal	PD signal	Velocity	Re	f	%DR*	fs	%DR**
3.879	3.683	11.608	69712	0.002	41.4%	0.003	39.4%
3.773	3.559	11.182	66224	0.002	40.3%	0.003	38.5%
3.689	3.462	10.843	63496	0.002	39.4%	0.003	37.7%
3.616	3.400	10.550	61149	0.002	38.0%	0.004	36.5%
3.573	3.363	10.376	59779	0.002	37.2%	0.004	35.7%
3.556	3.341	10.308	59239	0.002	37.1%	0.004	35.6%
3.530	3.329	10.203	58416	0.002	36.3%	0.004	34.8%
3.446	3.247	9.865	55780	0.002	34.8%	0.004	33.6%
3.231	3.019	9.000	49185	0.003	31.3%	0.004	30.5%
2.487	2.088	6.004	28249	0.003	25.4%	0.004	27.5%
2.296	1.875	5.235	23413	0.003	24.1%	0.004	27.4%
2.130	1.703	4.567	19418	0.003	23.0%	0.005	27.7%
2.009	1.588	4.080	16637	0.004	21.9%	0.005	27.6%
1.903	1.495	3.653	14300	0.004	20.8%	0.005	27.7%
1.825	1.427	3.339	12643	0.004	20.5%	0.005	28.4%
1.757	4.714	3.065	11245	0.004	14.8%	0.006	24.2%
1.664	3.968	2.691	9407	0.004	13.6%	0.006	24.5%
1.574	3.361	2.329	7716	0.005	10.3%	0.006	23.5%
1.512	2.960	2.079	6606	0.005	7.9%	0.006	22.8%
1.459	2.617	1.866	5695	0.005	6.7%	0.007	23.6%
1.405	2.305	1.648	4806	0.005	4.4%	0.007	23.2%
1.328	1.920	1.338	3612	0.006	-1.6%	0.008	22.0%
1.290	1.736	1.185	3059	0.006	-4.3%	0.008	22.5%
1.224	1.467	0.920	2160	0.008	-14.1%	0.009	19.1%
1.181	1.323	0.747	1623	0.009	-26.9%	0.010	14.5%
1.131	1.189	0.545	1055	0.012	-59.4%	0.012	2.6%
1.103	1.120	0.433	768	0.015	-92.5%	0.014	-9.5%

* Percent drag reduction based on Blasius equation

** Percent drag reduction based on Dodge-Metzner equation

Flow loop data for the PEO-CMC solution (250ppm CMC - 250ppm PEO) in 1-inch pipe

FR signal	PD signal	Velocity	Re	f	%DR*	fs	%DR**
3.820	3.942	11.407	82036	0.002	33.4%	0.003	28.2%
3.712	3.773	10.971	77770	0.002	32.9%	0.003	27.9%
3.628	3.659	10.632	74495	0.002	32.0%	0.003	27.1%
3.565	3.564	10.377	72064	0.002	31.6%	0.003	26.7%
3.470	3.445	9.994	68439	0.003	30.4%	0.003	25.7%
3.382	3.316	9.638	65127	0.003	29.8%	0.003	25.2%
3.168	3.033	8.774	57262	0.003	27.4%	0.004	23.4%
2.751	2.426	7.090	42764	0.003	26.4%	0.004	23.7%
2.594	2.233	6.456	37613	0.003	25.1%	0.004	23.1%
2.460	2.065	5.914	33362	0.003	24.8%	0.004	23.6%
2.285	1.866	5.208	28025	0.003	23.9%	0.004	23.7%
2.152	1.714	4.670	24143	0.003	24.5%	0.004	25.1%
2.025	1.594	4.158	20586	0.003	23.4%	0.005	25.2%
1.932	1.502	3.782	18082	0.004	24.1%	0.005	26.7%
1.868	1.446	3.524	16411	0.004	24.1%	0.005	27.3%
1.765	4.633	3.108	13816	0.004	18.3%	0.005	23.0%
1.707	4.205	2.873	12410	0.004	16.8%	0.005	22.6%
1.629	3.643	2.558	10585	0.004	15.1%	0.006	22.6%
1.557	3.157	2.267	8972	0.005	13.3%	0.006	22.3%
1.469	2.611	1.912	7104	0.005	10.6%	0.006	21.8%
1.388	2.224	1.585	5494	0.006	2.9%	0.007	18.3%
1.323	1.988	1.322	4287	0.007	-10.6%	0.007	10.2%
1.240	1.725	0.987	2872	0.009	-42.4%	0.009	-9.1%
1.163	1.567	0.676	1711	0.016	-127.0%	0.010	-58.6%
1.123	1.508	0.515	1177	0.026	-236.6%	0.012	-115.7%

* Percent drag reduction based on Blasius equation

** Percent drag reduction based on Dodge-Metzner equation

Flow loop data for the PEO-CMC solution (125ppm CMC - 375ppm PEO) in 1-inch pipe

FR signal	PD signal	Velocity	Re	f	%DR*	fs	%DR**
3.734	4.104	10.890	92805	0.003	25.0%	0.003	20.6%
3.662	3.986	10.604	89593	0.003	24.4%	0.003	20.1%
3.565	3.814	10.218	85309	0.003	24.0%	0.003	19.8%
3.421	3.581	9.646	79045	0.003	23.0%	0.004	19.0%
3.370	3.499	9.443	76855	0.003	22.6%	0.004	18.7%
3.210	3.241	8.807	70083	0.003	21.6%	0.004	18.0%
3.076	3.072	8.274	64531	0.003	19.3%	0.004	15.8%
2.686	2.452	6.723	49042	0.003	19.0%	0.004	16.7%
2.643	2.377	6.552	47399	0.003	19.7%	0.004	17.7%
2.423	2.102	5.677	39216	0.003	17.7%	0.004	16.5%
2.250	1.874	4.989	33058	0.004	18.5%	0.004	18.3%
2.061	1.664	4.237	26638	0.004	18.2%	0.005	19.2%
1.964	1.558	3.851	23480	0.004	19.2%	0.005	20.9%
1.878	1.483	3.509	20763	0.004	18.2%	0.005	20.6%
1.769	4.819	3.076	17441	0.004	14.1%	0.005	17.9%
1.703	4.221	2.813	15501	0.004	14.6%	0.005	19.1%
1.632	3.691	2.531	13478	0.004	13.4%	0.006	19.0%
1.573	3.273	2.296	11851	0.005	12.3%	0.006	19.0%
1.507	2.842	2.034	10094	0.005	10.7%	0.006	18.9%
1.455	2.546	1.827	8760	0.005	8.2%	0.006	17.7%
1.358	2.056	1.441	6402	0.006	0.8%	0.007	13.9%
1.284	1.737	1.147	4733	0.007	-9.3%	0.008	8.7%
1.212	1.515	0.861	3238	0.009	-36.2%	0.009	-7.9%
1.167	1.404	0.682	2379	0.012	-71.3%	0.010	-28.8%
1.137	1.329	0.562	1845	0.016	-108.2%	0.010	-50.7%
1.100	1.246	0.415	1235	0.024	-194.5%	0.012	-99.8%

* Percent drag reduction based on Blasius equation

** Percent drag reduction based on Dodge-Metzner equation

Flow loop data for the PEO-CMC solution (0ppm CMC - 500ppm PEO) in 1-inch pipe

FR signal	PD signal	Velocity	Re	f	%DR*	fs	%DR**
3.898	3.574	11.750	214532	0.002	44.6%	0.003	31.8%
3.786	3.480	11.297	203745	0.002	42.9%	0.003	29.7%
3.665	3.353	10.807	192242	0.002	41.4%	0.003	28.0%
3.523	3.211	10.232	178949	0.002	39.5%	0.003	25.7%
3.296	2.962	9.313	158180	0.002	36.8%	0.003	22.6%
3.123	2.794	8.613	142772	0.003	33.8%	0.003	19.2%
2.870	2.520	7.588	120938	0.003	30.1%	0.003	15.1%
2.655	2.296	6.718	103087	0.003	26.4%	0.003	11.1%
2.507	2.149	6.119	91205	0.003	23.3%	0.003	7.8%
2.337	1.982	5.431	77999	0.003	19.5%	0.004	3.8%
2.160	1.797	4.714	64793	0.004	16.6%	0.004	1.3%
2.019	1.649	4.143	54707	0.004	15.4%	0.004	0.5%
1.874	1.505	3.556	44778	0.004	14.7%	0.004	0.9%
1.811	1.445	3.301	40616	0.004	14.9%	0.004	1.5%
1.745	4.877	3.034	36362	0.004	9.1%	0.004	-4.4%
1.696	4.429	2.836	33277	0.005	9.0%	0.004	-3.8%
1.639	3.925	2.605	29773	0.005	9.3%	0.005	-2.9%
1.583	3.488	2.378	26423	0.005	8.6%	0.005	-2.9%
1.526	3.057	2.147	23114	0.005	8.5%	0.005	-2.1%
1.437	2.499	1.787	18168	0.005	5.5%	0.005	-3.6%
1.363	2.096	1.488	14284	0.006	1.3%	0.005	-6.0%
1.249	1.650	1.026	8778	0.008	-22.2%	0.006	-24.9%
1.201	1.493	0.832	6666	0.010	-42.4%	0.007	-41.3%
1.153	1.353	0.637	4703	0.013	-78.6%	0.008	-70.7%
1.110	1.260	0.463	3095	0.020	-156.0%	0.009	-130.0%

* Percent drag reduction based on Blasius equation

** Percent drag reduction based on Dodge-Metzner equation

Appendix C. PAM-SDS Experiment data

Appendix C-1. Bench-scale experiment data

Surface tension versus SDS concentration for the 1000ppm PAM solutions

SDS Concentration	Surface tension (Dynes/cm)				
	1	2	3	Average	RSD
0 ppm	67.6	68	67.8	67.8	0.3
5 ppm	64.3	64	64.1	64.1	0.2
10 ppm	64.6	64.5	64.8	64.6	0.2
50 ppm	53.4	53.6	53.5	53.5	0.2
100 ppm	44.8	44.1	44.5	44.5	0.8

Conductivity versus SDS concentration for the 1000ppm PAM solutions

SDS Concentration	Conductivity ($\mu\text{S}/\text{cm}$)				
	1	2	3	Average	RSD
0 ppm	1.131	1.133	1.14	1.135	0.4
5 ppm	1.169	1.172	1.173	1.171	0.2
10 ppm	1.148	1.142	1.148	1.146	0.3
50 ppm	1.166	1.17	1.167	1.168	0.2
100 ppm	1.217	1.202	1.202	1.207	0.7

Viscosity data for the 1000ppm PAM solution with 0ppm SDS

RPM	0.9	1.8	30	60	90	100	200
Ω	0.094	0.188	3.140	6.280	9.420	10.467	20.933
$\ln(\Omega)$	-2.362	-1.669	1.144	1.837	2.243	2.348	3.041
Dail Reading	15	16.5	31.5	40	46	48	64
Shear stress	0.9521	1.0843	2.4058	3.1546	3.6832	3.8594	5.2690
$\ln(\text{Shear stress})$	-0.049	0.081	0.878	1.149	1.304	1.351	1.662
N	2.4285	2.4285	2.4285	2.4285	2.4285	2.4285	2.4285
Shear rate	1.73	3.45	57.50	115.00	172.50	191.67	383.34
$\log(\text{Shear rate})$	0.2368	0.5378	1.7597	2.0607	2.2368	2.2826	2.5836
$\log(\text{Shear stress})$	-0.021	0.035	0.381	0.499	0.566	0.587	0.722
n	0.4109	0.4109	0.4109	0.4109	0.4109	0.4109	0.4109
k	0.450	0.450	0.450	0.450	0.450	0.450	0.450
η	0.3264	0.2170	0.0414	0.0275	0.0217	0.0204	0.0135

Viscosity data for the 1000ppm PAM solution with 5ppm SDS

RPM	0.9	1.8	30	60	90	100	200
Ω	0.094	0.188	3.140	6.280	9.420	10.467	20.933
$\ln(\Omega)$	-2.362	-1.669	1.144	1.837	2.243	2.348	3.041
Dail Reading	16	18	33	39.5	45.5	47.5	65.5
Shear stress	1.0402	1.2164	2.5379	3.1106	3.6392	3.8154	5.4012
$\ln(\text{Shear stress})$	0.039	0.196	0.931	1.135	1.292	1.339	1.687
N	2.4742	2.4742	2.4742	2.4742	2.4742	2.4742	2.4742
Shear rate	1.73	3.46	57.66	115.32	172.98	192.20	384.40
$\log(\text{Shear rate})$	0.2380	0.5390	1.7609	2.0619	2.2380	2.2838	2.5848
$\log(\text{Shear stress})$	0.017	0.085	0.404	0.493	0.561	0.582	0.732
n	0.3957	0.3957	0.3957	0.3957	0.3957	0.3957	0.3957
k	0.489	0.489	0.489	0.489	0.489	0.489	0.489
η	0.3513	0.2311	0.0422	0.0278	0.0217	0.0204	0.0134

Viscosity data for the 1000ppm PAM solution with 10ppm SDS

RPM	0.9	1.8	30	60	90	100	200
Ω	0.094	0.188	3.140	6.280	9.420	10.467	20.933
$\ln(\Omega)$	-2.362	-1.669	1.144	1.837	2.243	2.348	3.041
Dail Reading	16	18	32.5	40	46.5	47.5	65.5
Shear stress	1.0402	1.2164	2.4939	3.1546	3.7273	3.8154	5.4012
$\ln(\text{Shear stress})$	0.039	0.196	0.914	1.149	1.316	1.339	1.687
N	2.4484	2.4484	2.4484	2.4484	2.4484	2.4484	2.4484
Shear rate	1.73	3.45	57.57	115.14	172.71	191.90	383.80
$\log(\text{Shear rate})$	0.2373	0.5384	1.7602	2.0612	2.2373	2.2831	2.5841
$\log(\text{Shear stress})$	0.017	0.085	0.397	0.499	0.571	0.582	0.732
n	0.4039	0.4039	0.4039	0.4039	0.4039	0.4039	0.4039
k	0.472	0.472	0.472	0.472	0.472	0.472	0.472
η	0.3405	0.2253	0.0421	0.0279	0.0219	0.0205	0.0136

Viscosity data for the 1000ppm PAM solution with 50ppm SDS

RPM	0.9	1.8	30	60	90	100	200
Ω	0.094	0.188	3.140	6.280	9.420	10.467	20.933
$\ln(\Omega)$	-2.362	-1.669	1.144	1.837	2.243	2.348	3.041
Dail Reading	18	20	33	41	46.5	48	65.5
Shear stress	1.2164	1.3926	2.5379	3.2427	3.7273	3.8594	5.4012
$\ln(\text{Shear stress})$	0.196	0.331	0.931	1.176	1.316	1.351	1.687
N	2.5217	2.5217	2.5217	2.5217	2.5217	2.5217	2.5217
Shear rate	1.73	3.47	57.82	115.65	173.47	192.75	385.50
$\log(\text{Shear rate})$	0.2392	0.5403	1.7621	2.0631	2.2392	2.2850	2.5860
$\log(\text{Shear stress})$	0.085	0.144	0.404	0.511	0.571	0.587	0.732
n	0.3924	0.3924	0.3924	0.3924	0.3924	0.3924	0.3924
k	0.505	0.505	0.505	0.505	0.505	0.505	0.505
η	0.3610	0.2369	0.0429	0.0281	0.0220	0.0206	0.0135

Viscosity data for the 1000ppm PAM solution with 100ppm SDS

RPM	0.9	1.8	30	60	90	100	200
Ω	0.094	0.188	3.140	6.280	9.420	10.467	20.933
$\ln(\Omega)$	-2.362	-1.669	1.144	1.837	2.243	2.348	3.041
Dail Reading	15	18.5	32	41	46	47.5	65
Shear stress	0.9521	1.2605	2.4498	3.2427	3.6832	3.8154	5.3571
$\ln(\text{Shear stress})$	-0.049	0.231	0.896	1.176	1.304	1.339	1.678
N	2.4534	2.4534	2.4534	2.4534	2.4534	2.4534	2.4534
Shear rate	1.73	3.46	57.59	115.18	172.76	191.96	383.92
$\log(\text{Shear rate})$	0.2375	0.5385	1.7603	2.0614	2.2375	2.2832	2.5842
$\log(\text{Shear stress})$	-0.021	0.101	0.389	0.511	0.566	0.582	0.729
n	0.4042	0.4042	0.4042	0.4042	0.4042	0.4042	0.4042
k	0.470	0.470	0.470	0.470	0.470	0.470	0.470
η	0.3393	0.2245	0.0420	0.0278	0.0218	0.0205	0.0136

Apparent viscosity versus SDS concentration for the 1000ppm PAM solutions

SDS concentration	30rpm	90rpm	200rpm
0 ppm	0.0414	0.0217	0.0135
5 ppm	0.0422	0.0217	0.0134
10 ppm	0.0421	0.0219	0.0136
50 ppm	0.0429	0.0220	0.0135
100 ppm	0.0420	0.0218	0.0136

Surface tension versus SDS concentration for the 500ppm PAM solutions

SDS Concentration	Surface tension (Dynes/cm)				
	1	2	3	Average	RSD
0 ppm	69	68.8	69.1	69.0	0.2
5 ppm	68.1	68	68	68.0	0.1
10 ppm	65.5	65.5	65.7	65.6	0.2
50 ppm	61.0	61.0	61.1	61.0	0.1
100 ppm	52.1	52.2	52.2	52.2	0.1

Conductivity versus SDS concentration for the 500ppm PAM solutions

SDS Concentration	Conductivity ($\mu\text{S}/\text{cm}$)				
	1	2	3	Average	RSD
0 ppm	0.624	0.624	0.623	0.624	0.1
5 ppm	0.616	0.616	0.616	0.616	0.0
10 ppm	0.660	0.659	0.661	0.660	0.2
50 ppm	0.651	0.649	0.651	0.650	0.2
100 ppm	0.745	0.744	0.744	0.744	0.1

Viscosity data for the 500ppm PAM solution with 0ppm SDS

RPM	0.9	1.8	30	60	90	100	200
Ω	0.094	0.188	3.140	6.280	9.420	10.467	20.933
$\ln(\Omega)$	-2.362	-1.669	1.144	1.837	2.243	2.348	3.041
Dail Reading	9	11	20.5	25	28.5	29	40
Shear stress	0.4235	0.5997	1.4367	1.8331	2.1415	2.1855	3.1546
$\ln(\text{Shear stress})$	-0.859	-0.511	0.362	0.606	0.761	0.782	1.149
N	2.4127	2.4127	2.4127	2.4127	2.4127	2.4127	2.4127
Shear rate	1.72	3.45	57.45	114.89	172.34	191.49	382.98
$\log(\text{Shear rate})$	0.2364	0.5374	1.7593	2.0603	2.2364	2.2821	2.5832
$\log(\text{Shear stress})$	-0.373	-0.222	0.157	0.263	0.331	0.340	0.499
n	0.4083	0.4083	0.4083	0.4083	0.4083	0.4083	0.4083
k	0.267	0.267	0.267	0.267	0.267	0.267	0.267
η	0.1933	0.1283	0.0243	0.0161	0.0127	0.0119	0.0079

Viscosity data for the 500ppm PAM solution with 5ppm SDS

RPM	0.9	1.8	30	60	90	100	200
Ω	0.094	0.188	3.140	6.280	9.420	10.467	20.933
$\ln(\Omega)$	-2.362	-1.669	1.144	1.837	2.243	2.348	3.041
Dail Reading	11	12	20.5	24	27.5	29	40
Shear stress	0.5997	0.6878	1.4367	1.7450	2.0534	2.1855	3.1546
$\ln(\text{Shear stress})$	-0.511	-0.374	0.362	0.557	0.719	0.782	1.149
N	2.3511	2.3511	2.3511	2.3511	2.3511	2.3511	2.3511
Shear rate	1.72	3.43	57.23	114.47	171.70	190.78	381.56
$\log(\text{Shear rate})$	0.2348	0.5358	1.7577	2.0587	2.2348	2.2805	2.5816
$\log(\text{Shear stress})$	-0.222	-0.163	0.157	0.242	0.312	0.340	0.499
n	0.4129	0.4129	0.4129	0.4129	0.4129	0.4129	0.4129
k	0.256	0.256	0.256	0.256	0.256	0.256	0.256
η	0.1866	0.1242	0.0238	0.0159	0.0125	0.0117	0.0078

Viscosity data for the 500ppm PAM solution with 10ppm SDS

RPM	0.9	1.8	30	60	90	100	200
Ω	0.094	0.188	3.140	6.280	9.420	10.467	20.933
$\ln(\Omega)$	-2.362	-1.669	1.144	1.837	2.243	2.348	3.041
Dail Reading	10	12	20	26.5	30	30.5	40
Shear stress	0.5116	0.6878	1.3926	1.9653	2.2736	2.3177	3.1546
$\ln(\text{Shear stress})$	-0.670	-0.374	0.331	0.676	0.821	0.841	1.149
N	2.345	2.345	2.345	2.345	2.345	2.345	2.345
Shear rate	1.72	3.43	57.21	114.43	171.64	190.71	381.42
$\log(\text{Shear rate})$	0.2346	0.5356	1.7575	2.0585	2.2346	2.2804	2.5814
$\log(\text{Shear stress})$	-0.291	-0.163	0.144	0.293	0.357	0.365	0.499
n	0.4242	0.4242	0.4242	0.4242	0.4242	0.4242	0.4242
k	0.255	0.255	0.255	0.255	0.255	0.255	0.255
η	0.1865	0.1251	0.0248	0.0166	0.0132	0.0124	0.0083

Viscosity data for the 500ppm PAM solution with 50ppm SDS

RPM	0.9	1.8	30	60	90	100	200
Ω	0.094	0.188	3.140	6.280	9.420	10.467	20.933
$\ln(\Omega)$	-2.362	-1.669	1.144	1.837	2.243	2.348	3.041
Dail Reading	9.5	11	20	26	29.5	30	40
Shear stress	0.4676	0.5997	1.3926	1.9212	2.2296	2.2736	3.1546
$\ln(\text{Shear stress})$	-0.760	-0.511	0.331	0.653	0.802	0.821	1.149
N	2.3493	2.3493	2.3493	2.3493	2.3493	2.3493	2.3493
Shear rate	1.72	3.43	57.23	114.46	171.68	190.76	381.52
$\log(\text{Shear rate})$	0.2347	0.5358	1.7576	2.0586	2.2347	2.2805	2.5815
$\log(\text{Shear stress})$	-0.330	-0.222	0.144	0.284	0.348	0.357	0.499
n	0.4241	0.4241	0.4241	0.4241	0.4241	0.4241	0.4241
k	0.251	0.251	0.251	0.251	0.251	0.251	0.251
η	0.1842	0.1236	0.0245	0.0164	0.0130	0.0122	0.0082

Viscosity data for the 500ppm PAM solution with 100ppm SDS

RPM	0.9	1.8	30	60	90	100	200
Ω	0.094	0.188	3.140	6.280	9.420	10.467	20.933
$\ln(\Omega)$	-2.362	-1.669	1.144	1.837	2.243	2.348	3.041
Dail Reading	10	11	21	25.5	29.5	31.5	42.5
Shear stress	0.5116	0.5997	1.4807	1.8772	2.2296	2.4058	3.3749
$\ln(\text{Shear stress})$	-0.670	-0.511	0.393	0.630	0.802	0.878	1.216
N	2.2716	2.2716	2.2716	2.2716	2.2716	2.2716	2.2716
Shear rate	1.71	3.42	56.96	113.92	170.88	189.87	379.73
$\log(\text{Shear rate})$	0.2327	0.5337	1.7556	2.0566	2.2327	2.2784	2.5795
$\log(\text{Shear stress})$	-0.291	-0.222	0.170	0.273	0.348	0.381	0.528
n	0.4351	0.4351	0.4351	0.4351	0.4351	0.4351	0.4351
k	0.246	0.246	0.246	0.246	0.246	0.246	0.246
η	0.1820	0.1231	0.0251	0.0170	0.0135	0.0127	0.0086

Apparent viscosity versus SDS concentration for the 500ppm PAM solutions

SDS concentration	30rpm	90rpm	200rpm
0 ppm	0.0243	0.0127	0.0079
5 ppm	0.0238	0.0125	0.0078
10 ppm	0.0248	0.0132	0.0083
50 ppm	0.0245	0.0130	0.0082
100 ppm	0.0251	0.0135	0.0086

Appendix C-2. Flow loop experiment data

Flow loop data for the 1000ppm PAM solution with 0ppm SDS in 1.5-inch pipeline

FR signal	PD signal	Velocity	Re	f	%DR*	fs	%DR**
4.978	2.585	6.435	32295	0.002	48.4%	0.003	37.0%
4.862	2.508	6.248	30813	0.002	48.4%	0.003	37.2%
4.743	2.448	6.055	29320	0.002	47.6%	0.003	36.8%
4.639	2.384	5.887	28037	0.002	47.5%	0.003	37.0%
4.553	2.356	5.748	26993	0.002	46.3%	0.003	36.0%
4.458	2.315	5.595	25857	0.002	45.5%	0.003	35.3%
4.339	2.239	5.403	24459	0.002	45.4%	0.003	35.8%
4.234	2.209	5.233	23250	0.002	43.7%	0.003	34.1%
4.094	2.144	5.007	21673	0.002	42.5%	0.003	33.5%
3.962	2.074	4.793	20224	0.002	41.8%	0.003	33.2%
3.808	1.995	4.545	18581	0.002	40.9%	0.004	33.1%
3.653	1.926	4.294	16981	0.002	39.4%	0.004	32.3%
3.538	1.874	4.108	15828	0.003	38.2%	0.004	31.7%
3.411	1.812	3.903	14590	0.003	37.3%	0.004	31.7%
3.255	1.744	3.651	13121	0.003	35.6%	0.004	30.9%
3.128	1.692	3.446	11969	0.003	33.9%	0.004	30.1%
3.005	1.640	3.247	10891	0.003	32.3%	0.004	29.6%
2.867	1.578	3.024	9726	0.003	31.0%	0.004	29.4%
2.716	1.523	2.780	8509	0.003	27.9%	0.004	27.8%
2.558	1.456	2.525	7301	0.003	26.0%	0.005	27.9%
2.464	1.423	2.373	6616	0.004	23.8%	0.005	27.2%
2.332	1.378	2.160	5696	0.004	20.1%	0.005	26.2%
2.231	4.393	1.996	5027	0.004	11.8%	0.005	19.9%
2.162	4.104	1.885	4589	0.004	10.4%	0.006	20.7%
2.056	3.781	1.714	3944	0.005	4.6%	0.006	17.7%
1.971	3.449	1.576	3454	0.005	2.0%	0.006	17.6%
1.909	3.232	1.476	3111	0.005	-0.8%	0.006	17.1%
1.823	2.962	1.337	2659	0.006	-6.3%	0.007	15.9%
1.699	2.537	1.137	2054	0.006	-13.0%	0.008	16.8%
1.563	2.093	0.917	1460	0.007	-21.7%	0.009	18.1%
1.480	1.842	0.783	1136	0.008	-28.4%	0.010	18.1%
1.409	1.669	0.668	883	0.009	-40.4%	0.011	16.8%
1.318	1.431	0.521	595	0.011	-55.0%	0.013	19.3%
1.228	1.174	0.376	354	0.012	-56.2%	0.017	31.0%
1.172	1.119	0.285	228	0.017	-112.0%	0.022	21.9%
1.133	1.086	0.222	153	0.024	-190.0%	0.027	8.3%

Flow loop data for the 1000ppm PAM solution with 5ppm SDS in 1.5-inch pipeline

FR signal	PD signal	Velocity	Re	f	%DR*	fs	%DR**
5.077	2.499	6.516	34219	0.002	52.9%	0.003	39.9%
4.974	2.449	6.352	32844	0.002	52.4%	0.003	39.6%
4.831	2.379	6.124	30971	0.002	51.7%	0.003	39.3%
4.650	2.301	5.835	28660	0.002	50.5%	0.003	38.3%
4.437	2.184	5.494	26028	0.002	50.0%	0.003	38.5%
4.253	2.109	5.201	23831	0.002	48.5%	0.003	37.5%
4.102	2.041	4.960	22084	0.002	47.5%	0.003	37.0%
3.896	1.954	4.631	19782	0.002	45.9%	0.003	36.1%
3.582	1.816	4.129	16460	0.002	43.6%	0.004	35.2%
3.382	1.738	3.810	14467	0.002	41.5%	0.004	34.1%
3.209	1.662	3.534	12821	0.003	40.3%	0.004	34.1%
2.968	1.572	3.149	10656	0.003	37.2%	0.004	32.8%
2.809	1.513	2.895	9312	0.003	35.0%	0.004	31.9%
2.657	1.456	2.653	8092	0.003	33.0%	0.004	31.9%
2.462	4.884	2.341	6623	0.004	25.0%	0.005	26.1%
2.338	4.504	2.143	5748	0.004	20.6%	0.005	24.4%
2.151	3.896	1.845	4519	0.004	13.9%	0.005	21.5%
2.009	3.427	1.618	3661	0.005	8.3%	0.006	20.1%
1.907	3.109	1.455	3088	0.005	3.1%	0.006	19.4%
1.799	2.777	1.283	2523	0.006	-3.1%	0.007	17.6%
1.707	2.5	1.136	2075	0.006	-9.4%	0.007	16.9%
1.593	2.168	0.954	1568	0.007	-18.9%	0.008	15.8%
1.484	1.858	0.780	1135	0.008	-29.8%	0.009	14.6%
1.377	1.578	0.609	764	0.010	-45.3%	0.011	16.3%
1.288	1.345	0.467	499	0.011	-58.7%	0.014	20.4%
1.217	1.168	0.354	319	0.013	-68.5%	0.018	27.9%
1.146	1.114	0.240	172	0.023	-177.7%	0.024	6.2%
1.108	1.081	0.180	108	0.036	-307.5%	0.033	-10.5%

* Percent drag reduction based on Blasius equation

** Percent drag reduction based on Dodge-Metzner equation

Flow loop data for the 1000ppm PAM solution with 10ppm SDS in 1.5-inch pipeline

FR signal	PD signal	Velocity	Re	f	%DR*	fs	%DR**
4.976	2.449	6.355	32115	0.002	52.4%	0.003	41.0%
4.828	2.376	6.119	30231	0.002	51.8%	0.003	41.1%
4.656	2.296	5.844	28094	0.002	50.8%	0.003	40.1%
4.492	2.217	5.582	26112	0.002	50.0%	0.003	39.7%
4.334	2.147	5.330	24254	0.002	49.0%	0.003	39.0%
4.186	2.083	5.094	22561	0.002	47.9%	0.003	38.4%
3.967	1.983	4.744	20140	0.002	46.5%	0.003	37.8%
3.812	1.916	4.497	18490	0.002	45.3%	0.003	37.2%
3.600	1.830	4.158	16319	0.002	43.3%	0.004	36.1%
3.452	1.773	3.922	14864	0.002	41.6%	0.004	35.1%
3.288	1.698	3.660	13312	0.002	40.7%	0.004	35.3%
3.083	1.619	3.333	11463	0.003	38.3%	0.004	34.2%
2.937	1.568	3.100	10210	0.003	35.9%	0.004	33.0%
2.725	1.487	2.761	8489	0.003	33.1%	0.004	32.4%
2.589	1.439	2.544	7449	0.003	30.7%	0.005	31.7%
2.403	4.733	2.247	6110	0.004	22.4%	0.005	25.9%
2.324	4.487	2.121	5572	0.004	19.5%	0.005	25.0%
2.243	4.222	1.992	5040	0.004	16.7%	0.005	23.4%
2.180	3.990	1.891	4640	0.004	15.0%	0.005	23.4%
2.067	3.650	1.711	3954	0.005	9.7%	0.006	21.3%
1.94	3.243	1.508	3232	0.005	3.6%	0.006	19.9%
1.868	3.007	1.393	2848	0.005	0.1%	0.007	19.0%
1.774	2.717	1.243	2374	0.006	-5.6%	0.007	18.0%
1.688	2.448	1.106	1970	0.006	-11.1%	0.008	17.3%
1.57	2.105	0.917	1462	0.007	-21.3%	0.009	17.2%
1.495	1.887	0.797	1169	0.008	-28.4%	0.010	17.6%
1.43	1.702	0.694	936	0.009	-35.0%	0.010	17.6%
1.368	1.542	0.595	732	0.010	-44.1%	0.012	19.5%
1.278	1.324	0.451	471	0.011	-61.7%	0.014	19.6%
1.219	1.159	0.357	324	0.012	-61.4%	0.017	28.8%
1.178	1.130	0.291	234	0.017	-109.5%	0.020	17.2%
1.125	1.096	0.207	135	0.029	-238.0%	0.029	-1.8%

* Percent drag reduction based on Blasius equation

** Percent drag reduction based on Dodge-Metzner equation

Flow loop data for the 1000ppm PAM solution with 50ppm SDS in 1.5-inch pipeline

FR signal	PD signal	Velocity	Re	f	%DR*	fs	%DR**
5.086	2.544	6.603	34280	0.002	52.0%	0.003	38.6%
4.852	2.418	6.226	31182	0.002	51.2%	0.003	38.4%
4.661	2.304	5.917	28737	0.002	51.0%	0.003	38.8%
4.473	2.224	5.614	26405	0.002	49.6%	0.003	37.8%
4.290	2.147	5.318	24207	0.002	48.2%	0.003	36.7%
4.113	2.049	5.033	22150	0.002	47.9%	0.003	37.3%
3.916	1.975	4.715	19944	0.002	45.8%	0.003	35.7%
3.657	1.861	4.296	17178	0.002	43.8%	0.003	34.9%
3.464	1.769	3.985	15220	0.002	42.9%	0.004	35.0%
3.272	1.697	3.675	13362	0.002	40.5%	0.004	33.7%
3.066	1.617	3.342	11472	0.003	38.1%	0.004	32.8%
2.819	1.521	2.944	9353	0.003	35.1%	0.004	32.0%
2.603	1.442	2.595	7637	0.003	31.8%	0.005	31.1%
2.401	4.677	2.269	6154	0.004	23.9%	0.005	26.3%
2.266	4.220	2.051	5232	0.004	20.0%	0.005	24.9%
2.162	3.910	1.883	4561	0.004	15.6%	0.005	22.8%
2.012	3.444	1.641	3655	0.005	8.9%	0.006	21.0%
1.922	3.160	1.496	3149	0.005	4.6%	0.006	19.4%
1.811	2.823	1.316	2565	0.006	-2.0%	0.007	18.6%
1.688	2.449	1.118	1972	0.006	-10.3%	0.008	17.3%
1.572	2.097	0.931	1469	0.007	-18.8%	0.008	16.4%
1.437	1.734	0.713	956	0.009	-35.0%	0.010	15.5%
1.336	1.467	0.550	630	0.010	-49.5%	0.012	19.0%
1.223	1.178	0.367	329	0.012	-64.3%	0.017	28.5%
1.132	1.118	0.220	145	0.028	-231.5%	0.027	-4.3%
1.109	1.089	0.183	108	0.036	-310.9%	0.033	-11.7%

* Percent drag reduction based on Blasius equation

** Percent drag reduction based on Dodge-Metzner equation

Flow loop data for the 1000ppm PAM solution with 100ppm SDS in 1.5-inch pipeline

FR signal	PD signal	Velocity	Re	f	%DR*	fs	%DR**
5.064	2.375	6.589	33612	0.002	57.1%	0.003	46.6%
4.961	2.348	6.423	32264	0.002	56.0%	0.003	45.5%
4.817	2.287	6.189	30415	0.002	55.2%	0.003	45.0%
4.609	2.197	5.852	27816	0.002	54.1%	0.003	44.3%
4.363	2.086	5.454	24856	0.002	53.0%	0.003	43.7%
4.143	1.975	5.098	22316	0.002	52.6%	0.003	44.1%
3.856	1.874	4.633	19158	0.002	49.8%	0.003	42.2%
3.659	1.802	4.314	17096	0.002	48.0%	0.004	41.1%
3.451	1.711	3.977	15015	0.002	47.0%	0.004	41.1%
3.276	1.645	3.693	13344	0.002	45.4%	0.004	40.5%
3.037	1.561	3.306	11183	0.002	42.6%	0.004	39.4%
2.844	1.493	2.994	9544	0.003	40.3%	0.004	38.5%
2.627	1.420	2.642	7820	0.003	37.2%	0.005	37.4%
2.429	4.558	2.322	6361	0.003	29.0%	0.005	32.0%
2.274	4.096	2.071	5299	0.004	24.0%	0.005	30.1%
2.170	3.812	1.902	4628	0.004	19.5%	0.005	27.6%
2.083	3.523	1.761	4093	0.004	16.8%	0.006	27.3%
1.941	3.105	1.531	3274	0.005	10.3%	0.006	25.3%
1.809	2.736	1.317	2575	0.005	2.3%	0.007	23.2%
1.658	2.311	1.073	1856	0.006	-8.7%	0.008	20.8%
1.532	1.974	0.869	1325	0.007	-21.3%	0.009	18.1%
1.382	1.576	0.626	785	0.009	-40.1%	0.011	19.1%
1.301	1.303	0.495	540	0.009	-33.5%	0.014	32.0%
1.206	1.174	0.341	298	0.014	-85.6%	0.019	24.3%
1.15	1.127	0.250	182	0.022	-174.7%	0.024	5.0%
1.117	1.092	0.197	124	0.032	-268.1%	0.030	-8.3%
1.095	1.075	0.161	90	0.045	-387.6%	0.036	-22.5%

* Percent drag reduction based on Blasius equation

** Percent drag reduction based on Dodge-Metzner equation

Flow loop data for the 1000ppm PAM solution with 0ppm SDS in 1-inch pipeline

FR signal	PD signal	Velocity	Re	f	%DR*	fs	%DR**
4.069	2.107	12.404	75920	0.001	78.6%	0.002	68.6%
3.963	2.053	11.976	71802	0.001	78.4%	0.002	68.5%
3.892	2.027	11.690	69091	0.001	78.0%	0.002	68.1%
3.816	1.991	11.383	66233	0.001	77.8%	0.002	67.9%
3.672	1.909	10.802	60940	0.001	77.7%	0.003	68.1%
3.507	1.830	10.136	55079	0.001	77.3%	0.003	67.8%
3.354	1.763	9.518	49844	0.001	76.8%	0.003	67.4%
3.206	1.695	8.921	44966	0.001	76.4%	0.003	67.2%
3.086	1.640	8.437	41149	0.001	76.1%	0.003	67.1%
2.960	1.577	7.928	37278	0.001	76.0%	0.003	67.5%
2.840	1.539	7.444	33725	0.001	75.0%	0.003	66.6%
2.727	1.497	6.988	30502	0.001	74.4%	0.003	66.1%
2.617	1.456	6.544	27481	0.001	73.7%	0.003	65.8%
2.495	1.420	6.051	24268	0.001	72.3%	0.003	64.6%
2.411	4.905	5.712	22144	0.001	69.9%	0.003	61.9%
2.301	4.604	5.269	19472	0.001	67.8%	0.003	60.1%
2.175	4.349	4.760	16572	0.002	64.2%	0.004	56.6%
2.053	4.167	4.268	13932	0.002	58.9%	0.004	51.4%
1.784	3.743	3.182	8738	0.003	40.0%	0.004	34.6%
1.725	3.623	2.944	7722	0.003	34.1%	0.005	29.5%
1.667	3.450	2.710	6770	0.004	28.6%	0.005	25.4%
1.576	3.171	2.343	5371	0.004	17.7%	0.005	17.7%
1.517	2.988	2.104	4530	0.005	8.5%	0.006	11.4%
1.429	2.757	1.749	3377	0.006	-12.9%	0.006	-2.6%
1.364	2.575	1.487	2608	0.008	-35.9%	0.007	-16.3%
1.283	2.333	1.160	1758	0.011	-80.6%	0.008	-40.8%
1.211	2.138	0.869	1112	0.017	-160.2%	0.010	-78.7%
1.156	1.984	0.647	696	0.028	-284.3%	0.012	-130.7%
1.128	1.882	0.534	513	0.037	-389.9%	0.014	-167.2%

* Percent drag reduction based on Blasius equation

** Percent drag reduction based on Dodge-Metzner equation

Flow loop data for the 1000ppm PAM solution with 5ppm SDS in 1-inch pipeline

FR signal	PD signal	Velocity	Re	f	%DR*	fs	%DR**
4.079	2.095	12.296	79067	0.001	78.8%	0.002	67.5%
3.936	2.065	11.725	73268	0.001	77.6%	0.002	65.9%
3.825	2.029	11.283	68881	0.001	76.9%	0.002	65.0%
3.669	1.938	10.661	62891	0.001	76.7%	0.002	65.2%
3.419	1.811	9.664	53726	0.001	76.2%	0.003	65.0%
3.262	1.717	9.038	48252	0.001	76.4%	0.003	65.8%
2.989	1.617	7.949	39273	0.001	74.7%	0.003	64.2%
2.825	1.555	7.295	34219	0.001	73.7%	0.003	63.4%
2.643	1.482	6.569	28924	0.001	72.7%	0.003	62.9%
2.413	1.407	5.652	22725	0.001	70.2%	0.003	60.8%
2.247	4.485	4.990	18608	0.001	66.2%	0.003	56.8%
2.083	3.925	4.336	14854	0.002	63.4%	0.004	54.9%
1.990	3.755	3.965	12869	0.002	59.5%	0.004	51.2%
1.873	3.474	3.499	10528	0.002	54.5%	0.004	46.9%
1.734	3.105	2.945	7983	0.003	47.0%	0.004	41.4%
1.686	2.954	2.753	7167	0.003	44.4%	0.005	39.7%
1.612	2.778	2.458	5975	0.003	37.8%	0.005	34.7%
1.527	2.564	2.119	4710	0.004	28.2%	0.005	27.9%
1.459	2.386	1.848	3781	0.005	18.2%	0.006	21.8%
1.397	2.246	1.601	3003	0.006	4.3%	0.006	12.8%
1.331	2.070	1.338	2251	0.007	-14.7%	0.007	3.1%
1.203	1.763	0.827	1041	0.014	-99.8%	0.010	-39.5%
1.149	1.616	0.612	642	0.021	-185.0%	0.012	-69.1%
1.098	1.531	0.408	336	0.042	-415.0%	0.017	-147.3%

* Percent drag reduction based on Blasius equation

** Percent drag reduction based on Dodge-Metzner equation

Flow loop data for the 1000ppm PAM solution with 10ppm SDS in 1-inch pipeline

FR signal	PD signal	Velocity	Re	f	%DR*	fs	%DR**
4.039	2.071	12.136	74966	0.001	78.8%	0.002	68.3%
3.916	2.037	11.646	70189	0.001	77.9%	0.002	67.3%
3.834	2.001	11.319	67070	0.001	77.6%	0.002	67.0%
3.786	1.972	11.127	65269	0.001	77.6%	0.002	67.1%
3.706	1.922	10.808	62308	0.001	77.7%	0.002	67.4%
3.557	1.829	10.214	56931	0.001	77.9%	0.003	68.0%
3.388	1.789	9.540	51055	0.001	76.3%	0.003	66.2%
3.226	1.703	8.894	45649	0.001	76.2%	0.003	66.5%
3.059	1.679	8.228	40317	0.001	73.7%	0.003	63.4%
2.918	1.551	7.666	36010	0.001	76.0%	0.003	67.1%
2.793	1.513	7.167	32346	0.001	75.0%	0.003	66.1%
2.653	1.472	6.609	28419	0.001	73.5%	0.003	64.8%
2.434	1.391	5.736	22666	0.001	72.2%	0.003	64.1%
2.341	4.493	5.365	20373	0.001	70.1%	0.003	62.1%
2.118	4.078	4.476	15256	0.002	63.6%	0.004	55.8%
2.008	3.860	4.037	12940	0.002	59.4%	0.004	51.9%
1.937	3.756	3.754	11522	0.002	55.4%	0.004	48.4%
1.802	3.509	3.216	9000	0.003	46.5%	0.004	40.3%
1.714	3.301	2.865	7484	0.003	39.6%	0.005	35.0%
1.657	3.231	2.638	6559	0.003	32.2%	0.005	28.9%
1.488	2.882	1.964	4096	0.005	2.9%	0.006	7.3%
1.428	2.687	1.724	3329	0.006	-10.3%	0.006	-1.4%
1.323	2.382	1.306	2135	0.009	-49.8%	0.007	-25.0%
1.274	2.283	1.110	1648	0.012	-86.2%	0.008	-45.2%
1.232	2.149	0.943	1270	0.015	-125.0%	0.009	-63.5%
1.174	1.979	0.712	810	0.023	-220.6%	0.011	-105.5%
1.115	1.831	0.476	427	0.044	-463.4%	0.015	-193.7%

* Percent drag reduction based on Blasius equation

** Percent drag reduction based on Dodge-Metzner equation

Flow loop data for the 1000ppm PAM solution with 50ppm SDS in 1-inch pipeline

FR signal	PD signal	Velocity	Re	f	%DR*	fs	%DR**
4.103	2.191	12.529	80206	0.001	77.4%	0.002	65.1%
3.926	2.067	11.816	72989	0.001	77.6%	0.002	65.8%
3.801	2.001	11.312	68049	0.001	77.3%	0.002	65.7%
3.699	1.940	10.900	64116	0.001	77.3%	0.002	65.9%
3.475	1.824	9.997	55793	0.001	77.0%	0.002	65.9%
3.257	1.739	9.118	48120	0.001	75.8%	0.003	64.7%
3.049	1.637	8.279	41206	0.001	75.4%	0.003	64.8%
2.836	1.535	7.421	34555	0.001	75.1%	0.003	65.2%
2.680	1.478	6.792	29969	0.001	74.2%	0.003	64.6%
2.513	1.433	6.118	25338	0.001	72.0%	0.003	62.5%
2.351	1.369	5.465	21132	0.001	71.2%	0.003	62.4%
2.213	4.281	4.909	17782	0.001	66.7%	0.003	57.7%
2.084	3.911	4.389	14852	0.002	63.9%	0.004	55.4%
1.991	3.568	4.014	12865	0.002	62.5%	0.004	54.8%
1.873	3.402	3.538	10503	0.002	56.1%	0.004	48.7%
1.770	3.246	3.123	8593	0.003	48.7%	0.004	42.3%
1.674	3.115	2.735	6946	0.003	38.8%	0.005	33.8%
1.552	2.924	2.244	5051	0.004	20.7%	0.005	19.2%
1.474	2.819	1.929	3962	0.005	1.9%	0.006	5.1%
1.357	2.508	1.457	2524	0.008	-35.2%	0.007	-19.0%
1.300	2.368	1.227	1915	0.010	-67.3%	0.008	-36.7%
1.172	1.967	0.711	797	0.023	-220.8%	0.011	-103.2%
1.149	1.936	0.619	637	0.029	-298.4%	0.012	-135.6%
1.078	1.803	0.332	234	0.089	-939.0%	0.021	-333.0%

* Percent drag reduction based on Blasius equation

** Percent drag reduction based on Dodge-Metzner equation

Flow loop data for the 1000ppm PAM solution with 100ppm SDS in 1-inch pipeline

FR signal	PD signal	Velocity	Re	f	%DR*	fs	%DR**
4.062	2.187	12.404	76660	0.001	77.0%	0.002	65.7%
3.951	2.093	11.955	72279	0.001	77.4%	0.002	66.6%
3.889	2.046	11.705	69875	0.001	77.6%	0.002	66.9%
3.805	2.017	11.365	66666	0.001	77.1%	0.002	66.3%
3.665	1.919	10.798	61444	0.001	77.4%	0.002	67.1%
3.517	1.849	10.200	56098	0.001	77.0%	0.003	66.8%
3.297	1.766	9.310	48492	0.001	75.7%	0.003	65.5%
3.086	1.675	8.456	41594	0.001	74.7%	0.003	64.9%
2.872	1.614	7.591	35009	0.001	72.3%	0.003	62.3%
2.721	1.527	6.980	30622	0.001	72.6%	0.003	63.3%
2.555	1.481	6.308	26058	0.001	70.3%	0.003	61.1%
2.395	1.424	5.661	21923	0.001	68.5%	0.003	59.8%
2.242	4.132	5.042	18225	0.001	69.5%	0.003	62.1%
2.133	3.733	4.601	15749	0.001	68.6%	0.004	61.7%
2.041	3.529	4.229	13765	0.002	66.1%	0.004	59.7%
1.895	3.219	3.638	10828	0.002	61.0%	0.004	55.3%
1.750	2.981	3.052	8179	0.002	52.3%	0.004	47.9%
1.648	2.880	2.639	6487	0.003	41.4%	0.005	38.7%
1.544	2.686	2.219	4917	0.004	28.1%	0.005	28.6%
1.450	2.578	1.838	3642	0.005	5.9%	0.006	12.7%
1.381	2.431	1.559	2801	0.007	-15.0%	0.007	-1.1%
1.321	2.328	1.316	2138	0.009	-44.6%	0.007	-19.3%
1.248	2.177	1.021	1425	0.013	-102.7%	0.009	-52.7%
1.188	1.966	0.778	924	0.019	-174.7%	0.011	-80.6%
1.138	1.853	0.576	572	0.031	-318.6%	0.013	-140.5%
1.094	1.810	0.398	317	0.063	-665.4%	0.018	-252.9%

* Percent drag reduction based on Blasius equation

** Percent drag reduction based on Dodge-Metzner equation

Flow loop data for the 500ppm PAM solution with 0ppm SDS in 1.5-inch pipeline

FR signal	PD signal	Velocity	Re	f	%DR*	fs	%DR**
5.121	2.833	6.687	58763	0.002	44.0%	0.003	19.6%
4.934	2.699	6.384	54581	0.002	43.7%	0.003	19.9%
4.772	2.590	6.121	51051	0.002	43.3%	0.003	20.0%
4.570	2.467	5.794	46774	0.002	42.5%	0.003	19.6%
4.383	2.360	5.491	42940	0.002	41.5%	0.003	19.0%
4.174	2.240	5.152	38800	0.002	40.5%	0.003	18.6%
3.988	2.141	4.850	35249	0.002	39.2%	0.003	17.8%
3.816	2.050	4.572	32080	0.002	38.0%	0.003	17.3%
3.693	1.991	4.372	29882	0.003	36.8%	0.003	16.5%
3.519	1.902	4.090	26873	0.003	35.5%	0.003	16.0%
3.367	1.826	3.844	24343	0.003	34.3%	0.003	15.5%
3.213	1.751	3.594	21875	0.003	33.0%	0.003	15.1%
2.970	1.638	3.200	18185	0.003	30.6%	0.004	14.4%
2.839	1.584	2.988	16303	0.003	28.5%	0.004	13.2%
2.723	1.534	2.800	14701	0.003	27.0%	0.004	12.9%
2.569	1.465	2.550	12670	0.003	25.6%	0.004	13.1%
2.460	1.426	2.374	11302	0.004	23.0%	0.004	11.7%
2.344	4.808	2.186	9911	0.004	15.7%	0.004	5.3%
2.235	4.370	2.009	8667	0.004	13.1%	0.004	4.9%
2.148	4.039	1.868	7719	0.004	10.5%	0.005	4.1%
2.031	3.614	1.678	6509	0.005	6.4%	0.005	2.5%
1.947	3.306	1.542	5689	0.005	3.5%	0.005	2.2%
1.824	2.883	1.343	4564	0.005	-1.9%	0.006	1.4%
1.738	2.591	1.203	3833	0.006	-5.9%	0.006	1.3%
1.640	2.264	1.045	3060	0.006	-10.4%	0.006	2.1%
1.532	1.939	0.870	2285	0.007	-17.5%	0.007	2.4%
1.447	1.69	0.732	1737	0.008	-23.1%	0.008	3.6%
1.378	1.521	0.620	1334	0.009	-32.0%	0.009	2.7%
1.297	1.342	0.489	913	0.010	-47.9%	0.011	2.6%
1.232	1.221	0.383	620	0.013	-72.3%	0.012	-1.5%
1.153	1.098	0.255	325	0.019	-139.0%	0.018	-7.9%
1.118	1.048	0.198	218	0.026	-200.5%	0.022	-17.3%
1.093	1.034	0.158	151	0.038	-318.6%	0.027	-41.9%

* Percent drag reduction based on Blasius equation

** Percent drag reduction based on Dodge-Metzner equation

Flow loop data for the 500ppm PAM solution with 5ppm SDS in 1.5-inch pipeline

FR signal	PD signal	Velocity	Re	f	%DR*	fs	%DR**
5.123	2.358	6.575	58736	0.002	58.1%	0.003	40.2%
4.900	2.257	6.220	53780	0.002	57.3%	0.003	39.7%
4.759	2.216	5.995	50730	0.002	56.0%	0.003	38.2%
4.599	2.142	5.740	47350	0.002	55.5%	0.003	37.9%
4.428	2.078	5.468	43834	0.002	54.3%	0.003	36.8%
4.275	2.014	5.224	40774	0.002	53.5%	0.003	36.3%
4.124	1.953	4.984	37835	0.002	52.6%	0.003	35.6%
3.902	1.871	4.630	33663	0.002	50.8%	0.003	34.2%
3.763	1.814	4.408	31144	0.002	50.0%	0.003	33.7%
3.607	1.753	4.160	28404	0.002	48.9%	0.003	33.0%
3.416	1.687	3.856	25179	0.002	46.9%	0.003	31.6%
3.213	1.609	3.532	21911	0.002	45.3%	0.003	30.9%
3.045	1.550	3.265	19335	0.002	43.5%	0.003	29.9%
2.840	1.481	2.938	16357	0.003	40.9%	0.004	28.4%
2.678	1.422	2.680	14137	0.003	39.4%	0.004	28.2%
2.513	4.724	2.417	12000	0.003	32.0%	0.004	21.5%
2.406	4.379	2.247	10686	0.003	29.6%	0.004	20.3%
2.285	4.027	2.054	9268	0.004	25.8%	0.004	18.1%
2.175	3.685	1.879	8045	0.004	22.5%	0.005	16.6%
2.023	3.229	1.637	6463	0.004	17.2%	0.005	14.4%
1.912	2.915	1.460	5390	0.005	12.1%	0.005	12.4%
1.720	2.375	1.154	3712	0.005	1.8%	0.006	8.4%
1.595	2.050	0.955	2748	0.006	-7.9%	0.007	6.5%
1.502	1.818	0.807	2103	0.007	-17.3%	0.007	3.6%
1.433	1.643	0.697	1667	0.008	-24.5%	0.008	4.4%
1.325	1.389	0.525	1063	0.010	-40.2%	0.010	3.9%
1.245	1.238	0.397	683	0.012	-65.9%	0.012	0.7%
1.179	1.131	0.292	420	0.016	-108.6%	0.015	-7.0%
1.125	1.055	0.206	241	0.025	-185.3%	0.021	-19.4%

* Percent drag reduction based on Blasius equation

** Percent drag reduction based on Dodge-Metzner equation

Flow loop data for the 500ppm PAM solution with 10ppm SDS in 1.5-inch pipeline

FR signal	PD signal	Velocity	Re	f	%DR*	fs	%DR**
5.123	2.763	6.675	54848	0.002	46.1%	0.003	26.3%
5.009	2.682	6.491	52480	0.002	46.0%	0.003	26.6%
4.901	2.613	6.316	50272	0.002	45.7%	0.003	26.6%
4.726	2.511	6.033	46768	0.002	44.9%	0.003	26.1%
4.517	2.384	5.695	42707	0.002	44.3%	0.003	25.9%
4.314	2.288	5.367	38892	0.002	42.5%	0.003	24.6%
4.118	2.178	5.050	35334	0.002	41.6%	0.003	24.1%
3.854	2.043	4.623	30743	0.002	39.8%	0.003	23.1%
3.659	1.941	4.307	27503	0.002	38.6%	0.003	22.8%
3.470	1.852	4.002	24491	0.003	36.9%	0.003	21.9%
3.300	1.771	3.727	21893	0.003	35.5%	0.003	21.3%
3.095	1.676	3.395	18904	0.003	33.7%	0.004	20.6%
2.960	1.619	3.177	17024	0.003	32.0%	0.004	19.9%
2.753	1.534	2.842	14284	0.003	29.1%	0.004	18.6%
2.609	1.472	2.609	12484	0.003	27.5%	0.004	18.7%
2.477	1.421	2.396	10913	0.003	25.3%	0.004	17.7%
2.355	4.752	2.198	9531	0.004	17.9%	0.004	11.6%
2.247	4.335	2.024	8365	0.004	15.2%	0.005	10.7%
2.152	3.981	1.870	7387	0.004	12.5%	0.005	10.0%
2.015	3.509	1.649	6055	0.005	7.3%	0.005	8.2%
1.897	3.076	1.458	4988	0.005	3.6%	0.006	7.7%
1.787	2.732	1.280	4063	0.006	-2.4%	0.006	5.6%
1.652	2.282	1.062	3026	0.006	-8.4%	0.007	6.3%
1.558	2.015	0.910	2372	0.007	-15.8%	0.007	6.0%
1.428	1.646	0.699	1568	0.008	-26.1%	0.009	6.7%
1.307	1.361	0.504	935	0.010	-45.2%	0.011	6.9%
1.231	1.213	0.381	601	0.013	-70.2%	0.013	4.1%
1.162	1.108	0.269	348	0.018	-125.5%	0.017	-6.3%
1.115	1.047	0.193	206	0.027	-212.9%	0.023	-21.3%

* Percent drag reduction based on Blasius equation

** Percent drag reduction based on Dodge-Metzner equation

Flow loop data for the 500ppm PAM solution with 50ppm SDS in 1.5-inch pipeline

FR signal	PD signal	Velocity	Re	f	%DR*	fs	%DR**
5.122	2.741	6.677	55759	0.002	46.8%	0.003	26.9%
4.997	2.657	6.475	53120	0.002	46.6%	0.003	27.0%
4.805	2.546	6.164	49159	0.002	45.7%	0.003	26.5%
4.616	2.435	5.858	45371	0.002	45.0%	0.003	26.1%
4.374	2.304	5.467	40685	0.002	43.6%	0.003	25.3%
4.182	2.200	5.156	37101	0.002	42.6%	0.003	24.7%
3.986	2.098	4.839	33569	0.002	41.4%	0.003	24.1%
3.832	2.019	4.590	30885	0.002	40.4%	0.003	23.8%
3.658	1.938	4.308	27953	0.002	38.8%	0.003	23.0%
3.427	1.827	3.934	24228	0.003	37.0%	0.003	21.6%
3.272	1.750	3.684	21839	0.003	36.0%	0.003	21.6%
3.084	1.663	3.379	19065	0.003	34.4%	0.004	21.2%
2.904	1.586	3.088	16540	0.003	32.4%	0.004	20.5%
2.752	1.525	2.842	14513	0.003	30.3%	0.004	19.6%
2.594	1.461	2.586	12509	0.003	28.2%	0.004	19.0%
2.480	1.416	2.402	11132	0.003	26.6%	0.004	18.8%
2.341	4.655	2.177	9535	0.004	18.5%	0.004	12.1%
2.258	4.346	2.043	8624	0.004	16.3%	0.005	11.1%
2.138	3.924	1.849	7368	0.004	12.3%	0.005	9.5%
2.030	3.527	1.674	6301	0.005	9.0%	0.005	8.3%
1.930	3.186	1.512	5368	0.005	5.1%	0.005	7.8%
1.834	2.880	1.357	4525	0.005	0.2%	0.006	6.2%
1.698	2.414	1.137	3424	0.006	-5.0%	0.006	6.5%
1.601	2.121	0.980	2709	0.006	-10.9%	0.007	6.5%
1.509	1.855	0.831	2089	0.007	-17.4%	0.008	8.2%
1.404	1.572	0.661	1457	0.008	-26.6%	0.009	7.9%
1.319	1.369	0.523	1009	0.009	-37.9%	0.010	6.0%
1.223	1.197	0.368	579	0.013	-73.1%	0.014	4.7%
1.169	1.105	0.281	378	0.016	-107.4%	0.017	0.1%
1.133	1.062	0.222	262	0.022	-161.9%	0.020	-10.5%

* Percent drag reduction based on Blasius equation

** Percent drag reduction based on Dodge-Metzner equation

Flow loop data for the 500ppm PAM solution with 100ppm SDS in 1.5-inch pipeline

FR signal	PD signal	Velocity	Re	f	%DR*	fs	%DR**
5.122	2.935	6.601	52231	0.002	40.2%	0.003	20.8%
4.930	2.793	6.294	48478	0.002	39.9%	0.003	20.9%
4.723	2.655	5.963	44546	0.002	39.0%	0.003	20.6%
4.486	2.515	5.584	40194	0.002	37.5%	0.003	19.5%
4.331	2.418	5.336	37436	0.002	36.7%	0.003	19.1%
4.129	2.288	5.013	33950	0.002	35.9%	0.003	19.2%
3.983	2.203	4.779	31507	0.003	35.0%	0.003	18.7%
3.771	2.094	4.440	28079	0.003	32.9%	0.003	17.3%
3.561	1.974	4.104	24826	0.003	31.6%	0.003	17.0%
3.316	1.846	3.712	21217	0.003	29.4%	0.004	16.1%
3.142	1.756	3.434	18781	0.003	27.9%	0.004	15.8%
3.002	1.687	3.210	16900	0.003	26.4%	0.004	15.2%
2.786	1.590	2.864	14141	0.003	23.3%	0.004	13.8%
2.623	1.516	2.603	12178	0.004	21.1%	0.004	13.6%
2.462	1.445	2.346	10347	0.004	18.8%	0.004	13.2%
2.357	1.397	2.178	9211	0.004	18.0%	0.005	13.8%
2.213	4.377	1.948	7733	0.004	9.2%	0.005	7.7%
2.127	4.051	1.810	6895	0.005	6.3%	0.005	6.7%
1.995	3.538	1.599	5678	0.005	2.2%	0.005	5.9%
1.913	3.232	1.468	4966	0.005	-0.8%	0.006	5.5%
1.787	2.763	1.266	3941	0.006	-5.0%	0.006	5.7%
1.686	2.432	1.105	3183	0.006	-10.4%	0.007	5.6%
1.577	2.075	0.930	2433	0.007	-15.8%	0.007	6.5%
1.499	1.840	0.805	1942	0.007	-20.8%	0.008	6.6%
1.402	1.560	0.650	1389	0.008	-26.7%	0.009	10.3%
1.302	1.349	0.490	893	0.010	-47.2%	0.011	8.5%
1.201	1.161	0.329	478	0.014	-87.9%	0.015	4.2%
1.162	1.107	0.266	344	0.018	-126.5%	0.018	-4.3%
1.108	1.033	0.180	186	0.029	-227.4%	0.025	-18.7%

* Percent drag reduction based on Blasius equation

** Percent drag reduction based on Dodge-Metzner equation

Flow loop data for the 500ppm PAM solution with 0ppm SDS in 1-inch pipeline

FR signal	PD signal	Velocity	Re	f	%DR*	fs	%DR**
3.961	3.044	11.965	123482	0.001	57.6%	0.002	28.6%
3.852	2.954	11.525	116337	0.002	56.8%	0.002	27.5%
3.689	2.836	10.867	105950	0.002	55.0%	0.002	25.3%
3.558	2.712	10.339	97866	0.002	54.3%	0.002	24.6%
3.454	2.628	9.919	91620	0.002	53.3%	0.002	23.4%
3.349	2.547	9.496	85471	0.002	52.1%	0.002	22.1%
3.240	2.477	9.056	79257	0.002	50.3%	0.002	19.8%
3.121	2.373	8.576	72674	0.002	49.3%	0.002	18.8%
2.951	2.247	7.890	63643	0.002	46.8%	0.002	16.0%
2.823	2.147	7.373	57142	0.002	44.9%	0.003	14.1%
2.672	2.016	6.764	49812	0.002	43.4%	0.003	13.1%
2.558	1.936	6.304	44530	0.002	41.1%	0.003	10.8%
2.421	1.831	5.751	38479	0.003	38.8%	0.003	8.9%
2.270	1.722	5.142	32197	0.003	35.5%	0.003	6.2%
2.168	1.657	4.731	28194	0.003	32.3%	0.003	3.2%
1.987	1.557	4.000	21589	0.004	23.4%	0.003	-5.5%
1.865	1.502	3.508	17517	0.004	13.5%	0.004	-15.6%
1.688	1.414	2.794	12193	0.005	-5.3%	0.004	-32.8%
1.568	4.217	2.310	9006	0.006	-22.2%	0.004	-47.1%
1.492	3.506	2.003	7179	0.007	-23.8%	0.005	-42.5%
1.434	3.136	1.769	5891	0.007	-32.5%	0.005	-47.0%
1.400	2.991	1.632	5181	0.008	-43.0%	0.005	-54.2%
1.366	2.823	1.495	4505	0.009	-53.8%	0.006	-62.7%
1.289	2.512	1.184	3109	0.012	-95.1%	0.006	-89.9%
1.245	2.379	1.006	2401	0.015	-138.6%	0.007	-122.0%
1.177	2.263	0.732	1446	0.027	-285.2%	0.009	-213.5%
1.142	2.187	0.591	1028	0.039	-430.7%	0.010	-293.4%
1.112	2.138	0.470	714	0.060	-663.9%	0.012	-405.3%

* Percent drag reduction based on Blasius equation

** Percent drag reduction based on Dodge-Metzner equation

Flow loop data for the 500ppm PAM solution with 5ppm SDS in 1-inch pipeline

FR signal	PD signal	Velocity	Re	f	%DR*	fs	%DR**
4.132	2.776	12.479	134429	0.001	66.3%	0.002	43.2%
4.079	2.762	12.268	130842	0.001	65.6%	0.002	42.1%
3.969	2.705	11.830	123512	0.001	64.5%	0.002	40.6%
3.881	2.642	11.480	117761	0.001	64.0%	0.002	40.0%
3.806	2.586	11.182	112940	0.001	63.6%	0.002	39.6%
3.773	2.579	11.050	110843	0.001	63.0%	0.002	38.7%
3.674	2.501	10.657	104638	0.001	62.6%	0.002	38.2%
3.515	2.391	10.024	94953	0.001	61.4%	0.002	37.0%
3.308	2.252	9.200	82873	0.002	59.7%	0.002	35.1%
3.182	2.178	8.699	75822	0.002	58.2%	0.002	33.3%
3.091	2.119	8.337	70875	0.002	57.3%	0.002	32.3%
2.923	2.014	7.669	62071	0.002	55.3%	0.002	30.1%
2.727	1.888	6.889	52357	0.002	52.9%	0.003	27.7%
2.557	1.785	6.212	44437	0.002	50.2%	0.003	25.1%
2.434	1.717	5.723	39011	0.002	47.7%	0.003	22.4%
2.233	1.606	4.923	30721	0.002	42.7%	0.003	17.6%
2.099	1.531	4.390	25612	0.003	38.9%	0.003	14.2%
1.979	1.469	3.913	21335	0.003	34.4%	0.003	10.1%
1.788	1.368	3.153	15144	0.004	25.7%	0.004	3.4%
1.724	4.366	2.898	13249	0.004	15.5%	0.004	-7.8%
1.660	4.074	2.644	11450	0.005	8.9%	0.004	-13.8%
1.580	3.704	2.325	9341	0.005	-1.0%	0.004	-21.8%
1.479	3.243	1.923	6912	0.007	-18.1%	0.005	-34.8%
1.374	2.892	1.506	4686	0.009	-54.9%	0.006	-63.8%
1.278	2.604	1.124	2945	0.014	-122.3%	0.007	-113.7%
1.223	2.481	0.905	2089	0.020	-202.2%	0.008	-163.8%
1.182	2.418	0.742	1524	0.029	-311.5%	0.009	-235.1%
1.145	2.334	0.595	1072	0.042	-473.9%	0.010	-330.5%

* Percent drag reduction based on Blasius equation

** Percent drag reduction based on Dodge-Metzner equation

Flow loop data for the 500ppm PAM solution with 10ppm SDS in 1-inch pipeline

FR signal	PD signal	Velocity	Re	f	%DR*	fs	%DR**
4.141	2.746	12.705	124544	0.001	67.4%	0.002	47.6%
4.005	2.664	12.156	116165	0.001	66.5%	0.002	46.3%
3.909	2.590	11.768	110379	0.001	66.1%	0.002	46.1%
3.710	2.438	10.964	98735	0.001	65.4%	0.002	45.3%
3.696	2.453	10.907	97933	0.001	64.7%	0.002	44.4%
3.580	2.368	10.439	91387	0.001	64.1%	0.002	43.8%
3.314	2.202	9.365	77011	0.001	62.0%	0.002	41.4%
2.878	1.895	7.603	55460	0.002	59.4%	0.003	39.6%
2.703	1.775	6.897	47556	0.002	58.5%	0.003	39.2%
2.532	1.686	6.206	40270	0.002	55.9%	0.003	36.8%
2.375	1.596	5.572	33980	0.002	54.0%	0.003	35.4%
2.231	1.532	4.990	28561	0.002	50.4%	0.003	31.7%
2.111	1.481	4.505	24313	0.002	46.6%	0.003	28.0%
2.015	1.444	4.118	21098	0.003	42.5%	0.003	24.0%
1.901	4.759	3.657	17502	0.003	36.5%	0.004	18.4%
1.815	4.415	3.310	14955	0.003	31.0%	0.004	13.3%
1.724	4.030	2.942	12423	0.004	24.4%	0.004	7.7%
1.629	3.751	2.559	9968	0.005	11.8%	0.004	-4.0%
1.523	3.313	2.130	7469	0.006	-3.2%	0.005	-15.7%
1.432	2.635	1.763	5542	0.006	-4.4%	0.005	-10.8%
1.349	2.282	1.428	3975	0.007	-21.4%	0.006	-20.7%
1.254	1.906	1.044	2427	0.010	-55.4%	0.007	-39.5%
1.181	1.881	0.749	1438	0.019	-171.4%	0.009	-114.4%
1.122	1.722	0.511	787	0.035	-349.8%	0.012	-199.2%

* Percent drag reduction based on Blasius equation

** Percent drag reduction based on Dodge-Metzner equation

Flow loop data for the 500ppm PAM solution with 50ppm SDS in 1-inch pipeline

FR signal	PD signal	Velocity	Re	f	%DR*	fs	%DR**
4.194	2.178	12.926	130054	0.001	78.8%	0.002	65.6%
4.042	2.092	12.312	120448	0.001	78.6%	0.002	65.5%
3.939	2.043	11.896	114093	0.001	78.3%	0.002	65.3%
3.839	1.965	11.491	108045	0.001	78.7%	0.002	66.1%
3.668	1.901	10.800	97984	0.001	77.9%	0.002	65.1%
3.441	1.776	9.883	85193	0.001	77.8%	0.002	65.4%
3.231	1.689	9.034	73952	0.001	77.0%	0.002	64.7%
3.010	1.597	8.141	62763	0.001	76.2%	0.003	64.1%
2.763	1.527	7.143	51072	0.001	73.7%	0.003	61.2%
2.602	1.452	6.492	43935	0.001	73.6%	0.003	61.6%
2.492	1.424	6.048	39288	0.001	72.0%	0.003	59.8%
2.302	4.583	5.280	31720	0.001	68.1%	0.003	55.4%
2.165	4.210	4.726	26639	0.002	65.1%	0.003	52.3%
1.939	3.704	3.813	18991	0.002	56.8%	0.004	43.7%
1.853	3.540	3.465	16335	0.002	51.9%	0.004	38.5%
1.741	3.352	3.013	13101	0.003	42.8%	0.004	29.4%
1.671	3.233	2.730	11216	0.003	35.2%	0.004	21.9%
1.560	3.047	2.281	8452	0.004	18.2%	0.005	5.9%
1.449	2.755	1.832	5985	0.006	-4.1%	0.005	-12.1%
1.377	2.540	1.542	4558	0.007	-25.2%	0.006	-28.6%
1.306	2.316	1.255	3294	0.010	-55.9%	0.006	-48.9%
1.241	2.154	0.992	2275	0.014	-109.4%	0.007	-85.2%
1.165	1.950	0.685	1269	0.024	-238.6%	0.009	-159.0%
1.076	1.809	0.325	392	0.094	-989.5%	0.016	-483.8%

* Percent drag reduction based on Blasius equation

** Percent drag reduction based on Dodge-Metzner equation

Flow loop data for the 500ppm PAM solution with 100ppm SDS in 1-inch pipeline

FR signal	PD signal	Velocity	Re	f	%DR*	fs	%DR**
3.880	3.152	11.525	102368	0.002	52.8%	0.002	27.4%
3.724	3.006	10.902	93837	0.002	51.5%	0.002	26.0%
3.536	2.832	10.150	83918	0.002	49.9%	0.002	24.3%
3.437	2.723	9.755	78857	0.002	49.5%	0.002	24.2%
3.277	2.568	9.116	70921	0.002	48.3%	0.003	23.2%
3.087	2.415	8.356	61898	0.002	45.8%	0.003	20.5%
2.951	2.296	7.813	55716	0.002	44.2%	0.003	19.1%
2.798	2.172	7.202	49047	0.002	41.9%	0.003	17.0%
2.672	2.076	6.698	43788	0.002	39.6%	0.003	14.7%
2.468	1.909	5.883	35742	0.003	36.1%	0.003	11.9%
2.341	1.810	5.376	31036	0.003	33.5%	0.003	9.9%
2.201	1.705	4.816	26133	0.003	30.1%	0.003	7.3%
2.072	1.616	4.301	21891	0.003	25.9%	0.003	4.0%
1.936	1.541	3.758	17721	0.004	17.9%	0.004	-3.3%
1.828	1.481	3.326	14641	0.004	10.1%	0.004	-10.1%
1.733	1.438	2.946	12112	0.005	-0.8%	0.004	-20.1%
1.565	3.839	2.275	8082	0.006	-10.3%	0.005	-22.7%
1.480	3.258	1.936	6275	0.006	-18.1%	0.005	-25.4%
1.428	3.053	1.728	5254	0.007	-31.8%	0.005	-36.1%
1.396	2.924	1.600	4658	0.008	-42.1%	0.006	-42.6%
1.340	2.711	1.376	3680	0.010	-66.1%	0.006	-59.7%
1.308	2.611	1.248	3159	0.011	-86.5%	0.007	-73.3%
1.241	2.480	0.981	2165	0.017	-163.5%	0.008	-125.2%
1.186	2.409	0.761	1456	0.027	-293.0%	0.009	-202.1%
1.095	2.331	0.397	527	0.095	-1065%	0.014	-592.4%

* Percent drag reduction based on Blasius equation

** Percent drag reduction based on Dodge-Metzner equation